

An Investigation of Reaction Parameters for Carbon Dioxide Utilisation.

A Doctoral Thesis

by

Vanessa Silvestre González.

Submitted in partial fulfilment of the requirements for the award of Doctor
of Philosophy of Loughborough University.



INDEX

Index	3
Acknowledgements	9
List of Abbreviations	11
Abstract	15
Aims	17
1 Introduction	21
1.1 The Carbon Dioxide molecule, CO ₂	21
1.2 Global warming, Greenhouse Gases	23
1.3 Carbon fixation	24
1.4 Carbon dioxide capture and storage (CDCS)	24
1.5 Carbon dioxide capture and utilisation (CDU)	25
1.5.1 Mineral carbonation	25
1.5.2 Carbon Dioxide as a Chemical Feedstock	26
1.5.2.1 Fuels	28
1.5.2.2 Intermediates	28
1.5.2.2.1 Urea	28
1.5.2.2.2 Carbamates	29
1.5.2.3 Polymers	29
1.5.2.4 Inorganic complexes	29
1.5.2.5 Reactions	30
1.5.2.5.1 Carboxylation reaction	30
1.5.2.5.2 Cycloaddition or CO ₂ insertion reaction	31
1.5.2.5.3 Electrochemical CO ₂ reduction	31
1.5.3 Catalytic carboxylation from CO ₂	31
1.5.3.1 Metal and organometallic catalysts	31
1.5.3.1.1 Pd/Sn systems	32
1.5.3.1.2 Rh/B and Cu/B systems	32
1.5.3.1.3 Ni/Zn catalytic systems	33
1.5.3.1.4 Bimetallic aluminium complexes	34
1.5.3.2 Other catalysts	42
1.5.3.2.1 2,5-(2,6-diisopropylphenyl)iminomethyl pyrrole complexes	42
1.5.3.2.2 Selenium-catalysed cyclic carboxylation of diols	44
1.5.4 Electrochemical CO ₂ reduction	45
1.5.4.1 Reduction in Aqueous solution	45
1.5.4.2 Thermodynamic considerations	46
1.5.4.3 Electroreduction in non-aqueous medium	48
1.5.4.4 Electrochemical cell coupled to analytical instruments for in-line detection of species	49
1.5.5 Electrosynthesis of cyclic carbonates	50
1.5.5.1 Electrocarboxylation of epoxides	50
1.5.5.2 Electrocarboxylation of olefins	53
1.5.5.3 Study of the electrocatalytic activity of ammonium salts in the carbon dioxide electroreduction	55

1.5.5.4 Ionic liquids as solvent and catalyst for carboxylation of epoxides	55
1.6 introduction to the investigation.....	57
2 Results and discussion	61
2.1 Cyclic voltammetry	61
2.1.1 Electrode screening	61
2.1.1.1 Platinum disk working electrode.....	61
2.1.1.2 Glassy-Carbon disk working electrode.....	62
2.1.1.3 Gold disk working electrode.....	63
2.1.1.4 Copper rod working electrode.....	64
2.1.1.5 Electrode behaviour comparison for CO ₂ electroreduction in Bu ₄ NPF ₆ /ACN electrolyte.....	65
2.1.2 Magnesium counter electrode test.....	66
2.1.2.1 Copper rod working electrode (Platinum wire, RHE, Acetonitrile, Bu ₄ NBr).....	66
2.1.2.2 Copper rod and Magnesium ribbon.....	67
2.1.2.3 Comparison of Cu/Pt and Cu/Mg electrodes in Bu ₄ NBr/ ACN electrolyte.....	68
2.1.3 Electrode behaviour comparison for CO ₂ electroreduction in Bu ₄ NPF ₆ and Bu ₄ NBr electrolytes.....	69
2.1.4 Epoxide study under Cyclic voltammetry.....	70
2.1.4.1 Styrene oxide analysed by CV with copper rod and platinum wire electrodes.....	70
2.1.4.2 Styrene oxide analysed by CV with copper rod and magnesium ribbon electrodes.....	70
2.1.4.3 Electrode behaviour comparison for CO ₂ electroreduction in Bu ₄ NBr/ACN + Styrene oxide.....	71
2.1.4.4 Electrode behaviour comparison for CO ₂ electroreduction in Bu ₄ NBr/ACN and Bu ₄ NBr/ACN + Styrene Oxide.....	72
2.1.5 Conclusions.....	73
2.2 ICP analysis of Cu and Mg content on electrocatalytic cyclic carboxylation of epoxides ...	75
2.2.1 Styrene oxide electrochemical carboxylation.....	75
2.2.2 Fluorostyrene oxide electrochemical carboxylation	75
2.2.3 Bromostyrene oxide electrochemical carboxylation.....	76
2.2.4 1,2-Phenoxymethyl oxirane electrochemical carboxylation	77
2.2.5 1,2-Epoxyhexane	77
2.2.6 Allyl Glycidyl Ether.....	78
2.2.7 Comparison.....	79
2.2.8 Conclusions.....	79
2.3 Measure of the onset potential of the cell.....	80
2.4 DMS analytical technique to monitor in-situ electrocatalytic cyclic carboxylation of epoxides.....	81
2.5 Construction of a GC/MS for analysis of <i>in-situ</i> electrochemically assisted carboxylation reactions.....	82
2.5.1 Results.....	82
2.6 Background reactions.....	87
2.6.1 Electrocarboxylation of epoxides.....	87
2.6.2 Short Circuit reactions.....	88
2.6.3 Open circuit reaction	97

2.6.4	Carboxylation of epoxides (No Electrodes).....	98
2.6.4.1	Dilute reactions.....	98
2.6.4.2	MgCO ₃ and MgBr ₂ as cocatalyst for cyclic carboxylation of epoxides	103
2.6.4.3	Concentration Study.....	104
2.6.4.4	High concentrate cyclic carboxylation reactions.....	106
2.6.4.5	Glycidol and epichlorohydrin cyclic carboxylation.....	116
2.6.4.6	Cyclic carboxylation of 3-hydroxyoxetane	119
2.6.4.7	NH ₄ I catalyst for cyclic carboxylation of 1,2-phenoxymethyloxirane	119
2.6.4.8	Study of enantioselectivity of cyclic carboxylation of (S)-1,2-phenoxymethyloxirane	121
2.6.4.9	Solvent free reactions or neat reactions.....	126
2.6.4.10	Solvent screening study of the cyclic carboxylation reaction of 1,2-phenoxymethyloxirane	128
2.6.4.11	Phosphonium salts as catalysts.....	129
2.6.5	Conclusions	135
2.7	FTIR monitoring carboxylation reaction and calculation of reaction kinetics.....	139
2.7.1	Peaks.....	140
2.7.2	Infra Red reference spectra.	140
2.7.3	Temperature effect on IR measurements	144
2.7.4	Calibrations	144
2.7.5	Calculation of kinetics, reaction order of N-tetrabutylammonium iodide.....	147
2.7.5.1	Reaction of epichlorohydrin 1 M – TBAI 0.5 M.....	148
2.7.5.2	Reaction of epichlorohydrin 1 M – TBAI 0.25 M.....	149
2.7.5.3	Reaction of epichlorohydrin 1 M – TBAI 0.05 M.....	151
2.7.5.4	Determination of reaction order with respect to N-tetrabutylammonium iodide.	153
3	Conclusions and future work	159
3.1	Cyclic voltammetry.....	159
3.2	ICP analysis of Cu and Mg content on electrocatalytic cyclic carboxylation of epoxides..	160
3.3	Measure of the onset potential of the cell	161
3.4	Construction of a GC/MS for analysis of <i>in-situ</i> electrochemically assisted carboxylation reactions.....	161
3.5	Background reactions.....	161
3.5.1	Short Circuit reactions.....	162
3.5.2	Open circuit reaction.....	162
3.5.3	Carboxylation of epoxides (No Electrodes).....	162
3.5.3.1	Dilute reactions.....	162
3.5.3.2	MgCO ₃ and MgBr ₂ as cocatalyst for cyclic carboxylation of epoxides	163
3.5.3.3	Concentration Study.....	163
3.5.3.4	High concentrate cyclic carboxylation reactions	163
3.5.3.5	Glycidol and epichlorohydrin cyclic carboxylation.....	164
3.5.3.6	Cyclic carboxylation of 3-hydroxyoxetane	164
3.5.3.7	NH ₄ I catalyst for cyclic carboxylation of 1,2-phenoxymethyloxirane	164
3.5.3.8	Study of enantioselectivity of cyclic carboxylation of (S)-1,2-phenoxymethyloxirane	164
3.5.3.9	Solvent free reactions or neat reactions.....	165

3.5.3.10	Solvent screening study of the cyclic carboxylation reaction of 1,2-phenoxymethyloxirane.....	165
3.5.3.11	Phosphonium salts as catalysts.....	165
3.6	FTIR monitoring carboxylation reaction and calculation of reaction kinetics.....	166
4	Experimental.....	169
4.1	Electrochemical experiments.....	169
4.1.1	Reagents and apparatus.....	169
4.1.2	Electrochemical Cell design.....	169
4.2	ICP analysis of Cu and Mg content on electrocatalytic cyclic carboxylation of epoxides.....	171
4.3	Measure of the onset potential of the cell.....	172
4.4	DMS analytical technique to monitor in-situ electrocatalytic cyclic carboxylation of epoxides.....	172
4.5	Construction of a GC/MS for analysis of <i>in-situ</i> electrochemically assisted carboxylation reactions.....	174
4.6	Organic synthesis procedures.....	175
4.6.1	Reagents and apparatus.....	175
4.6.2	Reaction conditions and procedures.....	177
4.6.2.1	Product characterization.....	178
4.6.2.2	% of conversion Calculations.....	182
4.6.2.3	Initial improvements in procedure and work up.....	184
4.6.2.4	Electrocarboxylation of epoxides.....	186
4.6.2.5	Short Circuit reactions.....	186
4.6.2.6	Open circuit reaction.....	187
4.6.2.7	Carboxylation of epoxides (No Electrodes).....	188
4.6.2.8	Dilute reactions.....	188
4.6.2.8.1	MgCO ₃ and MgBr ₂ as cocatalyst for cyclic carboxylation of epoxides.....	188
4.6.2.8.2	Concentration study.....	189
4.6.2.8.3	High concentrate reactions.....	190
4.6.2.8.4	Glycidol and epichlorohydrin cyclic carboxylation.....	190
4.6.2.8.5	Cyclic carboxylation of 3-hydroxyoxetane.....	191
4.6.2.8.6	NH ₄ I catalyst for cyclic carboxylation of 1,2-phenoxymethyloxirane.....	191
4.6.2.8.7	Study of enantioselectivity of cyclic carboxylation of (S)-1,2-phenoxymethyloxirane.....	191
4.6.2.8.8	Solvent free reactions or neat reactions.....	192
4.6.2.8.9	Solvent screening study of the cyclic carboxylation reaction of 1,2-phenoxymethyloxirane.....	193
4.6.2.8.10	Phosphonium salts as catalysts.....	193
4.7	FTIR monitoring carboxylation reaction and calculation of reaction kinetics.....	196
5	Annexe.....	199
5.1	Gibbs free energy of CO ₂ and other molecules.....	201
5.2	Electrochemical cell set up.....	202
5.3	DMS experiment set up.....	203
5.4	Theoretical Mass spectra data.....	204

5.4.1	N ₂	204
5.4.2	O ₂	204
5.4.3	CO ₂	205
5.4.4	CO.....	205
5.4.5	Acetonitrile.....	206
5.4.6	Ethyl Acetate	206
5.4.7	Formic Acid.....	207
5.4.8	Methane	207
5.4.9	Methanol.....	208
5.4.9.1	Styrene oxide.....	208
5.4.9.2	Table of main peaks.....	209
5.5	ReactIR reaction set up.....	210
	References.....	211

ACKNOWLEDGEMENTS

I would like to acknowledge the Organic, Physical Chemistry and Analytical research teams in the University of Loughborough for their help and assistance in the labs. To Mark Edgar for advising and always helping with NMR analysis and to Al Daley for his always helpful attitude.

I want to thank Dr. Benjamin Buckley for his support, patience, teaching and guidance during the last three years and for making possible one of the best personal and professional experiences: a collaboration with the Chemistry Department in The University of Utah in Salt Lake City, USA. I want to thank Dr. Matt Sigman and his research group for hosting me during 6 weeks in their group and make me feel like one more in the group.

I want to make a special mention to Darren Walsh and his research group in the University of Nottingham for hosting me and guiding on the first year of this adventure. I would like to thank also Prof. Peter Licence and to Dr. Dan Mitchell from The University of Nottingham for spending time on introducing me to the synthesis of ionic liquids.

I want to thank my family for supporting me from Spain and to my second family (my friends in England) for their support every rainy and sunny day. They are Maria Mercedes Pardo, Nuria Lastra, Antonio LaFuente, Beatriz Fernandez, Shuqi Yang, Yuqi Li, and Volodymyr Tabas; to my “more than neighbours” Paula Cosar and Carlos Castelló, and to Ginés Escudero for sharing this amazing experience with me.

Finally, I would like to thank The Midlands Energy Consortium, Loughborough University and The University of Nottingham for funding this project.

LIST OF ABBREVIATIONS

ACN	acetonitrile
Bu ₄ NBr	n-Tetrabutylammonium bromide
Bu ₄ NI	n-Tetrabutylammonium iodide
CDCS	carbon dioxide capture and storage
CDCU	carbon dioxide capture and utilisation
CISO	chlorostyrene oxide
CV	cyclic voltammetry
d	doublet
DCM	dichloromethane
dd	doublet of doublets
DMF	dimethyl formamide
dppp	1,3-Bis(diphenylphosphino)propane
E	Energy
equiv	equivalents
EtOAc	ethyl acetate
EtOH	ethanol
FT	Fourier transform
GC	glassy-carbon
GCMS	gas chromatography mass spectrometry
h	hour
HER	hydrogen evolution reaction
i-PrOH	iso-propanol
IR	infra-red

lit.	literature
m	multiplet
MeCN	acetonitrile
MeOH	methanol
mp	melting point
MS	mass spectrometry
NE	no electrochemical system
NHE	normal hydrogen electrode
NMR	nuclear magnetic resonance
OC	open circuit system
PMO	1,2-phenoxyethyl oxirane
ppm	parts per million
ppmv	parts per million by volume
q	quartet
RHE	reference hydrogen electrode
rt	room temperature
s	singlet
SC	short Circuit system
SCE	saturated calomel electrode
SHE	standard hydrogen electrode
SO	styrene oxide
solv	solvent
t	triplet
TBABr	n-Tetrabutylammonium bromide
TBAI	n-Tetrabutylammonium iodide

TBAP	Tetrabutyl ammonium perchlorate
THPC	tetrakis(hydroxymethyl)phosphonium chloride
TIC	total ion current
TLC	thin layer chromatography
TMS	tetramethyl silane
UV	ultraviolet
V	volts

ABSTRACT

Carbon dioxide emissions per year have risen exponentially. It is widely known the contribution of CO₂ to global warming phenomena, so storage/utilisation of carbon dioxide has become a topical issue and an emerging research area. Despite the fact that utilization of CO₂ waste would not solve the problem of the huge quantities going to the atmosphere every year as only less than 1% of it could be reused for the industry, recycled carbon dioxide presents itself as a possible cheap and accessible chemical feedstock.

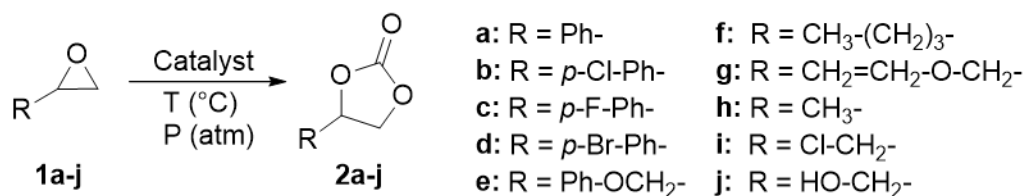
The challenge on recycling CO₂ is to minimize energy and cost efficiency of any suitable reaction. On previous investigations the electrochemical synthesis of 5-membered cyclic carbonate from epoxides was accomplished under mild conditions and optimized (1 atm CO₂ pressure, 60 mA constant current and 50 °C heating). In order to understand the mechanism of this electrochemical process a deep investigation on the variables of the synthesis of cyclic carbonates was carried out and is presented in this thesis. The variables studied include electrochemical system conditions (application of current through Cu/Mg electrodes, electrodes connected on a closed circuit system with no current, an open circuit system where electrodes were there was no connection between them, and reactions without electrodes), temperature of reaction, solvent screening, catalysts, epoxide substituents, concentration of species and ratio of reactants. As a result of the variables optimization, a new, cheap, simple and relatively fast method (5 to 24 hours of reaction time) for cyclic carboxylation of epoxides with CO₂ at atmospheric pressure in acetonitrile in the presence of ammonium salt (TBAI) at mild temperatures (50 - 75 °C) has been developed and improved. The concentration of the reactants, especially of the epoxide, was found to be the most important factor on the success of the reaction. The new reaction conditions also allow converting epoxides to carbonates without the help of any cocatalyst or electrochemical system obtaining excellent yields (50-100%) with the important saving on cost and energy of co-catalyst synthesis and recovery. Chlorostyrene oxide (1 M) reacted almost completely (94%) after 24 hours with TBAI (1 M), in 1 mL of acetonitrile at 75 °C and 1 atm pressure of CO₂. Epoxide carboxylation under neat conditions was feasible, producing 44% of chlorostyrene carbonate from chlorostyrene oxide in the presence of TBAI at 75 °C and 1 atm pressure of CO₂.

The main aim of the project was to optimize the procedure and conditions for the synthesis of cyclic carbonates from epoxides and carbon dioxide. The electrochemical carboxylation system previously developed by this research group (A. P. Patel, B. Buckley, U. Wijayantha)¹ was chosen as a starting point to analyse the catalytic processes happening during the electro-synthesis (Scheme 1.1).



Scheme 1.1.- Electro-synthesis of carbonates from epoxides under mild conditions.¹

The different epoxides (1a-j) selected for the formation of carbonates (2a-j) are summarized in the general reaction Scheme 1.2, all have been previously used for the same purpose and can be found in the literature with different reaction conditions and/or catalysts:



Scheme 1.2.-Epoxides selected for the synthesis of cyclic carbonates in the present project.

Fortunately, the findings of the research matched extremely well in some of the 12 principles of green chemistry,² as the optimized conditions for the reaction carried the reduction of solvent required, mild temperatures, no need of co-catalyst and atmospheric pressure of CO₂.

CHAPTER 1.
INTRODUCTION TO CO₂ UTILISATION

1 INTRODUCTION

The Introduction chapter summarizes the information available in the literature regarding carbon dioxide molecule and the role played in the global warming phenomena as one of the major contributors as a greenhouse gas.

A brief description of ways in which carbon dioxide is being fixated in nature (1.3 Carbon fixation), and artificially stored (1.4 Carbon dioxide capture and storage (CDCS)) are mentioned and a review on carbon dioxide capture and utilisation (CDCU) (1.5) is presented.

Carbon dioxide capture and utilisation section covers inorganic mineral carbonation (usually magnesium or calcium are transformed into magnesium or calcium carbonates), carbon dioxide insertion into different chemicals (producing the corresponding carbonates, cyclic carbonates, carbamates, etc.). A relevant selection for this project of the catalysis developed for carbon dioxide reactions is covered in more detail from section 1.5.3.

1.1 THE CARBON DIOXIDE MOLECULE, CO₂.

Carbon dioxide molecule is linear and non-polar with a double bond between the carbon and oxygen atoms (O=C=O). CO₂ is chemically unreactive under standard conditions of temperature and pressure (IUPAC definition of standard reference conditions: 273.15 °K (0 °C) and 100 KPa (1 bar)³) and therefore persists in the atmosphere.⁴⁻⁶

The Phase Diagram for CO₂ shows its physical state depending on temperature and pressure conditions (Figure 1.1).⁴ For pressures and temperatures such as the ones below the red and blue lines, CO₂ remains in vapour state. Over this line CO₂ can be at solid state (at very low temperatures, < -55 °C, over the corresponding sublimation pressure) or liquid state (from -55 °C to 40 °C, above the corresponding liquefaction pressure and below the corresponding melting pressure). The critical point is at temperature higher than 31 °C and pressure higher than 74 bar, where CO₂ gas density can be very large, even more than liquid water (important behaviour of CO₂ and relevant for its storage).

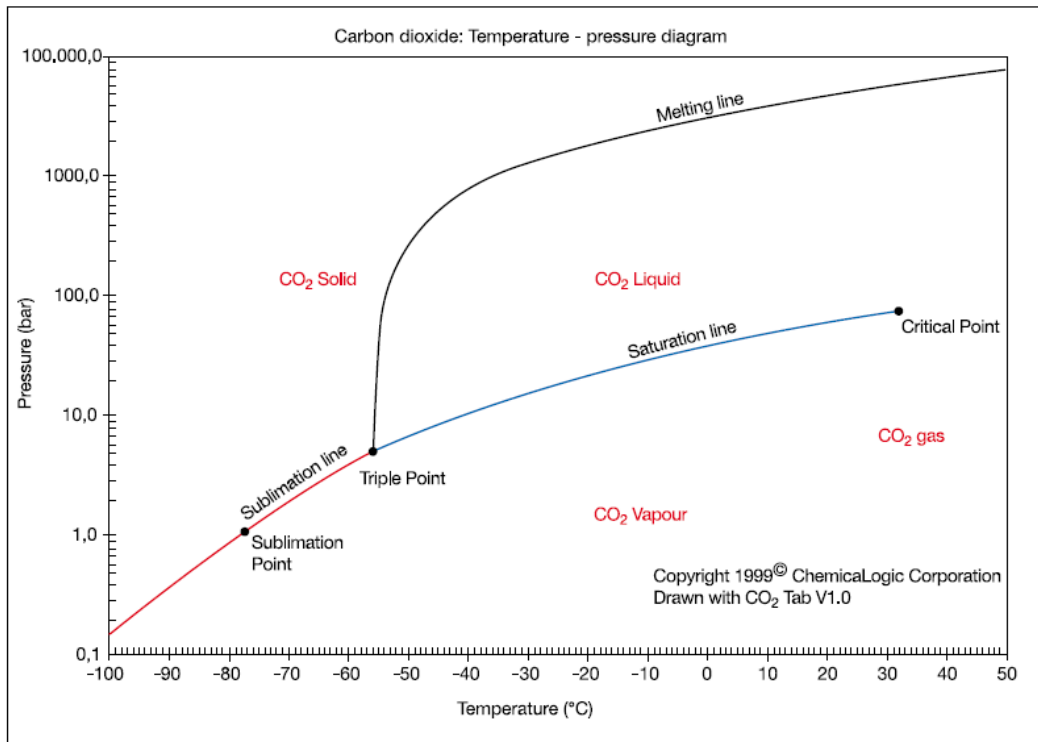


Figure 1.1.- Phase diagram for CO₂. Copyright © 1999 ChemicalLogic Corporation, 99 South Bedford Street, Suite 207, Burlington, MA 01803 USA. All rights reserved.

Volumetric concentration of CO₂ in the atmosphere is 0.040% (404 parts per million by volume, ppmv) as of July 2016 (Figure 1.2).⁷ CO₂ gas was generally thought to be harmless, in fact, CO₂ plays an important role in the earth's carbon cycle, and it is a necessary ingredient in the life cycle of animals and plants.⁸ Even though CO₂ is a non-flammable and chemically a non-toxic gas, there are some health and safety issues related to concentration in the atmosphere and storage or handling methods. For example: higher concentrations or exposures of longer duration are hazardous, either by reducing the concentration of oxygen in the air to below the required 16% level to sustain human life or by entering the body (bloodstream), and/or altering the amount of air taken in during breathing. When contained under pressure as in a gas cylinder, escape of CO₂ can also present serious hazards, for example asphyxiation, noise level (during pressure relief), frostbite, hydrates/ice plugs and high pressures.^{4,9}

Combustion of most carbon-containing substances produces CO₂. Energy utilization in modern societies today is based on combustion of carbonaceous fuels, which are dominated by the three fossil fuels: coal, petroleum, and natural gas.¹⁰

1.2 GLOBAL WARMING, GREENHOUSE GASES.

Carbon dioxide emissions per year by transport and industry have risen exponentially since the dawn of the industrial revolution (Figure 1.2). CO₂ gas is one of the main contributors to the Global warming phenomena¹¹ (Figure 1.3) and is one of the main reasons of why storage/utilization of carbon dioxide has become an important global issue.⁵

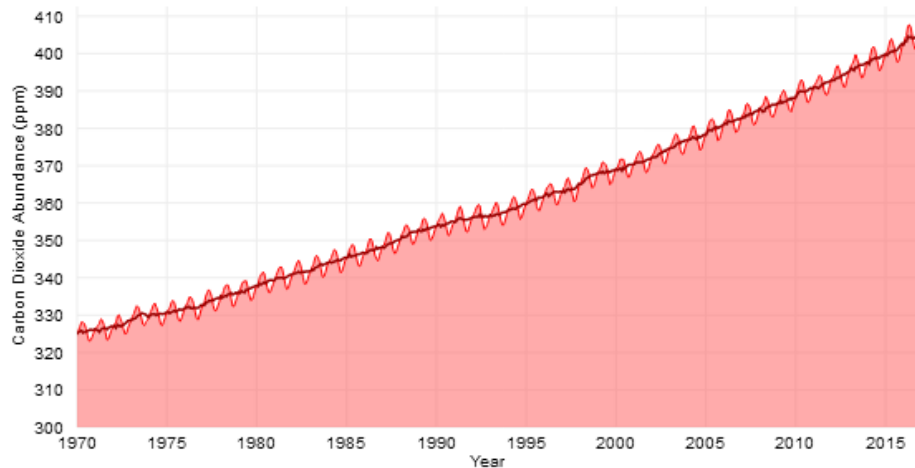


Figure 1.2.- Actual atmospheric CO₂ analysis during 1960–2016.⁷

Figure 1.3 shows a representation of the different gasses contributing to the greenhouse gas effect reported by NOAA Climate.gov in 2014 based on data collected up to 2016. Carbon dioxide produced in combustion of fossil fuel represents a 65% of the total of gases released to the atmosphere that contribute to this phenomena. An additional 11% of carbon dioxide comes from direct human-induced impacts on forestry and other land use (deforestation, degradation of soils and land clearing for agriculture). Agricultural activities, waste management, energy use, and biomass burning contribute to methane emissions (16% of total greenhouse gases emitted). Nitrous Oxide is the third abundant gas (6%) also coming from agricultural activities (like use of fertilizers) or biomass burning. Finally, a 2% of fluorinated gases (F-gases) are produced and released to the atmosphere from industrial processes, refrigeration, and use of products that include hydrofluorocarbons (HFCs), perfluorocarbons (PFCs), and sulfur hexafluoride (SF₆).

Global Greenhouse Gas Emissions by Gas

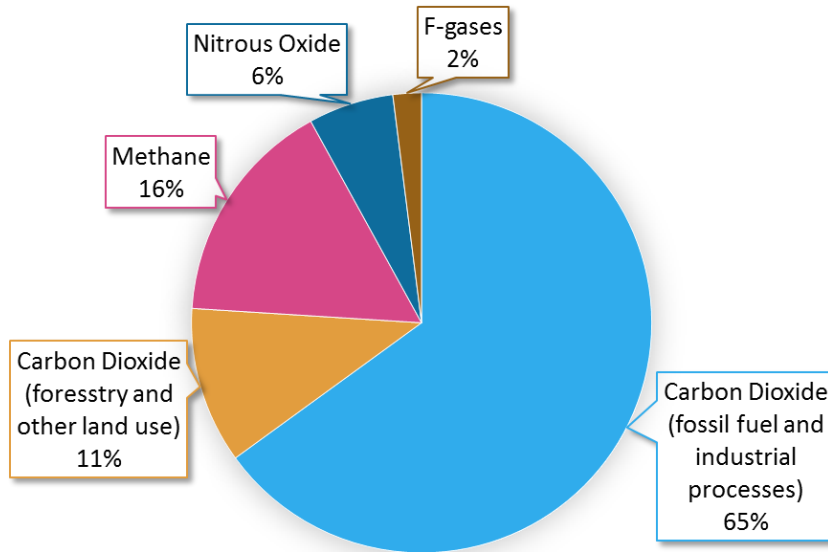


Figure 1.3.- Global greenhouse gas emissions by gas¹² based on global emissions from 2010 (Source: Intergovernmental panel on climate change, IPCC (2014)^{11,13}).

1.3 CARBON FIXATION

There are natural and artificial ways to capture the carbon to avoid emission into the atmosphere¹⁴ such as forestation, ocean fertilization, photosynthesis process,¹⁵ mineral carbonation¹⁶ and *in-situ* CO₂ capture.¹⁷

1.4 CARBON DIOXIDE CAPTURE AND STORAGE (CDCS)

One solution can be the capture and storage of CO₂.⁶ There exist in the literature several reviews about carbon dioxide capture^{4,14,18-20} and storage^{18,21,22}. In summary, capture of CO₂ can be carried out by different processes like pulverized coal combustion, gasification or oxy-combustion CO₂ separation and capture processes.¹⁴ Once the gas has been captured it may be stored in a geological reservoir (geological storage)²¹ or in mineral form (mineral carbonation).²²

1.5 CARBON DIOXIDE CAPTURE AND UTILISATION (CDCU)

There exist in the literature several reviews about carbon dioxide capture and utilisation.²²⁻²⁴ Next some of the general methods for utilisation of carbon dioxide in industry, such as mineral carbonation or carbon dioxide as chemical feedstock are summarized.

1.5.1 Mineral carbonation

Carbon dioxide is a chemical feedstock for the mineral carbonation process where minerals, generally calcium or magnesium silicates are transformed with CO₂ into calcium or magnesium carbonates. Magnesium and calcium carbonates have a lower energy state than CO₂ (Figure 1.4). Therefore, theoretically the process could produce energy. The magnesium and calcium oxide carbonation reaction can be shown by the equations 1.1 and 1.2. Carbonation reaction of magnesium or calcium are exothermic and release. For comparison, the heat produced in carbon combustion is 400 kJ/mole.

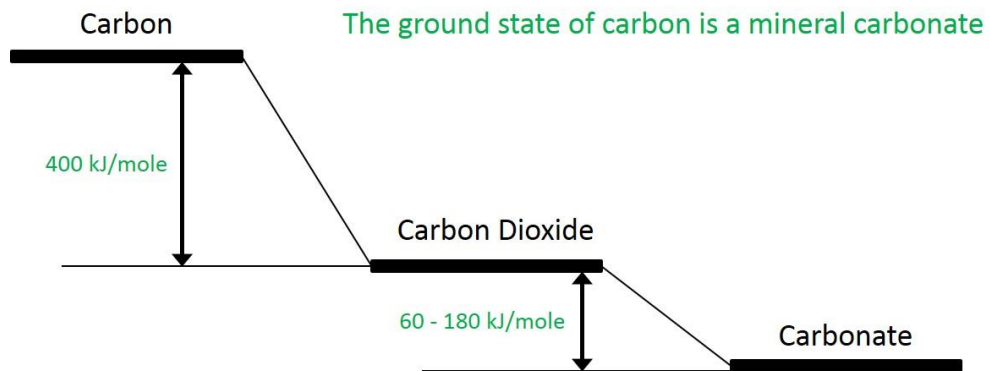
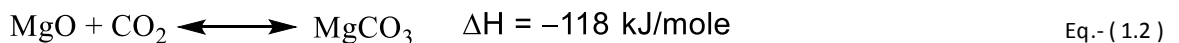
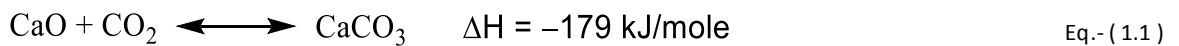
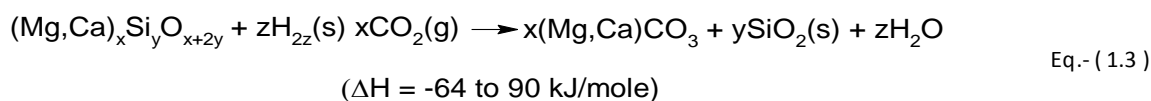


Figure 1.4.- Energy states of carbon.²⁵



However, calcium and magnesium cannot be usually found in nature as pure oxides but are typically found in silicate minerals.⁶ The reaction for common calcium and magnesium silicate

minerals is still exothermic, but less heat is released compared to the carbonation reaction of magnesium or calcium (Equation 1.3).



1.5.2 Carbon Dioxide as a Chemical Feedstock

CO₂ waste from an existing chemical process, previously separated from the stream, could be used as a chemical feedstock for the synthesis of other chemicals.⁶ The energy required for this process could be supplied by renewable energy sources (e.g., wind or solar energy).

CDCU alone cannot remediate all CO₂ emissions because they are much higher than the CO₂ volume that could be used as feedstock in chemical industry. It has been suggested from VCI and DECHEMA in Germany that chemical industry could convert around 1% of global CO₂ emissions in the fine and bulk chemicals sector and 10% into synthetic fuels.²⁶ Despite the fact that a very little percentage of CO₂ waste can be reused, can be a possible cheap and accessible chemical feedstock.

CO₂ is already used as an additive in food in countries like EU member countries²⁷ (listed as E290), US²⁸, Australia and New Zealand²⁹ (listed by its INS number 290). Examples of carbon dioxide use in the food industry are: carbonation of drinks³⁰, meat preservative³¹ or accelerated production of greenhouse tomatoes³². Carbon dioxide is also used as feedstock in commercial processes (i.e., synthesis of urea from ammonia and carbon dioxide³³) and as solvent in processes such as dry fabric cleaning³⁴ and decaffeination³⁵. But, the CO₂ is always released back to the atmosphere so these are recycling rather than mitigation technologies.

As a consequence of CO₂ low reactivity there has to be an energy trade off or a reduction in the activation energy for the reaction through the use of catalyst for CO₂ to be converted into economically valuable products.

Utilisation and storage of CO₂ closes the 'carbon cycle' by storing in a solid form (construction materials, polymers or chemical feedstock) the carbon previously released to the atmosphere as carbon dioxide. However, if CO₂ is converted to fuels, capturing carbon from the atmosphere would be necessary to maintain the cycle as shown in Figure 1.5.

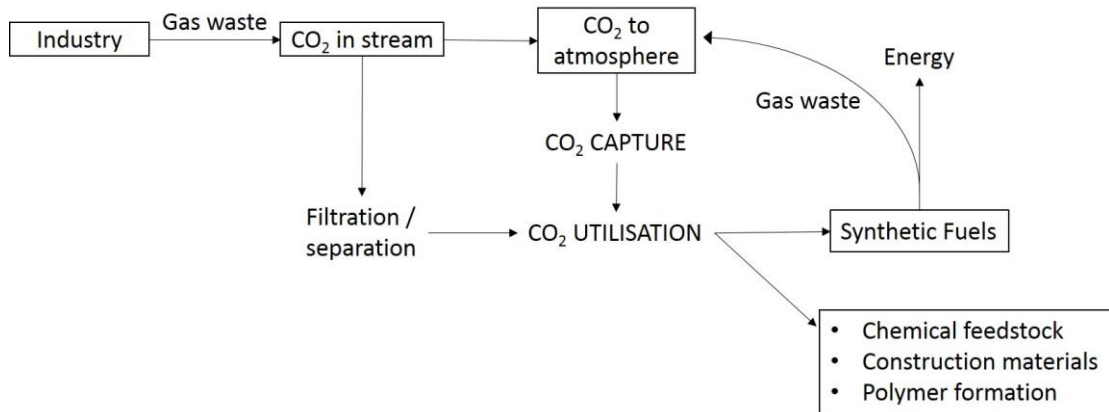


Figure 1.5.- Carbon dioxide industrial waste cycle.

Figure 1.6 represents a small sub-set of the important transformations of CO₂ of the whole chemicals landscape that have been reported.

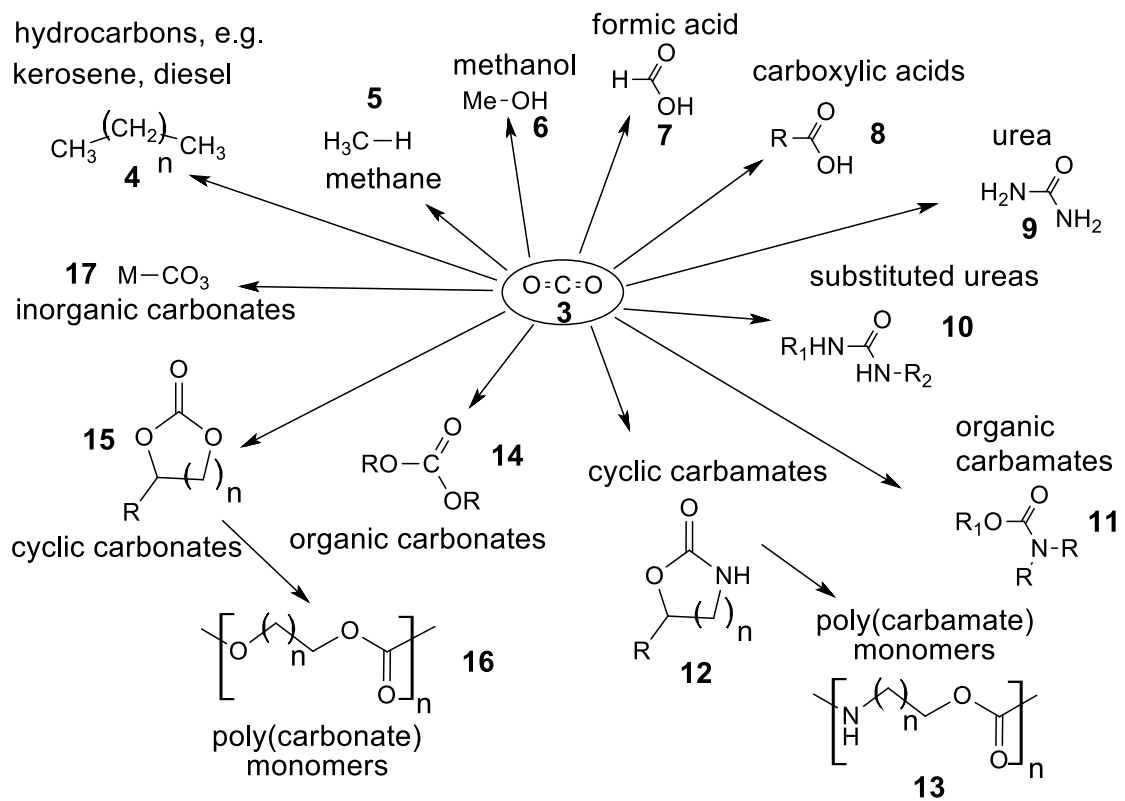


Figure 1.6.- A brief overview of some of chemicals from carbon dioxide.⁶

Gibbs free energy of CO₂ and related substances are shown in Figure 5.1 of the Annex.⁵ As a consequence of CO₂ high stability, it is necessary a substantial input of energy, effective activation reaction conditions and often active catalysts for chemical conversion of CO₂ (reactions involve positive change in enthalpy and thus they are endothermic).

The use of CO₂ as a single reactant is more energy-demanding than if it is used as a co-reactant with another substance with a higher Gibbs free energy, such as CH₄, carbon (graphite) or H₂.

1.5.2.1 Fuels

Both, methanol and formic acid have been targeted as products by hydrogenation of CO₂ over a wide range of catalysts.²³ While methanol synthesis requires three equivalents of hydrogen per CO₂ molecule (two incorporated into the product and the third consumed in the by-product, water), formic acid requires only one equivalent of hydrogen (without the formation of by-products), so it is a valuable product that can store hydrogen in a more manageable liquid form. Decomposition of formic acid releases the hydrogen when required but also the CO₂.³⁶

Sandia laboratories in New Mexico, USA reported the synthesis of synthetic diesel from CO₂.³⁷⁻⁴⁰ The project was called "Sunshine to petrol" as energy source was a solar furnace. Air Fuel Synthesis Ltd in the UK have used atmospheric CO₂ and wind energy to produce aviation fuels (rate of 1 litre per day).⁴¹

1.5.2.2 Intermediates

A part from direct products, intermediates are also a target representing a huge potential market.⁶ Some of them are commented bellow.

1.5.2.2.1 Urea

Large quantities of CO₂ are already consumed through reaction with ammonia (Figure 1.7) from the Haber-Bosch process to produce urea (H₂N-(C=O)-NH₂), a key ingredient in fertilisers.⁴²

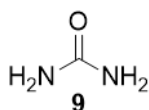


Figure 1.7.- Urea molecule (9).

The Haber-Bosch process which was developed by Fritz Haber and Carl Bosch, is the most economical for the fixation of nitrogen and with modifications continues in use as one of the basic processes of the chemical industry in the world.⁴³

1.5.2.2.2 Carbamates

The reaction of a variety of N-nucleophiles (like primary and secondary amines^{44,45}, metals and metal salts^{46,47}, metal complexes⁴⁶⁻⁴⁹, and p-block-amides⁴⁶⁻⁵¹) with carbon dioxide results in the formation of N-carbonyl compounds⁵², including carbamates which have applications ranging from pesticides for agricultural processes⁵³ to polymers for construction and protection⁵⁴.

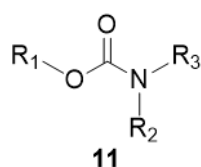


Figure 1.8.- General structure of organic carbamates (**11**).

Carbamates (**11**) differ from ureas (**9**) in that the central carbon of the C=O group is also bonded to a nitrogen and an oxygen, rather than two nitrogens. They are used as a replacement for the extremely toxic phosgene in organic synthesis^{6,55,56} and as a precursor in the synthesis of isocyanates which are used in the formation of polyurethanes.⁵⁵

1.5.2.3 Polymers

Cyclic carbonates with six atoms or more can be ring-opened to give a hydroxyl carboxylic acid that can polymerise to give polycarbonates.^{57,58} However, direct synthesis of polymers from epoxides and CO₂ is being studied as a simpler process.^{59,60}

Polycarbonates are used in construction materials (in place of glass)^{61,62} and in security and personal protection products due to their properties (high strength and impact resistance while being extremely light and mouldable).⁶³ Polycarbonates have very high impact-resistance and optical transparency^{55,64-66} that gives them applications in the manufacture of CDs, DVDs, eyeglasses, aircraft windows, etc. Polymers chemical and mechanical properties can be tuned by altering the composition of the side chain group.⁶⁷

1.5.2.4 Inorganic complexes

A diversity of metal cations is used as the molecular template for the production of inorganic carbonates which have several applications in construction as well as catalysis.⁶⁸ The best known examples of inorganic carbonates produced and used throughout history are limestone, for construction as “crush rock”, soda, for washing and papermaking activities, and sodium bicarbonate (or baking powder) used as a food additive.⁶⁹ Potassium carbonates have been used

as fertilizer and in production of glass or soap. Other bicarbonates much less used compared to the calcium, sodium or potassium are the carbonates of magnesium, barium, lithium and strontium, that have been used in rubber processing, the production of glass, ceramics, photochemicals, cosmetics and medicine, catalysts and batteries.⁷⁰ Precipitated calcium carbonate is used in paper industry, plastics and rubber, and paint production.⁷¹

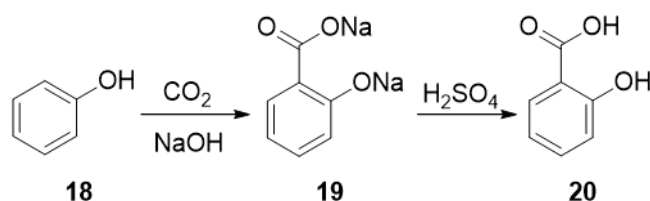
Industrial scale production of sodium bicarbonate proceeds via the Solvay process where CO₂ is combined with sodium from seawater.⁷² Production methods of potassium bicarbonate involve the carbonation of potassium hydroxide which is produced by electrolysis of aqueous potassium chloride solutions.⁷³ Magnesium carbonate (magnesite) can be produced by carbonating a magnesium chloride brine.⁷⁴ Carbonates of barium, strontium and lithium are typically achieved by carbonating barium sulfate⁷⁵ (barite), strontium sulfate⁷⁶ (celestine) and lithium⁷⁷ brines.

1.5.2.5 Reactions

Two types of reactions involving carbon dioxide addition are described below.

1.5.2.5.1 Carboxylation reaction

It consists on the direct addition of CO₂ to a receptor molecule by a single bond to the carbon atom on CO₂ to form a carboxylate group (or a carboxylic acid). This reaction is 100% atom efficient in that all atoms are incorporated to the product. An example of this reaction is the Kolbé-Schmitt reaction to produce salicylic acid from phenol (Scheme 1.1).^{78,79}



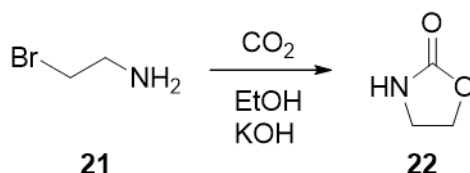
Scheme 1.1.- Kolbé-Schmitt reaction to produce salicylic acid.⁷⁹

Linear and cyclic organic carbonates are also formed from CO₂.⁸⁰ When CO₂ is inserted into an organic epoxide leads to the formation of the cyclic carbonate which will be explained in more detail in section “1.5.3 Catalytic carboxylation from CO₂”.

A part from the uses previously commented, organic carbonates can also be used as green solvents, additives to gasoline,^{70,81} thickeners for cosmetics⁶⁵ and electrolytes for lithium batteries⁶⁴⁻⁶⁶. Diethyl carbonate is also used as an intermediate for phenobarbital synthesis.⁸²

1.5.2.5.2 Cycloaddition or CO₂ insertion reaction

In this reaction two bonds are formed, one to the carbon and a second to one of the heteroatoms (i.e. oxygen or nitrogen).⁸³ An example of cycloaddition of CO₂ reaction is shown in Scheme 1.2 where an haloamine reacts with CO₂ to give a cyclic carbamate.⁸⁴



Scheme 1.2.- Cyclization of 2-bromoethanamine with carbon dioxide. Reaction conditions: 2 mmol substrate, 1.2 equiv KOH, 10 mL EtOH, 65 °C, 35 bar CO₂, 1 h. Product obtained >99%.

1.5.2.5.3 Electrochemical CO₂ reduction

It usually requires the use of an electric current (possibly created from a renewable energy source) to produce the required electrons. Some of the products that can be formed by electrochemical reduction of carbon dioxide are formic acid, carbon monoxide, methanol, methane and other hydrocarbons. Barton Cole and Bocarsly (2010) have reviewed electrochemical reduction processes in detail and Silvestri and Scialdone (2010) have reviewed some recent advances in electrochemical carboxylation.^{85,86}

Electrochemical carbon dioxide reduction process will be further discussed in section 1.5.4.

1.5.3 Catalytic carboxylation from CO₂

Literature reviews about catalytic carboxylation are numerous, some of them focus on metal complexes and non-metal catalysts for transformation of carbon dioxide into carbonates^{55,87-89}, and others summarize the electrocatalytic reactions of carbon dioxide⁹⁰⁻⁹⁵ or photoreduction of carbon dioxide⁹⁶. A number of key publications has been selected to be studied due to their relevance with the present research project.

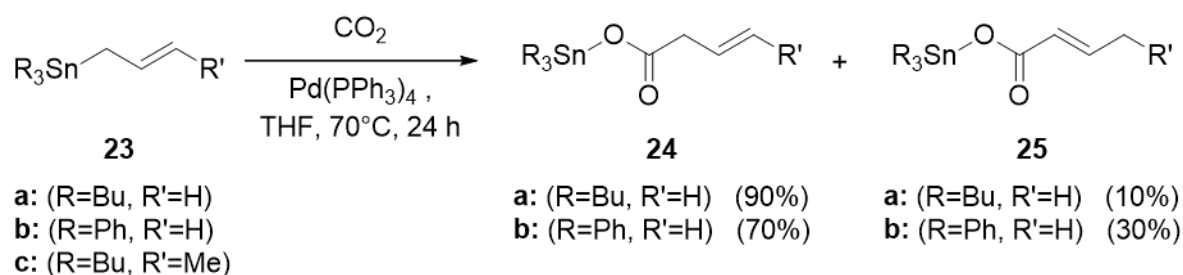
1.5.3.1 Metal and organometallic catalysts

The first successful attempt on producing carboxylic acids from CO₂ and reactive organometallic derivatives was accomplished by Victor Grignard and Philippe Barbier in 1980.⁹⁷ "Grignard reagents" (organomagnesium reagents) are strong nucleophiles that react fast with CO₂ to form carboxylic acids and related products.⁹⁸ Organolithium,⁹⁷ organocopper⁹⁹ and

organomanganese¹⁰⁰ reagents are also known to react with CO₂. However, the most frequent drawback of these standard reactions is that unwanted side products may be produced some of which might represent an additional problem for the environment. In order to overcome this disadvantage, the development of new methods to achieve versatile carboxylations with CO₂ has been investigated by many research groups. Some of them are detailed below.

1.5.3.1.1 Pd/Sn systems.

One of the first examples of bimetallic catalytic systems that allowed the insertion of CO₂ into the rather unreactive tin-carbon bond was reported by Shi *et al.*¹⁰¹ The aim was to combine in the same system the ability of a transition metal to catalyse crosscoupling reactions and CO₂ activation. For example, tributyl(allyl)tin (23a) does not react with CO₂, but when palladium(0) species (Pd(PPh₃)₄ or Pd(PBu₃)₄) are present in the solution the reaction evolves to afford carboxylates 24a (90%) and 25a (10%) (Scheme 1.3). The mechanism proposed for this reaction was through the transfer of the allylic moiety to the palladium(0) via oxidative coupling, followed by an insertion of CO₂ into the Pd-C bond.¹⁰²

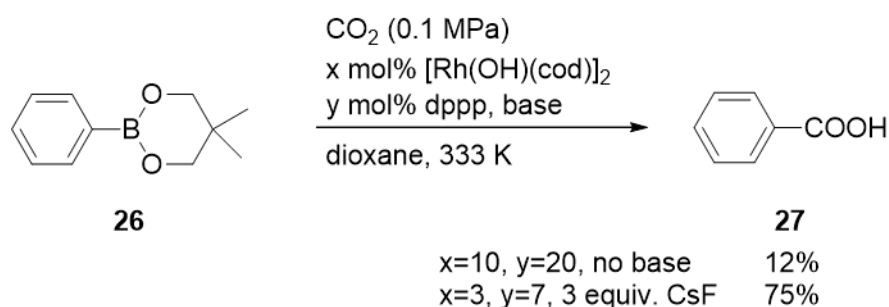


Scheme 1.3.- Formation of tin carboxylates with a dual allylstannanes/Pd(PPh₃)₄ catalytic system.¹⁰¹

Further improvements to the Pd/Sn bimetallic system have been achieved by different research groups.^{103–106}

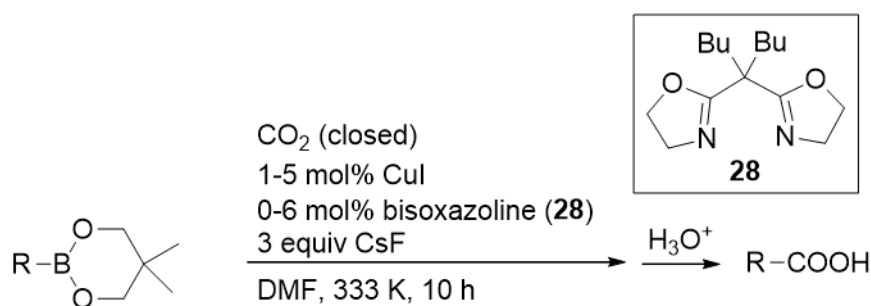
1.5.3.1.2 Rh/B and Cu/B systems.

An alternative with a rhodium(I)-catalyzed carboxylation of aryl- and alkenylboronic esters proceeding under mild conditions was proposed by Ukai *et al.* in 2006.¹⁰⁷ The Rh/B system permitted the reaction to evolve while leaving ancillary reactive functional groups such as carbonyl- and cyano unreacted (Scheme 1.4).



Scheme 1.4.- Rhodium-catalyzed carboxylation of alkylboronic esters under mild conditions (dppp ligand: 1,3-Bis(diphenylphosphino)propane).¹⁰⁷

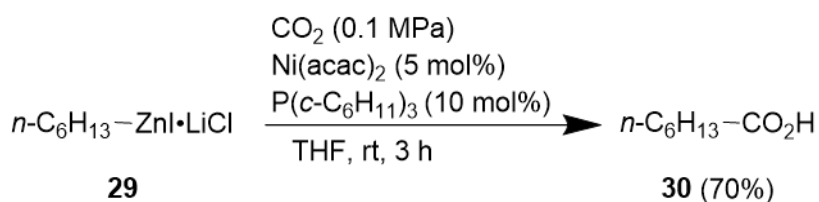
This reaction was particularly useful for the synthesis of functionalized arylcarboxylic acids. However, the corresponding alkylboronic esters could not be carboxylated with the Rd(I) catalytic system under the conditions detailed in Scheme 1.4. Furthermore it was found that arylboronic esters containing a bromide would generate complex mixtures of products, limiting the utility of this approach. The same research group studied and reported other metallic systems which could also promote this type of carboxylation reaction with a wider functional group compatibility, such as the case of a boronic ester/copper(I) salt/CsF catalytic system.¹⁰⁸ The best results were obtained when a copper(I) iodide/bisoxazoline system was used giving substituted benzoic acid in high yields and purities (up to 95% for *para*-methoxy-benzoic acid) (Scheme 1.5).



Scheme 1.5.- Optimized copper - catalyzed carboxylation of alkylboronic esters.¹⁰⁸

1.5.3.1.3 Ni/Zn catalytic systems.

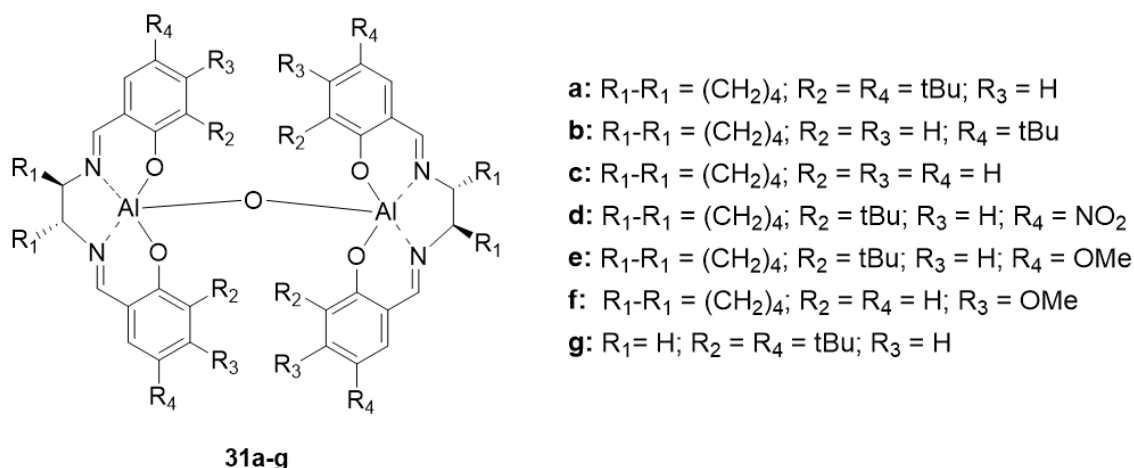
Ochiai *et al.* reported the synthesis of saturated carboxylic acid in good yields under mild conditions with a bimetallic Ni/Zn catalytic system (0.1 MPa CO₂, 4 to 8 h reaction time, temperatures ranging from room temperature to 323 K).¹⁰⁹ An example of the reaction of hexylzinc iodide-lithium chloride complex with carbon dioxide in the presence of the Ni(acac)₂ is shown in Scheme 1.6.

Scheme 1.6.- Ni-catalyzed carboxylation of organozinc iodide reagents under mild conditions.¹⁰⁹

More investigations involving Ni/Zn catalytic system were carried out by different research groups. When zero-valent nickel species were used to produce reactive cyclic nickel-carboxylates a second organometallic counterpart (ZnR₂) was not necessarily required.¹¹⁰⁻¹¹⁴

1.5.3.1.4 Bimetallic aluminium complexes

North's group has a wide background on research on catalytic synthesis of cyclic carbonates.¹¹⁵ They focused on the study of bimetallic catalysts, especially of aluminium (due to its price-efficiency relationship compared to other metals like platinum) and a range of different ligands (Figure 1.9) were tested as catalysts for the carboxylation of epoxides with CO₂ in the presence of tetrabutylammonium bromide under solvent free conditions. The bimetallic complexes showed a high catalytic activity at atmospheric pressure and room temperature. The ammonium salt was stable for over 60 reactions, though it was found to decompose *in situ* by a retro-Menschutkin reaction forming tributylamine (also found to be a participant in the reaction mechanism) (see Scheme 1.7).

Figure 1.9.- Bimetallic aluminium complexes tested as catalysts for the carboxylation of epoxides.¹¹⁶

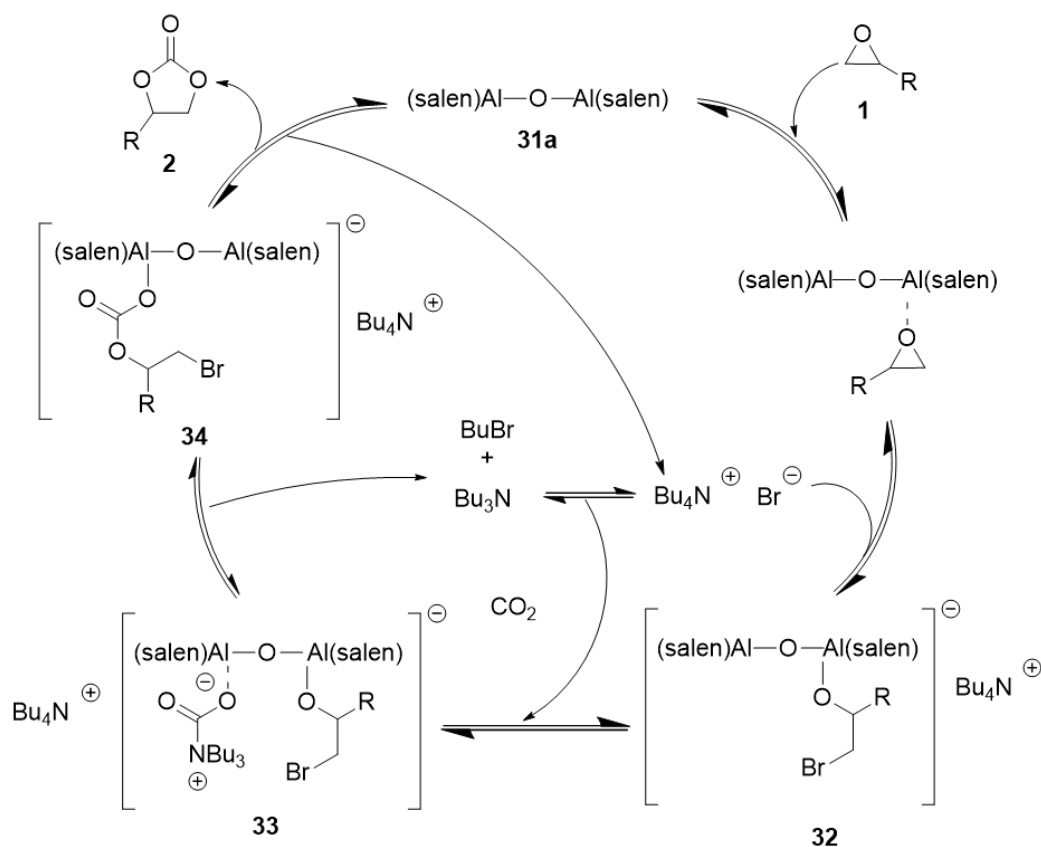
A full analysis of the reaction kinetics with *in situ* IR scans was carried out over the synthesis of styrene carbonate with CO₂ catalyzed by 31a and TBABr in propylene carbonate as solvent. The

carbonate peak was masked by that of the solvent so the peak selected to follow the reaction was the one at 876 cm⁻¹ which corresponds to C-O bond of styrene oxide.

GC-MS was chosen as a second method to confirm that concentration of epoxide calculated through IR measurements were correct. Concentration of styrene oxide along the reaction was calculated through calibrations of the IR and the GC-MS previously carried out. The reaction kinetics showed that reaction was first order in aluminium complex concentration, first order in epoxide concentration, first order in carbon dioxide concentration (except when used in excess, that produces saturation of the solvent) and second order in TBABr concentration (Eq.- (1.4)). Also, addition of butyl bromide to revert tributylamine into TBABr resulted in inhibition of the reaction.

$$R = k[\text{epoxide}][\text{CO}_2][\text{catalyst}][\text{Bu}_4\text{NBr}]^2 \quad \text{Eq.- (1.4)}$$

Although no kinetic resolution of racemic epoxides was possible, it was shown that if enantiomerically pure styrene oxide was used as substrate, then enantiomerically pure styrene carbonate was formed.¹¹⁷ The catalytic cycle on Scheme 1.7 was proposed to explain the high catalytic activity of the bimetallic complexes.



Scheme 1.7.- Catalytic cycle for the cyclic carbonate synthesis by using complex 31a and Bu_4NBr by North *et al.*¹¹⁷

North and co-workers also presented a study on the influence of temperature and pressure on cyclic carbonate synthesis catalysed by bimetallic aluminium complexes¹¹⁸ where they analysed the conversion of styrene oxide to styrene carbonate using TBABr as cocatalyst and two different structures of aluminium complexes ($[(\text{salen})\text{Al}]_2\text{O}$ structure 31a from Figure 1.9 and $[(\text{acen})\text{Al}]_2\text{O}$ structure 35 from Figure 1.10).

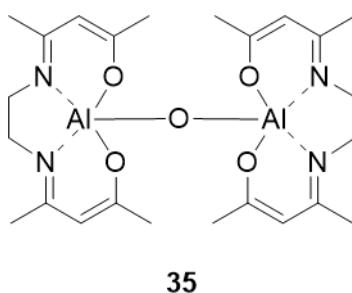
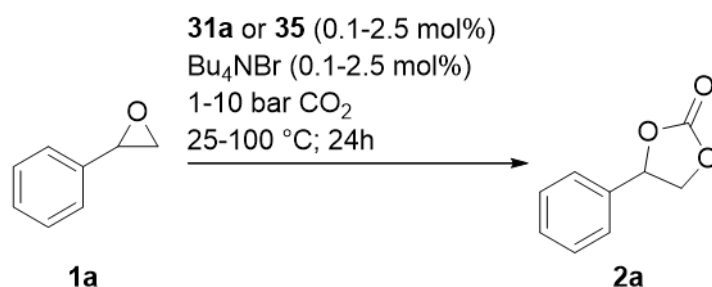


Figure 1.10.- Bimetallic aluminium complex used for the catalysis of cyclic carbonate synthesis ($[(\text{acen})\text{Al}]_2\text{O}$).¹¹⁸

The study was carried out over a set of reactions in order to compare performances of catalysts 31a and 35 (varying concentration from 0.1 to 2.5 mol%). Different pressures of CO₂ (1 to 10 bar) were also tested over a range of temperatures (25 to 100 °C) during 24 hours (Scheme 1.8).



Scheme 1.8.- Conversion of styrene oxide into styrene carbonate using catalysts $[(\text{salen})\text{Al}]_2\text{O}$ (31a) or $[(\text{acen})\text{Al}]_2\text{O}$ (35).¹¹⁸

In general, both catalysts showed a high efficiency on catalysing the carboxylation of epoxides. However, in comparison, catalyst 35 performed usually lower than 31a or in some cases the reaction under catalyst 35 did not evolve.

Table 1.1 shows conversion of styrene oxide at 25 °C during 24 h using catalyst 31a or 35 at pressures of CO₂ of 1, 5 and 10 bars. The background reactions using only metal catalysts with no presence of TBABr led to 0% of conversion (entry 1, Table 1.1). When TBABr was used without metal catalyst (entry 2, Table 1.1) the reaction gave as much as 6% of carbonate. When used TBABr together with 31a conversions went from 58% (0.5 mol% of TBABr and 0.5 mol% catalyst, 5 bar, entry 6, Table 1.1) to 100% (2.5 mol% of TBAI and 2.5 mol% of catalyst, 5 and 10 bar CO₂,

entries 11 and 20, Table 1.1). When catalyst 35 was used instead performance was lower in comparison producing generally less carbonate than catalyst 31a (see column 'conv. 35 (%)' of Table 1.1).

Table 1.1.- Synthesis of styrene carbonate 2 using catalyst 31a or 35 at 25 °C.^{a, 118}

Entry	31a or 35 (mol%)	Bu ₄ NBr (mol%)	CO ₂ (bar)	conv. 31a (%)	conv. 35 (%)
1	2.5		1	0	0
2		2.5	1	6	6
3	2.5	2.5	1	98	93
4	0.5		5	0	0
5		0.5	5	4	4
6	0.5	0.5	5	58	21
7		1.0	5	5	5
8	1.0	1.0	5	79	49
9	2.5		5	0	0
10		2.5	5	6	6
11	2.5	2.5	5	100	63
12	0.5		10	0	
13		0.5	10	5	5
14	0.5	0.5	10	69	
15	1.0		10	0	
16		1.0	10	5	5
17	1.0	1.0	10	95	
18	2.5		10	0	
19		2.5	10	6	6
20	2.5	2.5	10	100	75

^aAll reactions carried out for 24 h.

When reactions were carried out at 60 °C (Table 1.2) with TBABr alone, conversions went from 3% at 1 CO₂ bar (entry 2) to 28% at 10 CO₂ bar (entry 22). Meanwhile conversions of reactions adding catalyst 31a went from 32% at 1 bar (entry 3) to 100% at 1, 5 and 10 bar (entries 5, 6, 12, 14, 17 and 21). Catalyst 35 showed slightly lower performance than catalyst 31a when reactions were run under 1 bar pressure of CO₂ (entries 3 and 5).

The reactions were also studied at 100 °C (Table 1.3), TBABr alone produced only 4 to 52% of cyclic carbonate (entries 1 and 7), while addition of catalyst 31a gave conversions in the range of 49 to 98% (entries 2 and 9) and catalyst 35 of the range of 0 to 97% (entries 2 and 5).

Table 1.2.- Synthesis of styrene carbonate 2 using catalyst 31a or 35 at 60 °C.^{a,118}

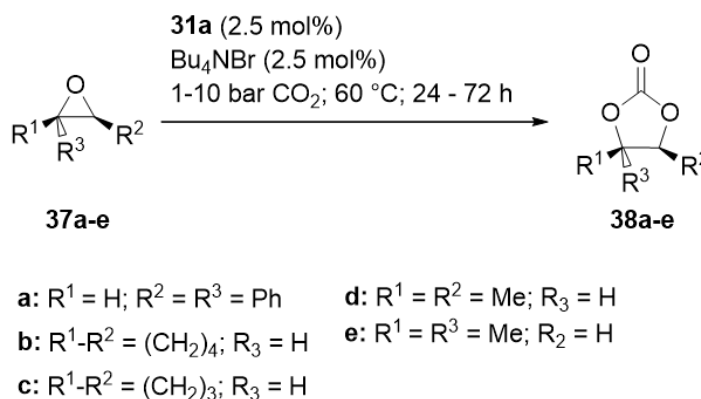
Entry	31a or 35 (mol%)	Bu ₄ NBr (mol%)	CO ₂ (bar)	conv. 31a (%)	conv. 35 (%)
1	0.1		1	0	0
2		0.1	1	3	3
3	0.1	0.1	1	32	23
4		0.5	1	7	7
5	0.5	0.5	1	100	78
6		1.0	1	10	10
7	1.0	1.0	1	100	
8		0.1	5	3	3
9	0.1	0.1	5	36	33
10	0.5		5	0	0
11		0.5	5	9	9
12	0.5	0.5	5	100	
13		1.0	5	13	13
14	1.0	1.0	5	100	
15	2.5		5	0	0
16		2.5	5	24	24
17	2.5	2.5	5	100	100
18		0.1	10	6	6
19	0.1	0.1	10	58	47
20		0.5	10	13	13
21	0.5	0.5	10	100	
22		2.5	10	28	28
23	2.5	2.5	10	100	100

^aAll reactions carried out for 24 h.Table 1.3.- Synthesis of styrene carbonate 2 using catalyst 31a or 35 at 100 °C.^{a,118}

Entry	31a or 35 (mol%)	Bu ₄ NBr (mol%)	CO ₂ (bar)	conv. 31a (%)	conv. 35 (%)
1		0.1	1	4	4
2	0.1	0.1	1	49	
3	0.5		1	0	0
4		0.5	1	7	7
5	0.5	0.5	1	75	97
6	2.5		1	0	0
7		2.5	1	52	52
8	0.5	2.5	1	85	
9	1.0	2.5	1	98	
10		0.1	5	6	6
11	0.1	0.1	5	65	59
12	0.1		10	0	0
13		0.1	10	8	8
14	0.1	0.1	10	82	73

^aAll reactions carried out for 24 h.

Conversions of disubstituted epoxides to cyclic carbonates using catalyst 31a were also successful (Scheme 1.9).¹¹⁸



Scheme 1.9.- Conversion of disubstituted epoxides 37a–e into cyclic carbonates 38a–e using catalysts 31a or 35.¹¹⁸

As shown in Table 1.4, best performances required CO₂ pressures of 10 bar, time reaction was from 24 to 72 hours, and yields went from 26% of conversion to carbonate 38e at 10 bar of CO₂ after 24 hours (entry 7) to 100% of conversion to 38a (entry 4) or to 38e carbonate (entry 8), both after 72 hours.

Table 1.4.- Synthesis of disubstituted cyclic carbonates 37a–e using catalyst 31a at 60 °C.^{a, 118}

Entry	epoxide	CO ₂ (bar)	time (h)	yield (%)
1	37b	1.0	24	35
2	37b	10.0	24	65
3	37a	10.0	24	32
4	37a	10.0	72	100
5	37c	10.0	24	71
6	37d	10.0	24	49
7	37e	10.0	24	26
8	37e	10.0	72	100

^aReaction conditions as in Scheme 1.9: 31a 2.5 mol%, TBABr 2.5 mol%, 60 °C.

In this study the viability of using compressed air instead of CO₂ for the catalytic carboxylation of styrene oxide was checked under different pressures (10 and 25 bar) and temperatures (20 or 50 °C) (see Table 1.5). Performance of the reaction when using compressed air was of 64% of conversion after 24 hours at 10 bar of CO₂ and 50 °C (entry 1, Table 1.5), lower than when pure CO₂ was used (100% of conversion after 24 hours at 10 CO₂ bar and 60 °C; entry 23, Table 1.2). Even when the reactions were run for longer times or at higher pressures the conversion was not complete (78% after 72 hours, entry 2, Table 1.5; 79% after 24 hours at 25 bar of CO₂, entry 3, Table 1.5). However, the results demonstrate that the synthesis of the cyclic carbonate under

compressed air is possible (same reaction exposed to air under atmospheric pressure and low temperature did not evolve).

Table 1.5.- Synthesis of styrene oxide with catalyst 31a using compressed air.^{a, 118}

Entry	air (bar)	T (°C)	t (h)	conv. (%)
1	10.0	50	24	61
2	10.0	50	72	78
3	25.0	50	24	79
4	25.0	20	24	19

^aReaction conditions: 31a catalyst 2.5 mol%, TBABr 2.5 mol%, 24 h.

As a need to test the carboxylation of epoxides in a realistic industrial CO₂ waste flow or flue gas, North, Wang and Young (2011) investigated the exposure of an immobilized bimetallic aluminium complex catalyst (Figure 1.11)¹¹⁵ to flue gas for different periods of time and compared their catalytic activity for the carboxylation of epoxide.^{115,119,120} Reactions were carried out with presence of TBABr and CO₂ obtained from dry ice in a gas-phase reactor previously designed for ethylene carbonate synthesis.¹²⁰ In batch reactions results showed some decrease in catalyst activity (Graph 1.1). Samples of catalyst that were exposed to flue gas produced by combustion of coal had their catalytic activity more deteriorated than those exposed to flue gas produced by combustion of gas. After 7, 15 and 22 cycles TBABr co-catalyst was reactivated by treatment with benzyl bromide and conversion of carbonate restore its initial values. They suggested that the loss of activity is due to changes to the catalyst morphology resulting in the reactants not being able to access catalyst sites. In contrast, when reactions were carried out in a gas-phase flow reactor, there was no apparent loss of catalyst activity when the catalyst was exposed to flue gas formed by combustion of coal. Although the reason is unknown, they attribute it to the substrates short residence time in the flow reactor resulting in the more easily obstructed catalyst sites not being involved in the catalysis and therefore their blocking has no appreciable effect on catalyst activity.

1.5.3.2 Other catalysts

1.5.3.2.1 2,5-(2,6-diisopropylphenyl)iminomethyl pyrrole complexes

Babu and Muralidharan (2012) published their work on the synthesis of Zn(II), Cd(II) and Cu(II) complexes of 2,5-(2,6-diisopropylphenyl)iminomethyl pyrrole ligands and their catalytic activity for cyclic carbonate synthesis.¹²² Figure 1.12, shows the two different structures of the complexes studied for cyclic carbonate synthesis catalysis.

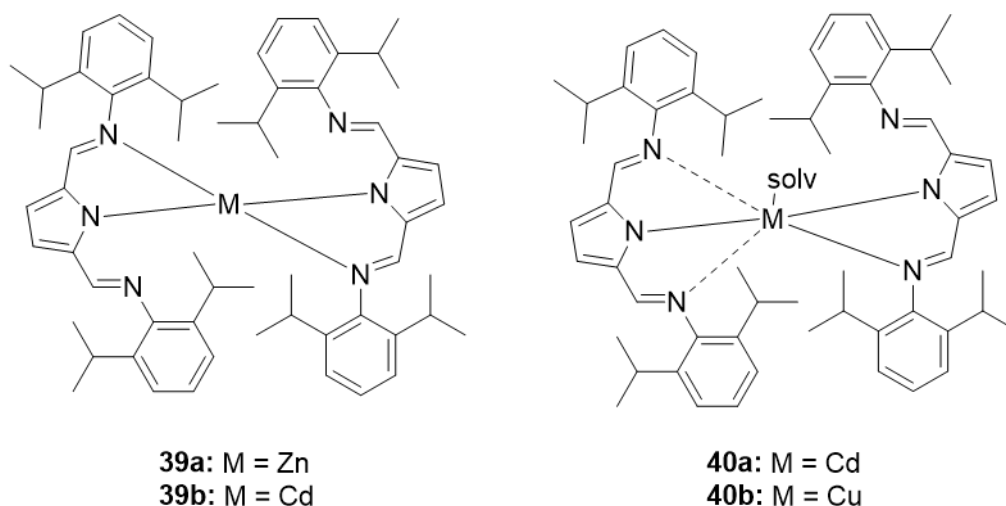
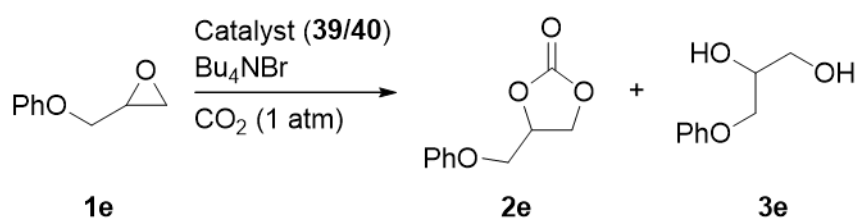


Figure 1.12.- 2,5-(2,6-diisopropylphenyl)iminomethyl pyrrole complexes of Zn(II), Cd(II) and Cu(II).¹²²

Carboxylation reactions were carried out under solvent free conditions, mild temperatures (from 30 °C to 105 °C and CO₂ atmospheric pressure), and N-tetrabutylammonium bromide as co-catalyst.



Scheme 1.10.- Synthesis of 1,2-phenoxyethyl oxirane (2e) with catalyst 39 under mild reaction conditions.¹²²

Synthesis of 2e was carried out in presence of catalysts 39a,b and 40a,b. Table 1.6 shows the results of a selection of reactions. When 39a was used, best performance occurred under reaction conditions on entry 4 of Table 1.6. Background reactions with no catalyst showed considerably high conversions to cyclic carbonate (45%) at 105 °C after 4 hours of reaction (entry 1, Table 1.6). Among all four catalysts, the Cu(II) metal complex, 40b, showed to be a better catalyst for the

synthesis of 2e, converting 96% of the epoxide and did not produce the diol 3e as a subproduct of the reaction (entry 9, Table 1.6).

Table 1.6.- Screening studies for the synthesis of 2e with catalysts 39a and 40b.¹²²

Entry	Catalyst (mol%)	TBABr (mol%)	T (°C)	time (h)	Conv (%)	
					2e	3e
1	-	5.0	105	4	45	-
2	39a (2.5)	1.0	30	24	31	-
3	39a (2.5)	2.5	60	10	72	8
4	39a (2.5)	5.0	60	10	84	8
5	39a (2.5)	5.0	60	20	60	35
6	39a (2.5)	5.0	105	2	59	34
7	39b (2.5)	5.0	60	10	51	14
8	40a (2.5)	5.0	60	10	48	10
9	40b (2.5)	5.0	60	20	96	-

^aReaction condition: CO₂ (1 atm, balloon) and solvent free conditions.

A ¹H NMR study of the reaction of 2-phenyloxirane in the presence of TBABr and Zn(II) complex catalyst under 1 atmospheric pressure of CO₂ at 105 °C after 5 min, 1, 2, 5 and 10 h as independent experiments led to conclusion that diol was forming after cyclic carbonate degradation. Figure 1.13 shows how diol signals (at 3.7 ppm) start appearing with presence of the cyclic carbonate (signals at 4.3, 4.8 and 5.7 ppm) after 1 hour of reaction and keeps forming after all epoxide has reacted (signals at 2.8, 3.2 and 3.8 ppm) after 2 hours. All carbonate transformed to diol after 10 hours of reaction.

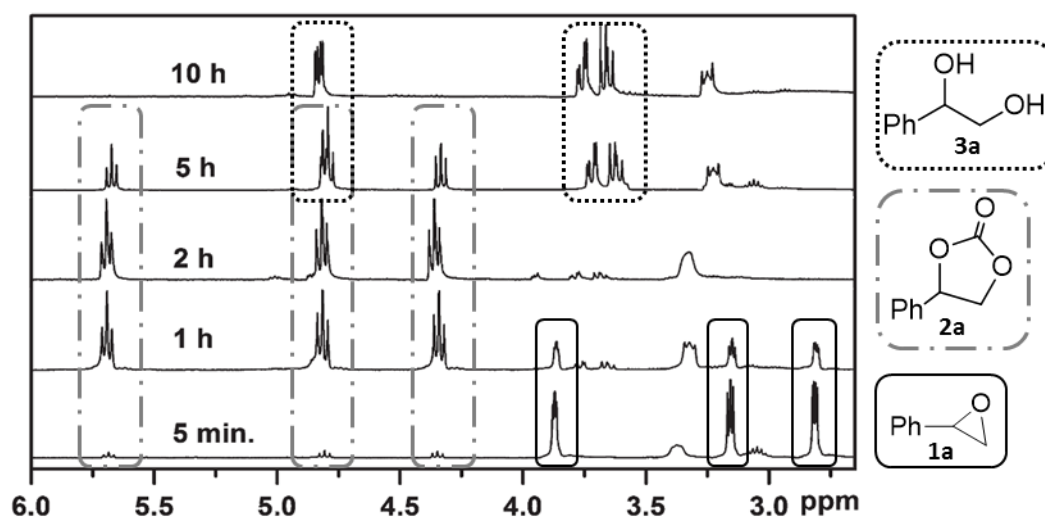


Figure 1.13.- Progress of diol formation monitored by ¹H NMR (modified image).¹²²

glycerol in DMF showed that best performance was achieved when 10 mmol of K₂CO₃ and 3 mmol of Se were used (entry 3). When other bases were tested (entries 9 to 12) there was production of carbonate only in the case of NaH (entry 9) giving 40% of conversion. When THF was used as solvent the reaction did not evolve (entry 13).

Table 1.7.- Influence of various conditions on synthesis of 2j.¹²⁴

Entry	Base (mmol)	Se (mmol)	Solvent	Isolated Yield (%) ^a
1	K ₂ CO ₃ , 10	10	DMF	22
2	K ₂ CO ₃ , 10	5	DMF	55
3	K ₂ CO ₃ , 10	3	DMF	84
4	K ₂ CO ₃ , 10	2	DMF	83
5	K ₂ CO ₃ , 10	1	DMF	61
6	K ₂ CO ₃ , 20	10	DMF	43
7	K ₂ CO ₃ , 20	20	DMF	45 ^b
8	K ₂ CO ₃ , 50	20	DMF	58 ^b
9	NaH, 10	3	DMF	40
10	Triethylamine, 10	3	DMF	NR
11	1-Methylpyrrolidine, 10	3	DMF	NR
12	DBU, 10	3	DMF	— ^c
13	K ₂ CO ₃ , 10	3	THF	NR

^a Yields based on selenium. Glycerol 10 mmol. ^b Yields based on glycerol. ^c Tar was formed.

1.5.4 Electrochemical CO₂ reduction

1.5.4.1 Reduction in Aqueous solution

The most common carbon dioxide reduction reactions are as follows (The values are estimated from thermodynamic data at pH 7 in aqueous solution versus normal hydrogen electrode (NHE), at 25 °C, 1 atmosphere pressure for the gases, and 1 M for the other solutes).^{91,93}



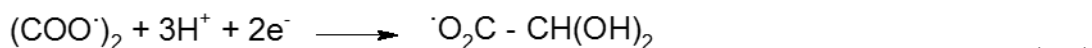
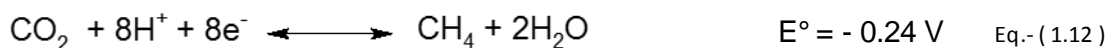
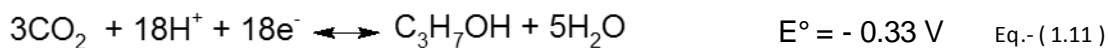
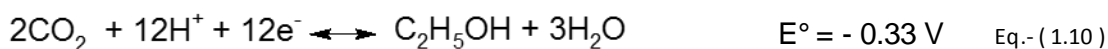
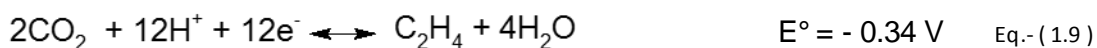
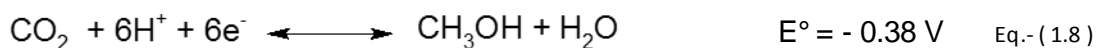
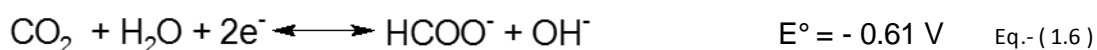
The main reduction products are formic acid, methanol, hydrocarbons and oxalic acid.⁹³ Photosynthesis (biological and artificial), photocatalytic and electrochemical reduction seem to be three of the most effective methods for carbon dioxide insertion reactions.

The potential for the reduction of CO₂ to CO₂⁻ is -1.9 V vs. NHE, and typical reduction potentials required at either Pt or Hg working electrodes are -2.0 V to -2.5 V, depending on the solvents and electrolytes used.⁹³

The products obtained of the electrochemical CO₂ reduction depend mainly on three factors: the electrocatalytic activity of the cathodic metal, the composition of the supporting electrolyte (aqueous or nonaqueous solutions), and the experimental reaction parameters (cathode potential, current density, temperature and pressure).⁹³

1.5.4.2 Thermodynamic considerations

Despite the fact that chemical reactivity of CO₂ is low, the equilibrium potentials of CO₂ reduction are not very negative as compared with that of the hydrogen evolution reaction (HER) in aqueous electrolyte solutions. Equation 1.4 shows the electrochemical reduction potentials of CO₂ to HCOO⁻ in aqueous solution at pH 7.0 at 25 °C with respect to the standard hydrogen electrode (SHE). The standard electrode potential of HER at pH 7.0 is -0.414 V vs. SHE at 25 °C.⁹¹



The CO₂ reduction in aqueous solution involves H₂O and OH⁻, and the equilibrium potential varies in accordance with the pH of the electrolyte. As an example of formation of HCOOH from CO₂ at 25 °C, Figure 1.15 represents the equilibrium potential vs. pH relations (Pourbaix diagram) constructed on the basis of thermodynamic data. Thermodynamically stable regions of related species of CO₂ and HCOOH are shown with respect to pH and potential. The equilibrium potential of CO₂ reduction is in the same range as HER in aqueous media, or, in other words, hydrogen formation competes with the electrochemical reduction of CO₂.

However, CO₂ reduction does not take place easily, and the actual electrolysis potentials for CO₂ reduction are much more negative in most cases than the equilibrium ones. The reason is that the intermediate species CO₂^{-•}, formed by an electron transfer to a CO₂ molecule, proceeds as the first step at highly negative potential, such as -2.21 V (vs. saturated calomel electrode (SCE) measured in dimethyl formamide (DMF)). As is shown in Figure 1.15, HER prevails over CO₂ reduction in acidic solutions.

The mechanism for the electrochemical reduction of CO₂ in NaHCO₃ aqueous solution with copper electrode was investigated.¹²⁵ Based on the experimental results from the literature reports, the pathways by which methane, ethylene and formic acid on Cu electrode are formed in aqueous solution can be estimated as shown in Figure 1.16.⁹³ However, the large number of mechanisms proposed for the electroreduction of carbon dioxide indicates that this topic is not understood completely.⁹³

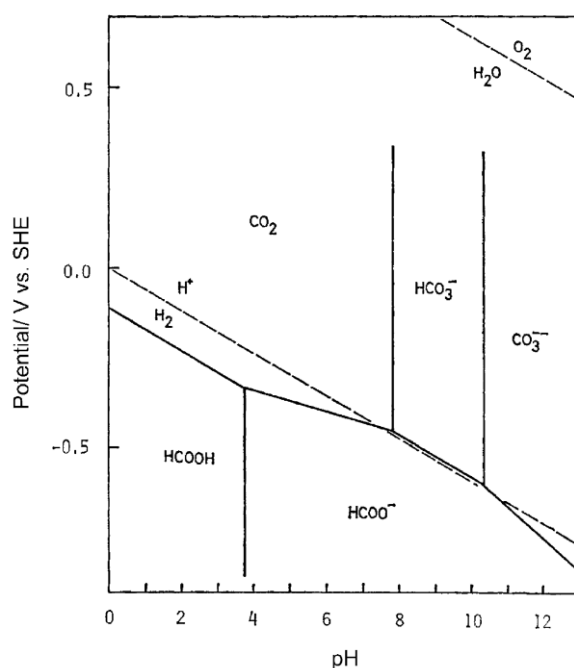


Figure 1.15.- pH potential diagram of CO₂ and its related substances. pH potential relations for water are shown in broken lines.¹²⁶

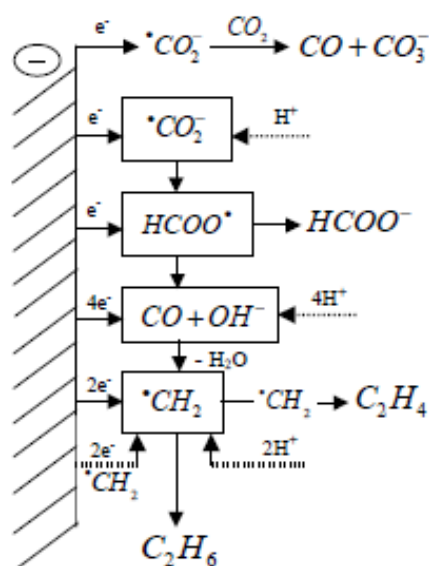


Figure 1.16.- Pathways for ethane, ethylene and formate formation on Cu electrode.⁹³

1.5.4.3 Electroreduction in non-aqueous medium

Organic solvents tend to dissolve CO₂ reasonably well as its solubility is usually higher than in water (Table 1.8). For example, solubility of CO₂ in acetonitrile at 25 °C is eight times compared to that in water at ambient temperature.^{93,127,128}

Table 1.8.- Solubility of carbon dioxide in some solvents at 25 °C.^{127,128}

Substance	Solvent density (g L ⁻¹)	Solubility (mg g ⁻¹)	Solubility (g L ⁻¹)
Glycerol	1250	13.8	17.2
Glycerol carbonate	1400	7.9	11.0
Tetraglyme	1011	4.8	4.9
PEGDME 150	1089	6.4	6.9
PEG 200	1124	13.4	15.1
PEG 300	1124	13.5	15.1
PEG 600	1124	7.7	8.7
Poly(ethylenimine)	1030	>3.0	>3.1
Methanol	788	7.7	6.1
Acetonitrile ¹²⁸	780	15.1	11.9
Water	997	1.5	1.5

In addition, several metals that have been previously found inactive in aqueous CO₂ electroreductions (like Pt, Mo, Ru, Os)^{94,128} have shown some electrocatalytic activity in non aqueous media.⁹³ Main carbon dioxide electroreduction products in organic solvents were found to be carbon monoxide, oxalic acid and formic acid.⁹⁴

In aprotic solvents, where there are no protons available to be involved in CO₂ reduction, the primary products are CO and oxalate, and all reductions must proceed through the CO₂ radical anion, •CO₂⁻.^{86,129} The relevant reactions in aprotic media are summarized below:



1.5.4.4 Electrochemical cell coupled to analytical instruments for in-line detection of species.

As it has just been exposed, exists in the literature a wide collection of publications supporting the different electrochemically produced species from CO₂ reduction detailed above in different media and conditions. The analytical techniques utilised for the detection of these

products are of different nature (IR¹³⁰, GC/LC¹³¹, GCMS¹³², MS¹³³) or combinations of them^{134,135}.

Mass spectrometry used as an online detector coupled to an electrochemical cell has been widely used before and for the first time by Wolter and Heitbaum in 1984.¹³⁶ The technique has been called "Differential Electrochemical Mass Spectrometry".¹³⁵⁻¹⁵⁰

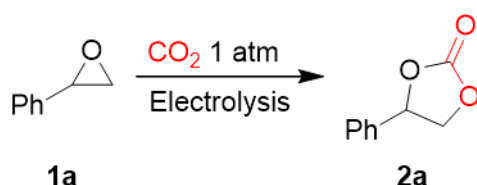
One of the studies on CO₂ electroreduction carried out by Mul, Baltrusaitis *et al.* confirmed that CO₂ electroreduction produced volatile compounds such as CO, ethylene, methane, ethane in aqueous media.¹⁴¹

In the present project, a GCMS detector has been built on-line to an electrochemical cell in order to analyse the species produced in the reduction of CO₂ (see section 2.5). Another analytical technique on its initial development state called Differential Mobility Spectrometer (DMS) has been tested for the detection of species of CO₂ reduction in acetonitrile (see section 2.4).

1.5.5 Electrosynthesis of cyclic carbonates

1.5.5.1 Electrocarboxylation of epoxides

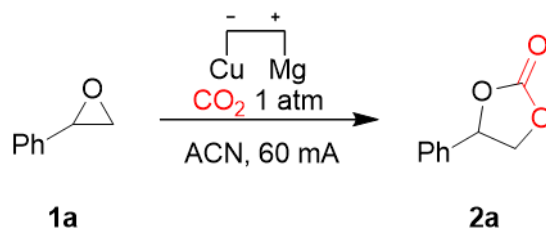
Electrocatalytic carboxylation methods are able to efficiently transform epoxides to cyclic carbonates generally in few hours, at temperatures below 100 °C and at atmospheric pressure. Buckley & Wijayantha studied the effect of different electrodes and electrolytes in the electrocarboxylation of epoxides in acetonitrile.¹ When different pair of electrodes were tested (Table 1.9), Cu and Mg pair performed extremely well (entry 1), followed by Graphite-Mg (entry 3) and Steel-Mg (entry 2) or Cu-Al (entry 4). Cu-Sn (entry 5) and Cu-Zn pair (entry 6) had the lowest catalytic activity converting only 10 and 5% of epoxide 1a to carbonate 2a.

Table 1.9.- Electrode screening ^a

Entry	Cathode	Anode	Conv. (%) ^b
1	Cu	Mg	>99
2	Steel	Mg	75
3	Graphite	Mg	80
4	Cu	Al	75
5	Cu	Sn	10
6	Cu	Zn	5

^a General conditions: CO₂ (1 atm, balloon), Bu₄NBr (2.0 eq.), MeCN, single compartment cell, 60 mA, 7 h rt, 12 h 50 °C. ^b Conversion evaluated from the ¹H NMR spectrum by integration of epoxide vs. cyclic carbonate peaks.

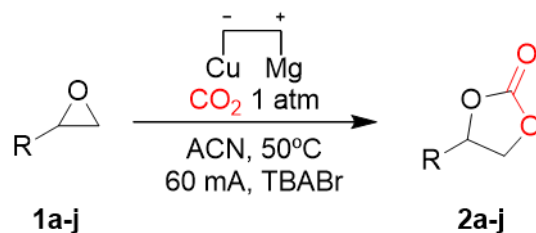
Table 1.10 collects the optimization studies regarding electrolyte (Bu₄NBr or Bu₄NPF₆) (entries 4 and 5), epoxide to electrolyte ratio (0.5 equivalents to 2.0 equivalents in entries 1 to 3), temperature (rt, 25 or 50 °C in entries 2, 4 and 5), and reaction time (entries 2, 6 and 8).

Table 1.10.- Optimization studies.^a

Entry	Supporting electrolyte		t (h)	Conv. (%) ^b
	(equiv.)	T (°C)		
1	Bu ₄ NBr (2.0)	7 h, rt, 12 h 50 °C	19	>99
2	Bu ₄ NBr (1.0)	7 h, rt, 12 h 50 °C	19	98
3	Bu ₄ NBr (0.5)	7 h, rt, 12 h 50 °C	19	80
4	Bu ₄ NBr (1.0)	25 °C	6	77
5	Bu ₄ NPF ₆ (1.0)	50 °C	6	17
6	Bu ₄ NBr (1.0) ^c	50 °C	6	99
7	Bu ₄ NBr (1.0)	25 °C	6	77
8	Bu ₄ NBr (1.0)	50 °C	3.5	76

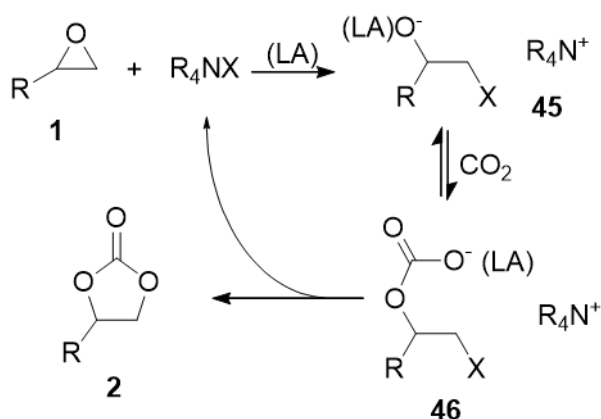
^a General conditions: Cu cathode, Mg anode, CO₂ (1 atm, balloon), MeCN, single compartment cell, 60 mA. ^b Conversion evaluated from the ¹H NMR spectrum by integration of epoxide vs. cyclic carbonate peaks. ^c On average 90-95% of the Bu₄NBr is recovered after each reaction by precipitation with EtOAc.

The method optimization resulted in the conditions outlined below in Scheme 1.12, corresponding to the reaction on entry 6 of the previous table:



Scheme 1.12.- Electrocarboxylation of styrene oxide at mild conditions in a acetonitrile solution. Copper cathode and magnesium anode, 60 mA of current, epoxide, carbon dioxide (1 atm) at 50 °C for 7h in acetonitrile solution and TBABr as electrolyte.

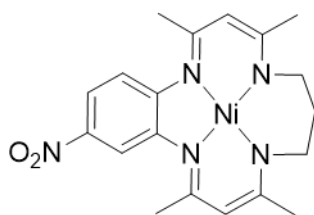
Buckley & Wijayantha proposed that mechanism of the reaction could be related to that proposed by North and co-workers in their catalytic carboxylation reaction as it follows:¹¹⁷



Scheme 1.13.- Reaction mechanism in the cyclic carbonate synthesis (LA = Lewis Acid).¹¹⁷

M. North *et al.* conclusions were founded on a wide range of experiments and tests of different epoxides, catalysts, and reaction conditions.¹¹⁷ One of the determining analysis that provided kinetic information consisted on monitoring the catalytic carboxylation of styrene oxide by FTIR in line. Reaction orders of TBAI (as cocatalyst) and styrene oxide (of reactions with bimetallic aluminium-salen complexes as catalyst) were found to be of 2nd order for ammonium salt concentration and of 1st order for styrene oxide concentration. This technique has been selected in the project that is presented in this thesis to try to elucidate the kinetic profile of the carboxylation of epichlorohydrin (discussion of results in section 2.7).

A nickel complex (Figure 1.17) was used under electrocatalytic conditions for the synthesis of cyclic carbonates from epoxides by Hossein Khoshro, Hamid R. Zare, *et al.*¹⁵¹ showing an excellent electrocatalytic activity for the reduction of carbon dioxide by cyclic voltammetry.



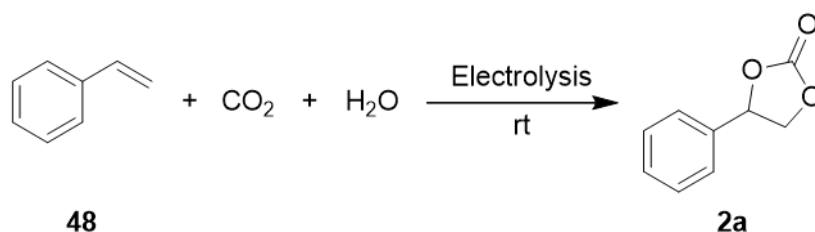
47

Figure 1.17.- 2,4,10,12-tetramethyl-1,5,9,13-(14-nitrobenzo) tetraazacyclopentadecinato (2-)nickel(II) complex.¹⁵¹

The electrolysis was carried out in a three-electrode electrochemical cell (containing a glassy carbon working electrode, a Pt counter electrode wire and an Ag/Ag⁺ reference electrode (0.01 M AgNO₃ in 0.1 M TBAP acetonitrile solution)) in 50 mL of ACN solution of 0.1 mol/L TBAP, 3.0 mmol of 1,2-propylene oxide (1e), and 0.3 mmol of the Ni(II) complex catalyst (47). The interaction of 1e and CO₂ in ACN and TBAP at room temperature in the absence of Ni complex did not show redox peaks in the scan region of -0.7 to -2.0 V. When catalyst 47 was added to the solution the voltammogram showed a marked increase in the cathodic current and a decreased in the anodic current. The results showed the epoxide conversion was about 100% after passing 2.0 F/mol of the starting substrates through the cell at room temperature.

1.5.5.2 Electrocarboxylation of olefins

Cyclic carbonates can also be synthesized through electrochemistry from olefins. Xiaofang Gao, Gaoqing Yuan and co-workers achieved high rates of conversion of olefins to cyclic carbonates (95%) using an electrochemical cell that consisted on graphite anode and Ni sheet cathode at 80 mA with NH₄I as supporting electrolyte in DMSO (10 mL) / H₂O (1 g) containing olefin (3 mmol) in a stainless steel undivided cell with Teflon packing. CO₂ was flushed at 4.9 atm pressure and at room temperature during 3 hours.¹⁵²

Scheme 1.14.- Synthesis of cyclic carbonates from olefins and CO₂ through electrochemistry.¹⁵²

Other reaction conditions also produced the desired cyclic carbonate in lower yields as detailed in Table 1.11. Solvent screening study (entries 1 to 7) showed DMSO to be the preferred solvent with 78% of conversion to carbonate (entry 2). A study on the anion of the

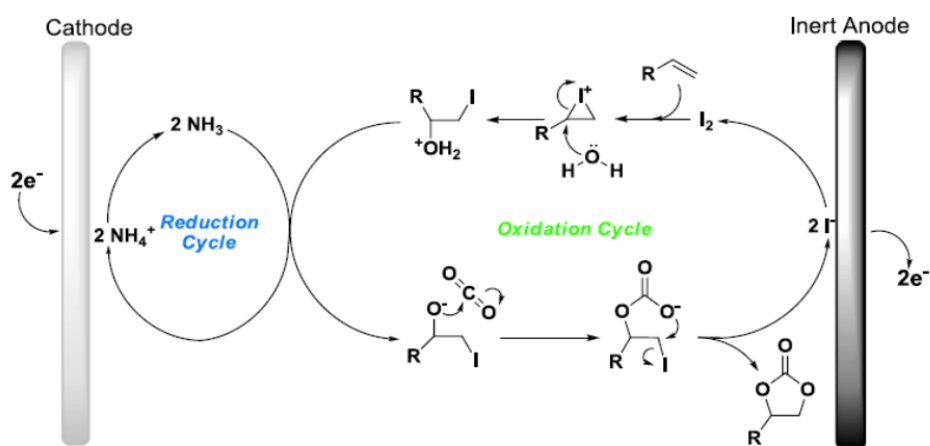
ammonium salt (entries 2, and 8 to 16) showed that when used Iodide (TBAI in entry 8 or NH₄I in entry 13) results improved to about 95% of conversion. Electrode screening (entries 13, and 17 to 21) confirmed C-Ni as the most catalytic pair of electrodes for the conversion of styrene to styrene carbonate.

Table 1.11.- Optimization of reaction conditions.^a

Entry	Anode-cathode	Electrolyte	Yield (%) ^b
1	C-Ni	<i>n</i> -Bu ₄ NBr/DMF	8
2	C-Ni	<i>n</i> -Bu ₄ NBr/DMSO	78
3	C-Ni	<i>n</i> -Bu ₄ NBr/MeCN	63
4	C-Ni	<i>n</i> -Bu ₄ NBr/CH ₂ Cl ₂	6
5	C-Ni	<i>n</i> -Bu ₄ NBr/dioxane	28
6	C-Ni	<i>n</i> -Bu ₄ NBr/acetone	19
7	C-Ni	<i>n</i> -Bu ₄ NBr/THF	23
8	C-Ni	<i>n</i> -Bu ₄ NI/DMSO	94 (88)
9	C-Ni	<i>n</i> -Bu ₄ NCl/DMSO	40
10	C-Ni	<i>n</i> -Bu ₄ NBF ₄ /DMSO	0
11	C-Ni	NH ₄ Cl/DMSO	Trace
12	C-Ni	NH ₄ Br/DMSO	68
13	C-Ni	NH ₄ I/DMSO	95 (90)
14	C-Ni	NaI/DMSO	0
15	C-Ni	NaBr/DMSO	0
16	C-Ni	NaCl/DMSO	0
17	Al-Ni	NH ₄ I/DMSO	0
18	Zn-Ni	NH ₄ I/DMSO	0
19	C-Cu	NH ₄ I/DMSO	85
20	C-Al	NH ₄ I/DMSO	88
21	C-Zn	NH ₄ I/DMSO	91

^a Reaction conditions: styrene (3 mmol), H₂O (1 g), solvent (10 mL), supporting electrolyte (1.0 mol/L), CO₂ (4.9 atm), undivided cell, current density 16 mA/cm², 3h, electricity 3 F/mol, rt. ^b Yields were determined by ¹H NMR integration. Number in parentheses is the isolated yield.

The reaction mechanism proposed is shown in Scheme 1.15.

X. Gao et al. / *Electrochemistry Communications* 34 (2013) 242–245

Scheme 1.15.- Reaction mechanism of electrosynthesis of cyclic carbonates from olefins with NH₄I as supporting electrolyte.

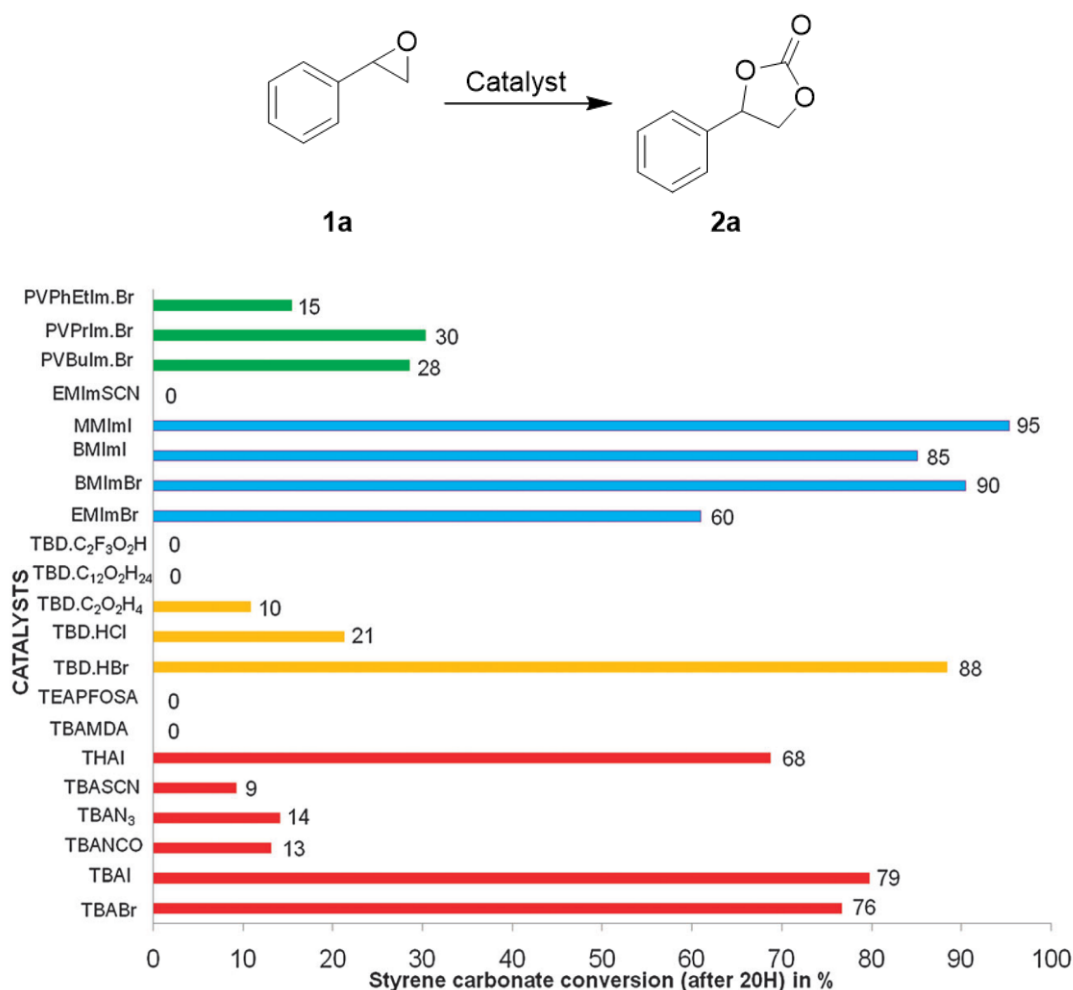
1.5.5.3 Study of the electrocatalytic activity of ammonium salts in the carbon dioxide electroreduction.

In a paper published in 2014 by Timothy C. Berto *et al.* the electrocatalytic activity of tetraalkylammonium ions on CO₂ electroreduction was investigated under cyclic voltammetry technique.¹⁵³ Scan rate dependence showed that the process is diffusion-controlled and largely independent of working electrode material. Different R groups on NR₄⁺ showed little effect on the reduction potential, meaning that catalysis through NR₄[•] species is not a viable mechanism for electroreduction of CO₂. Instead, reduction of CO₂ occurs via outer-sphere electron transfer according to the mechanism put forth by Savéant and co-workers.¹⁵⁴ The full analysis of the reaction products which consisted exclusively of CO and CO₃²⁻, and solvent decomposition products at the counter electrode, supported this view. They also observed no degradation of NR₄⁺ ions which suggests that there is no formation of NR₄[•] radical species during electroreduction.

1.5.5.4 Ionic liquids as solvent and catalyst for carboxylation of epoxides

Recent studies of the carboxylation of styrene oxide reaction in ionic liquids look promising. Stephanie Foltran & colleagues compared the catalytic activity of several ionic salts like tetraalkylammonium salts (TBABr, TBAI...), Imidazolium salts (EMImBr, BMImBr...) and guanidinium salts (TBDHBr...) among others in a closed system with supercritical carbon dioxide at T = 80 °C and P = 8 MPa. Although TBABr and TBAI show good results on the

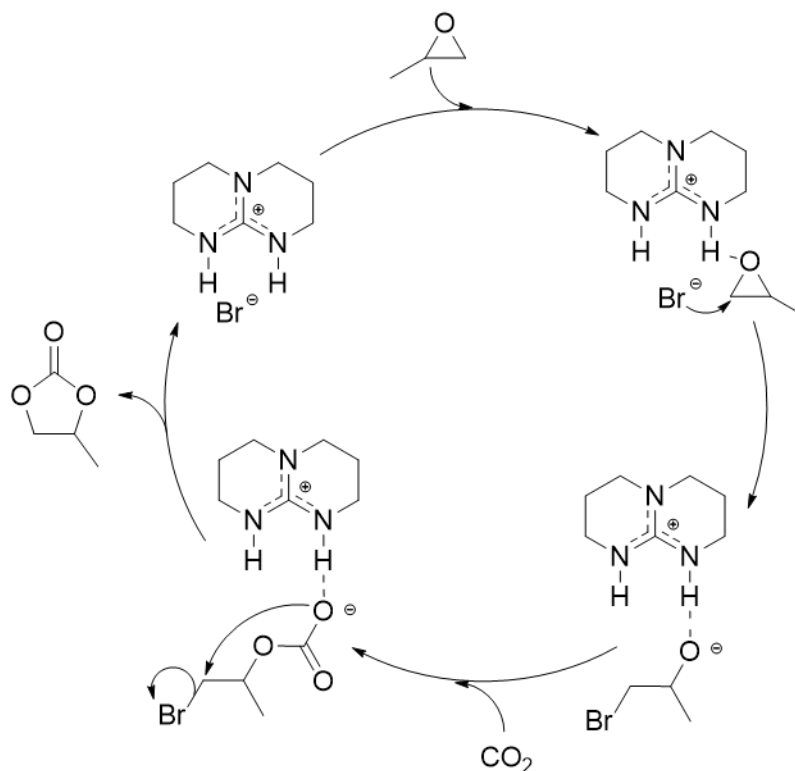
conversion of styrene oxide to styrene carbonate (76 and 79%, Figure 1.18), ionic liquids such as MImI, BMImI and BMImBr yield higher conversion after 20 h of reaction (95, 85 and 90%, Figure 1.18).¹⁵⁵



PVPhEtIm.Br = polyvinyl phenyl ethyl imidazolium bromide; PVPrIm.Br = polyvinyl propyl imidazolium bromide; PVBulm.Br = polyvinyl butyl imidazolium bromide; EMImSCN = ethyl methyl imidazolium thiocyanate; MImI = methyl methyl imidazolium iodide; BMImI = butyl methyl imidazolium iodide; BMImBr = butyl methyl imidazolium bromide; EMImBr = ethyl methyl imidazolium bromide; TBD.C₂F₃O₂H = (1,5,7-triaza-bicyclo[4.4.0]dec-5-enium.1,1,1-trifluoro-2-hydroperoxyethane); TBD.C₁₂O₂H₂₄ = (1,5,7-triaza-bicyclo[4.4.0]dec-5-enium.dodecanoic acid); TBD.C₂O₂H₄ = (1,5,7-triaza-bicyclo[4.4.0]dec-5-enium.acetic acid); TBD.HCl = (1,5,7-triaza-bicyclo[4.4.0]dec-5-enium.hydrochloric acid); TBD.HBr = (1,5,7-triaza-bicyclo[4.4.0]dec-5-enium.hydrobromic acid); TEAPFOSA = tetraethylammonium heptadecafluorooctane sulphonate; TBAMDA = malondialdehyde tetrabutylammonium salt; THAI = tetrahexylammonium iodide; TBASCN = tetrabutylammonium thiocyanate; TBAN₃ = tetrabutylammonium azide; TBANCO = tetrabutylammonium cyanate; TBAI = tetrabutylammonium iodide; TBABr = tetrabutylammonium bromide.

Figure 1.18.- Styrene carbonate conversion at T = 80 °C and P = 8 MPa with styrene oxide (1a) and 1 mol% of catalyst after 20 h of reaction.¹⁵⁵

The proposed mechanism was as follows:



Scheme 1.16.- Proposed mechanism of the cycloaddition of propylene oxide with CO₂ by TBD·HBr.¹⁵⁵

1.6 INTRODUCTION TO THE INVESTIGATION

In order to understand the electrochemical synthesis of carbonates previously carried out and reported in 2011 by A. P. Patel, B. Buckley and W. Wijayantha¹ (section 1.5.5.1), the cyclic voltammetry technique was chosen to help explain the catalytic activity of the components of the reaction system. A common analytical technique used in-line with electrochemical cells found in the literature (and presented in the introduction in section 1.5.4.4) is the gas chromatography mass spectrometry.¹³² In the present project, a GCMS detector has been built on-line to an electrochemical cell in order to analyse the species produced in the reduction of CO₂.

Another analytical technique on its initial development state called Differential Mobility Spectrometer (DMS) has been tested for the detection of species of CO₂ reduction in acetonitrile.

The study of the reaction variables in the present research, involved background reactions with different electrode set ups, temperatures, catalysts, concentration of species, and methodology. The result is an optimization of all variables to achieve the most efficient method for the synthesis of carbonates from a range of epoxides.

Kinetics calculations to determine the reaction order with respect to TBAI were carried out using a ReactIR to on-line monitoring the conversion of epichlorohydrine to carbonate.

CHAPTER 2

RESULTS AND DISCUSSION

2 RESULTS AND DISCUSSION

2.1 CYCLIC VOLTAMMETRY

Electrochemical reduction of carbon dioxide in acetonitrile solution has been studied by cyclic voltammetry technique. Different electrodes have been tested and compared to identify the best performance system conditions. As previously discussed, electrode material is crucial in the mechanism of carbon dioxide reduction and the product of the reaction depends on the electrocatalytic activity of the cathodic metal and on other factors like the composition of the supporting electrolyte (aqueous or nonaqueous solutions), and the experimental reaction parameters (cathode potential, current density, temperature and pressure).

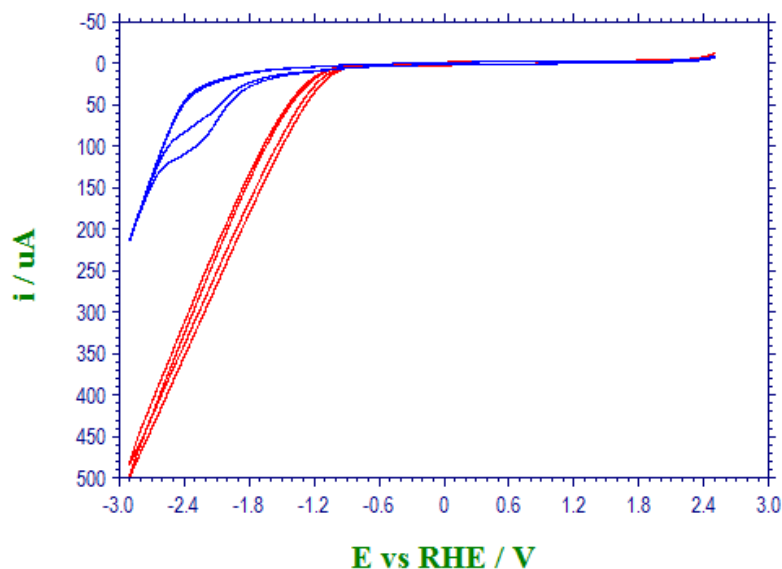
Platinum, Glassy-carbon, gold and copper electrodes were tested for carbon dioxide electrochemical reduction in acetonitrile with Bu_4NPF_6 or Bu_4NBr as electrolyte. See more details of the experimental procedure on section 4.1.2.

2.1.1 Electrode screening

Different working electrodes have been tested versus platinum wire counter electrode, Reversible Hydrogen Electrode (RHE) as reference electrode in an acetonitrile solution of tetrabutylammonium hexafluorophosphate as electrolyte (1%).

2.1.1.1 Platinum disk working electrode.

Platinum disk working electrode was tested for carbon dioxide reduction in acetonitrile in the presence of Bu_4NPF_6 electrolyte vs. RHE and Platinum wire as counter electrode. Graph 2.1 shows the overlapped spectra for the blank and the CO_2 saturated solution measures.

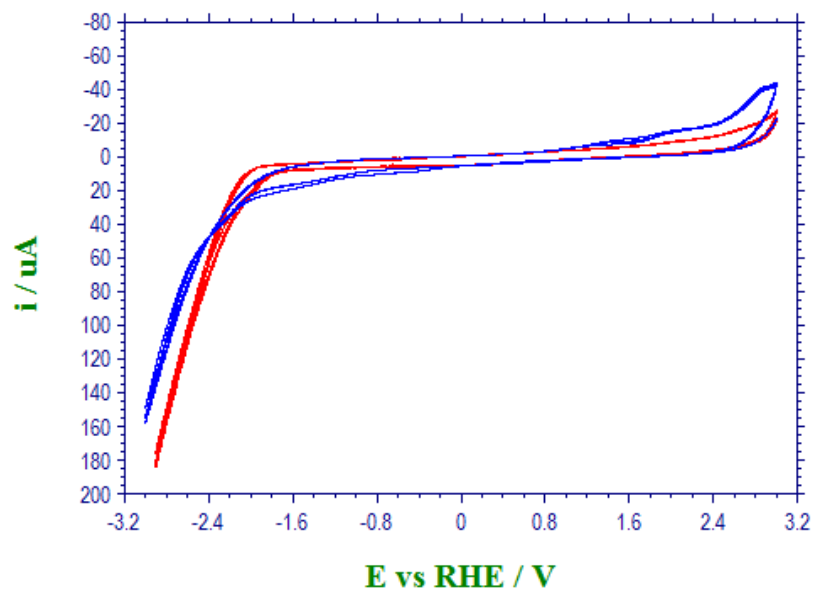


Graph 2.1.-Cyclic voltammogram of Pt disk working electrode in 0.1% w/v Bu₄NPF₆ acetonitrile solution, Pt wire as counter electrode, RHE, under N₂ atmosphere (red line) and in CO₂ saturated solution (blue line).

It is clearly shown on the cyclic voltammogram that platinum electrode in CO₂ saturated acetonitrile solution (blue line) is catalyzing a reaction as a later peak appears in comparison with the blank (N₂ atmosphere, red line). In the blank decomposition of the solvent starts at -0.6V while in carbon dioxide saturated solution decomposition takes place at a higher reduction potential and a new peak appears at -1.4V.

2.1.1.2 Glassy-Carbon disk working electrode.

Glassy-Carbon disk working electrode was tested for carbon dioxide reduction in acetonitrile in the presence of Bu₄NPF₆ electrolyte vs. RHE and Platinum wire as counter electrode. Graph 2.2 shows the overlapped spectra for the blank and the CO₂ saturated solution measures.

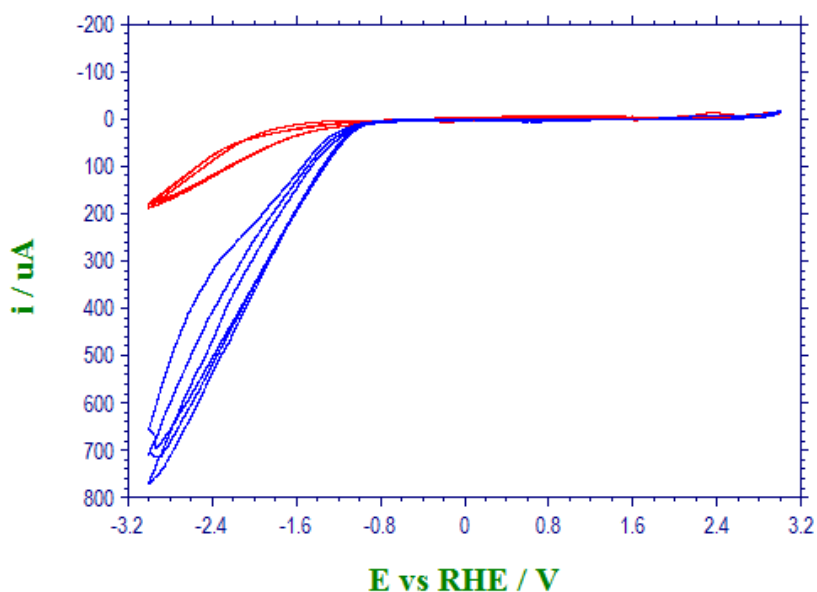


Graph 2.2.- Cyclic voltammogram of GC disk working electrode in 0.1% w/v Bu_4NPF_6 acetonitrile solution, Pt wire as counter electrode, RHE, under N_2 atmosphere (red line) and in CO_2 saturated solution (blue line).

Differences between the blank (N_2 atmosphere, red line) and CO_2 saturated solution (blue line) can be appreciated at -0.8V, reduction potential at which a broad peak probably due to CO_2 reduction appears, and a slightly later decomposition of the solvent takes place.

2.1.1.3 Gold disk working electrode.

Performance of gold disk working electrode for carbon dioxide electroreduction in acetonitrile, in the presence of Bu_4NPF_6 electrolyte vs. RHE and Platinum wire as counter electrode is shown in Graph 2.3.

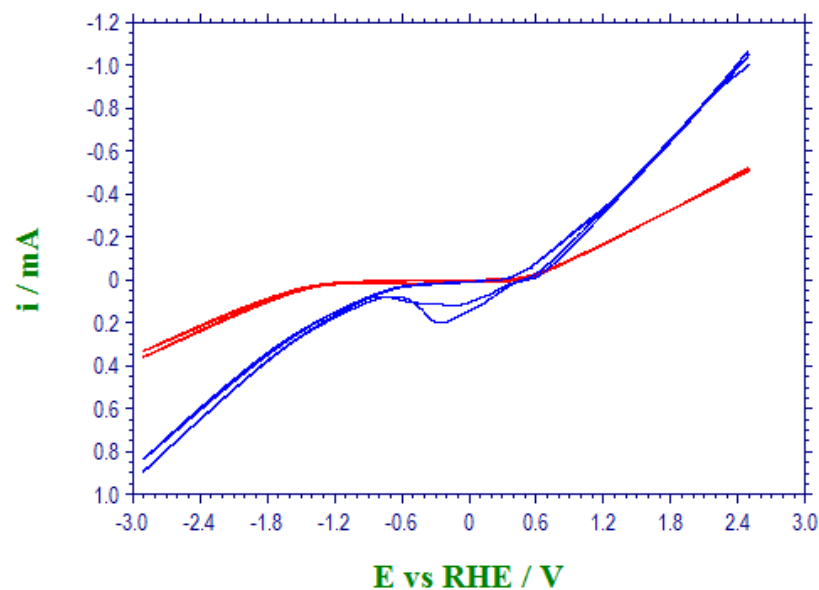


Graph 2.3.- Cyclic voltammogram of Gold disk working electrode in 0.1% w/v Bu₄NPF₆ acetonitrile solution, Pt wire as counter electrode, RHE, under N₂ atmosphere (red line) and in CO₂ saturated solution (blue line).

A high peak appears at -0.9V for CO₂ saturated solution (blue line), showing that carbon dioxide reduction is happening. It was visible that bubbles were forming on the gold electrode surface while scanning down -0.9V and that has been reported to be the formation of carbon monoxide by Hori, Y.⁹¹

2.1.1.4 Copper rod working electrode.

Copper rod working electrode was tested for carbon dioxide electroreduction in acetonitrile, in the presence of Bu₄NPF₆ electrolyte vs. RHE and Platinum wire as counter electrode. Graph 2.4 shows the overlapped spectra for the blank and the carbon dioxide saturated solution measures.

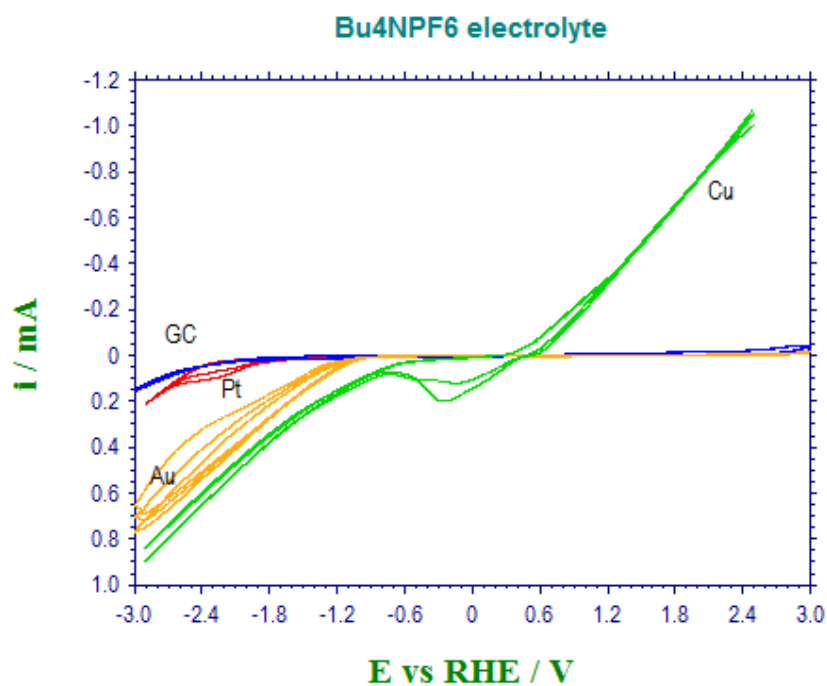


Graph 2.4.- Cyclic voltammogram of Copper rod working electrode in 0.1% w/v Bu_4NPF_6 acetonitrile solution, Pt wire as counter electrode, RHE, under N_2 atmosphere (red line) and in CO_2 saturated solution (blue line).

Copper dissolves in higher concentration when solution is saturated in CO_2 (blue line) possibly due to a slightly acidification of the solution because of the presence of water in the CO_2 stream.

2.1.1.5 Electrode behaviour comparison for CO_2 electroreduction in $\text{Bu}_4\text{NPF}_6/\text{ACN}$ electrolyte

All voltammograms of carbon dioxide saturated solution are shown together in Graph 2.5.



Graph 2.5.- Comparison of performance of Pt, GC, Au and Cu electrodes in CO_2 acetonitrile solution, Bu_4NPF_6 electrolyte, Pt wire as counter electrodes, vs. RHE.

When comparing voltammograms it can be seen that CO₂ reduction peaks appear at lower reduction potentials when gold or copper electrodes were used. This means that less energy is required in the reduction process in comparison with the GC or Pt working electrodes.

It can be concluded from this experiment that gold and copper electrodes had better performance for carbon dioxide reduction when Bu₄NPF₆ electrolyte was used.

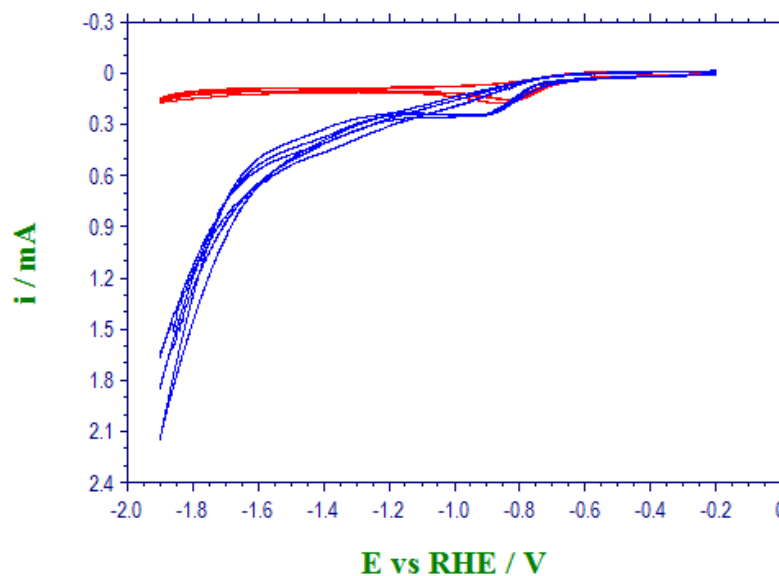
2.1.2 Magnesium counter electrode test

The electrocarboxylation reaction conditions with best results used by Anish P. Patel¹ for the cyclic carboxylation of styrene oxide involved the use of Cu and Mg as electrodes, under 60 mA of current flow and ammonium salt as catalyst. Magnesium electrode is therefore a target of study under cyclic voltammetry.

Cyclic voltammograms of copper working electrode vs Platinum wire; and copper vs magnesium ribbon in 1% Bu₄NBr solution in acetonitrile were recorded and are shown below. However, due to its sacrificial nature (magnesium irreversibly dissolves during the reaction), the cv obtained does not provide more information.

2.1.2.1 Copper rod working electrode (Platinum wire, RHE, Acetonitrile, Bu₄NBr)

Copper rod working electrode was tested for carbon dioxide electroreduction in acetonitrile, in the presence of Bu₄NBr electrolyte vs. RHE and platinum wire as counter electrode. Graph 2.6 shows the overlapped spectra for the blank and the carbon dioxide saturated solution measures. A variation on the CV happens when solution is saturated with CO₂ (blue line) showing that carbon dioxide reduction occurs at -1.2V.

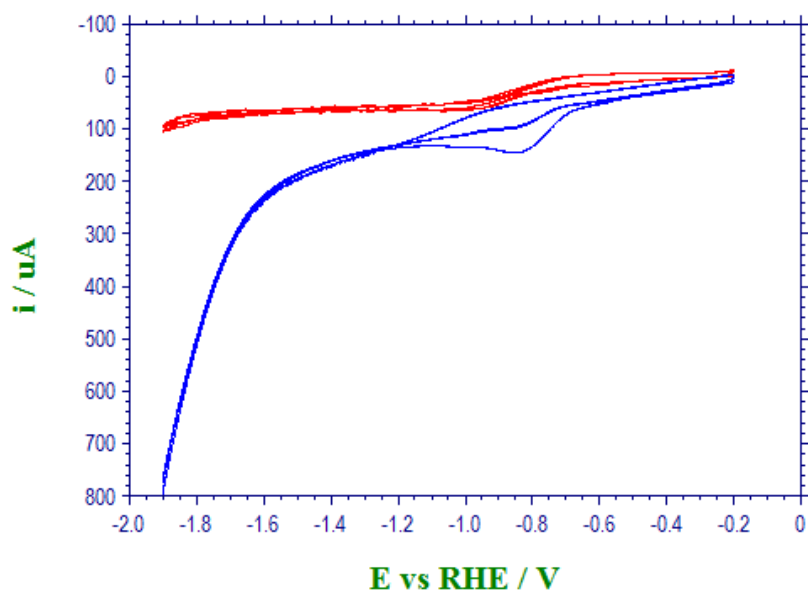


Graph 2.6.- Cyclic voltammogram of Copper rod working electrode in 0.1M Bu₄NBr acetonitrile solution, Pt wire as counter electrode, RHE, under N₂ atmosphere (red line) and in CO₂ saturated solution (blue line).

It is worth noting that the solution went to clear purple color after several scans. The change in color suggests that a Cu (I) coordination complex ($[\text{CuBr}_4][(\text{Bu}_4\text{N})_3]$) could be forming. As found in literature this complex could thermally degrade to produce $[\text{Et}_4\text{N}][\text{CuBr}_3]$ (s) + EtBr (g) + Et₃N (g).¹⁵⁶

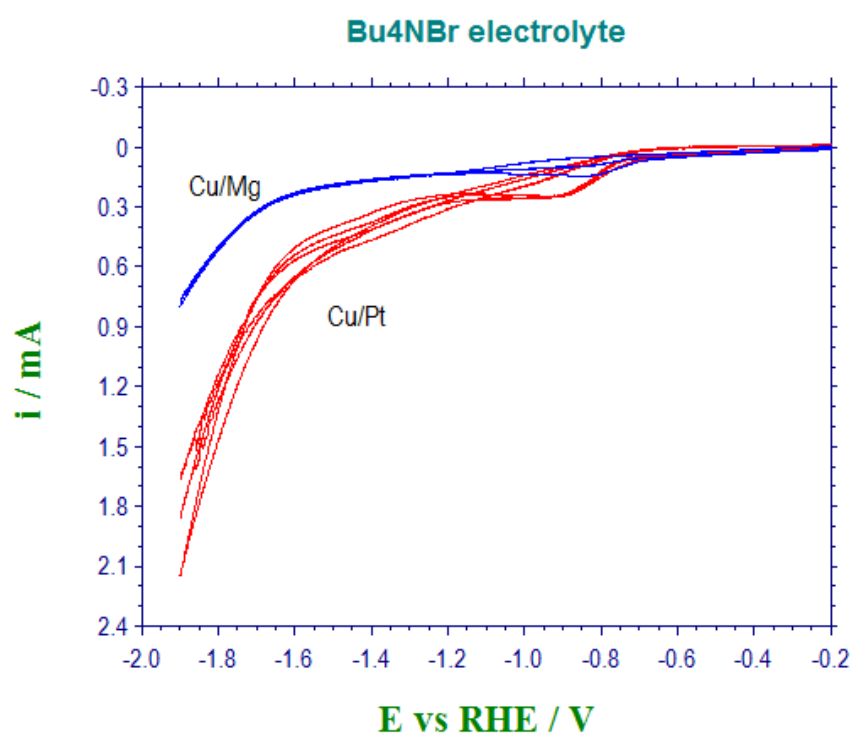
2.1.2.2 Copper rod and Magnesium ribbon.

Copper rod working electrode was tested for carbon dioxide electroreduction in acetonitrile, in the presence of Bu₄NBr electrolyte vs. RHE and Magnesium ribbon as counter electrode. Graph 2.7 shows the overlapped spectra for the blank and the carbon dioxide saturated solution measures. As in the previous experiment, it is clear that carbon dioxide reduction is taking place at -1.2V.



Graph 2.7.- Cyclic voltammogram of Copper rod working electrode in 0.1M Bu_4NBr acetonitrile solution, Mg ribbon as counter electrode, RHE, under N_2 atmosphere (red line) and in CO_2 saturated solution (blue line).

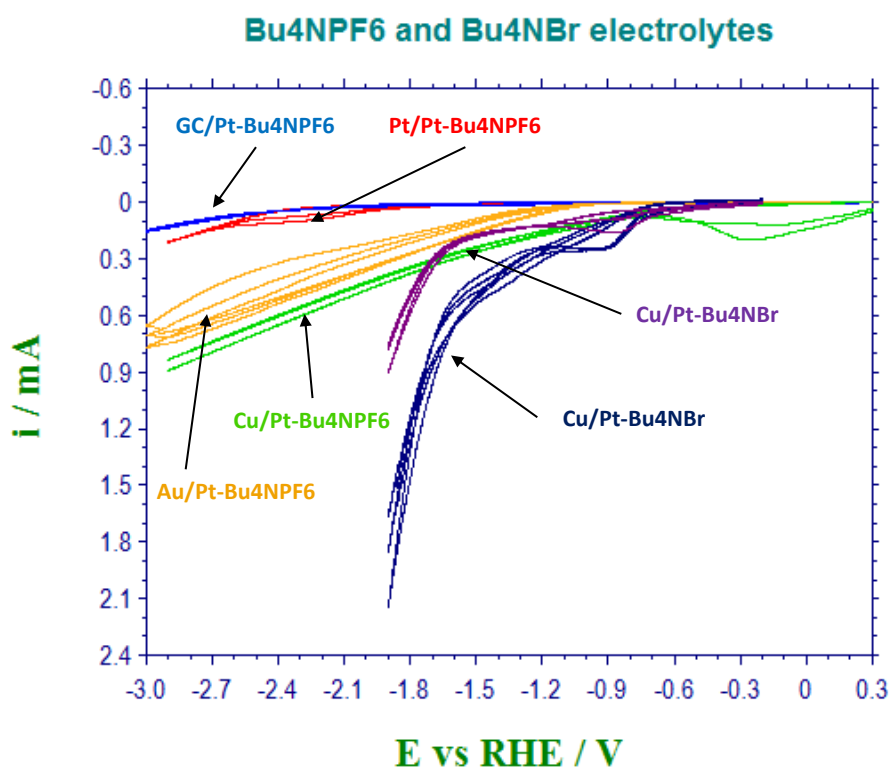
2.1.2.3 Comparison of Cu/Pt and Cu/Mg electrodes in $\text{Bu}_4\text{NBr}/\text{ACN}$ electrolyte



Graph 2.8.- Comparison of performance of Cu/Pt and Cu/Mg electrodes in CO_2 acetonitrile solution, Bu_4NPF_6 electrolyte, Pt wire as counter electrodes, vs. RHE.

When comparing both pair of electrodes, Cu/Pt is the one with higher electrocatalytic activity for carbon dioxide reduction. However, the cheaper cost of Magnesium make Cu/Mg pair of electrodes more desirable.

2.1.3 Electrode behaviour comparison for CO₂ electroreduction in Bu₄NPF₆ and Bu₄NBr electrolytes



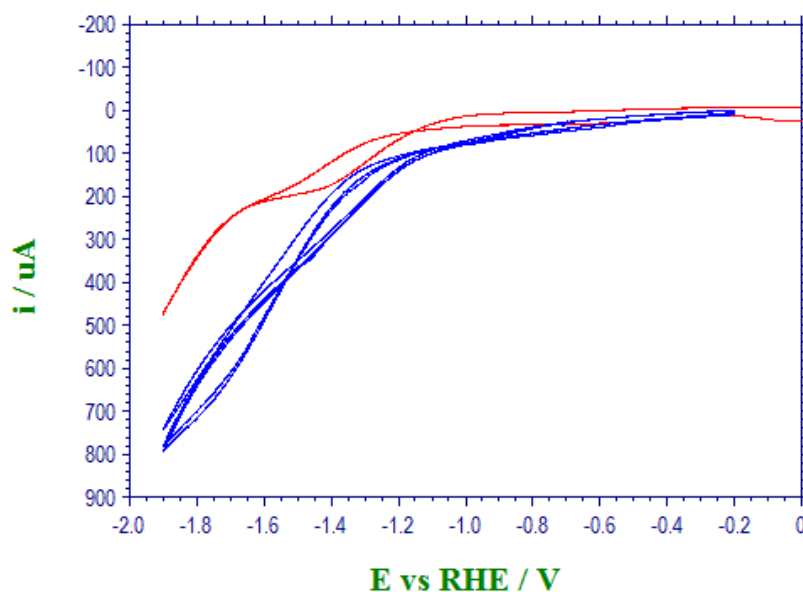
Graph 2.9.- Comparison of Pt, GC, Au and Cu electrodes in CO₂ saturated acetonitrile solution, Bu₄NPF₆ or Bu₄NBr electrolyte, Pt wire or Mg ribbon as counter electrode, vs. RHE.

An overview of the comparative Graph 2.9 tell us that when used Bu₄NBr electrolyte better carbon dioxide electroreduction response was obtained. This fact matches with the experimental method optimization results of “electrocarboxylation of styrene oxide”¹ that indicate that Bu₄NBr is a better catalyst for the reaction.

2.1.4 Epoxide study under Cyclic voltammetry

2.1.4.1 Styrene oxide analysed by CV with copper rod and platinum wire electrodes

Copper rod working electrode was tested for carbon dioxide electroreduction in acetonitrile, in the presence of styrene oxide and Bu_4NBr electrolyte vs. RHE and Platinum wire as counter electrode. Graph 2.10 shows the overlapped spectra for the blank and the carbon dioxide saturated solution measures.

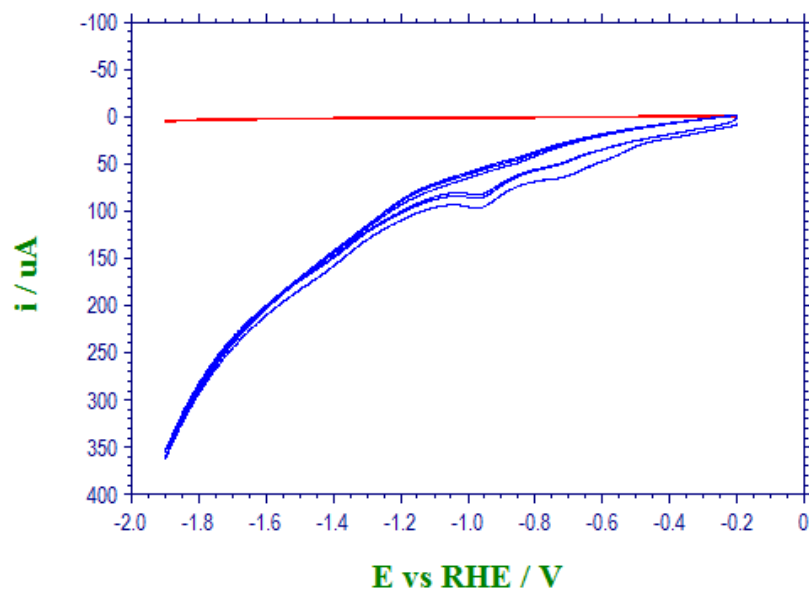


Graph 2.10.- Cyclic voltammogram of Copper rod working electrode in 0.1M Bu_4NBr acetonitrile solution, Pt wire as counter electrode, RHE, and 0.06M styrene oxide, under N_2 atmosphere (red line) and in CO_2 saturated solution (blue line).

When solution was saturated in carbon dioxide (blue line), the current dropped slightly. Possible styrene oxide- CO_2 reduction is taking place below -0.6V.

2.1.4.2 Styrene oxide analysed by CV with copper rod and magnesium ribbon electrodes

Copper rod working electrode was tested for carbon dioxide electroreduction in acetonitrile, in the presence of styrene oxide and Bu_4NBr electrolyte vs. RHE and Magnesium wire as counter electrode. Graph 2.11 shows the overlapped spectra for the blank and the carbon dioxide saturated solution measures.



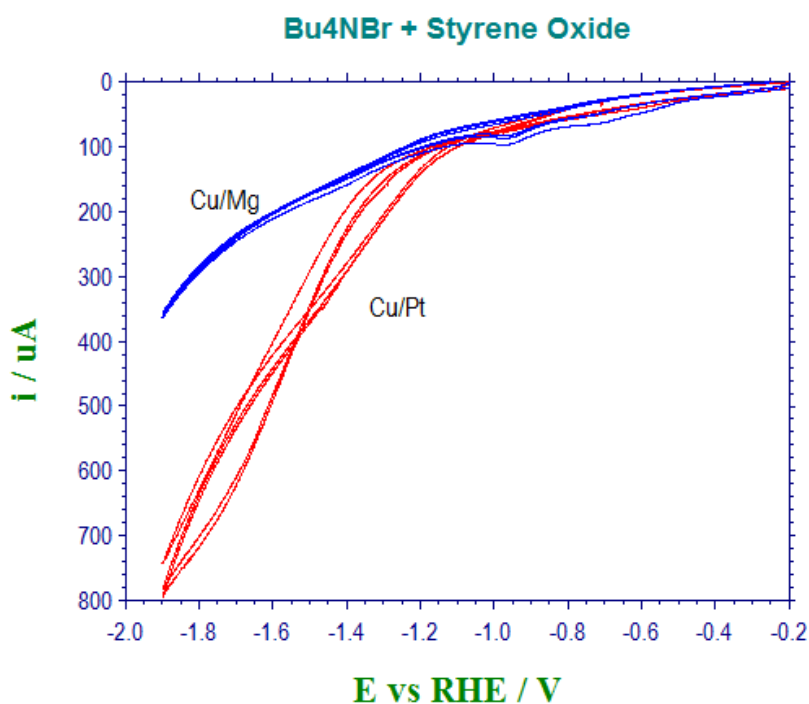
Graph 2.11.- Cyclic voltammogram of Copper rod working electrode in 0.1M Bu_4NBr acetonitrile solution, Mg ribbon as counter electrode, RHE, and 0.06M styrene oxide, under N_2 atmosphere (red line) and in CO_2 saturated solution (blue line).

When styrene oxide was added to the solution using Cu/Mg pair of electrodes, differences between blank and carbon dioxide saturated solution were noticeable. The whole curve shape changed and four peaks appeared at -0.4, -0.6, -0.8 and -1.1V.

2.1.4.3 Electrode behaviour comparison for CO_2 electroreduction in $\text{Bu}_4\text{NBr}/\text{ACN}$ + Styrene oxide.

Graph 2.12 shows together Cu/Pt and Cu/Mg pair of electrodes in carbon dioxide saturated acetonitrile solution in the presence of styrene oxide and Bu_4NBr as electrolyte vs. RHE.

Comparison between pair of electrodes show that Cu/Pt needs less energy to reduce CO_2 than Cu/Mg, but again Cu/Mg is a cheaper option.

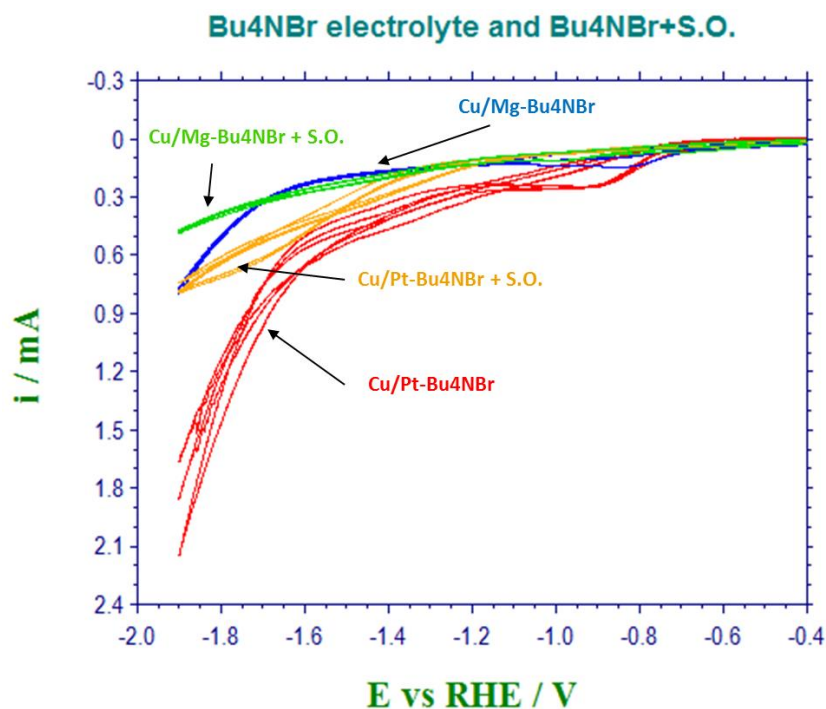


Graph 2.12.- Comparison of Cu rod electrodes in CO₂ saturated acetonitrile solution, in the presence of styrene oxide and Bu₄NBr electrolyte, Pt wire or Mg ribbon as counter electrode, vs. RHE.

2.1.4.4 Electrode behaviour comparison for CO₂ electroreduction in Bu₄NBr/ACN and Bu₄NBr/ACN + Styrene Oxide.

Graph 2.13 shows together Cu/Pt and Cu/Mg pair of electrodes in carbon dioxide saturated acetonitrile solution with Bu₄NBr as electrolyte vs. RHE. Orange (Cu/Pt) and green (Cu/Mg) curves are in the presence of styrene oxide.

Comparison shows that Cu/Pt is in both cases more catalytic than Cu/Mg. However, the advantage of Cu/Mg is the low cost of those metals.



Graph 2.13.- Comparison of Cu rod electrodes in CO₂ saturated acetonitrile solution, Bu₄NBr electrolyte, Pt wire or Mg ribbon as counter electrode, vs. RHE. Green and orange lines are in the presence of Styrene oxide.

In order to know more about the mechanism of the reactions behind the electrochemistry, a series of non-electrochemical experiments regarding carboxylation of styrene oxide in the presence (or not) of the metal electrodes will be carried out. Some of them are explained in next section, Organic synthesis & Control reactions.

2.1.5 Conclusions

Comparison of the different working electrodes CVs showed that their ability for CO₂ reduction when Bu₄NPF₆ catalyst was used can be ranked from higher to lower as follows: Cu > Au > Pt > GC

From comparing the two different electrolytes used and the pairs of electrodes, a classification of performance can be listed as follows (working/counter electrodes-electrolyte 1%):

GC/Pt-Bu₄NPF₆ < Pt/Pt-Bu₄NPF₆ < Au/Pt-Bu₄NPF₆ < Cu/Pt-Bu₄NPF₆ < Cu/Pt-Bu₄NBr < Pt/Pt-Bu₄NBr

This sequence would be consistent with the experimental results obtained previously on catalyst screening for carboxylation of epoxides, being Bu₄NBr a better catalyst than Bu₄NPF₆.

The addition of styrene oxide to the system of Cu/Pt electrodes with Bu₄NBr showed a CV looking as an irreversible process. However, when the electrode pair used was Cu/Mg, a very different curve was acquired with at least three processes going on when CO₂ was flushed. Due to the complexity of the system more experiments should be carried out in order to determine the processes taking place.

A 2015 January publication by Berto, T. C., Zhang, L., Hamers, R. J. & Berry, J. F. reported a deeper analysis on this matter concluding that “the “catalytic” role of NR₄⁺ salts in CO₂ electroreduction is non-existent.¹⁵³ None of the current data supports a strong electrostatic interaction between either NR₄⁺ and CO₂ or NR₄⁺ and the electrode surface, and the diffusion-controlled electroreduction best fits a simple direct outer-sphere reduction of dissolved CO₂, the mechanism which was originally put forth by Savéant and co-workers.¹⁵⁴

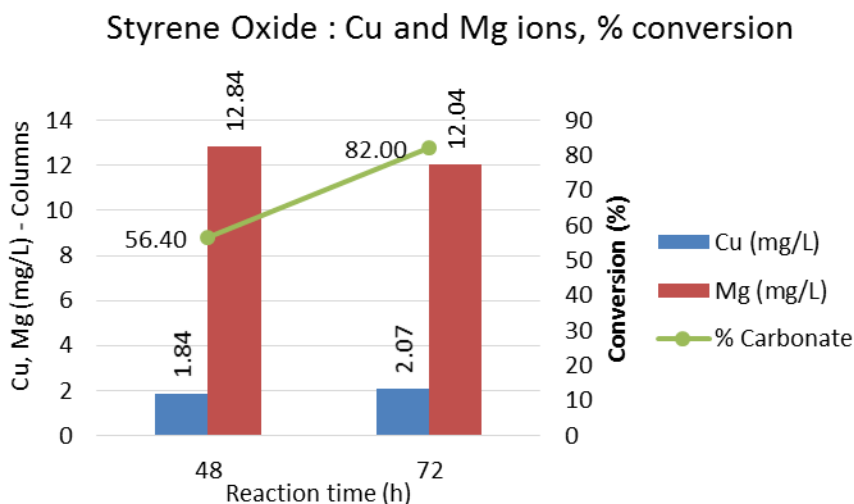
Experiments using no current were designed to further understand the mechanism of the reaction.

2.2 ICP ANALYSIS OF CU AND MG CONTENT ON ELECTROCATALYTIC CYCLIC CARBOXYLATION OF EPOXIDES

In order to find a correlation between the copper and magnesium content in solution and the production of cyclic carbonate both ions were measured by Atomic Absorption Spectrometry (Experimental specifications in section 4.2).

2.2.1 Styrene oxide electrochemical carboxylation

It was found by ICP analysis that Cu and Mg electrodes were degrading to the solution. Cu and Mg content in solution during the electrocarboxylation of styrene oxide (1a) in acetonitrile (1 atm pressure of CO₂, at 75 °C with the presence of TBAI) were stable through reaction time as shown in Graph 2.14 for 48 and 72 hours of reaction times.

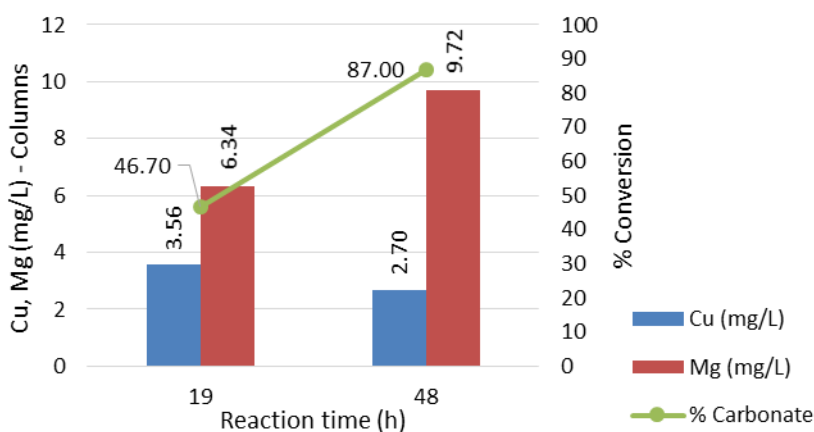


Graph 2.14.- Cu and Mg content in solution in mg/L (blue and red columns respectively) and % of conversion (green line) to the corresponding carbonate of styrene oxide at different reaction times (h). At a concentration of 0.02M, Ratio: 1:1, temperature of 75 °C, and Bu₄NI as electrolyte.

2.2.2 Fluorostyrene oxide electrochemical carboxylation

In the case of electrochemical carboxylation of fluorostyrene oxide, Mg ions slowly increase with time and Cu ions decrease while carbonate production highly increases (Graph 2.15).

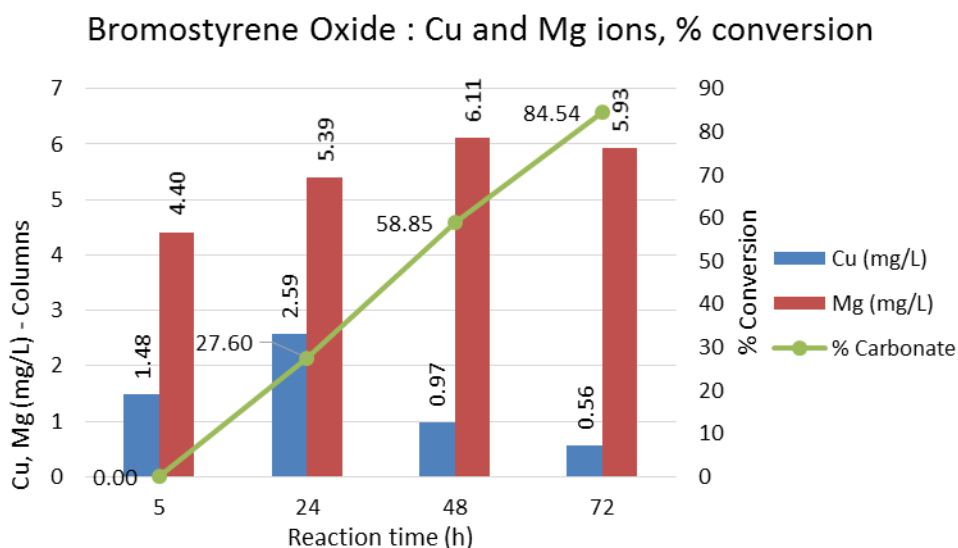
Fluorostyrene Oxide : Cu and Mg ions, % conversion



Graph 2.15.- Cu and Mg content in solution in mg/L (blue and red columns respectively) and % of conversion (green line) to the corresponding carbonate of fluorostyrene oxide at different reaction times (h). At a concentration of 0.02M, Ratio: 1:1, temperature of 75 °C, and Bu₄NI as electrolyte.

2.2.3 Bromostyrene oxide electrochemical carboxylation

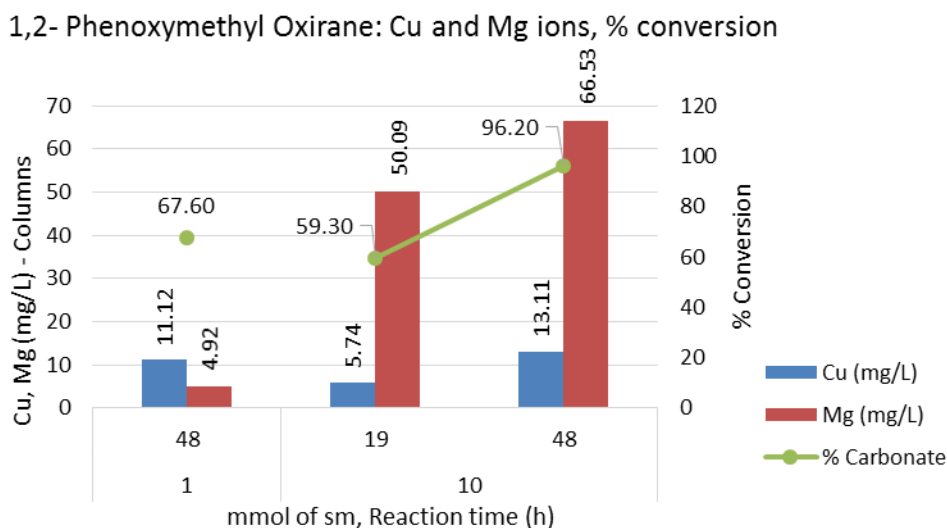
In the reaction with bromostyrene oxide as starting material, Magnesium ions increase with time, Copper ions increase first but decrease after, and a slower conversion to carbonate takes place compared to the previous reactions (Graph 2.16).



Graph 2.16.- Cu and Mg content in solution in mg/L (blue and red columns respectively) and % of conversion (green line) to the corresponding carbonate of bromostyrene oxide at different reaction times (h). At a concentration of 0.4M, Ratio: 1:1, temperature of 75 °C, and Bu₄NI as electrolyte.

2.2.4 1,2-Phenoxymethyl oxirane electrochemical carboxylation

When the reaction was concentrated more, Mg highly dissolves and performance improves by achieving almost the same conversion in half the time: when 1 mmol of starting material reacted after 48 hours, 67% of carbonate was produced. However, when 10 mmol of starting material reacted, 60% of conversion was accomplished in only 19 hours (Graph 2.17).

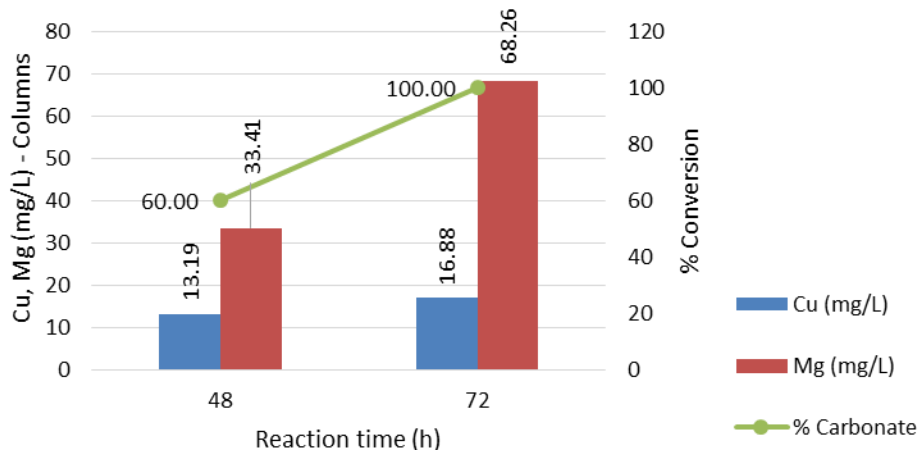


Graph 2.17.- Cu and Mg content in solution in mg/L (blue and red columns respectively) and % of conversion (green line) to the corresponding carbonate of 1,2-phenoxymethyl oxirane at different reaction times (h). At two different concentrations: 1 mmol or 10 mmol of starting material, Ratio: 1:1, temperature of 75 °C, and Bu₄NI as electrolyte.

2.2.5 1,2-Epoxyhexane

In this case both Cu and Mg ions increased with time but a highest difference is seen on magnesium ions in solution. % of conversions for 1,2-epoxy-hexane is also slower (as in the case of bromostyrene oxide).

1,2- Epoxy hexane: Cu and Mg ions, % conversion

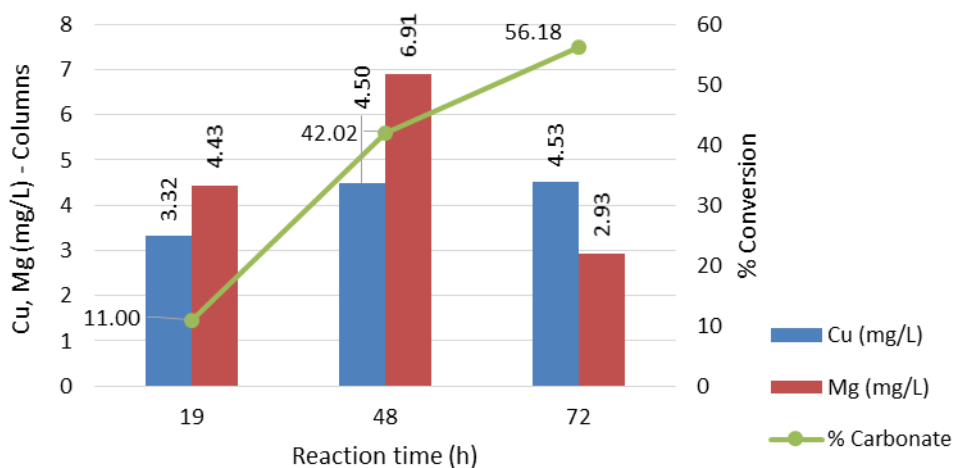


Graph 2.18.- Cu and Mg content in solution in mg/L (blue and red columns respectively) and % of conversion (green line) to the corresponding carbonate of 1,2- epoxyhexane at different reaction times (h). At a concentration of 0.2M, Ratio: 1:1, temperature of 75 °C, and Bu_4NI as electrolyte.

2.2.6 Allyl Glycidyl Ether

Cu and Mg content in solution was very low for the allyl glycidyl ether reaction. Conversion was also slow and not higher than 56% after 72 hours.

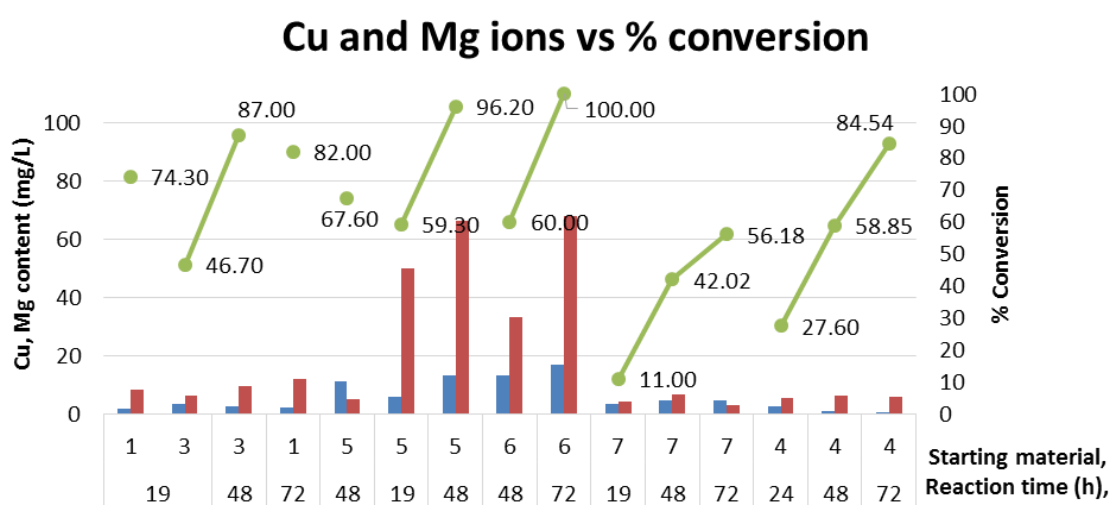
Allyl Glycidyl Ether: Cu and Mg ions, % conversion



Graph 2.19.- Cu and Mg content in solution in mg/L (blue and red columns respectively) and % of conversion (green line) to the corresponding carbonate of allyl glycidyl ether at different reaction times (h). At a concentration of 0.31M, Ratio: 1:1, temperature of 75 °C, and Bu_4NI as electrolyte.

2.2.7 Comparison

The plotting of all starting materials together shows that no comparison between different chemical species can be achieved (Graph 2.20). Copper and Magnesium content in solution is independent of concentration between different starting materials but it is dependent on time within the same reactant. Some reactions at higher concentration showed more Mg ions than others but reaction rates were slower (roughly based on the difference on slopes of data representation) (e.g. starting material 1,2-epoxyhexane).



Graph 2.20.- Cu and Mg content in solution in mg/L (blue and red columns respectively) and % of conversion (green line) to the corresponding carbonate of all different starting materials (1 = styrene oxide (1a); 3 = fluorostyrene oxide (1c); 4 = bromostyrene oxide (1d); 5 = 1,2-phenoxyethyl oxirane (1e); 6 = 1,2-epoxyhexane (1f); 7 = allyl glycidyl ether (1g)) reaction at different reaction times (h).

Due to the difference on the chemical behaviour some starting materials such as styrene oxide (number 1 in Graph 2.20) has higher % of conversion to carbonate (87%) at low concentrations (0.02 M) after 48 hours while others like 1,2- epoxyhexane (number 6 in Graph 2.20) had less conversion rate (60%) at higher concentration (0.2 M) after the same period of time (48 hours).

2.2.8 Conclusions

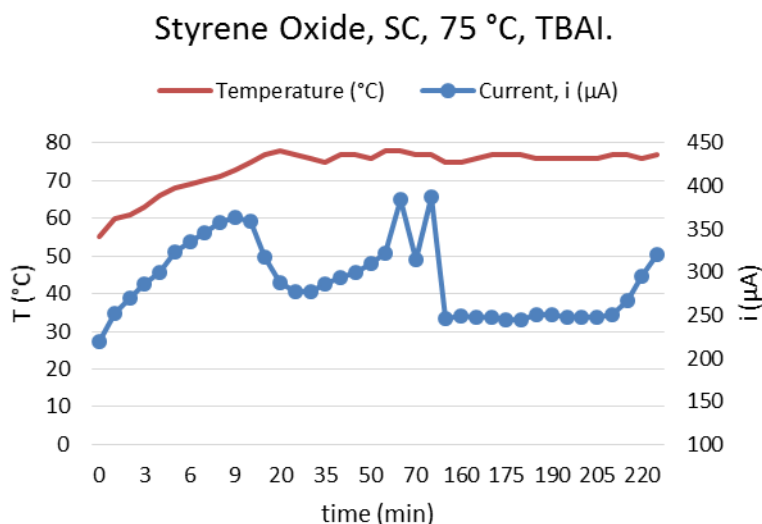
Cu and Mg content usually rose with time and so did the carbonate within the same reaction, however when comparing different starting materials, trends were not consistent. For example, after 48 hours of reaction of styrene oxide (with TBAI in ACN at 75 °C and 1 atm of CO₂) at a concentration of 0.02 M conversion to carbonate was of 87% containing less than 10 mg/L in Cu

and Mg ions. In contrast, after the same time of reaction, 1,2-epoxyhexane conversion to carbonate was of 60% while Cu and Mg ions content was more than 45 mg/L. It can be concluded that a straight relation cannot be identified between Cu and Mg in solution and concentrations and conversion when comparing different starting materials.

2.3 MEASURE OF THE ONSET POTENTIAL OF THE CELL

Some Short Circuit reactions were monitored looking at the onset potential of the cell. This was simply measured by connecting a multimeter to the Cu and Mg electrodes on the voltmeter mode. The usual response was in a range from 0.8 to 1 volt which is the potential at which CO₂ has been found to start to reduce at different electrodes.^{91,157,158} If this occurs, the products of the reduction could be determined by analysing the system by LCMS coupled to the electrochemical cell. An attempt to do so with a GCMS is reported on section 2.5. The experimental procedure of the reaction set up is the same as explained on section 4.6.2.4.

The current response of a short circuit mode reaction with styrene oxide as starting material is shown in Graph 2.21.



Graph 2.21.- Measures of current (μA in blue) and temperature ($^{\circ}\text{C}$ in red) of a short circuit mode reaction of styrene oxide and Bu₄NI, up to 75 °C.

Differences in the current may indicate reactions taking place on the electrodes surfaces. It would be convenient to monitor the current flowing in the reaction for longer time (as long as the reaction takes place) together with periodical analysis of the solution by LCMS and ¹H-NMR spectroscopy. With the present equipment this was not possible but a new handmade

multimeter with a range of channels and connected to a computer has been built for this purpose by A. Sertap Kavasoglu, a colleague from Hacettepe University, Engineering Faculty in Beytepe /Ankara, TURKEY during his visit to the Energy Research Lab in Loughborough University carrying on a collaborative project. The device will need to be set up and calibrated before its use.

2.4 DMS ANALYTICAL TECHNIQUE TO MONITOR IN-SITU ELECTROCATALYTIC CYCLIC CARBOXYLATION OF EPOXIDES.

The electrochemical cell was successfully coupled to the differential mobility spectrometer and a change in response with respect to background experiments was detected by the instrument and recorded in a computer for its analysis. However, a first analysis of the data did not expose significant information about the system due to saturation of acetonitrile response. Acetonitrile sequesters the positive charge because of its high proton affinity saturating the signal.

Further investigation would require changing the solvent to one whose proton affinity is less than that of methanol in order for resolving the signal response. However, this change should be previously studied in terms of the viability of the electrochemical reaction under the new conditions since it would affect the performance. Table 2.1 shows proton affinities for acetonitrile and methanol both used in this experiment, and some proposed solvents to be tested in future research.

Table 2.1.- Proton affinities of solvents

Solvent (neutral molecules)	Proton affinity (kJ/mol)
<i>Acetonitrile</i>	788
<i>Methanol</i>	761
Benzene	759
Formaldehyde	718
Water	697
Hydrogen peroxide	678

2.5 CONSTRUCTION OF A GC/MS FOR ANALYSIS OF *IN-SITU*

ELECTROCHEMICALLY ASSISTED CARBOXYLATION REACTIONS

As explained in the introduction research groups have used MS (usually LCMS^{ref}) as an analytical method to identify subproducts and/or intermediates in the electrocarboxylation of epoxides.

A similar system consisting of a MS or GC-MS coupled to the electrochemical cell will be developed in order to detect volatile products produced during the electrochemical carboxylation of styrene oxide with CO₂.

An attempt of determining all compounds produced in the electrocarboxylation of epoxides was made by building a mass spectrometer in the laboratory next to a fumehood in where a electrochemical cell was placed to run the reaction. More details about the instrument specifications can be found on section 4.5. Experimental procedure of this reaction set up is as explained on the experimental section 4.6.2.4.

2.5.1 Results

Some of the mass spectra patterns of molecules of interest (such us CO₂, CO, Acetonitrile...) are collected in the Annexe.

First blank (Figure 2.1) shows an injection of CO₂ gas at room temperature (top spectrum green colour), the background spectrum where only carrier gas should be present (middle spectrum red colour) and the TIC (bottom, sum of all spectra recorded, purple colour).

Second blank, Figure 2.2, shows an injection of CO₂ gas flushed through the cell containing acetonitrile (top spectrum green colour) at room temperature, the background spectrum when only carrier gas should be present, (middle spectrum red colour), and the TIC (bottom, sum of all spectra recorded, black colour).

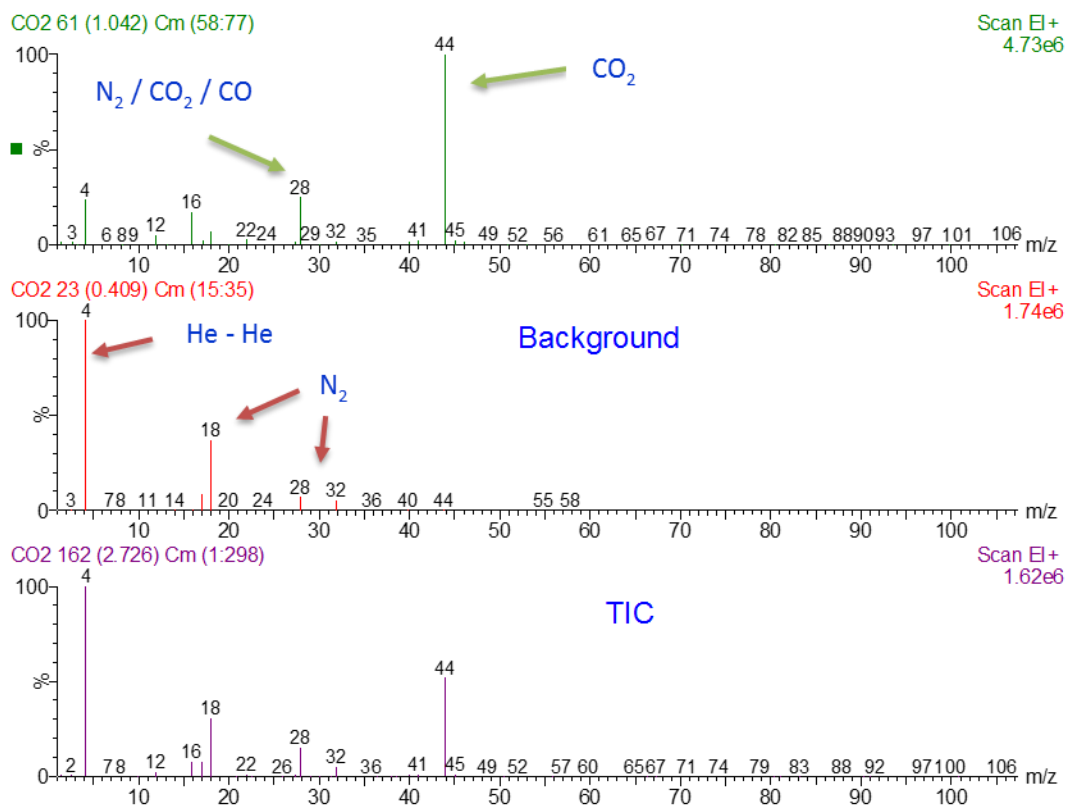


Figure 2.1.- TIC (bottom), background (middle) and CO₂ (top) mass spectra signals at room temperature.

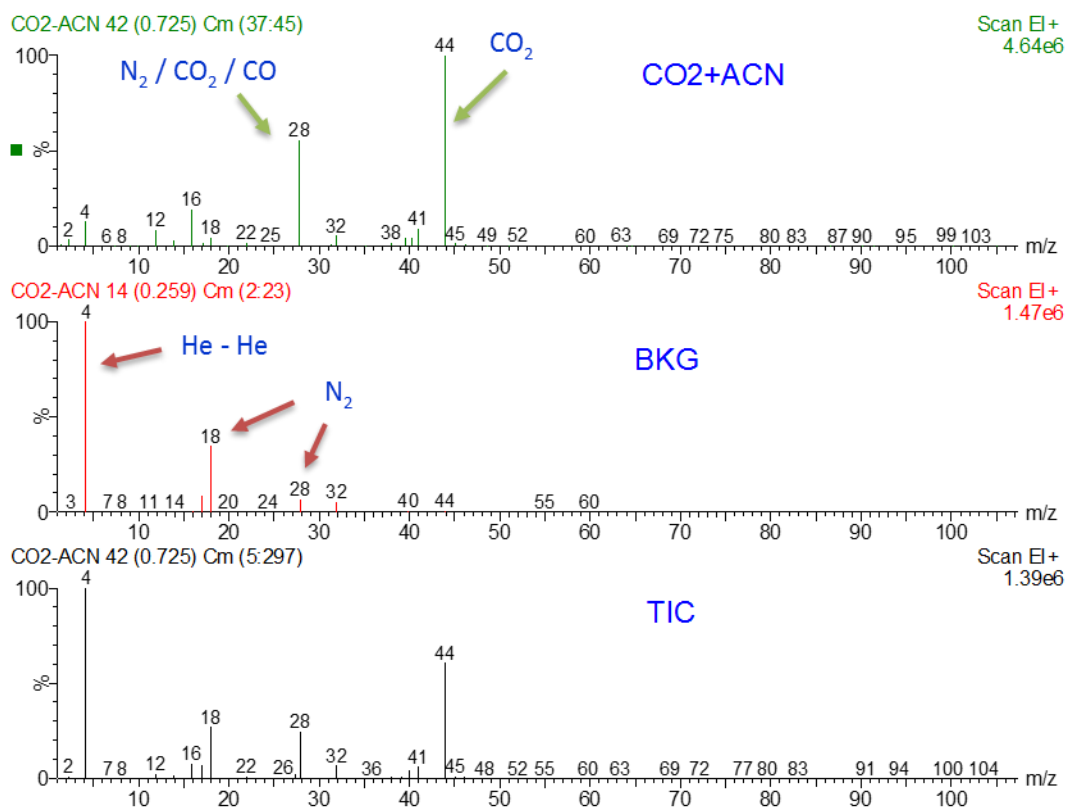


Figure 2.2.- TIC (bottom), background (middle) and CO₂ flushed through a flask containing acetonitrile (top) mass spectra signals at room temperature.

The same experiment at 75 °C was carried out. Figure 2.2 shows the chromatograms for the two injections of CO₂ flushed through a flask containing 50 mL of ACN at 75 °C. On the bottom, on red, there is the TIC chromatogram that shows one first peak corresponding to a first injection and a second and broad peak corresponding to the second injection. This broad peak is due to the condensation of ACN vapour along the glass capillary which is about 2 m long and is currently at room temperature. To avoid condensation in the system which can highly damage the detector the length of the inlet tube and capillary must be shortened to the minimum possible. The length of the second peak plateau shows that a minimum of 4 minutes was needed to “clean” the system.

The chromatogram in the middle shows the times at which all signals for the peak of ACN (41 m/z) appear along the analysis. As it can be spotted, it has the same shape than the TIC, meaning that every time an injection is taken, ACN is present in the sample.

The top chromatogram, on black colour, shows the times at which all signals for CO₂ peak (44 m/z) appear. In this case it is clear that both injections contained CO₂, but the second one it did only at the first stage and did not last until the end of the plateau.

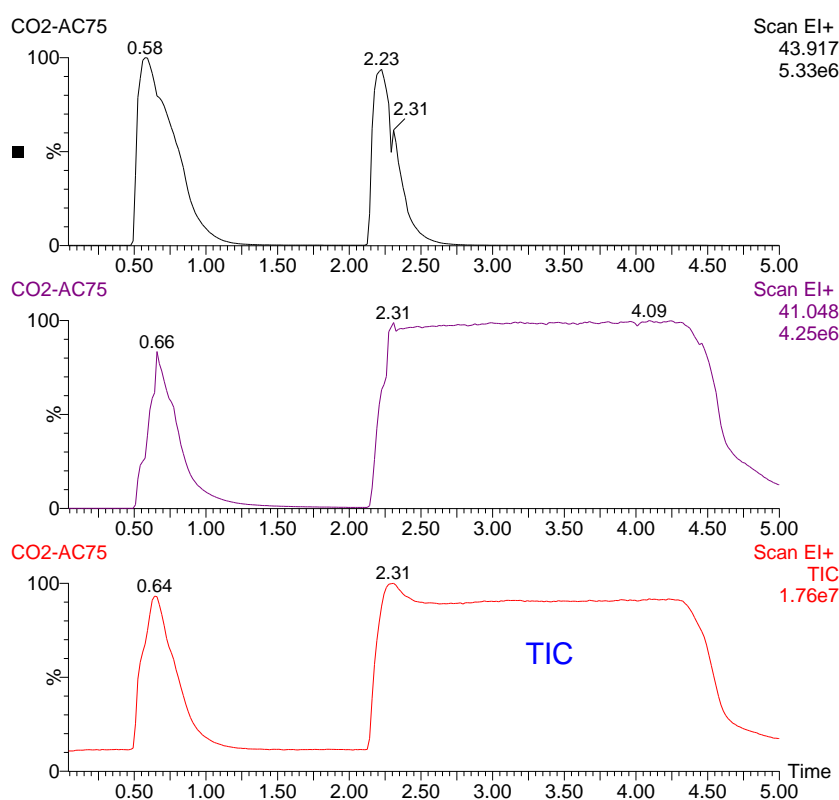


Figure 2.3.- Chromatograms of two injections containing CO₂ flushed through a flask filled with 50 mL of a acetonitrile at 75 °C. TIC chromatogram (bottom on red colour); Acetonitrile chromatogram (middle on purple colour) shows times of peaks at 41 m/z; CO₂ chromatogram (top on black colour) shows times of peaks at 44 m/z.

The same conclusion can be drawn from the Mass spectra (Figure 2.4). Image number 1, shows the TIC spectrum where all recorded spectra are collected. Signals corresponding to CO₂ at 44 m/z, ACN and its pattern from 38-41 m/z, N₂ at 28 and 18 m/z, and He at 4 m/z can be distinguished. If a spectrum corresponding to the background is isolated, then only He and N₂ signals appear (Figure 2.4, number 2). When a spectrum selected from the first peak of the TIC chromatogram in Figure 2.3 is isolated, ACN and CO₂ peaks are the most intense signals (shown in Figure 2.4, number 3). The same pattern is shown when the isolated spectrum corresponded to the first minute of the second peak (second injection) of the TIC chromatogram on Figure 2.3 before the signal becomes flat. However, on a spectrum from the flat signal of the second peak of the chromatogram, only ACN is present, corresponding to the condensed ACN in the capillary (Figure 2.4, number 4).

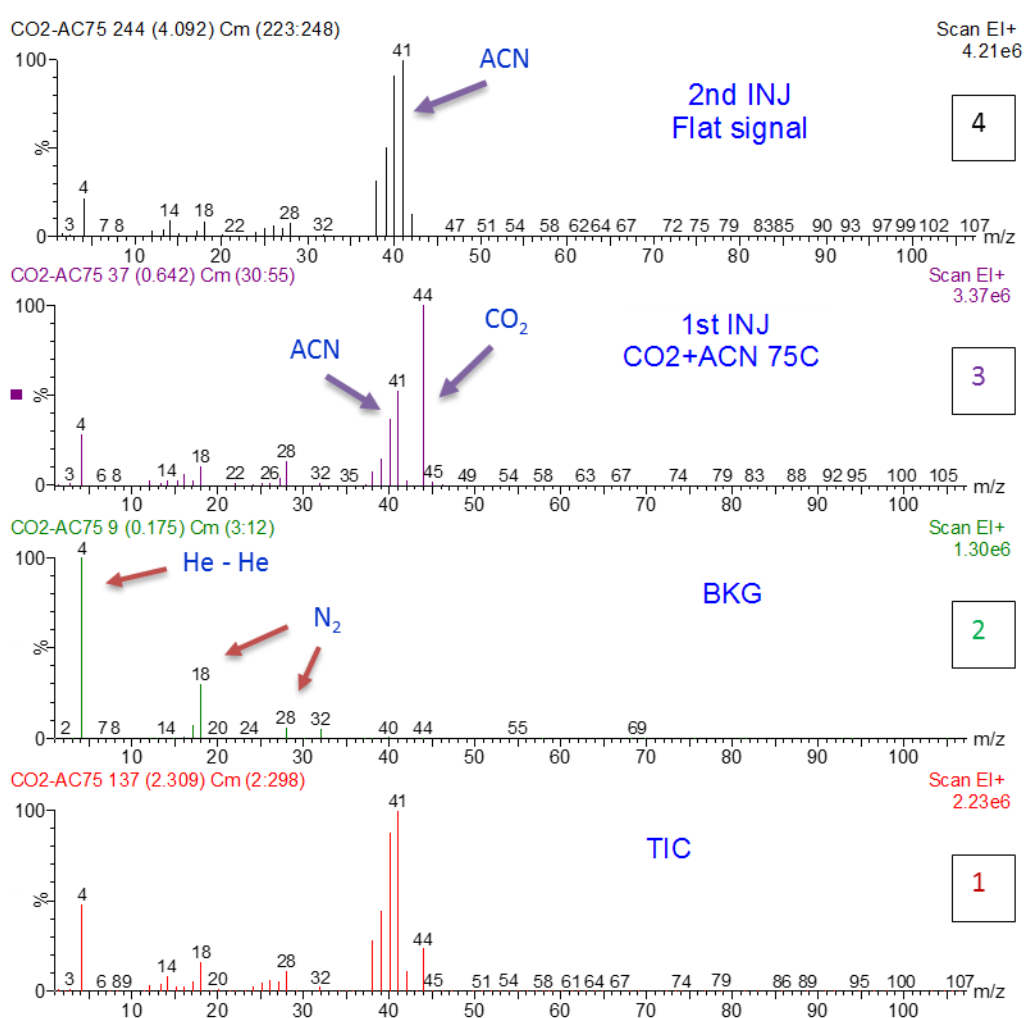


Figure 2.4.- Mass spectrum of two injections containing CO₂ flushed through a flask filled with 50 mL of acetonitrile at 75 °C. TIC spectrum (1, on red colour); background spectrum (2, on green colour); 1st injection spectrum (3, on purple colour); Plateau spectrum (4, on black colour).

Figure 2.5 compares the spectra of injections of CO₂ at room temperature (bottom, on red colour), CO₂ flushed through a flask containing ACN at room temperature (middle, on green colour) and at 75 °C (top, on purple colour). The difference in temperature can be spotted due to the higher amount of ACN present in the CO₂ flow going into the detector.

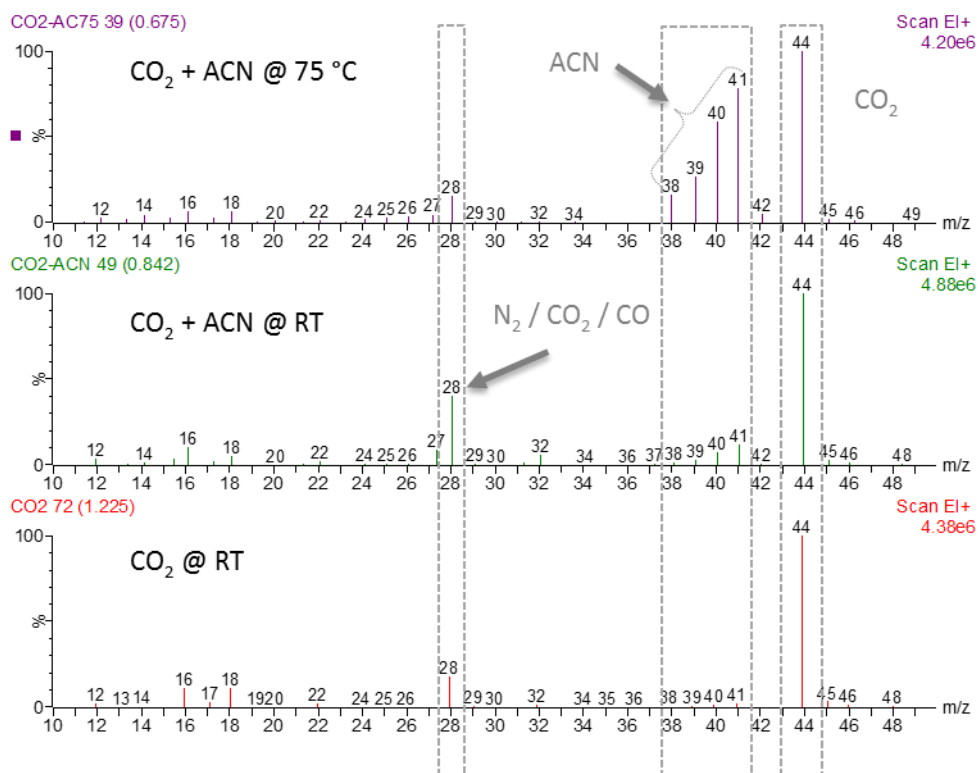


Figure 2.5.- Mass spectra comparison. CO₂ at room temperature (bottom on red colour), CO₂ and ACN vapours at room temperature (middle on green colour), CO₂ and ACN vapours at 75 °C (top on purple colour).

In summary, the system is working properly, efficiently identifying every compound and apparently responding with the correct intensities. However, if the intention is to identify other compounds products or subproducts coming from the CO₂ electroreduction in the cell such as CO, which m/z peak overlaps with the 2nd main peak of CO₂ pattern (at 28 m/z), prior separation of the gases is required. A gas chromatography device was purchased and installed in conjunction with the MS detector. A calibration of the detector with CO₂ as calibrant is desired in order to compare accurately intensities of its pattern peaks. The ideal set up would consist of a Liquid Chromatography – Mass Spectrometry system coupled with the electrochemical cell. The disadvantages of a GCMS vs LCMS are that only compounds in their gas state can be measured, so the possibility of finding any other key compound produced in the electro-reduction of CO₂ and dissolved in the ACN (e.g. formic acid) is lost.

2.6 BACKGROUND REACTIONS

A wide research on the electrocarboxylation of epoxides was carried out by Anish P. Patel and is presented in his PhD thesis and publication¹. As was suspected after the cyclic voltammetry study of the carboxylation of epoxides in the present investigation and supported by a recent publication¹⁵³, the activity of the ammonium salt is not electrocatalytic, therefore further research on the reaction mechanism is needed. The best performance conditions of these reactions were chosen as starting point for the following background reaction experiments.

Due to the finding that electrocatalysis does not take place, and to the influence of numerous variables in the reaction, the following experiments were designed only focusing on the electrochemical system. First, current was not applied, but the electrodes were connected with a wire to close the circuit system and allow electrons to travel (short circuit reactions); Second, the same electrodes system with no current, and without any wire connection (Open circuit); Finally, reactions with no electrodes were carried out (No electrodes reactions). The results of these experiments are discussed below.

2.6.1 Electrocarboxylation of epoxides

The following reactions were reproduced from Anish P. Patel work in this research group.¹

Procedure of reaction on entry 1 of Table 2.2:

The epoxide (1b, 2 mmol) was added to a solution of supporting electrolyte (Bu_4NBr) in acetonitrile (60 mL) in a ratio of (1:1), the resulting solution was flushed with CO_2 for 1h, followed by heated electrolysis for 5h at 75 °C and constant current (60mA) with constant stirring and constant CO_2 flow, in a single compartment cell containing a magnesium anode (30 cm of Mg ribbon) and copper cathode (60 cm of Cu rod) previously sanded (to remove the oxide layer).

On completion the reaction mixture was filtered if any precipitate was formed and later concentrated under reduced pressure (in ice bath if required). EtOAc (5 mL) was added to precipitate Bu_4NI . After precipitation the solid was removed by filtration and the solvent evaporated to afford the corresponding carbonate (88% of 2b evaluated from ^1H NMR spectrum).

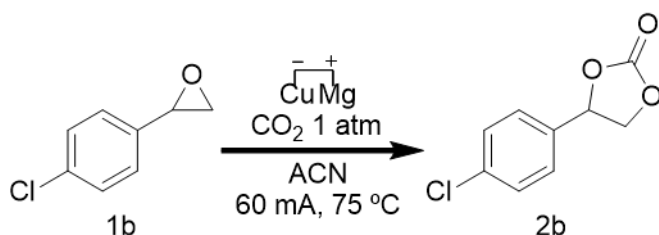


Table 2.2.- Electrochemical carboxylation of chlorostyrene oxide.

Entry	Starting material	Time (h)	Carbonate (%) ^a
1	Chlorostyrene oxide	5	88

^aGeneral reaction conditions: copper rod, magnesium ribbon, 60 mA of current, Bu₄Nl as supporting electrolyte, CO₂ constant flow, CH₃CN, 75 °C; ^aEvaluated from ¹H NMR spectrum.

Electrochemical carboxylation of styrene oxide was also reproduced performing as follows:

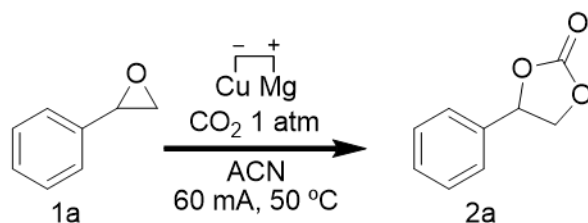


Table 2.3.- Electrochemical carboxylation of styrene oxide.

Entry	Starting material	Time (h)	Carbonate (%) ^a
1	Styrene Oxide	19	73

^aGeneral reaction conditions: copper rod, magnesium ribbon, 60 mA of current, Bu₄NBr as supporting electrolyte, CO₂ constant flow, CH₃CN, 50 °C; ^aEvaluated from ¹H NMR spectrum.

2.6.2 Short Circuit reactions

Procedure of reaction on entry 10 of Table 2.4:

The epoxide (1a, 2 mmol) was added to a solution of supporting electrolyte (Bu₄Nl) in acetonitrile (50 mL), the resulting solution was flushed with CO₂ for 1h, followed by heating at 50 °C with constant stirring for 48 hours under constant CO₂ flow, in a single compartment cell containing a magnesium anode (15 cm of Mg ribbon) and copper cathode (30 cm of Cu rod) previously sanded. A wire connection between Cu and Mg electrodes was used to close the system, but no current was applied.

On completion the reaction mixture was concentrated under reduced pressure (in ice bath if required) and EtOAc (5 mL) was added to precipitate Bu_4NI . After precipitation the solid was removed by filtration and the solvent evaporated to afford the corresponding carbonate (97% of 2a evaluated from $^1\text{H NMR}$ spectrum).

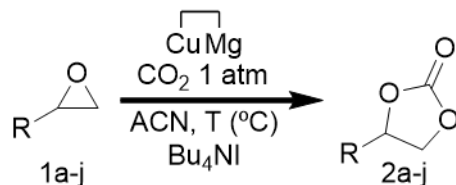
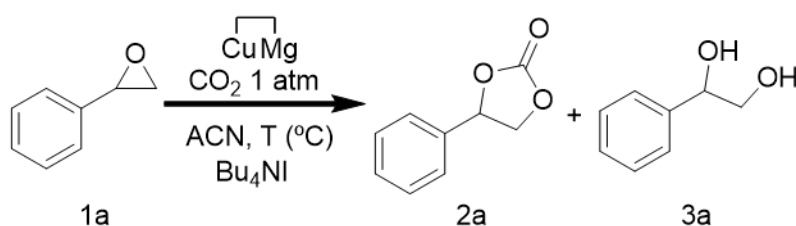


Table 2.4.- Short Circuit reaction conditions and results of styrene oxide carboxylation with TBAI.^a



Entry	Ratio (1a:TBAI)	CO ₂	Temp (°C)	time (h)	Carbonate (%) ^b	Diol (%) ^b
1 ^c	1:1	X	0	96	0	100
2	1:1	√	0	96	2	98
3	1:1	√	30	0	0	0
4	1:1	√	30	5	4	0
5	1:1	√	30	24	67	0
6	1:1	√	30	48	89	0
7	1:1	√	50	0	0	0
8	1:1	√	50	5	7	0
9	1:1	√	50	24	65	0
10	1:1	√	50	48	97	0
11	1:1	√	75	0	0	0
12	1:1	√	75	19	56	16
13	1:1	√	75	48	83	13
14	1:1	√	75	19	76	14
15	1:1	√	75	19	74	3
16	1:1	√	100	0	0	0
17	1:1	√	100	19	2	0
18 ^d	1:10	√	0	19	3	3
19 ^d	1:10	√	75	19	74	3

^aGeneral reaction conditions: copper rod, magnesium ribbon, wire connection between electrodes, Bu_4NI as supporting electrolyte, CO_2 constant flow, CH_3CN , 0 to 100 °C; ^bEvaluated from $^1\text{H NMR}$ spectrum. Mg ribbon was replaced for a freshly sanded if consumed after 48 hours. ^cA background reaction without CO_2 after 96 h gave as only product the corresponding diol (29). ^dCatalyst concentration was increased by ten times to compare the performance at 1:10 ratio (entries 16 and 17) at two different temperatures.

Regarding the formation of diol, it was suspected that it was produced directly from the epoxide remaining in solution as it is widely reported in the literature.^{118,159–162} However, the possibility of the diol coming from the cyclic carbonate was also considered as a degradation of the carbonate in presence of some organometallic complexes used for its synthesis from epoxides was previously reported by Muralidharan & Heeralal.¹²²

The investigation of formation of diol as product led to the modification of the work up conditions as explained in 184. It was found that diol proceeds from the remaining epoxide when solution was treated with dilute HCl in the initial method. The first experiment to investigate this issue consisted on subjecting the cyclic carbonate to the electrocarboxylation conditions in presence of 0.5 mL of H₂O followed by addition of 0.5 mL of 0.1 M HCl. Results of this test showed that the carbonate was not degrading (see Table 2.5). Styrene epoxide and carbonate were washed separately with dilute HCl, extracted with EtOAc and rota evaporated the product. ¹H NMR showed that carbonate remained pure, while epoxide transformed to the corresponding diol (Scheme 2.1).

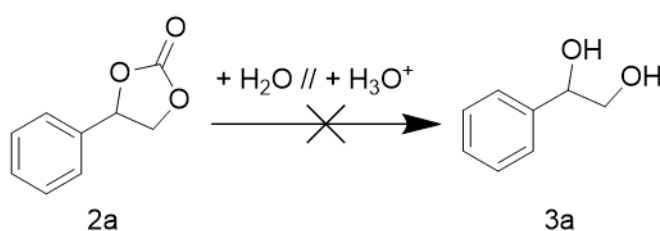
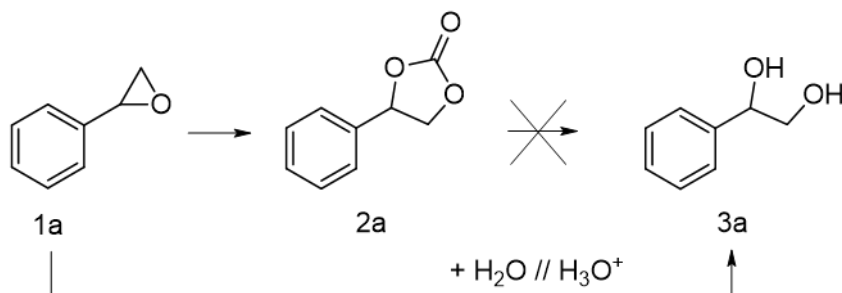


Table 2.5.- Degradation study of 4-phenyl-1,3-dioxolan-2-one under short circuit mode.

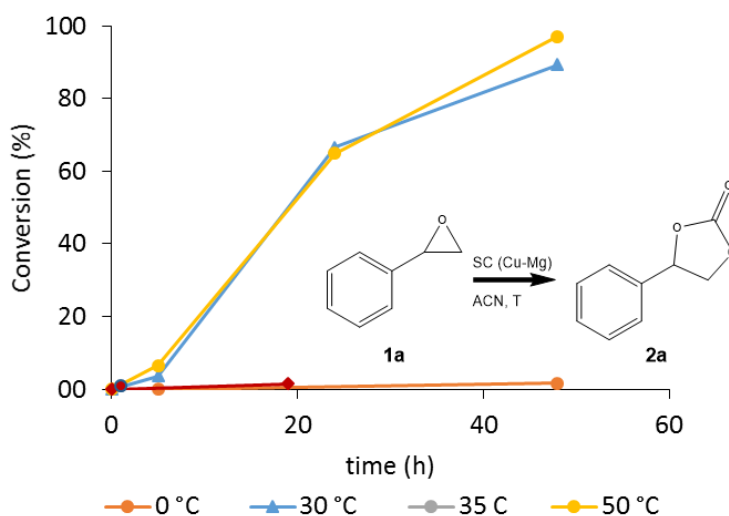
Time (h)	Carbonate (%) ^a	diol (%) ^a
19	100	0
48	100	0

General reaction conditions: 4-phenyl-1,3-dioxolan-2-one as starting material, copper rod and magnesium ribbon (Short circuit mode), Bu₄Ni as supporting electrolyte, CO₂ constant flow, CH₃CN, 75 °C; ^aEvaluated from ¹H NMR spectrum. R_i refers to the code given to each reaction.

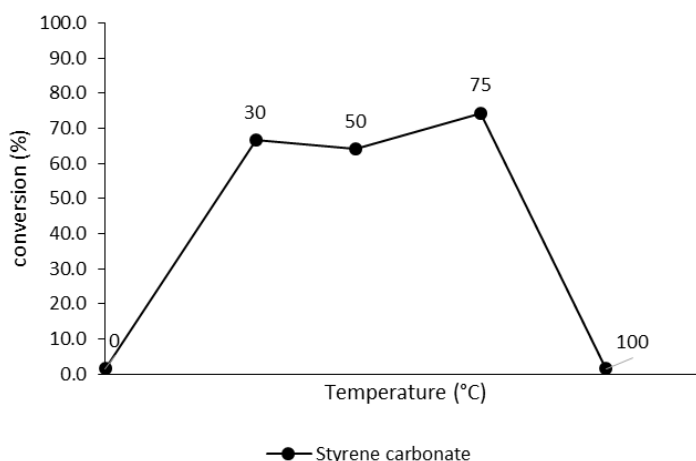


Scheme 2.1.- Evolution of styrene oxide carboxylation reaction.

Graph 2.22 shows the synthesis of styrene carbonate from styrene oxide under short circuit conditions of Cu and Mg electrodes in acetonitrile, at different temperatures (Entries 1 to 17 of Table 2.4). Reactions run at 0 °C or at 100 °C or higher temperature gave very low or no conversion to carbonate. Note that boiling point of acetonitrile is reached at 82 °C at atmospheric pressure, so reactions over that temperature experience degasification of the solution and no CO₂ is left to react. Reactions carried out at 30, 50 and 75 °C under short circuit conditions performed very similarly. Temperature profile of the reaction after 19 hours is represented in Graph 2.23.

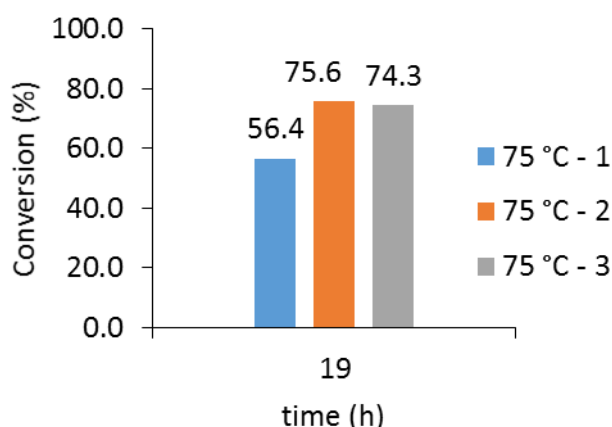


Graph 2.22.- Styrene oxide carboxylation under SC conditions at different temperatures.



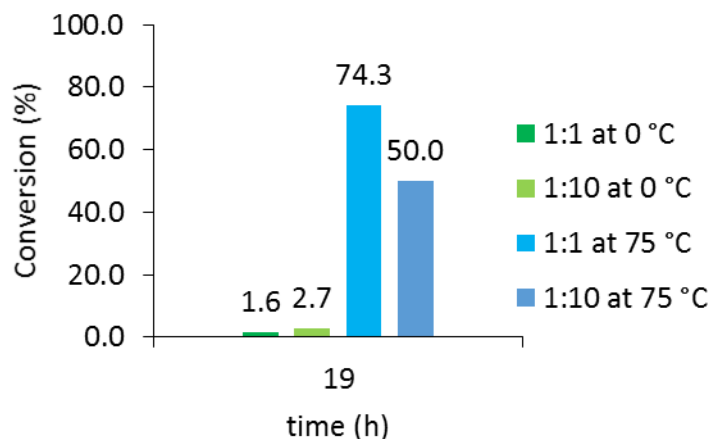
Graph 2.23.- Profile of styrene carbonate conversion at different temperatures after 19 hours of reaction under SC conditions.

Reproducibility of the reaction was within a range of at least 20% range of difference in performance. Three replicates of the synthesis of styrene carbonate at 75 °C in acetonitrile under short circuit conditions (Entries 12, 14 and 15 of Table 2.4) are shown in Graph 2.24. This wide range of different conversions could be due to weaknesses in the experimental procedure, like the fact that CO₂ flow usually stopped overnight probably due to the change of room temperature and had to be restarted in the morning. This leads to an uncertainty on the actual time of the reaction because of the intermittent absence of one of the reactants.



Graph 2.24.- Three replicates of styrene carbonate synthesis under short circuit conditions (Cu and Mg electrodes), ACN, TBAI (1:1), after 19 hours of reaction.

Entries 18 and 19 of Table 2.4 correspond to experiments increasing the proportion of the ammonium salt catalyst (ratios epoxide:catalyst 1:10), at two different temperatures after 19 hours of reaction. The comparison to the analogue experiments at 1:1 ratio is shown in Graph 2.25. Only a 1% more of carbonate was achieved at 0 °C when TBAI was 10 times higher, and 24% less carbonate when the reaction was held at 75 °C. There is no significant difference among the data of reactions with ratios 1 to 1 or reactions with ratios 1 to 10 as the variability study led to a wide range of conversion % under the same conditions.



Graph 2.25.- Effect of escalation of TBAI to 10 mmol in the synthesis of styrene carbonate in acetonitrile at two different temperatures after 19 hours of reaction under short circuit conditions (Cu and Mg electrodes).

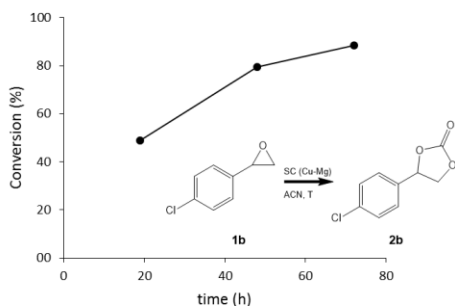
Synthesis of carbonates from epoxides 1b to 1g under short circuit conditions (Cu-Mg electrodes) in acetonitrile was successfully achieved and results are listed in Table 2.6. Graphical representation of the data of Table 2.6 is shown on Graph 2.26 to Graph 2.31. All reactions were run at 0.04 M concentration except one of 1,2-phenoxy methyloxirane (entries 10 and 11) that was run at a 0.14 M concentration and the allyl glycidyl ether reactions of 0.31 M (entries 18 to 24). Temperature of reactions was maintained at 75 °C, ratio of epoxide regarding TBAI was 1:1, and carbon dioxide supplied from a cylinder.

Table 2.6.- Synthesis of cyclic carbonates from epoxides under short circuit conditions (Cu-Mg) in acetonitrile.^a

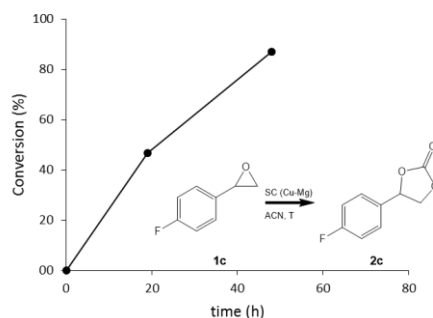
Entry	Epoxide	time (h)	epoxide (M)	Carbonate (%) ^b
2. Chlorostyrene oxide (1b)				
1	SC2_11.2a	19	0.04	49
2	SC2_11.2b	48	0.04	80
3	SC2_11.2C	72	0.04	86
3. Fluorostyrene oxide (1c)				
4	SC3_14a	19	0.04	47
5	SC3_14b	48	0.04	87
4. Bromostyrene oxide (1d)				
6	SC4_19a	5	0.04	0
7	SC4_19b	24	0.04	28
8	SC4_19c	48	0.04	59
9	SC4_19d	72	0.04	85
5. 1,2-Phenoxymethyloxirane^c (1e)				
10	SC5_16b	19	0.14	59
11	SC5_16c	48	0.14	96
12	SC5_9	19	0.04	28
13	SC5_9.2a	48	0.04	68
14	SC5_9.2b	96	0.04	70
6. 1,2-Epoxyhexane (1f)				
15	SC6_12a	19	0.04	30
16	SC6_12b	48	0.04	60
17	SC6_12c	72	0.04	100
7. Allyl Glycidyl ether^d (1g)				
18	SC7_13	19	0.04	0
19	SC7_13.1	48	0.31	56
20	SC7_13.2a	19	0.31	13
21	SC7_13.2b	48	0.31	26
22	SC7_13.2c	120 ^e	0.31	76
23	SC7_13.3a	19	0.31	11
24	SC7_13.3b	48	0.31	42
25	SC7_13.3c	72	0.31	56

^aGeneral reaction conditions: copper rod, magnesium ribbon, wire connection between electrodes, Bu₄NI as supporting electrolyte (1:1), CO₂ constant flow, CH₃CN, 75 °C; ^bEvaluated from ¹H NMR spectrum. Mg ribbon was replaced for a freshly sanded if consumed after 48 hours. ^cConcentration of 1,2-phenoxymethyloxirane was increased to 0.14 M (Entries 10 and 11). ^dThree replicates of allyl glycidyl ether were run at 0.31 M. ^eReaction was left overweekend with a balloon of CO₂.

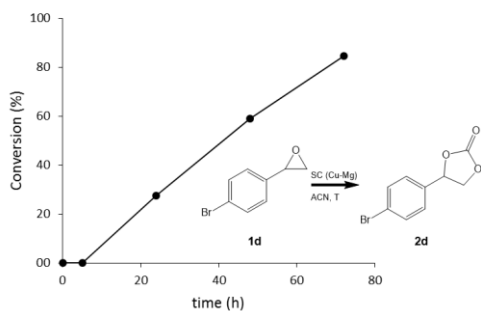
Carboxylation of epoxides (**1b** to **1g**) under short circuit conditions: Cu-Mg, ACN, TBAI (1:1).
Data from Table 2.6.



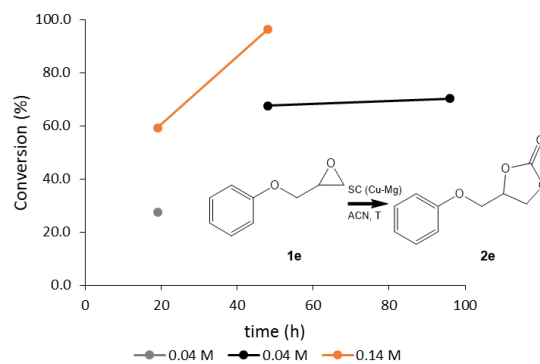
Graph 2.26.- Chlorostyrene oxide carboxylation



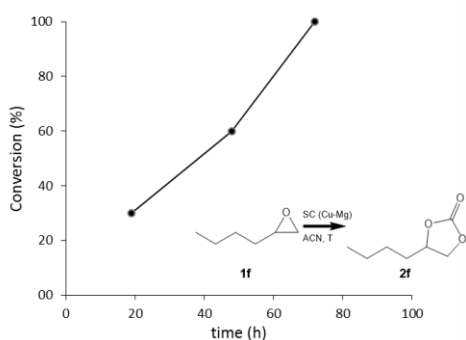
Graph 2.27.- Fluorostyrene oxide carboxylation.



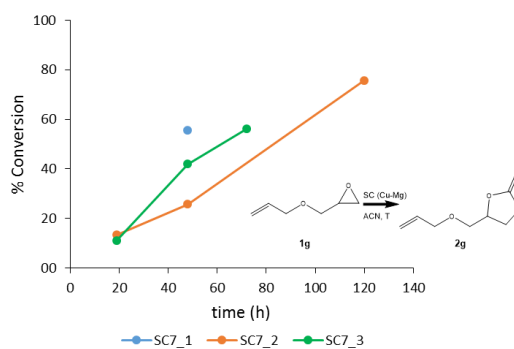
Graph 2.28.- Bromostyrene oxide carboxylation.



Graph 2.29.- 1,2-Phenoxymethyl oxirane carboxylation.



Graph 2.30.- 1,2-Epoxyhexane carboxylation.



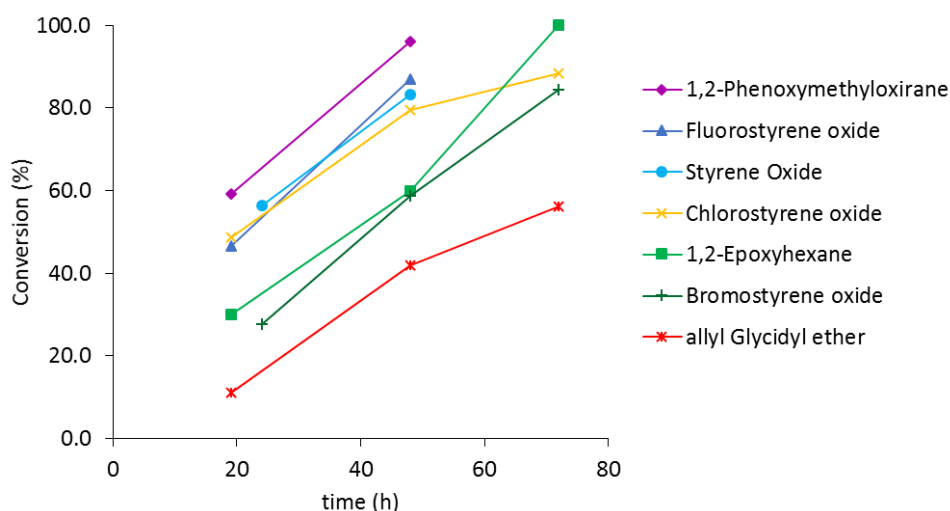
Graph 2.31.- Allylglycidyl ether carboxylation.

As it is noticeable reactions develop at different rates depending on the R group bonded to the epoxide.

One reaction of 1,2-phenoxyethyl oxirane was carried out at a concentration of 0.14 M (orange line in Graph 2.29) to compare the result with the dilute reaction (0.04 M, black line of the same graph). The reaction developed at a higher speed rate as expected when rising the concentration of any of the reactants.

A first reaction at 0.04 M of allyl glycidyl ether was attempted and no carbonate was produced. The concentration of epoxide was raised up to 0.3 M to double check the no conversion to carbonate surprisingly achieving conversions from 11% after 19 h of reaction to 72 after 120 hours. Three replicates of allyl glycidyl ether (Graph 2.31) after 48 hours of reaction showed a high dispersion of results in conversion (from 26 to 55%). This could be, as spotted previously, due to a weak set up (like the fact that CO₂ supply was failing overnight).

Graph 2.32 collects the previous reactions under short circuit conditions in order to better visualize the differences between them.



Graph 2.32.- Comparison of synthesis of cyclic carbonates from epoxides under short circuit conditions.

The classification on reaction rate depending on the epoxide under these conditions can be extracted from data represented in Graph 2.32:

1,2-Phenoxyethyl oxirane > fluorostyrene oxide > styrene oxide > chlorostyrene oxide > 1,2-epoxyhexane > bromostyrene oxide > allyl glycidyl ether.

2.6.3 Open circuit reaction

Procedure of reaction on entry 1 of Table 2.7:

Epoxide (1a, 2 mmol) was added to a solution of supporting electrolyte (Bu_4NBr) in acetonitrile (1:1), the resulting solution was flushed with CO_2 for 1h, followed by heating at $50\text{ }^\circ\text{C}$, constant stirring and constant CO_2 flow, for 19 hours in a single compartment cell containing a magnesium ribbon (15 cm of Mg ribbon) and copper rod (30 cm of Cu rod) previously sanded. No connection was made between the electrodes or current applied.

On completion the reaction mixture was concentrated under reduced pressure (in ice bath if required) and EtOAc (5 mL) was added to precipitate Bu_4NI . After precipitation the solid was removed by filtration and the solvent evaporated to afford the corresponding carbonate (46% of 2a evaluated from $^1\text{H NMR}$ spectrum).

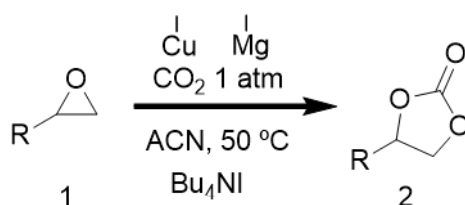


Table 2.7.- Open circuit reaction conditions of three different starting materials, with and without electrolyte.^a

Entry	Epoxide	Catalyst	time (h)	epoxide (M)	Carbonate ^b (%)
1	Styrene Oxide	TBABr	19	0.04	46
2	Styrene Oxide ^c	x	19	0.04	0
3	Chlorostyrene oxide	TBAI	19	0.04	20
4	1,2-Phenoxymethyloxirane	TBAI	5	0.15	10
5	1,2-Phenoxymethyloxirane	TBAI	5	0.15	12

^aGeneral reaction conditions: copper rod, magnesium ribbon, supporting electrolyte (1:1), CO_2 constant flow, no connection between electrodes, CH_3CN ; ^bEvaluated from $^1\text{H NMR}$ spectrum. ^cNo supporting electrolyte.

Reaction of styrene oxide (1a) in acetonitrile at a concentration of 0.04 M containing TBABr and in the presence of Cu and Mg electrodes without any connection between them (open circuit conditions) was heated up to $75\text{ }^\circ\text{C}$ and flushed with CO_2 (entry 1 of Table 2.7) producing 46% of carbonate (2a). This reaction showed that carboxylation takes place even without electrode connection. Same conditions without TBABr did not produce styrene carbonate (entry 2, Table 2.7). The solution of TBABr would be doing the job of transferring electrons from one electrode to

another although with a lot more resistance than would present the wire connection between electrodes.

Chlorostyrene oxide was also used as starting material under the same conditions to confirm that cyclic carboxylation can be extrapolated to other epoxides under open circuit conditions, using TBAI as catalyst at a concentration of 0.04 M. Reaction produced only 20% of carbonate after 19 hours (entry 3, Table 2.7).

Two replicates of 1,2-phenoxyethyl oxirane carboxylation under open circuit conditions after 5 hours (entries 4 and 5, Table 2.7) were examined in order to compare with other condition reactions of the same starting material.

The urge of attempting carboxylation of epoxides without electrodes was even stronger after these results, so a series of experiments at low concentration were carried out and are explained below.

2.6.4 Carboxylation of epoxides (No Electrodes)

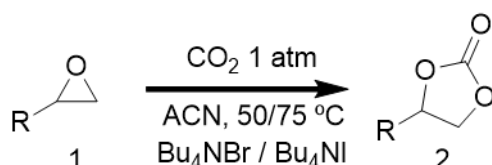
Three different ranges of concentrations of reactants were studied under No Electrodes conditions (dilute reactions from 0.02 to 0.26 M, concentrated reactions from 1 to 20 M, and neat conditions). The general procedures are described in section 4.6.2.6.

2.6.4.1 Dilute reactions

Procedure of reaction on entry 16 of Table 2.8:

Epoxide (1f, 0.17 M) was added to a solution of supporting electrolyte (Bu_4NI) (1:1) in acetonitrile and heated to 75 °C. Constant CO_2 flow (1 atm pressure). No electrodes were placed in the solution.

On completion the reaction mixture was concentrated under reduced pressure (in ice bath if required) and EtOAc (5 mL) was added to precipitate Bu_4NI . After precipitation the solid was removed by filtration and the solvent evaporated to afford the corresponding carbonate (42% of 2f evaluated from $^1\text{H NMR}$ spectrum).

Table 2.8.- Carboxylation of epoxides no electrocatalytic.^a

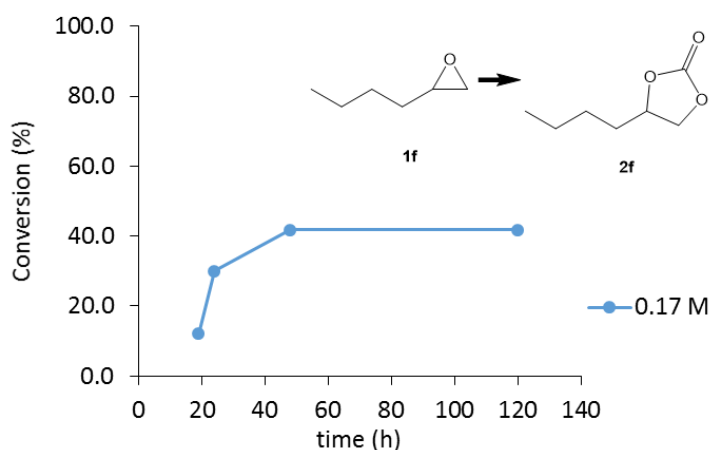
Entry	Catalyst/Epoxide	Temp (°C)	Epoxide (mol/L)	Time (h)	Carbonate ^b (%)
TBABr/ Styrene Oxide (1a)					
1	NE1_3	50	0.02	19	3
2	NE1_3.2	50	0.02	19	1
TBAI/ Styrene oxide (1a)					
3	NE1_3.3a	75	0.02	5	1
4	NE1_3.3b	75	0.02	19	5
Chlorostyrene oxide (1b)					
5	NE2_15a	75	0.04	5	0
6	NE2_15b	75	0.04	24	7
7	NE2_15c	75	**	48	70
Fluorostyrene oxide (1c)					
8	NE3_14a	75	0.05	5	0
9	NE3_14b	75	0.05	24	4
10	NE3_14c	75	**	48	92
1,2-Phenoxymethyloxirane (1e)					
11	NE5_6	50	0.02	19	0
Allyl Glycidyl ether (1g)					
12	NE7_13a	75	0.04	24	5
13	NE7_13b	75	0.04	48	7
1,2-Epoxyhexane (1f)					
14	NE6_9a	75	0.17	19	12
15	NE6_9b	75	0.17	24	30
16	NE6_9c	75	0.17	48	42
17	NE6_9d	75	0.17	120	42

^aGeneral reaction conditions: Bu₄NI supporting electrolyte, starting material (1:1), in Acetonitrile, at 75 °C. ^bConversion calculated from ¹H NMR. ** Solution dried off during overnight CO₂ gas flow.

A series of experiments carried out without electrodes is presented in Table 2.8. Styrene oxide was dilute in acetonitrile in the presence of TBABr (entries 1 and 2), or TBAI (entries 3 and 4), heated up to 50 or 75 °C at a concentration of 0.02 M and CO₂ was supplied from a cylinder for 19 hours. Low conversion to styrene carbonate took place under these conditions (less than 4.7%).

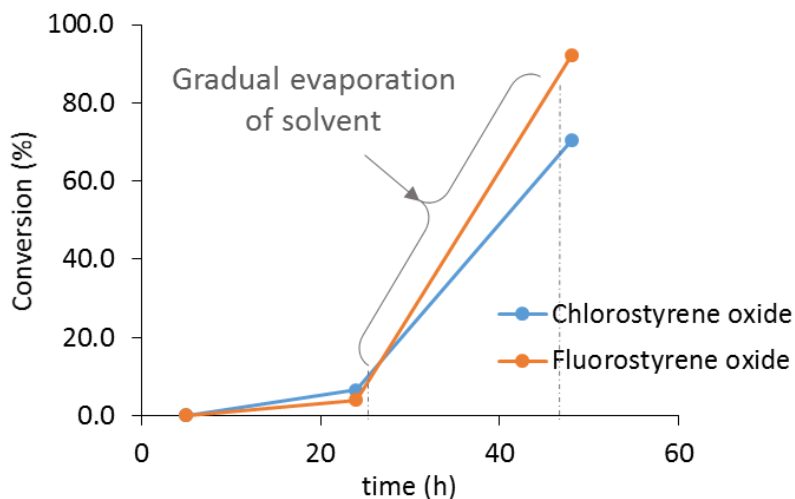
Allyl glycidyl ether at 0.04 M, 75 °C was transformed to its corresponding cyclic carbonate only in 7.4% after 48 hours (entry 13). 1,2-Phenoxymethyloxirane did not produce any carbonate after 19 hours (entry 11).

1,2-Epoxyhexane was used as starting material under these conditions, at 0.17 M concentration at 75 °C (entries 14 to 17, Table 2.8). Graph 2.33 shows the carboxylation conversion trend of this epoxide during 120 hours of reaction which reached a maximum of 42% after 48 hours of reaction.



Graph 2.33.- 1,2- Epoxyhexane carboxylation under no electrodes conditions.

In the case of chlorostyrene oxide and fluorostyrene oxide reactions (entries 5 to 10, Table 2.8) very low conversion (< 7%) was observed after 24 h of reaction at a concentration of 0.04 M, however, when the solvent was accidentally evaporated overnight the conversion rose to 70% and 92% respectively (Graph 2.34). This accidental evaporation took place due to the instability of the CO₂ supply system when room temperature dropped overnight and gas pressure changed allowing a lot more gas flow passing through the cell and dragging the solvent vapours.



Graph 2.34.- Synthesis of chlorostyrene and fluorostyrene carbonate when accidental evaporation of solvent happened.

When the determination of the percentage conversion was made on the $^1\text{H-NMR}$ spectrum of the crude reaction mixture, signals from the Bu_4NI and the epoxide and carbonate were compared to confirm that no starting material was evaporated with the solvent (unlike styrene oxide which is volatile under reduced pressure and ambient temperature), so ratios were still (1:1) : ([epoxide + carbonate] : Bu_4NI). See example on Figure 2.6.

The integration for the methyl groups in Bu_4NI is set at 12 (3 protons x 4 methyl groups = 12 protons in 1 molecule) and the sum of the integral values of one proton corresponding to the starting material and one proton corresponding to the product gives a total value of 1 (0.70 + 0.30 = 1).

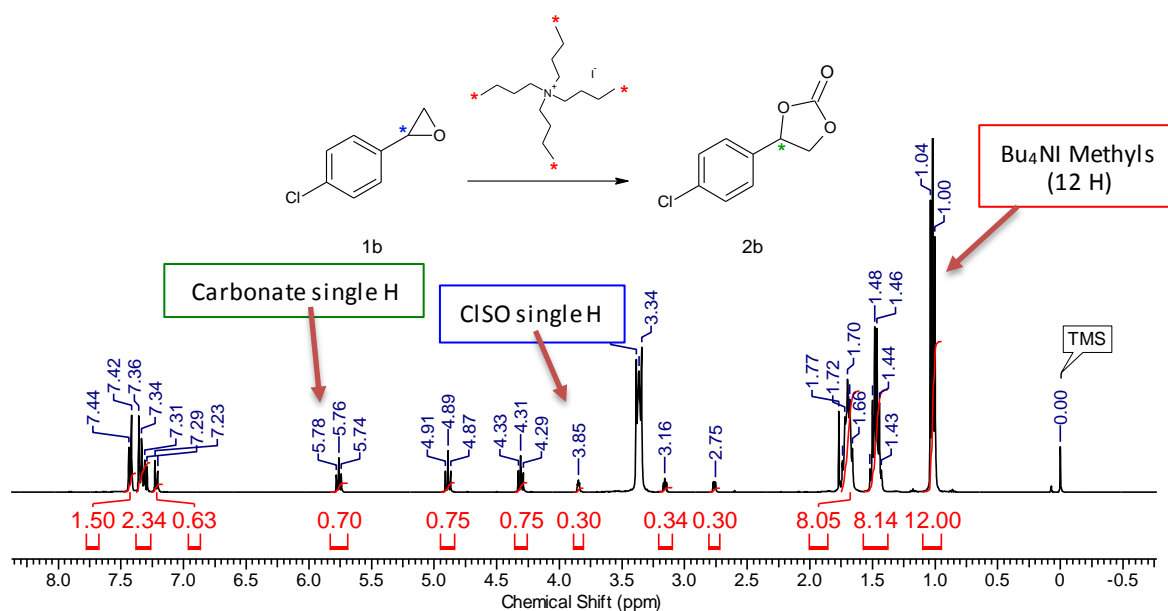


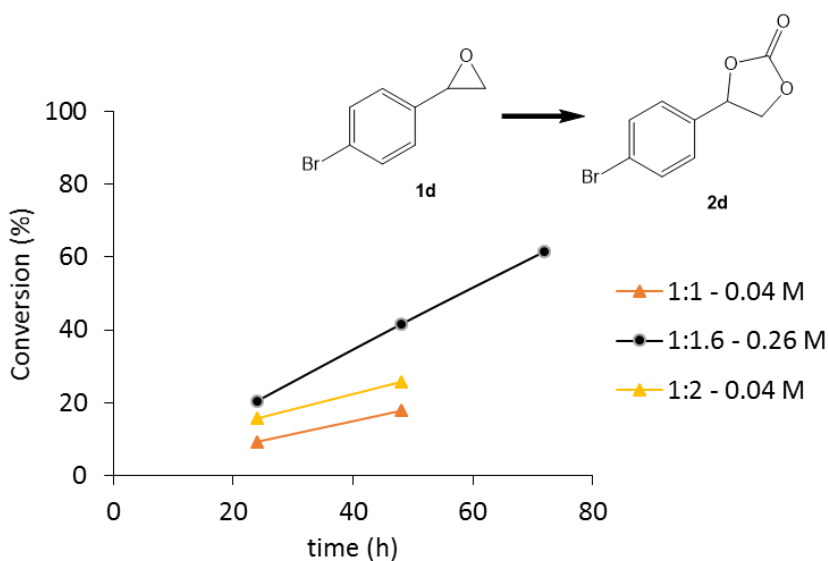
Figure 2.6.- $^1\text{H-NMR}$ of crude of chlorostyrene oxide carboxylation (CISO) reaction after 48 hours. Integrals related to 12 protons from the methyls from Bu_4NI . Tetramethyl silane (TMS) as reference.

In a controlled experiment previously carried out in order to elucidate the implications of the variables of concentration and ratio between epoxide and ammonium salt, the importance of concentration over the ratio was clear. Table 2.9 presents the results of this experiment and Graph 2.35 shows its representation.

Table 2.9.- Study of concentration and catalyst ratio in bromostyrene oxide carboxylation.

Entry	Epoxide	Ratio (1d:TBAI)	Epoxide (mol/L)	Time (h)	Carbonate (%)
Bromostyrene oxide					
1	NE4_11a	1:1	0.04	24	9.3
2	NE4_11b	1:1	0.04	48	17.8
3	NE4_10a	1:1.6	0.26	24	20.5
4	NE4_10b	1:1.6	0.26	48	41.5
5	NE4_10c	1:1.6	0.26	72	61.5
6	NE4_12a	1:2	0.04	24	15.7
7	NE4_12b	1:2	0.04	48	25.7

^aGeneral reaction conditions: bromostyrene oxide as starting material, Bu₄Ni supporting electrolyte, (1a:TBAI) ratio, in Acetonitrile, at 75 °C.



Graph 2.35.- Bromostyrene oxide carboxylation in acetonitrile in the presence of TBAI at different ratios and concentrations.

In this set of experiments, two different ratio (1:1 and 1:2) of the same concentration of bromostyrene oxide reaction and TBAI catalyst were carried out (Table 2.9, entries 1 and 2 (orange line in Graph 2.35); entries 6 and 7 (yellow line in Graph 2.35)) showing better performance when TBAI was double than bromostyrene oxide. The slope of the reaction (reaction rate) did not vary noticeable though.

However, a third experiment of a ratio equal to 1:1.6, which results were expected to fall between the 1:1 and 1:2 reaction results, performed a lot better due to the higher concentration of the reactants that was 5 times more concentrated.

These promising results on rising the concentration of bromostyrene oxide (and the posterior accidentally evaporation of the solvent of chlorostyrene oxide and fluorostyrene oxide carboxylation reactions) led to the experimental design of a highly improved experimental method for carboxylation of epoxides without involving electrodes or any other catalyst than the ammonium salt.

2.6.4.2 MgCO₃ and MgBr₂ as cocatalyst for cyclic carboxylation of epoxides

If the reaction with no electrocatalyst does not evolve or performs very poorly at low concentrations as it has been discussed in the previous section of background reactions, one might wonder what the mechanism involved in the reaction is that activates the carboxylation of epoxides (even at low concentrations) when electrodes are used. Some experiments trying to elucidate this mechanism were carried out and are explained below.

From the observation of the Magnesium electrode being a sacrificial anode and the formation of an inorganic solid (not soluble in any of the usual solvents) in solution, one of the reaction catalysts hypothesis of the electrocarboxylation of epoxides with Mg and Cu as electrodes was that Mg metal reduced to Mg²⁺ and formed MgCO₃ (with CO₂ in solution) and/or MgBr₂ (with free bromide in solution coming from the N-tetrabutylammonium bromide). In order to confirm the catalytic activity of this specie in the carboxylation of epoxides, MgCO₃ and MgBr₂ were added to a solution of styrene oxide.

All attempts to produce the cyclic carbonate through these added Mg²⁺ to solution failed as seen in Table 2.10. One of the main obstacles for these reactions to take place was the low solubility of the inorganic cocatalysts (MgCO₃ and MgBr₂) in acetonitrile.

Procedure of reaction on entry 1 of Table 2.10:

Styrene oxide (0.1 mmol) was dissolved in acetonitrile (60 mL) and heated to 50 °C. One equivalent of different catalyst/cocatalyst were tested as detailed in the table below. One reaction contained 0.1 mmol of MgBr₂ and CO₂ was supplied with a balloon at atmospheric pressure. Another reaction was carried out with N-tetrabutylammonium bromide (0.1 mmol) and MgCO₃ (0.1 mmol) that were added to the reaction mixture, however no CO₂ was supplied during

the reaction. Entry 3 contained all three catalysts under study, N-tetrabutylammonium bromide (0.1 mmol), MgBr_2 (0.1 mmol) and MgCO_3 (0.1 mmol), but no CO_2 was supplied. And entry 4 contained MgBr_2 (0.1 mmol) and MgCO_3 (0.1 mmol), no CO_2 was supplied to the reaction. ^1H NMR analysis were carried out after 19 hours of reaction. 0% of conversion to carbonate 2a for all attempts.

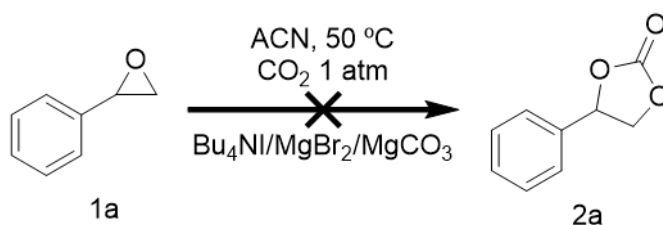


Table 2.10.- MgCO_3 and MgBr_2 presumed catalytic activity test.^a

Entry	Catalyst / Epoxide	Cocatalyst	Temp (°C)	Epoxide (mol/L)	Time (h)	Carbonate ^b (%)
TBABr						
1	Styrene Oxide	MgBr_2	50	0.02	19	0
2	Styrene Oxide	MgCO_3	50	0.02	19	0
3	Styrene Oxide ^c	$\text{MgCO}_3/\text{MgBr}_2$	50	0.02	19	0
4	Styrene Oxide	$\text{MgCO}_3/\text{MgBr}_2$	50	0.02	19	0
TBAI						
5	Styrene Oxide	MgBr_2	75	0.02	19	0
6	Styrene Oxide ^d	MgBr_2	75	0.02	19	0
7	1,2-Phenoxymethyloxirane	MgBr_2	50	0.02	19	0
8	1,2-Epoxyhexane	MgBr_2	75	0.02	168	0

^aGeneral reaction conditions: Epoxide starting material and N-tetrabutylammonium bromide or iodide catalyst (ratio 1:1), in Acetonitrile (0.02 M). When MgBr_2 was used as catalyst (entry 1) CO_2 was supplied with a balloon at 1 atm pressure. All reactions were carried out at 50 °C (entries 1-4 and 7) or at 75 °C (entries 5, 6 and 8). ^bEvaluated from ^1H NMR spectrum.

^cRatio of cocatalysts is 1 mmol of MgCO_3 to 0.5 mmol of MgBr_2 . ^dThis reaction is a replicate of entry 5.

2.6.4.3 Concentration Study

A study on the influence of the concentration of epoxide on the performance of the cyclic carboxylation was carried out using 1,2-phenoxymethyl oxirane as starting material.

Procedure of reaction of Table 2.11:

1,2-Phenoxymethyloxirane (1e, 0.1M) was added to a solution of the catalyst (Bu_4NI) in acetonitrile at a 1 to 1 ratio previously heated to 75 °C. Reactions were run at concentrations of 0.1, 0.5, 1.0 and 2.0 M. CO_2 atmosphere (1 atm pressure) was maintained with balloons. No

electrodes were placed in the solution. ^1H NMR analysis of the aliquots were made at 5 hours and 24 hours of reaction.

Table 2.11 and Graph 2.36 show the results of this study. It is important to notice that the reaction carried out at 2.0 M concentration of epoxide (entry 4, Table 2.11; yellow square in Graph 2.36) had completed the conversion to carbonate when the sample was analysed under ^1H NMR after 24 hours, but the reaction time to reach 100% carbonate is probably less than 24 hours. However, at this concentration, TBAI was not completely soluble in acetonitrile at 75 °C so the final ratio is 1 of epoxide to < 1 of catalyst. It can be appreciated that for the rest of the series (entries 2 to 4) the reaction rate increases with increasing concentration of epoxide.

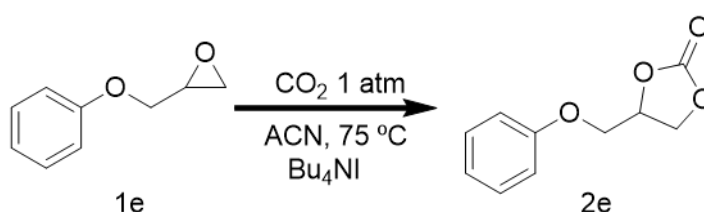
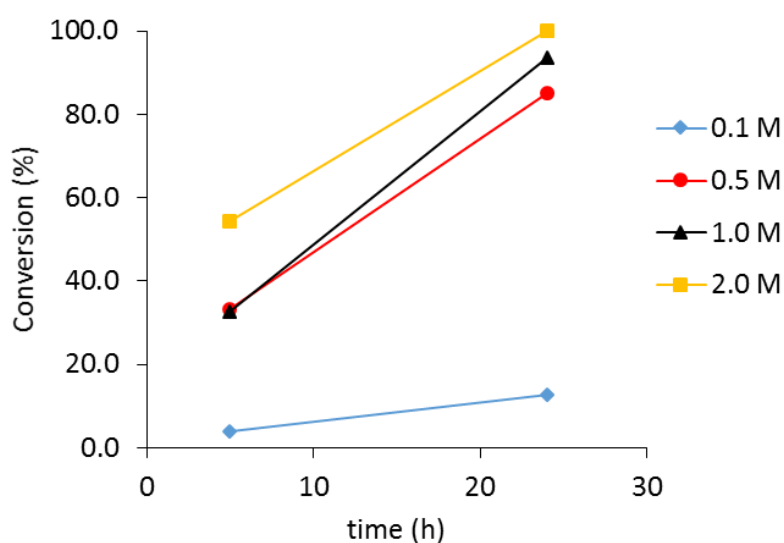


Table 2.11.- Molarity study of the cyclic carboxylation of 1,2-phenoxymethyl oxirane reaction.^a

Entry	1,2-Phenoxymethyloxirane Concentration (mol/L)	Carbonate ^b (%)	
		5 h	24 h
1	0.1	3.8	12.7
2	0.5	33.3	85.0
3	1.0	32.7	93.5
4	2.0 ^c	54.3	100.0

^aGeneral reaction conditions: Bu_4NI catalyst, 1 mmol of 1,2-phenoxymethyloxirane starting material (1:1), in Acetonitrile, 1 atm pressure of CO_2 , at 75 °C. ^bEvaluated from ^1H NMR spectrum. ^cCatalyst did not dissolve completely.



Graph 2.36.- Molarity study of 1,2-phenoxymethyl oxirane carboxylation. Data from Table 2.11.

2.6.4.4 High concentrate cyclic carboxylation reactions

As a result of the initial concentration screening experiments, it was confirmed that higher concentration led to increasing the rate of the reaction and a ratio 1:1 was preferred among other ratios. In the process it was also found that 1 M was the concentration at which acetonitrile gets saturated of N-tetrabutylammonium iodide at 75 °C. Due to this limitation the concentration chosen to be to improve the cyclic carboxylation experimental procedure was 1 M and the ratio of epoxide to ammonium salt of 1 to 1. The general procedure of this set of reactions can be found on section 4.6.2.8.3 and the results are presented below.

Procedure of reaction on entry 2 of Table 2.12:

Epoxide (1a, 10 M) was added to a concentrate solution of supporting electrolyte (Bu₄NI, 1 M) in acetonitrile and heated to 75 °C. No electrodes were placed in the solution.

On completion the reaction mixture was concentrated under reduced pressure (in ice bath if required) and EtOAc (5 mL) was added to precipitate Bu₄NI. After precipitation the solid was removed by filtration and the solvent evaporated to afford the corresponding carbonate (28% of 2a after 24 hours, evaluated from ¹H NMR spectrum).

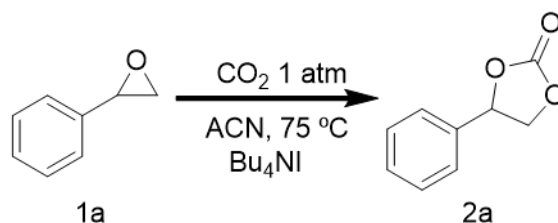
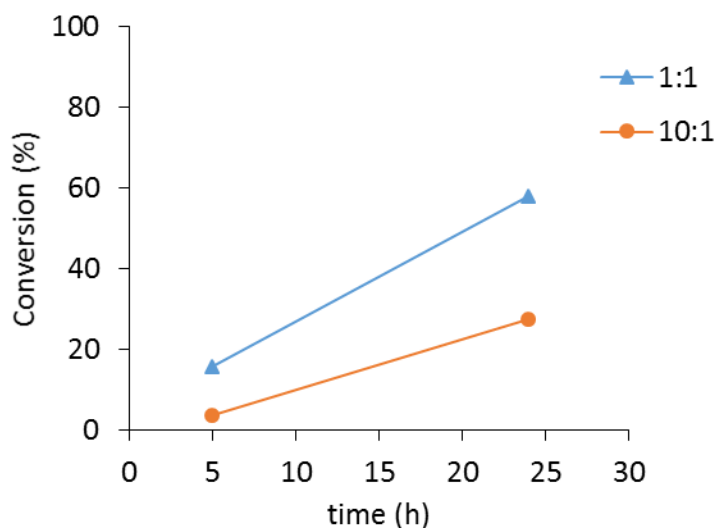


Table 2.12.- Cyclic carboxylation at high concentration of styrene oxide and N-tetrabutylammonium iodide in acetonitrile.^a

Entry	Styrene oxide (mol/L)	TBAI (mol/L)	Carbonate ^b (%)	
			5 h	24 h
1	1.0	1.0	15.8	58
2	10.0	1.0	3.6	28

^aGeneral reaction conditions: Bu₄NI catalyst (1 M) and styrene oxide as starting material at ratio 1:1 (entry 1); ratio 10:1 (entry 2) in Acetonitrile, 1 atm pressure of CO₂ supplied with balloon, at 75 °C. ^bEvaluated from ¹H NMR spectrum.



Graph 2.37.- Styrene carbonate synthesis with TBAI in acetonitrile at 1 M concentration.

Chlorostyrene carbonate synthesis among others was carried out using two different sources of carbon dioxide. A gas flow was used in the reaction in entry 1 of Table 2.13 and a balloon was used in entries 2 and 3 in order to compare performances. It was confirmed, with a similar calculation than the one explained in page 190 on the ^1H NMR integrals that no chlorostyrene oxide had been evaporated while gas flow was used.

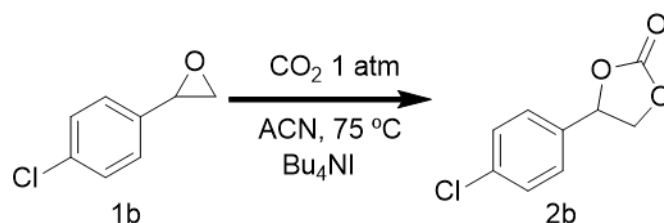
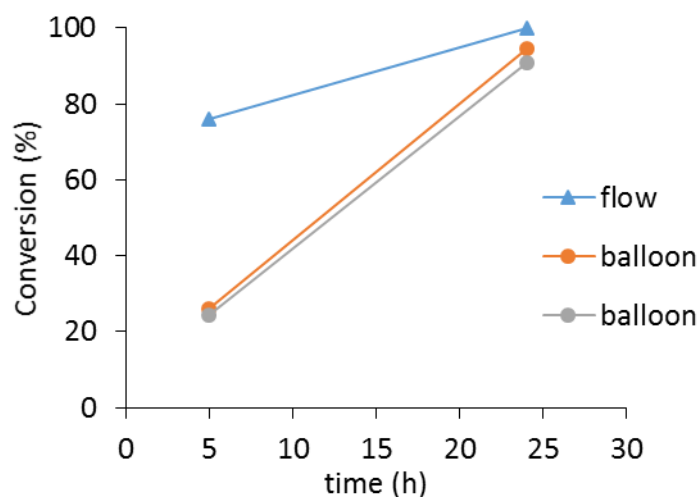


Table 2.13.- Cyclic carboxylation at high concentration of chlorostyrene oxide and N-tetrabutylammonium iodide in acetonitrile.^a

Entry	Chlorostyrene oxide (mol/L)	Carbonate ^b (%)		CO ₂
		5 h	24 h	
1 ^d	1.0	76	100	flow
2	1.0	26	95	Balloon
3	1.0	24	91	Balloon

^aGeneral reaction conditions: Bu₄NI catalyst (1 M) and chlorostyrene oxide (1 M) as starting material in acetonitrile, 1 atm pressure of CO₂, at 75 °C. ^bEvaluated from ^1H NMR spectrum. ^dEntry 1 was carried out using a source of CO₂ gas flow to the reaction.



Graph 2.38.- Chlorostyrene carbonate synthesis with TBAI in acetonitrile at 1 M concentration.

Fluorostyrene oxide carboxylation was also selected to compare performances of the reaction with CO₂ gas flow and CO₂ balloon. Table 2.14 and Graph 2.39 show the results of the two replicates of each technique.

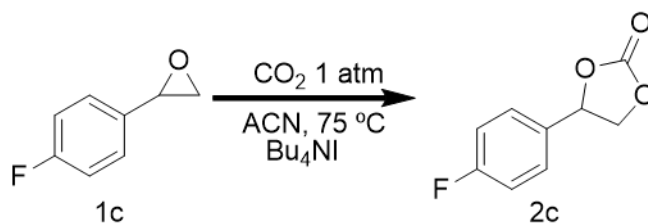
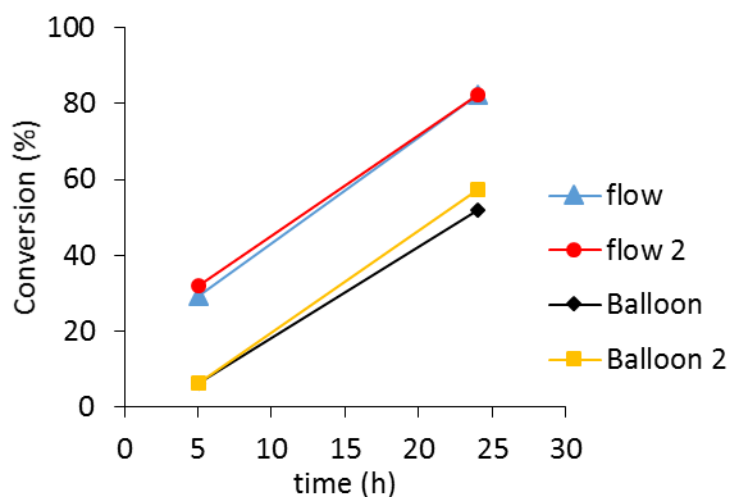


Table 2.14.- Cyclic carboxylation at high concentration of fluorostyrene oxide and N-tetrabutylammonium iodide in acetonitrile.^a

Entry	Fluorostyrene oxide (mol/L)	Carbonate ^b (%)		CO ₂
		5 h	24 h	
1	1.0	29	82	flow
2	1.0	32	82	flow
3	1.0	6	52	Balloon
4	1.0	6	57	Balloon

^aGeneral reaction conditions: Bu₄NI catalyst (1 M) and fluorostyrene oxide (1M) as starting material in acetonitrile, 1 atm pressure of CO₂ (CO₂ flow in reactions on entries 1 and 2 and CO₂ balloon in reactions on entries 3 and 4), at 75 °C.

^bEvaluated from ¹H NMR spectrum.



Graph 2.39.- Fluorostyrene carbonate synthesis with TBAI in acetonitrile at 1 M concentration.

Bromostyrene oxide carboxylation reaction is next to be analysed. Table 2.15 and Graph 2.40 collect the data obtained in this experiment. It's important to notice that when gas flow was used to supply CO₂ (entry 1 of Table 2.15, blue square in Graph 2.40), the reaction probably finished before the sample was taken after 24 hours.

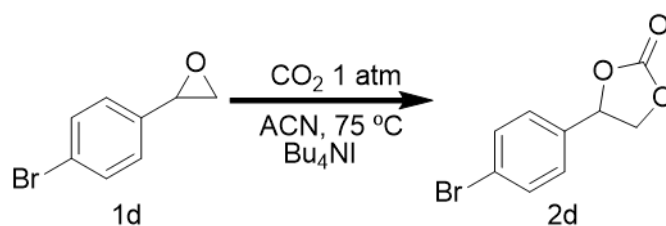
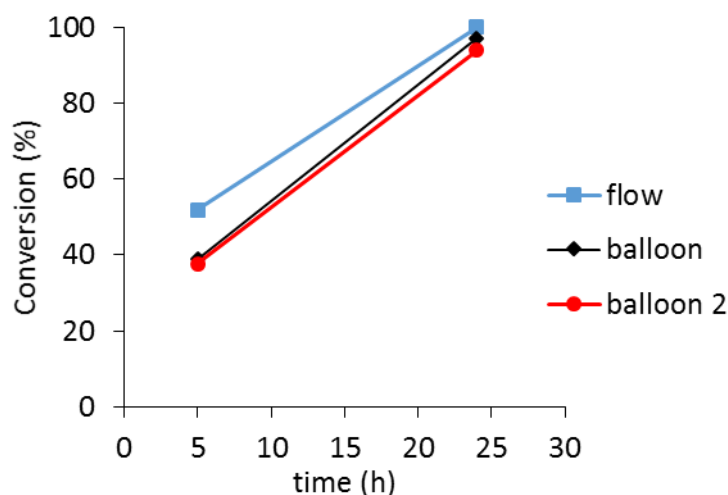


Table 2.15.- Cyclic carboxylation at high concentration of bromostyrene oxide and N-tetrabutylammonium iodide in acetonitrile.^a

Entry	Bromostyrene oxide (mol/L)	Carbonate ^b (%)		CO ₂
		5 h	24 h	
1	1.0	52	100	flow
2	1.0	39	97	Balloon
3	1.0	38	94	Balloon

^aGeneral reaction conditions: Bu₄Ni catalyst (1 M) and bromostyrene oxide (1M) as starting material in acetonitrile, 1 atm pressure of CO₂ (CO₂ flow in reactions on entry 1 and CO₂ balloon in reactions on entries 2 and 3), at 75 °C.

^bEvaluated from ¹H NMR spectrum.



Graph 2.40.- Bromostyrene carbonate synthesis with TBAI in acetonitrile at 1 M concentration.

1,2-Phenoxymethyl oxirane was selected among the rest of the chemicals to be the reactant of a series of experiments designed in order to study different variables of the cyclic carboxylation reaction of epoxides. This chemical was chosen due to its considerably lower toxicity and price and the easy purification of the corresponding carbonate (4-(phenoxymethyl)-1,3-dioxolan-2-one).

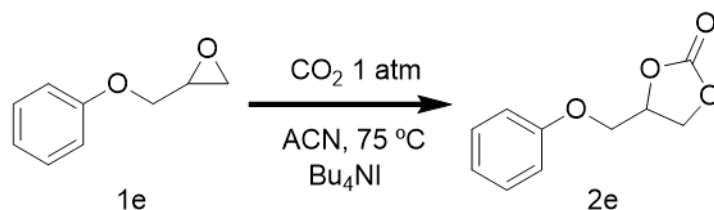
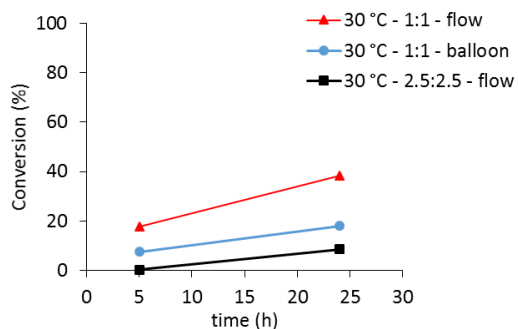


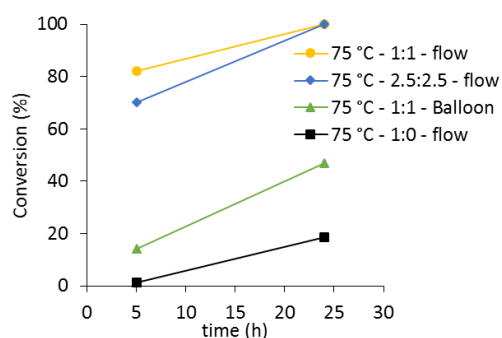
Table 2.16.- Cyclic carboxylation at high concentration of 1,2-phenoxymethyl oxirane and N-tetrabutylammonium iodide in acetonitrile at ratio 1:1.^o

Entry	T (°C)	Epoxide (mol/L)	TBAI (mol/L)	Carbonate ^b (%)		CO ₂
				5 h	24 h	
1	30	1.0	1.0	8	18	balloon
2	30	1.0	1.0	18	39	flow
3	30	2.5	2.5 ^c	0.2	9	flow
4	75	1.0	0.0	1	18	flow
5	75	1.0	1.0	82	100	flow
6	75	2.5	2.5 ^c	70	100	flow
7	75	1.0	1.0	14	47	balloon

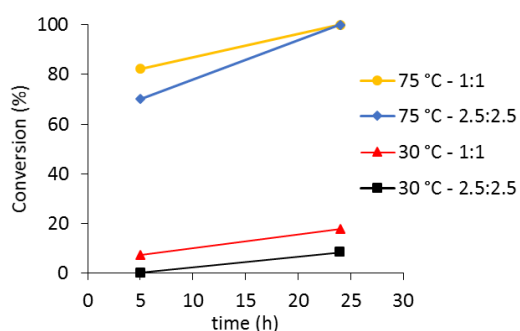
^oGeneral reaction conditions: Bu₄NI catalyst and fluorostyrene oxide as starting material in Acetonitrile, 1 atm pressure of CO₂, at 75 °C. ^bEvaluated from ¹H NMR spectrum.



Graph 2.41.- 1,2-Phenoxymethyl oxirane carboxylation at 30 °C at different concentrations and with different CO₂ supplies.



Graph 2.42.- 1,2-Phenoxymethyl oxirane carboxylation at 75 °C at different concentrations and with different CO₂ supplies.



Graph 2.43.- 1,2-Phenoxymethyl oxirane carboxylation at 30 and 75 °C at different concentrations.

Reactions at 30 °C are represented in Graph 2.41, showing a better performance when CO₂ gas flow was used at 1 M concentration. The fact that 2.5 M reaction produces less carbonate in comparison is again due to the low solubility of TBAI in acetonitrile. This affect directly to the proportion of epoxide and ammonium salt in solution, increasing the first in relation to the second.

Reactions at 75 °C are plotted in Graph 2.42 showing the same behaviour regarding CO₂ source and concentration. A background reaction with no ammonium salt was carried out (entry 4, Table 2.16) producing a total of 18% of carbonate after 24 hours of reaction.

Performance increases considerably in comparison with the reactions carried out at 30 °C (up to 82% more after 5 hours) as seen in Graph 2.43.

Next, 1,2-epoxyhexane carboxylation with TBAI in acetonitrile at 1 M concentration is summarized in Table 2.17 and Graph 2.44. Similar trends than the ones previously explained happen.

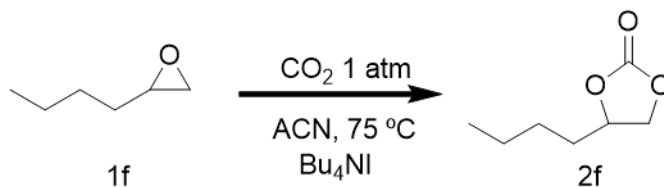
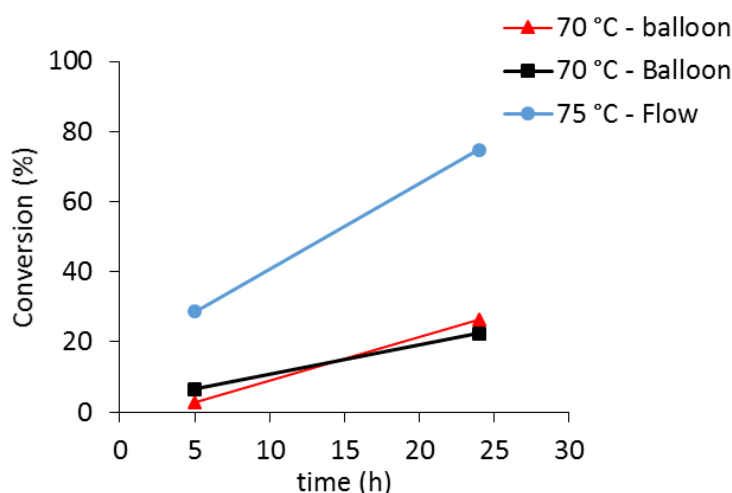


Table 2.17.- Cyclic carboxylation at high concentration of 1,2-epoxyhexane and N-tetrabutylammonium iodide in acetonitrile.^o

Entry	T (°C)	Epoxide (mol/L)	TBAI (mol/L)	Carbonate ^b (%)		CO ₂
				5 h	24 h	
1	75	1.0	1.0	29	75	flow
2	70	1.0	1.0	3	27	balloon
3	70	1.0	1.0	7	23	balloon

^oGeneral reaction conditions: Bu₄NI catalyst (1 M) and fluorostyrene oxide (1M) as starting material in Acetonitrile, 1 atm pressure of CO₂ (CO₂ flow in reaction on entry 1 and CO₂ balloon in reactions on entries 2 and 3), at 75 °C.

^bEvaluated from ¹H NMR spectrum.



Graph 2.44.- 1,2-Epoxyhexane cyclic carboxylation with TBAI in acetonitrile (1 M) at 70 and 75 °C.

Reactions at higher concentrations (1 M or higher) were carried out with different CO₂ source. When a direct flow from the CO₂ cylinder was flushed through the cell reaction rates always performed better, especially after 5 hours of reaction, than when CO₂ was supplied by a balloon that was refilled as needed (expect overnight, when the balloon was left until the next day). This could be due to the fact that when heating at 75 °C the pressure in the cell is positive towards outside due to partial evaporation of the solvent. That means that the CO₂ contained in the

balloon is coming to the cell at a lower rate. If instead the CO₂ is flushed with a constant flow rate, the concentration of CO₂ will be maintained. The fact that some solvent can evaporate out of the cell with the CO₂ flow, means that the actual concentration of species in solution when CO₂ flow is used could be higher than the initial one (usually 1 M). This could be improving the yields as compared to the balloon source. Also, the balloon needle got sometimes solvent condensed inside and had to be emptied in order for the CO₂ to keep flowing (that was accomplished only by applying pressure on the balloon so the solvent would drop back to the reaction mixture).

However, due to the high volatility of styrene oxide the balloon source was chosen to avoid the loss of the starting material and maintained in order to compare with the rest of epoxides performance.

Allyl glycidyl ether (1g) carboxylation produced 100% of carbonate (2g) in less than 24 hours under reaction conditions showed in Table 2.18.

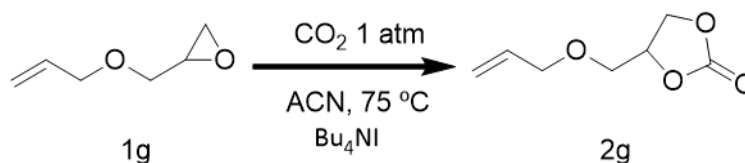
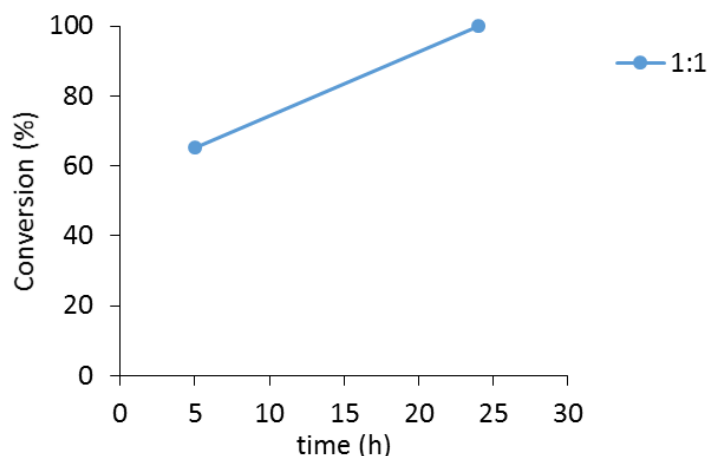


Table 2.18.- Cyclic carboxylation at high concentration of allyl glycidyl ether and N-tetrabutylammonium iodide in acetonitrile.^o

Entry	T (°C)	Epoxide (mol/L)	TBAI (mol/L)	Carbonate (%) ^a	
				5 h	24 h
1	75	1.0	1.0	65	100

^aGeneral reaction conditions: Bu₄NI catalyst (1 M) and fluorostyrene oxide (1M) as starting material in Acetonitrile, 1 atm pressure of CO₂ flow, at 75 °C. ^bEvaluated from ¹H NMR spectrum.



Graph 2.45.- Allyl glycidyl ether cyclic carboxylation with TBAI in acetonitrile (1 M) at 75 °C.

Propylene oxide carboxylation with TBAI at 30 °C in acetonitrile was attempted and results are shown next. The high volatility of the epoxide caused the loss of most of the starting material even with a CO₂ balloon and so the rate of produced carbonate is less than what was initially calculated. The more accurate percentage of conversion presented in Table 2.19 (in the column called *Corrected (%)) was obtained by comparing the integral value of the carbonate to the TBAI integral (used for the calculation as internal standard) in the final ¹H NMR spectrum.

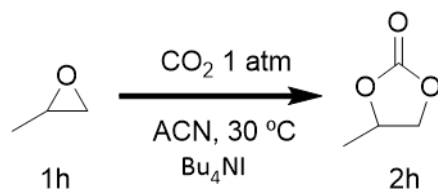


Table 2.19.- Cyclic carboxylation at high concentration of propylene oxide and N-tetrabutylammonium iodide in acetonitrile.^o

Entry	Epoxide (mol/L)	TBAI (mol/L)	Carbonate ^b (%)		*Corrected ^b (%)	
			5 h	24 h	5 h	24 h
1	0.5	1.0	3	19	2	8
2	1.0	1.0	16	81	9	18

^oGeneral reaction conditions: Bu₄NI catalyst (1 M) and propylene oxide (0.5M or 1M) as starting material in Acetonitrile, 1 atm pressure of CO₂ (balloon, as starting material is highly volatile), at 30 °C. ^bEvaluated from ¹H NMR spectrum.

Epichlorohydrin carboxylation with TBAI in acetonitrile at 75 °C developed in a record time producing 90% of carbonate in only 5 hours of reaction (Table 2.20).

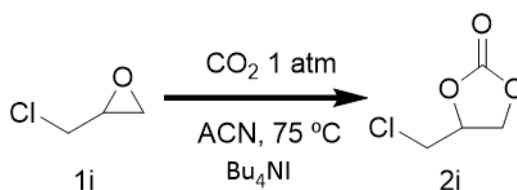


Table 2.20.- Cyclic carboxylation at high concentration of epichlorohydrin and N-tetrabutylammonium iodide in acetonitrile.^o

Entry	Epoxide (mol/L)	TBAI (mol/L)	Carbonate ^b (%)	
			5 h	24 h
1	1.0	1.0	90	100

^oGeneral reaction conditions: Bu₄NI catalyst (1 M) and epichlorohydrin (1M) as starting material in Acetonitrile, 1 atm pressure of CO₂, at 75 °C. ^bEvaluated from ¹H NMR spectrum.

In the case of glycidol carboxylation, the reaction finished even earlier than 5 hours (Table 2.21).

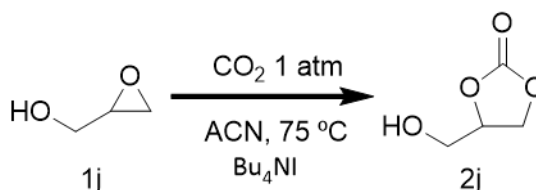


Table 2.21.- Cyclic carboxylation at high concentration of glycidol and N-tetrabutylammonium iodide in acetonitrile.^o

Entry	Epoxide (mol/L)	TBAI (mol/L)	Carbonate ^b (%)	
			5 h	24 h
1	1.0	1.0	100	100

^oGeneral reaction conditions: Bu₄NI catalyst (1 M) and glycidol (1M) as starting material in Acetonitrile, 1 atm pressure of CO₂, at 75 °C. ^bEvaluated from ¹H NMR spectrum.

In order to accurately know the reaction time for glycidol (and for epichlorohydrin) extra experiments were carried out sampling every hour and are detailed in the next section.

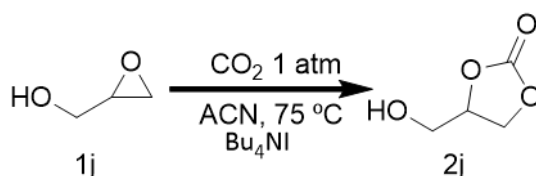
2.6.4.5 Glycidol and epichlorohydrin cyclic carboxylation

As seen in the previously, in Table 2.20 and Table 2.21 epichlorohydrin and glycidol had been completely converted to carbonate after 5 hours of reaction. In order to accurately know the time on completion of the reaction for these two epoxides, further reactions with sampling every hour were carried out.

Procedure of reaction on entry 1 of Table 2.22:

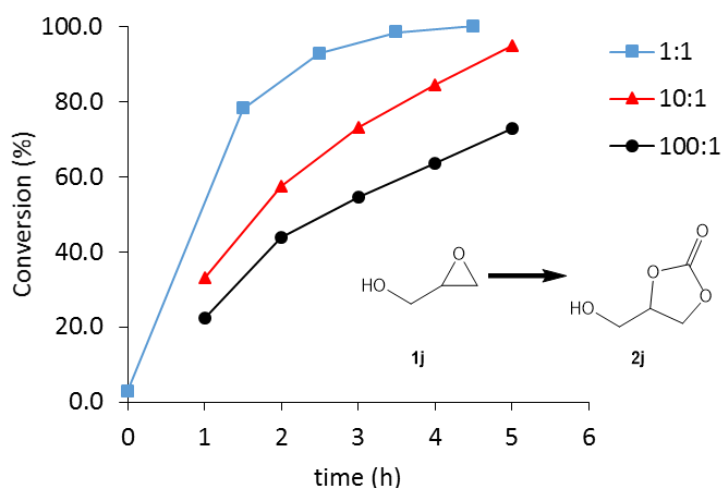
Epoxide (1j, 1 M) was added to a 1 M solution of supporting electrolyte (Bu_4NI) in acetonitrile and heated to 75 °C. CO_2 was supplied with balloons. No electrodes were placed in the solution. On completion the reaction mixture was concentrated under reduced pressure and EtOAc (5 mL) was added to precipitate Bu_4NI . After precipitation the solid was removed by filtration and the solvent evaporated to afford the corresponding carbonate (100% of 2j after less than 5 hours, evaluated from ^1H NMR spectrum).

Table 2.22 shows the results for glycidol cyclic carboxylation reaction with TBAI catalyst in ACN, 75 °C, at different ratios (1:1; 10:1 and 100:1) and reaction times. Graphical representation of the data is shown in Graph 2.46. After 1.5 hours of reaction conversion to carbonate was 78% when ratio epoxide to TBAI was 1:1 (entry 2 of Table 2.22; blue square of Graph 2.46). As it was expected, reaction rate reduced as the ratio increased, although performance was still high obtaining 73% of carbonate after 5 hours of a reaction with a ratio epoxide to catalyst 100:1 (entry 4 of Table 2.22, black circles in Graph 2.46).

Table 2.22.- Glycidol cyclic carboxylation with Bu_4NI .^a

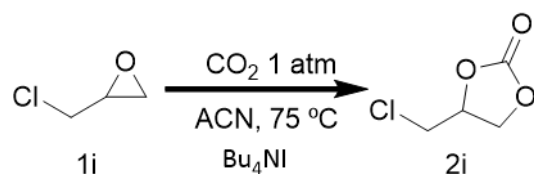
Entry	Glycidol (mol/L)	TBAI (mol/L)	Conversion ^b (%)				
			0 h	1.5 h	2.5 h	3.5 h	5 h
1	1	1					100
2	1	1	3	78	93	98	100
			1 h	2 h	3 h	4 h	5 h
3	10	1	33	58	65	84	95
4	100	1	22	44	55	64	73

^aGeneral reaction conditions: Bu_4NI catalyst (at 1 M concentration) and glycidol as starting material at different ratios, in Acetonitrile, 1 atm pressure of CO_2 , at 75 °C. ^bEvaluated from ^1H NMR spectrum.



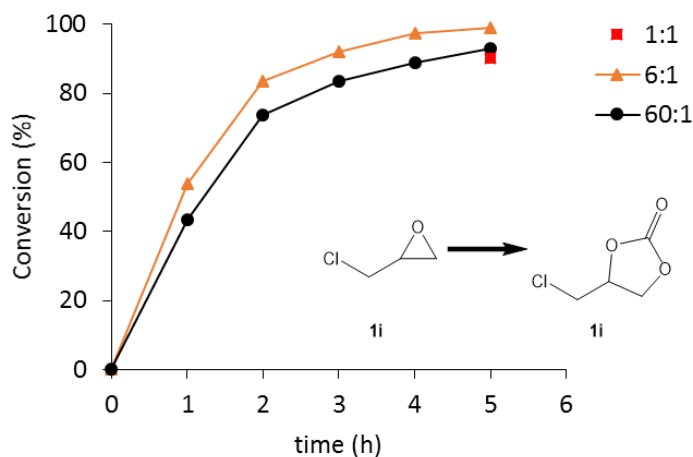
Graph 2.46.- Glycidol cyclic carboxylation with TBAI in ACN at different ratios.

Table 2.23 shows the results for the reactions carried out of epichlorohydrin cyclic carboxylation and graphical representation is presented in Graph 2.47. The behaviour of epichlorohydrin is similar to the glycidol's.

Table 2.23.- Epichlorohydrin cyclic carboxylation with Bu_4NI .^a

Entry	Epichlorohydrin (mol/L)	TBAI (mol/L)	Carbonate ^b (%)					
			1 h	2 h	3 h	4 h	5 h	24 h
1	1	1					90	100
2	6	1	54	84	92	97	99	
3	60	1	44	74	84	89	93	

^aGeneral reaction conditions: epichlorohydrin as starting material at ratios 1:1, 6:1 and 60:1, being Bu_4NI catalyst 1 M concentrated, in Acetonitrile, 1 atm pressure of CO_2 , at 75 °C. ^bEvaluated from ^1H NMR spectrum.



Graph 2.47.- Epichlorostyrene oxide cyclic carboxylation with TBAI in ACN at different ratios.

Carboxylation of glycidol and epichlorohydrin were analysed at 5 hours and 20 or 24 hours by sampling and running ^1H NMR of the crude. For all starting materials that got 100% of conversion at 24 hours the time at which the reaction finished was uncertain as it probably finished overnight but was not tested until the next morning. This was the case of epichlorohydrin and glycidol at 1 M in acetonitrile with TBAI (1:1) that got 100% of conversion to the corresponding carbonate after only 5 hours. Further experiments sampling hourly were carried out at different epoxide:TBAI ratios (1:1 ; 10:1 and 100:1). Again, ratio 1:1 presented a higher conversion rate particularly differentiated for the glycidol carboxylation.

2.6.4.6 Cyclic carboxylation of 3-hydroxyoxetane

3-Hydroxyoxetane was chosen to undergo the improved cyclic carboxylation reaction conditions under four membered rings to produce six membered cyclic carbonates with no success.

Procedure of reaction in Table 2.24:

3-Hydroxyoxetane (1k, 1 M) was added to a 1 M solution of supporting electrolyte (Bu_4NI) in acetonitrile and heated to 75 °C. CO_2 was supplied with balloons. No electrodes were placed in the solution. $^1\text{H NMR}$ analysis were carried out after 5 and 24 hours of reaction with no success.

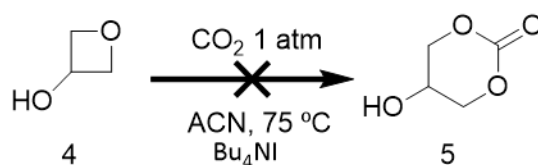


Table 2.24.- 3-hydroxyoxetane cyclic carboxylation with Bu_4NI .^a

Entry	Epoxide	Carbonate ^b (%)	
		5 h	24 h
1	3-hydroxyoxetane	0	0

^aGeneral reaction conditions: Bu_4NI catalyst and 3-hydroxyoxetane as starting material at ratios 1:1, 1 M concentration in Acetonitrile, 1 atm pressure of CO_2 , at 75 °C. ^bEvaluated from $^1\text{H NMR}$ spectrum.

2.6.4.7 NH_4I catalyst for cyclic carboxylation of 1,2-phenoxymethyloxirane

As reported in the literature and previously discussed in the introduction chapter synthesis of cyclic carbonates from olefins was achieved using an electrochemical system with NH_3/I_2 (NH_4^+/I^- electrochemically reduced/oxidized species) as catalyst¹⁵². The aim of this experiment was to test NH_4I as a viable catalyst under the improved cyclic carboxylation reaction conditions.

Procedure of reaction on entry 1 of Table 2.25:

Epoxide (1e, 1 M) was added to a concentrate suspension of catalyst (NH_4I , 1 M) in acetonitrile in a flask that has been previously flushed with CO_2 and heated to 75 °C. CO_2 1 atm pressure was maintained with balloons. No electrodes were placed in the solution. $^1\text{H NMR}$ analysis was carried out after 5 and 24 hours of reaction. (18% of 2e after 24 hours, evaluated from $^1\text{H NMR}$ spectrum).

A second product (1-iodo-3-phenoxypropan-2-ol) was obtained as main product when NH_4I was used together with TBAI in acetonitrile at 75 °C. The halogenated alcohol is probably formed by ring opening of the epoxide with the proton of the ammonium iodide and the subsequent halogenation leaving a molecule of NH_3 free. Background reactions under neat conditions did not produce alcohol and only 1.5% of carbonate after 24 hours of reaction was achieved (entry 5, Table 2.25). When no TBAI was added (entries 3 and 4) the reaction did not produce any carbonate or alcohol.

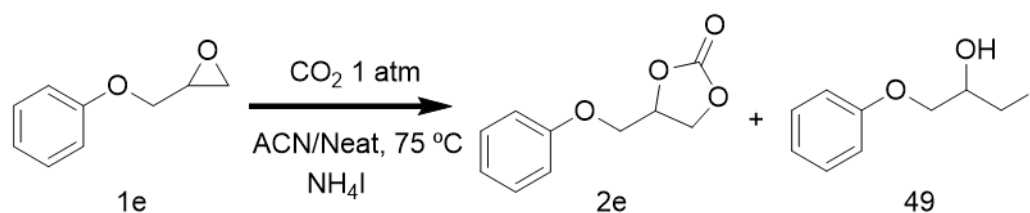
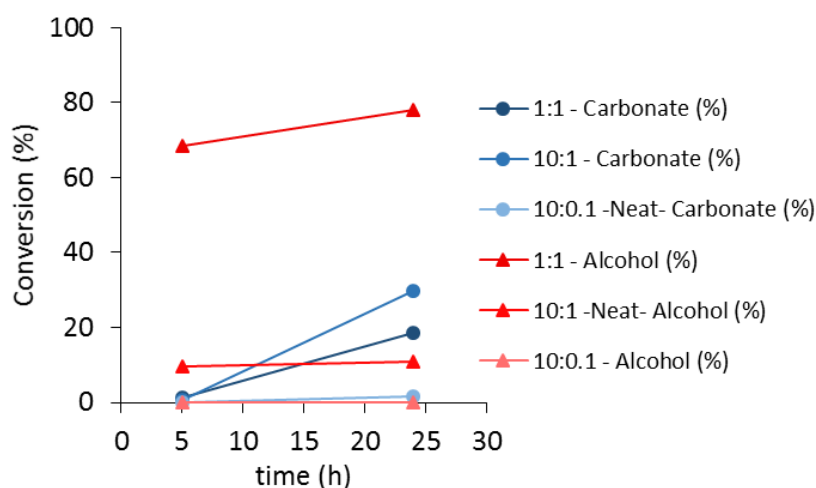


Table 2.25.- NH_4I catalyst for cyclic carboxylation of 1,2-phenoxyethyloxirane.^a

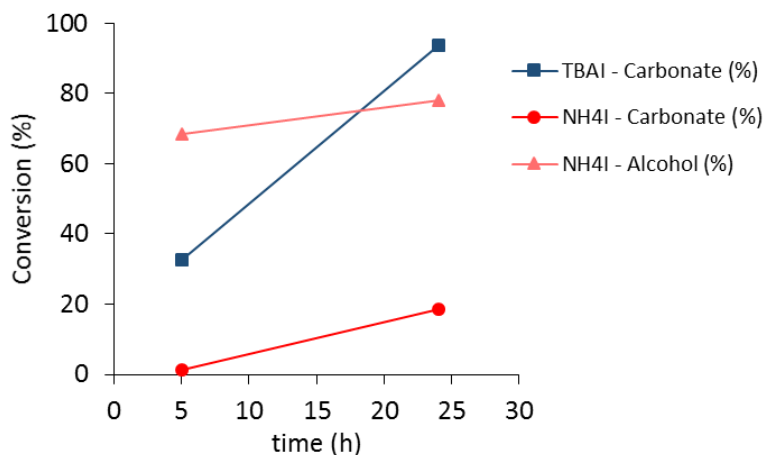
Entry	Epoxide (mmol)	NH_4I (mmol)	Epoxide (mol/L)	Carbonate ^b (%)		Alcohol ^b (%)	
				5 h	24 h	5 h	24 h
1	1.0	1.0	1.0	1	18	69	78
2	10.0	1.0	10.0	1	30	10	11
3	1.0	0.0	Neat	0	0	0	0
4	10.0	0.0	Neat	0	0	0	0
5	10.0	0.1	Neat	0	2	0	0

^aGeneral reaction conditions: 1,2-Phenoxyethyloxirane starting material and NH_4I catalyst (ratios 1:1; 10:1 and 100:1), in Acetonitrile (except entries 5 and 6 which are neat reactions), 1 atm pressure of CO_2 balloon, at 75 °C. ^bEvaluated from ^1H NMR spectrum.



Graph 2.48.- 1,2-Phenoxyethyloxirane carboxylation with NH_4I and TBAI in acetonitrile at 75 °C.

Graph 2.49 shows the comparison of carbonate conversions using ammonium iodide results (red-circle and pink-triangle) against the carboxylation of 1,2-phenoxy methyl oxirane with TBAI (blue-square).



Graph 2.49.- Comparison of two catalysts for carboxylation of 1,2-phenoxymethyl oxirane.

2.6.4.8 Study of enantioselectivity of cyclic carboxylation of (S)-1,2-phenoxymethyloxirane

An interesting aspect of the reaction to be studied is the stereogenic centre of the molecule located in the carbon number 2 to which the epoxide and the R group are bonded. One of the questions to be answered about the mechanism of the reaction is if the epoxide opens by breaking the bond to the chiral or to the non-chiral carbon.

An experiment using (S)-1,2-phenoxymethyl oxirane was carried out (Table 2.26) in order to analyse the reaction products by chiral HPLC. The analysis showed that an enantiomerically pure carbonate was produced from enantiomerically pure epoxide (Image 2.1 and Image 2.2). The racemic 1,2-phenoxymethyl oxirane form was previously used as a reactant (entry 5 of Table 2.16) and chiral HPLC analysis of the starting material and the product (Image 2.3 and Image 2.4) show the two peaks corresponding to the R and S forms. HPLC analysis of a mixture of (S) and (±)-4-(phenoxymethyl)-1,3-dioxolan-2-one was also carried out in order to confirm the origin of the peaks (Image 2.5).

Procedure of reaction on entry 1 of Table 2.26:

Epoxide (**1**, 3.6 M) was added to a 1 M solution catalyst (Bu_4NI) in acetonitrile in a flask that has been previously flushed with CO_2 and heated to 75 °C. CO_2 1 atm pressure was maintained with balloons. No electrodes were placed in the solution.

On completion the reaction mixture was concentrated under reduced pressure and EtOAc (5 mL) was added to precipitate Bu_4NI . After precipitation the solid was removed by filtration and the solvent evaporated to afford the corresponding carbonate (100% of conversion of **2** after 24 hours, evaluated from $^1\text{H NMR}$ spectrum).

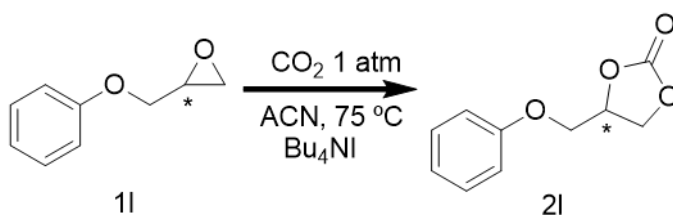


Table 2.26.- Enantiomeric study of the cyclic carboxylation reaction of (*S*)-1,2-phenoxymethyl oxirane.^a

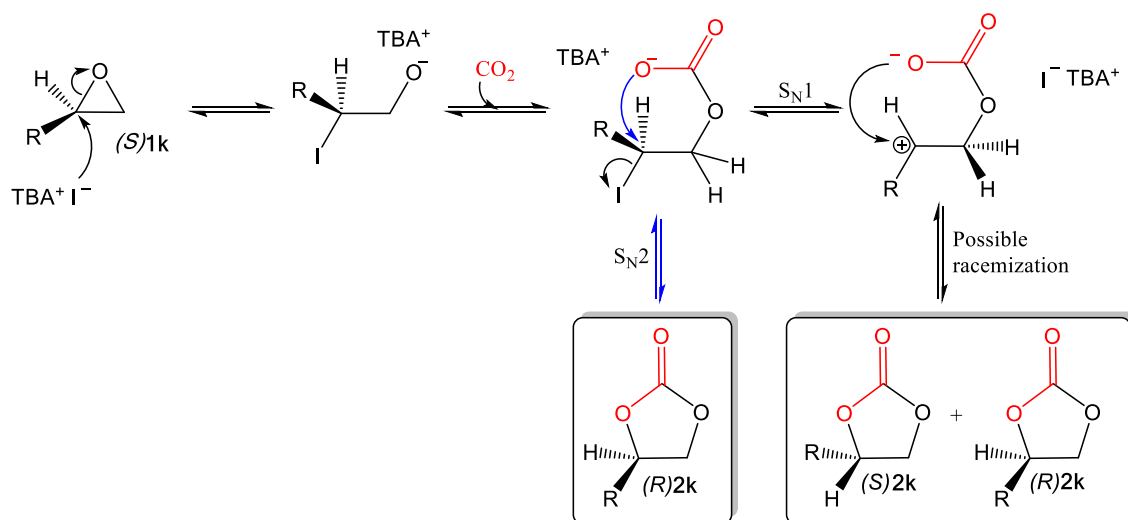
Entry	Epoxide (mol/L)	TBAI (mol/L)	Carbonate ^b (%)	
			5 h	24 h
1	3.6	1.0	31	100

^aGeneral reaction conditions: (*S*)-1,2-phenoxymethyl oxirane and 1M Bu_4NI catalyst in acetonitrile, 1 atm pressure of CO_2 (flow), at 75 °C. ^bEvaluated from $^1\text{H NMR}$ spectrum.

By adding the product of the carboxylation of (*S*)-phenoxymethyl oxirane to the product obtained from the reaction of the form (\pm) and analysing the mixture (Image 2.5) it is confirmed that the second peak appearing at 49 min in the mixture corresponds to the product formed from epoxide (*S*). Nevertheless, the enantiomeric form (*R* or *S*) of the carbonate cannot be known from this experiment. In order to find it out through this technique, a commercial pattern of one of the enantiomers of 4-(phenoxymethyl)-1,3-dioxolan-2-one should be analysed and the retention time compared with the sample's at the same chromatographic conditions. A usually more accessible way to test the chirality of the product is to determine its specific rotation of light and compare it with the reported data for the pure product in literature ($[\alpha]_D^{25} = +5.46^\circ$; $c = 0.39$ in EtOH)¹⁶³.

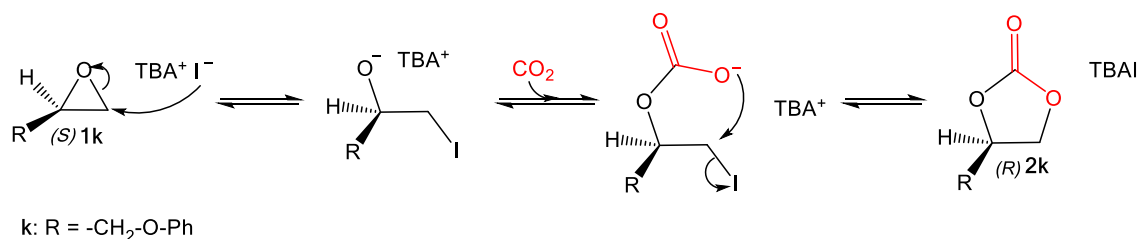
When considering the mechanism of the reaction, two possible routes exist. One would take place if the iodide bonds the chiral carbon (Scheme 2.2) and the other one if bonds the non-chiral carbon (Scheme 2.3).

If the chiral carbon plays an active role in the reaction mechanism, then two different outcomes can happen depending on the mechanism of CO₂ insertion. This is, if the reaction mechanism is stepwise (S_N1), and the new bond takes place between the chiral carbon and the oxygen of the CO₂, then racemization could occur when the carbocation is formed on the first step of breaking bonds and the final product could be a mixture of enantiomeric carbonates, (*R*) and (*S*). If the reaction goes through one transition state where old bonds break and new bonds form simultaneously (S_N2), then the stereochemistry would be maintained (as it would be 100% inverted twice, first due to the insertion of the iodide and ring opening, and second due to the insertion of carbonate). However, the final carbonate becomes (*R*) in this case (**2k**) due to reorganization of the preference in nomenclature of the Cahn–Ingold–Prelog priority rules to determining the stereo configuration.

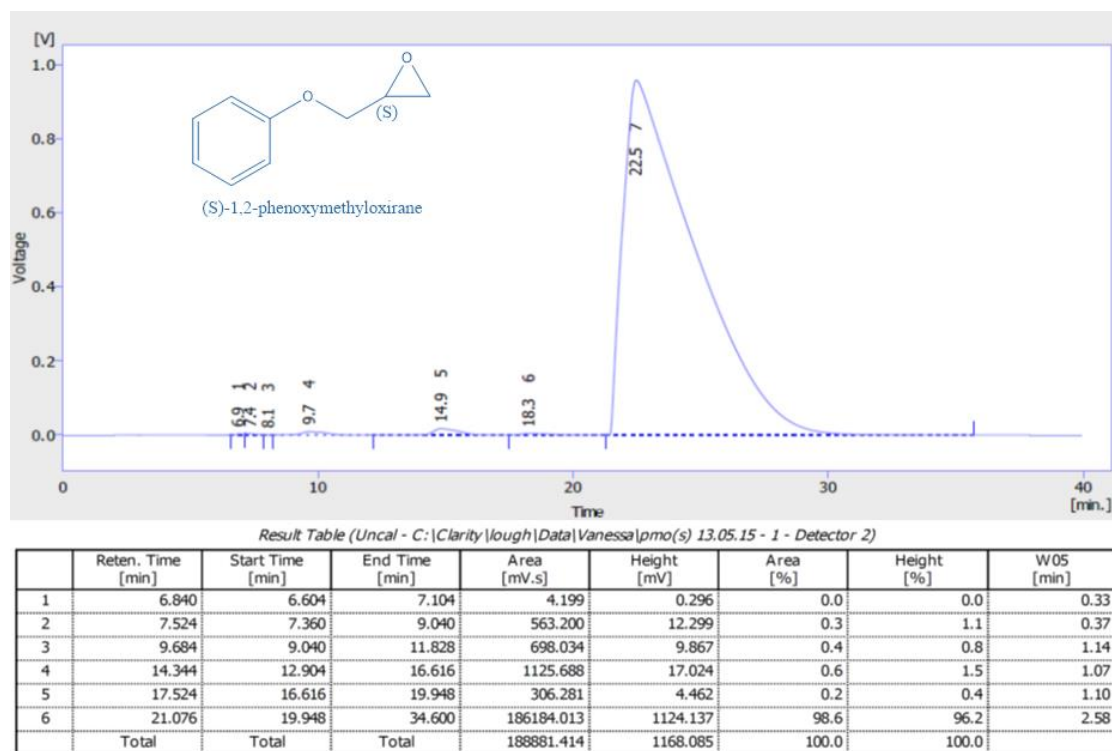


Scheme 2.2.- Mechanism of insertion of CO₂ in the chiral carbon of **1k**.

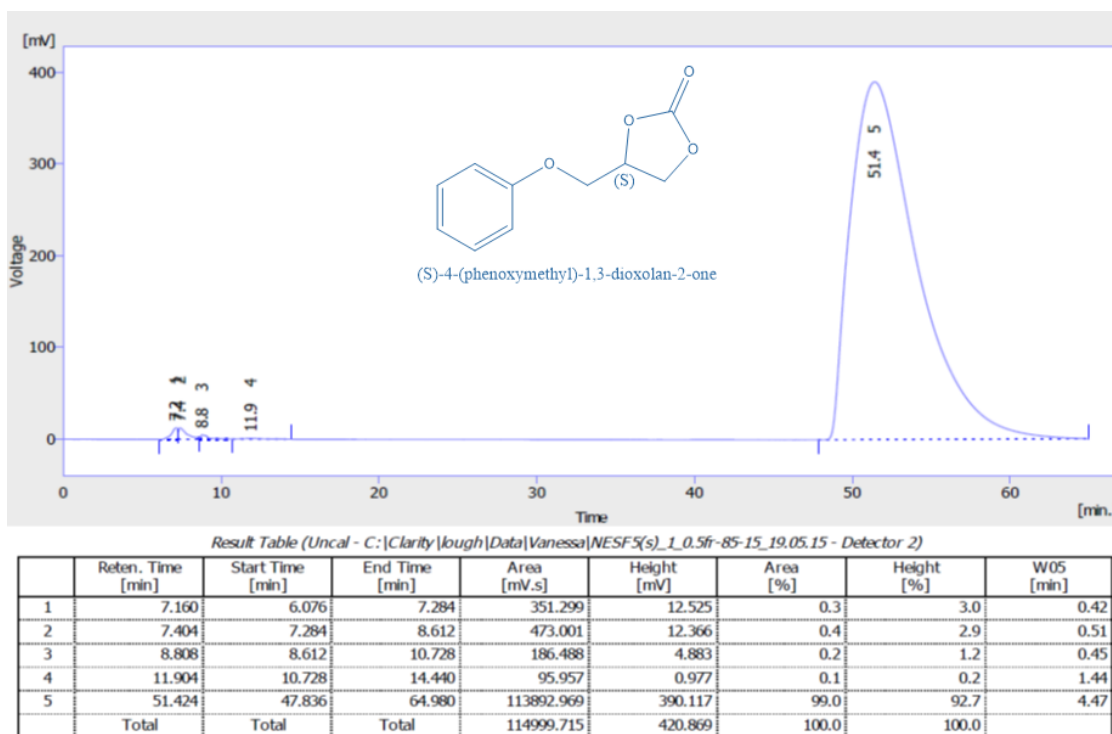
If, on the other hand, the new bond is formed between the oxygen of CO₂ and the non-chiral carbon, despite that the reaction could also undergo S_N1 or S_N2, there would be only one possible product since the chiral carbon will remain intact. Also in this case, as previously explained, the carbonate (**2k**) becomes (*R*).



Scheme 2.3.- Mechanism of insertion of CO₂ in the non-chiral carbon of **1k**.

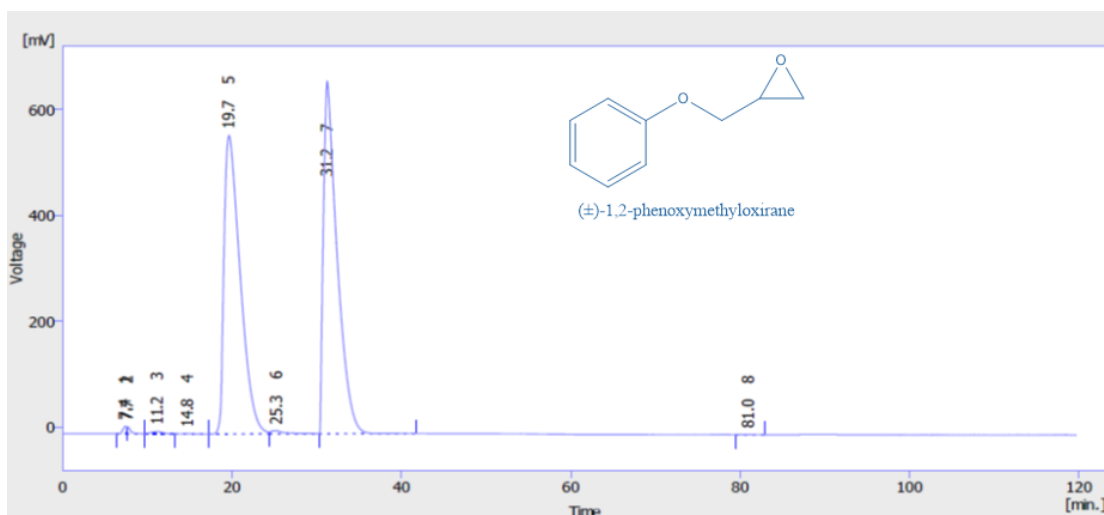
Image 2.1.- HPLC analysis of pure (S)-1,2-phenoxymethyl oxirane.^a

^aCarrier solvent mixture of hexane:isopropanol 99:1, flow rate of 0.5 mL/min.

Image 2.2.- HPLC analysis of (S)-4-(phenoxymethyl)-1,3-dioxolan-2-one.^a

^aCarrier solvent mixture of hexane:isopropanol 85:15, flow rate of 0.5 mL/min.

Image 2.3.- HPLC analysis of pure (±)-1,2-phenoxymethyl oxirane.^a

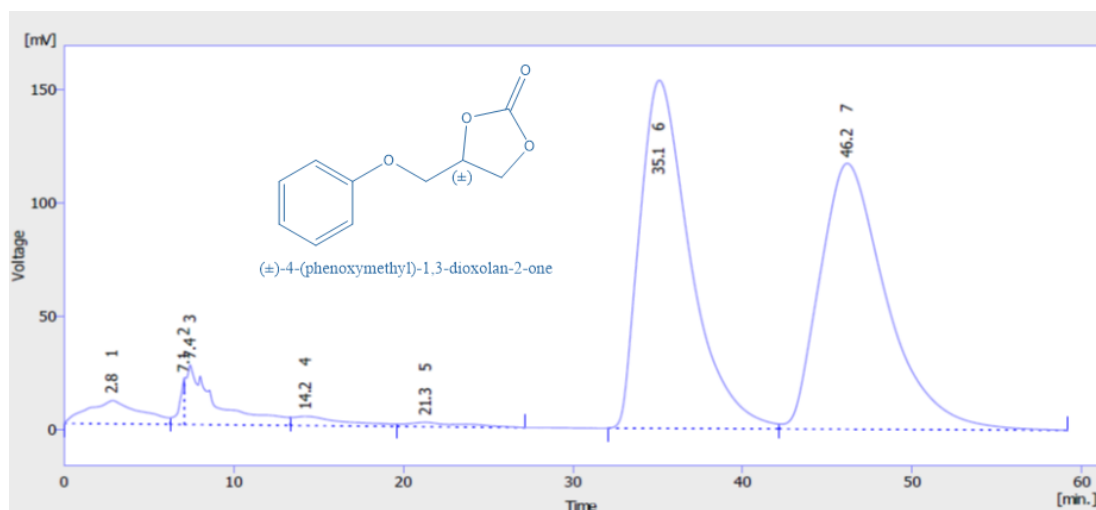


Result Table (Uncal - C:\Clarity\lough\Data\Vanessa\pmo(+)- 13.05.15 - 3 - Detector 2)

	Reten. Time [min]	Start Time [min]	End Time [min]	Area [mV.s]	Height [mV]	Area [%]	Height [%]	W05 [min]
1	7.380	6.396	7.552	378.021	14.228	0.2	1.1	0.45
2	7.660	7.552	9.744	445.155	13.389	0.3	1.1	0.44
3	11.196	9.744	13.276	446.247	4.454	0.3	0.4	1.62
4	14.792	13.276	17.196	74.862	0.635	0.0	0.1	1.93
5	19.660	17.196	24.452	74662.723	563.831	49.3	44.4	2.08
6	25.292	24.452	30.296	731.016	6.107	0.5	0.5	1.41
7	31.248	30.296	41.692	74605.650	666.052	49.3	52.5	1.71
8	81.004	79.496	82.860	39.049	0.510	0.0	0.0	0.99
	Total	Total	Total	151382.724	1269.206	100.0	100.0	

^aCarrier solvent mixture of hexane:isopropanol 99:1, flow rate of 0.5 mL/min.

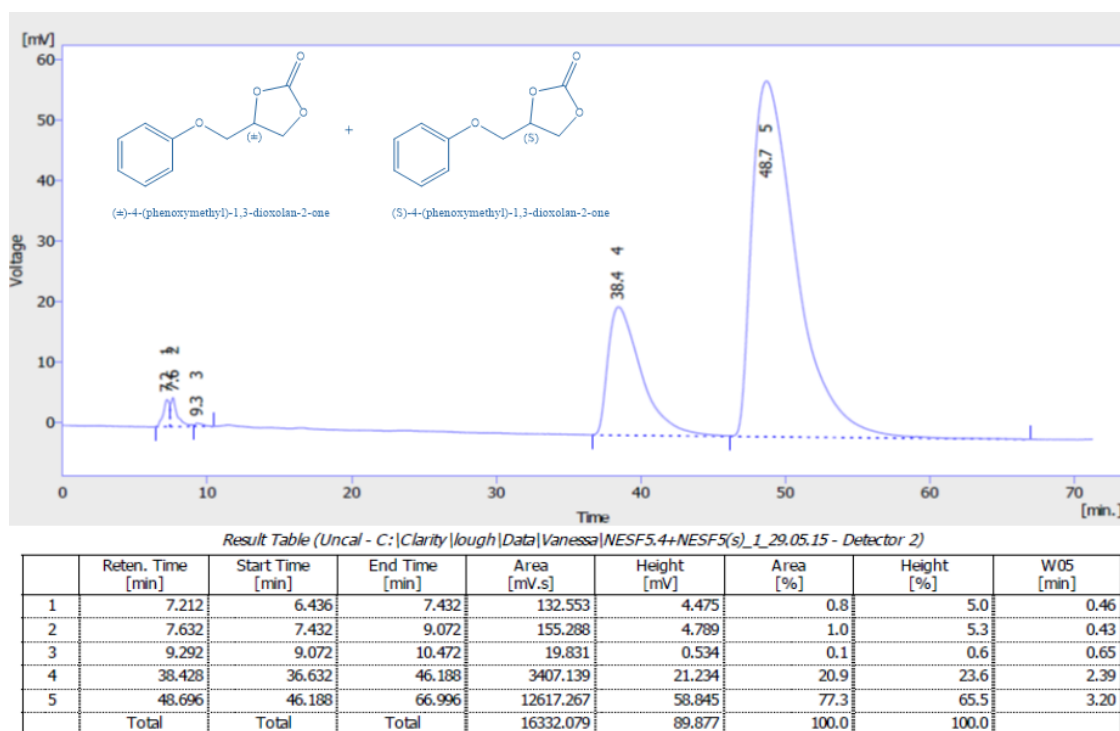
Image 2.4.- HPLC analysis of (±)- 4-(phenoxymethyl)-1,3-dioxolan-2-one. ^a



Result Table (Uncal - C:\Clarity\lough\Data\Vanessa\NESF5.4_7_0.5f-85-15_19.05.15 - Detector 2)

	Reten. Time [min]	Start Time [min]	End Time [min]	Area [mV.s]	Height [mV]	Area [%]	Height [%]	W05 [min]
1	2.848	0.008	6.248	2238.944	10.314	3.2	3.1	3.80
2	7.084	6.248	7.088	390.991	20.234	0.6	6.1	0.26
3	7.436	7.088	13.332	3336.542	26.266	4.7	7.9	1.56
4	14.244	13.332	19.640	867.858	4.089	1.2	1.2	2.69
5	21.324	19.640	27.200	474.263	1.959	0.7	0.6	3.00
6	35.080	32.076	42.156	31591.751	153.500	44.6	46.0	3.10
7	46.160	42.156	59.144	31962.506	117.247	45.1	35.1	4.10
	Total	Total	Total	70862.855	333.608	100.0	100.0	

^aCarrier solvent mixture of hexane:isopropanol 85:15, flow rate of 0.5 mL/min.

Image 2.5.- HPLC analysis of a mixture of (±)- 4-(phenoxyethyl)-1,3-dioxolan-2-one and (S)- 4-(phenoxyethyl)-1,3-dioxolan-2-one.^a

^aCarrier solvent mixture of hexane:isopropanol 85:15, flow rate of 0.5 mL/min.

2.6.4.9 Solventfree reactions or neat reactions

Carboxylation of epoxides under neat conditions was successfully achieved and the results are presented in Table 2.27.

Procedure of reaction on entry 7 of Table 2.27:

The catalyst (Bu_4NI , 0.1 mmol) was added to the epoxide (1e, 10 mmol) in absence of solvent and heated to 75 °C. The catalyst (Bu_4NI) dissolved in the epoxide when temperature increased up to 70 °C (only if ratio epoxide:salt was equal to or lower than 100:1 regarding the catalyst). No electrodes were placed in the solution.

On completion the reaction mixture usually became an amalgam due to slow precipitation of the carbonate mixed with the non-reacted epoxide and the ammonium salt. Due to rigidity of the mixture the reaction stopped at a lower percentage of conversion compared to when the reaction took place using a solvent, as shown by NMR analysis. The mixture was homogenised by grinding it with a mortar and analysed by ^1H NMR to calculate the conversion % and further dissolved in 1 mL of EtOAc to be purified by flash chromatography (solvent petroleum ether :

ethyl acetate, 1:1) to completely remove salt traces from the product and to afford the pure carbonate (2a to 2j).

In general, the reaction stopped when the mixture got saturated on carbonate and became solid, meaning that final conversions were usually lower than in high concentrate dissolved form.

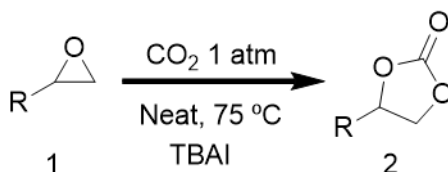
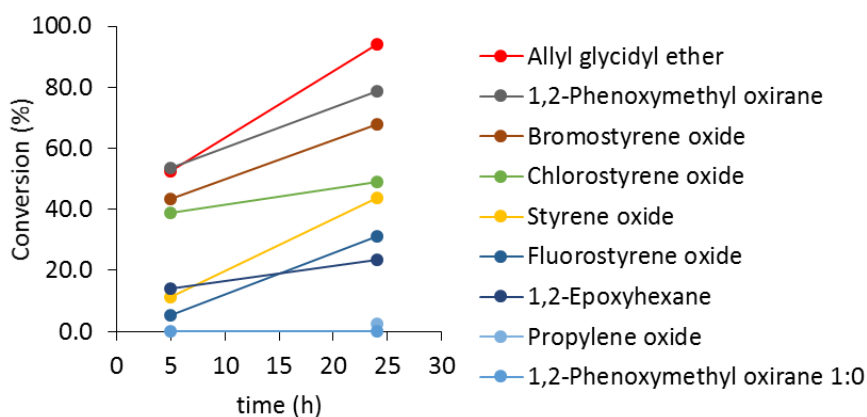


Table 2.27.- Cyclic carboxylation of epoxides (1a to 1h) under neat condition reactions.^a

Entry	Epoxide	Epoxide (mmol)	Catalyst (mmol)	Carbonate ^b (%)	
				5 h	24 h
1	Styrene Oxide (1a)	10.0	0.10	11	44
2	Chlorostyrene oxide (1b)	1.0	0.01	39	49
3	Fluorostyrene oxide (1c)	1.0	0.01	5	31
4	Bromostyrene oxide (1d)	1.0	0.01	43	68
5	1,2-Phenoxy methyloxirane (1e)	1.0	0.00	0	0
6	1,2-Phenoxy methyloxirane (1e)	10.0	0.00	0	2
7	1,2-Phenoxy methyloxirane (1e)	10.0	0.10	54	79
8	1,2-Epoxyhexane (1f)	10.0	0.10	14	24
9	Allyl Glycidylether (1g)	10.0	0.10	52	94
10	Propylene oxide ^c (1h)	10.0	0.10	0	3

^aGeneral reaction conditions: Epoxides from a1 to a8 and Bu₄NI catalyst, (100:1), under neat conditions, 1 atm pressure of CO₂ (balloon), at 75 °C. ^bEvaluated from ¹H NMR spectrum. ^c Room temperature (24 °C) was used in this case due to high volatility of the starting material.

Graphical representation of the data in Table 2.27 is shown below.



Graph 2.50.- Synthesis of cyclic carbonates from different epoxides under neat conditions.

2.6.4.10 Solvent screening study of the cyclic carboxylation reaction of 1,2-phenoxymethyloxirane

A study on the influence of the solvent on the cyclic carboxylation of epoxides was carried out. Table 2.28 and Graph 2.51 show the results of these experiments.

Procedure of reaction on entry 4 of Table 2.28:

A study on the influence of the solvent on the cyclic carboxylation of epoxides was carried out. 1,2-Phenoxymethyloxirane (1e, 1 M) was added to a 1 M solution of catalyst (Bu_4NI) in acetonitrile while heating up to 75 °C. CO_2 at 1 atm pressure was maintained with balloons. ^1H NMR analysis of the aliquots were made at 5 hours and 24 hours of reaction.

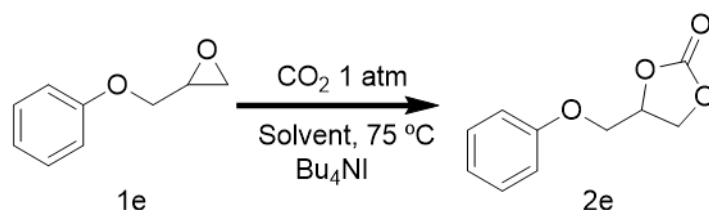
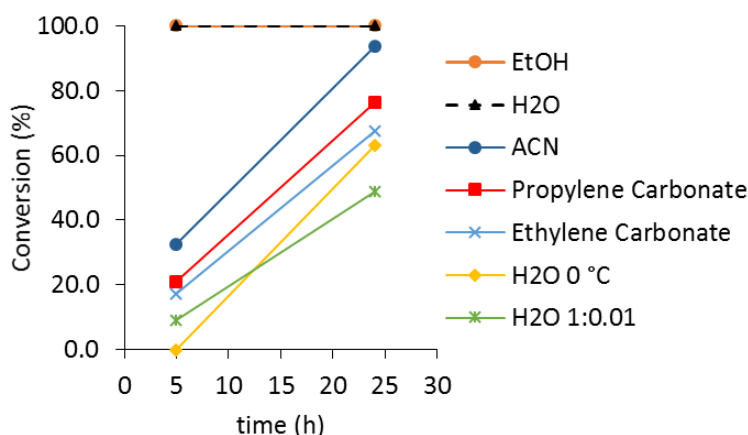


Table 2.28.- Solvent screening of cyclic carboxylation of 1,2-phenoxymethyloxirane.^a

Entry	Solvent	Temp (°C)	Epoxide (mol/L)	Catalyst (mol/L)	Carbonate ^b (%)	
					5 h	24 h
1	Ethylene Carbonate	75	1.00	1.00	17	68
2	Propylene Carbonate	75	1.00	1.00	21	76
3	ACN	75	1.00	1.00	33	94
4	EtOH	75	1.00	1.00	100	100
5	H ₂ O	75	1.00	1.00	100	100
6	H ₂ O ^c	75	1.00	0.01	9	49
7	H ₂ O ^d	0	1.00	1.00	0	63

^aGeneral reaction conditions: Bu_4NI catalyst, 1,2-phenoxymethyloxirane starting material (at 1M concentration, and ratio 1:1 in reactions on entries 1 to 5), in different solvents, 1 atm pressure of CO_2 , at 75 °C. ^bEvaluated from ^1H NMR spectrum.

^cRatio 1:0.01 in water. ^dTemperature of 0 °C in water.



Graph 2.51.- Solvent screening for the cyclic carboxylation of 1,2-phenoxymethyl oxirane. From data in Table 2.28.

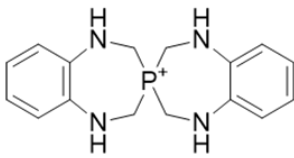
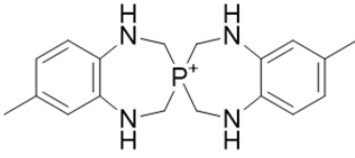
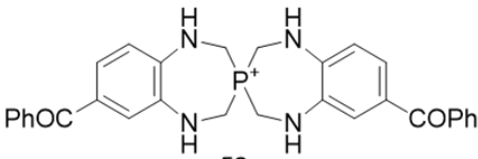
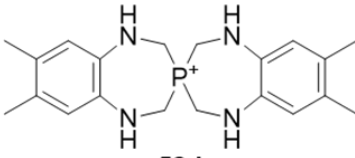
Ethylene carbonate and propylene carbonate as solvents (entries 1 and 2, Table 2.28) for the carboxylation reaction of 1e, produced 26 and 18% less carbonate (2e) after 24 hours than acetonitrile (entry 3, Table 2.28) that produced 94% of conversion after the same time. When ethanol and water were used as solvents (entries 4 and 5), reaction performance was the highest, achieving 100% of conversion in less than 5 hours. Reduction of the catalyst to 1% in water at 75 °C (entry 6) gave a conversion rate of only 49% after 24 hours. When the reaction was held at 0 °C in water (entry 7) conversion after 24 hours rose up to 63%.

The solvent screening study revealed that the more polar the solvent the higher the yield of carbonate conversion. Also protic solvents showed excellent conversions with 100% achieved after 5 hours. Conditions were 1:1 at 75 °C. Reaction in H₂O went by two phases. Presence of hydrogen bonds from solvents –OH to carbon dioxide could be the answer to the good performance of these solvents. Also, that could be the explanation as well for the exceptional conversion rates for the glycidol compared to other starting materials.

2.6.4.11 Phosphonium salts as catalysts.

In collaboration with Professor Martin Smith from Inorganic Chemistry department in Loughborough University, Matias Gimenez Toledo (Erasmus student from The University of Valencia, Spain) synthesized a series of Phosphonium salts that were tested as catalysts for the reaction of cyclic carboxylation of epoxides. Procedure of the synthesis can be found in the literature.^{164,165} The structures of the phosphonium salts tested as catalysts for the carboxylation of epoxides are listed in Table 2.29.

Table 2.29.- Phosphonium salts structure and molecular data.

Cation Shortname	Anion	Cation Structure	Molecular formula	Molecular weight (g/mol)
PS1	Cl ⁻	 52a	C ₁₆ H ₂₀ ClN ₄ P	334,78
	Br ⁻		C ₁₆ H ₂₀ BrN ₄ P	379,23
	I ⁻		C ₁₆ H ₂₀ I ₄ N ₄ P	426,24
	BF ₄ ⁻		C ₁₆ H ₂₀ N ₄ PBF ₄	386,14
	BPh ₄ ⁻		C ₄₀ H ₄₀ BN ₄ P	618,56
PS2	Cl ⁻	 52b	C ₁₈ H ₂₄ ClN ₄ P	362,84
	I ⁻		C ₁₈ H ₂₄ I ₄ N ₄ P	454,29
PS3	Cl ⁻	 52c	C ₃₀ H ₂₈ ClN ₄ O ₂ P	543,00
PS4	Cl ⁻	 52d	C ₂₀ H ₂₈ ClN ₄ P	390,89

Molecular data of Phosphonium salt catalysts. Synthesis of Phosphonium salts can be found in literature.^{164,165} ¹H-NMR, ¹³C-NMR, ³¹P-NMR, IRs, X-Ray and MS analysis of samples were carried out as part of the compound characterization.¹⁶⁶

An initial screening study regarding catalyst performance of different anions of the phosphonium salts (PS1) over 1,2-phenoxymethyl oxirane (**1e**) was conducted producing the results shown in Table 2.30 and Graph 2.52. It is important to notice that because the reactions are run under neat conditions, again most of the reactions ended as a solid mixture, so conversion stopped when solution was not fluid any more.

Procedure of reaction on entry 5 of Table 2.30:

The PS1I phosphonium catalyst was added to the epoxide (**1e**) on a ration epoxide:salt of 100:1, under neat conditions and heated to 75 °C. The catalyst did not dissolve in the epoxide at low temperatures, but it did when reaction temperature was reached.

On completion, the reaction mixture became an amalgam due to slow precipitation of the carbonate (2e) mixed with the non-reacted epoxide and the phosphonium salt. The mixture was homogenised by grinding it with a mortar and analysed by $^1\text{H NMR}$ to calculate the conversion %.

An initial screening study regarding catalyst performance of different anions of the phosphonium salts (PS1) over 1,2-phenoxymethyl oxirane (1e) was conducted producing the results shown in Table 2.30. Experimental procedure was performed as detailed above using an amount of 0.1 mmol of Phosphonium (1% of catalyst loading) salt that was added to 10 mmol of epoxide.

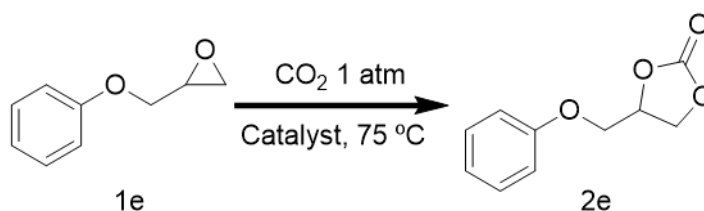
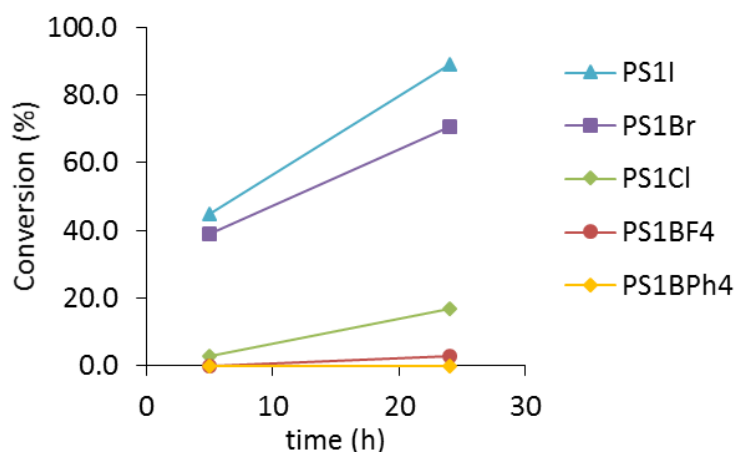


Table 2.30.- Phosphonium salt catalysts for cyclic carboxylation of 1,2-phenoxymethyl oxirane, a nion screenings study.^a

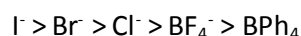
Entry	Catalyst	Carbonate ^b (%)	
		5 h	24 h
1	PS1BPh ₄	0	0
2	PS1BF ₄	0	3
3	PS1Cl	3	17
4	PS1Br	39	70
5	PS1I	45	89

^aGeneral reaction conditions: Phosphonium salt catalyst and 1,2-phenoxymethyl oxirane as starting material at ratios 100:1, under neat conditions, 1 atm pressure of CO₂ balloon, at 75 °C. ^bEvaluated from $^1\text{H NMR}$ spectrum.



Graph 2.52.- Anion screening study for phosphonium salt catalysts for the cyclic carboxylation of 1,2-phenoxymethyl oxirane. Data from Table 2.30.

There is a clear trend on anion activity, sorted by higher to lower performance as follows:



Performance of the phosphonium salt with Cl^- anion was much lower than the salt with Br^- or I^- anions, being iodide the best performer. Nevertheless synthesis of PS1I is carried out beginning with PS1Cl and LiI, so it was suggested to run the reaction with PS1Cl and LiI that would produce PS1I *in situ*. In this way, a whole step on the synthesis of the catalyst would be saved by producing it within the reaction mixture.

Table 2.31 shows results of a series of reactions using different ratio of PS1Cl:LiI (Entries 3 to 6). In order to discard LiI acting as a catalyst for the formation of the cyclic carbonate or other subproducts, a control reaction was carried out by adding LiI to 1,2-phenoxymethyl oxirane under the same reaction conditions (result shown in entry 1 of Table 2.31). Entries 6 to 8 correspond to three replicates of the same reaction in order to estimate the variability of the result. As previously explained, the reaction mixture solidified when carbonate concentration reached the saturation point and no more carbonate could be formed due to rigidity of the mixture so speed of reactions cannot be compared.

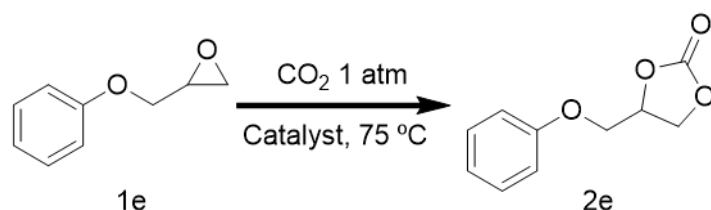


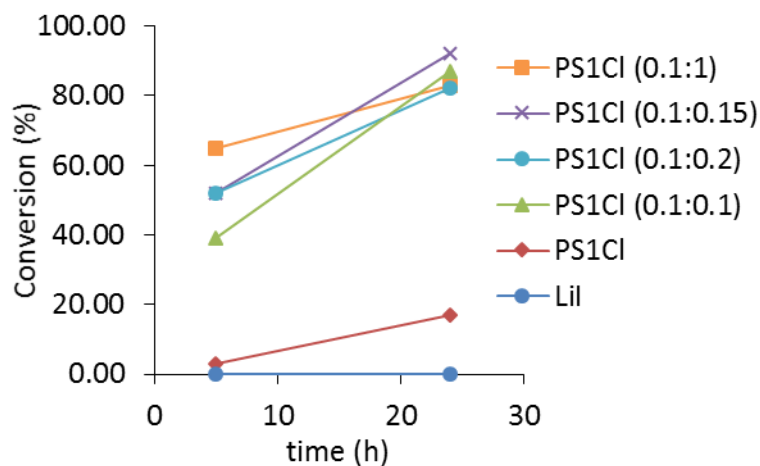
Table 2.31.- Cyclic carboxylation of 1,2-phenoxymethyl oxirane by producing PS1I catalyst *in situ*.^a

Entry	1,2-Phenoxymethyloxirane (mmol)	PS1Cl (mmol)	LiI (mmol)	Carbonate ^b (%)	
				5 h	24 h
1	10	0.00	0.10	00	0
2	10	0.10	0.00	3	17
3	10	0.10	0.10	39	87
4	10	0.10	0.15	52	92
5	10	0.10	0.20	52	82
6	10	0.10	1.00	65	83
7	10	0.10	1.00	34	84
8	10	0.10	1.00	23	91

^aGeneral reaction conditions: Phosphonium salt (0.1 mmol) as catalyst and LiI as cocatalyst (PS1Cl + LiI → PS1I), 1,2-phenoxymethyl oxirane (10 mmol) as starting material, under neat conditions, 1 atm pressure of CO₂ balloon, at 75 °C.

^bEvaluated from ¹H NMR spectrum.

Entry 1 corresponds to a control reaction using LiI as catalyst; Entry 2 corresponds to PS1Cl catalyst reaction; Entries 3-6 show results of reactions using different stoichiometric amounts of PS1Cl:LiI; Entries 6-8 show three replicates of the same reaction.



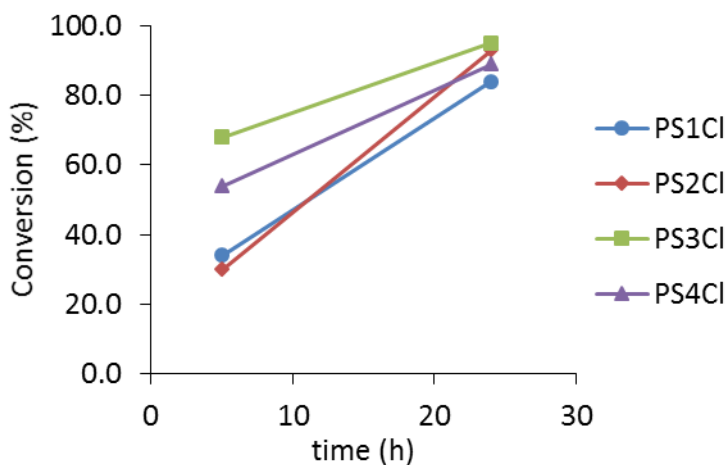
Graph 2.53.- Phosphonium salt (PS1) as catalysts generated *in situ* for cyclic carboxylation of 1,2-phenoxyethyl oxirane.

In order to evaluate the efficiency of different phosphonium cations the structures on Table 2.29 were synthesized and tested as catalyst for the cyclic carboxylation of epoxides under neat conditions. All salts were synthesized with Cl⁻ anion and later mixed with LiI (1:10) within the reaction mixture to produce *in situ* the corresponding phosphonium iodide as discussed above. Table 2.32 shows results for PS1, PS2, PS3 and PS4 catalysis for the cyclic carboxylation of 1,2-phenoxyethyl oxirane (Table 2.32, Graph 2.54), allyl glycidyl ether (Table 2.33, Graph 2.55), and styrene oxide (Table 2.34, Graph 2.56).

Table 2.32.- Phosphonium salt anion screening for cyclic carboxylation of 1,2-phenoxyethyl oxirane.^a

N	Catalyst	LiI (mmol)	Carbonate (%)	
			5 h	24 h
1	PS1Cl	1.0	34	84
2	PS2Cl	1.0	30	93
3	PS3Cl	1.0	68	95
4	PS4Cl	1.0	54	89

^a General reaction conditions: Phosphonium salt as catalyst (0.1 mmol) and LiI as cocatalyst (1 mmol), (PS1Cl + LiI → PS1I), 1,2-phenoxyethyl oxirane (10 mmol) or allyl glycidyl ether (10 mmol) or styrene oxide (10 mmol) as starting material, under neat conditions, 1 atm pressure of CO₂ balloon, at 75 °C. ^bEvaluated from ¹H NMR spectrum.



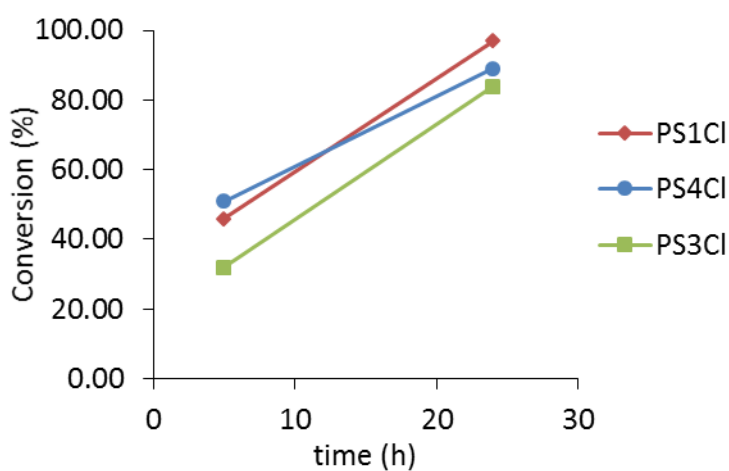
Graph 2.54.- Cation screening study of phosphonium catalysts for the cyclic carboxylation reaction of 1,2-phenoxyethyl oxirane.

Table 2.33.- Phosphonium salt anion screening for cyclic carboxylation of allyl glycidyl ether.^a

N	Catalyst	Carbonate ^b (%)	
		5 h	24 h
allyl Glycidyl ether			
1	PS1Cl	46	97
2	PS3Cl	32	84
3	PS4Cl	51	89

^a General reaction conditions: Phosphonium salt as catalyst (0.1 mmol) and LiI as cocatalyst (1 mmol), (PS1Cl + LiI → PS1I), allyl glycidyl ether (10 mmol) as starting material, under neat conditions, 1 atm pressure of CO₂ balloon, at 75 °C.

^bEvaluated from ¹H NMR spectrum.



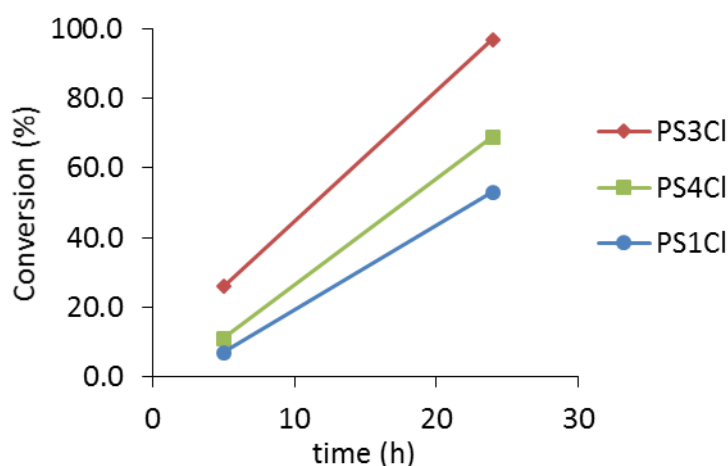
Graph 2.55.- Cation screening study of phosphonium catalysts for the cyclic carboxylation reaction of allyl glycidyl ether.

Table 2.34.- Phosphonium salt anion screening for cyclic carboxylation of styrene oxide.^a

N	Catalyst	Carbonate ^b (%)	
		5 h	24 h
Styrene Oxide			
1	PS1Cl	7	53
2	PS3C	26	97
3	PS4Cl	11	69

^a General reaction conditions: Phosphonium salt as catalyst (0.1 mmol) and LiI as cocatalyst (1 mmol), (PS1Cl + LiI → PS1I), styrene oxide (10 mmol) as starting material, under neat conditions, 1 atm pressure of CO₂ balloon, at 75 °C.

^b Evaluated from ¹H NMR spectrum.



Graph 2.56.- Cation screening study of phosphonium catalysts for the cyclic carboxylation reaction styrene oxide.

2.6.5 Conclusions

Three different conditions of background reactions regarding the electrodes were carried out showing conversion of epoxides to carbonates in all of them at different levels: short circuit (when a wire connected both electrodes and no current was applied), open circuit (when electrodes were placed in the solution but no connection between them) and electrodes free (no electrodes were used in the reaction). The performance of these conditions at a given concentration (0.02 M) of analytes followed the order as expected: Current > Short circuit > open circuit > no electrodes.

When reactions were run under short circuit conditions, yields were of 75% of conversion of styrene carbonate after 20 hours under short circuit conditions (in acetonitrile at 75 °C). Different

epoxides were tested under these conditions giving different conversion rates as follows: 1,2-phenoxymethyloxirane > fluorostyrene oxide > styrene oxide > chlorostyrene oxide > 1,2-epoxyhexane > bromostyrene oxide > allyl glycidyl ether.

Open circuit conditions produced a 45% of styrene carbonate after 20 hours, but only 20% of chlorostyrene oxide under the same conditions. 12% of 1,2-phenoxymethyl oxirane converted to carbonate after 5 hours of reaction.

Carboxylation of epoxides under no electrodes conditions was as low as 5% at a concentration of 0.02 M in acetonitrile at 75 °C after 24 hours. However, and before concentration was purposely risen, two reactions suffered slow evaporation of the solvent while overnight reaction due to a difference in pressure of the CO₂ flow possibly caused by the change of temperature in the laboratory room during the night and morning. The conversion on these reactions rose from 7% after 24 hours for chlorostyrene carbonate to 70% in the next 24 hours; and from 4% after 24 hours to 92% in the next 24 hours for fluorostyrene carbonate. The ¹H NMR analysis of the crude comparing integral values of starting material and tetrabutylammonium iodide confirmed that despite the higher flow rate of CO₂ causing evaporation of the solvent, the starting materials did not evaporate.

A study on the ratio epoxide:catalyst showed that influence of concentration of the species on the reaction is higher than the influence of the catalyst ratio.

The possibility of MgBr₂ and MgCO₃ species causing the formation of carbonate was rejected by a series of experiments that produced no conversion after 20 to 72 hours. Although these species might form when electrodes and current are used, the inorganic form is not catalysing the carboxylation of epoxides as concluded from these experiments.

A molarity study using 1,2-phenoxymethyl oxirane and TBAI (1:1) showed the clear reaction rate improvement when increasing concentration.

When a direct flow from the CO₂ cylinder was flushed through the cell reaction rates always performed better. This could be due to the fact that when heating at 75 °C the pressure in the cell is positive towards outside due to partial evaporation of the solvent. That means that the CO₂ contained in the balloon is coming to the cell at a lower rate. If instead the CO₂ is flushed with a constant flow rate, the concentration of CO₂ will be maintained. The fact that some solvent can evaporate out of the cell with the CO₂ flow, means that the actual concentration of species in

solution when CO₂ flow is used could be higher than the initial one (usually 1 M). This could be improving the yields as compared to the balloon source. However, due to the high volatility of styrene oxide the balloon source was chosen to avoid the loss of the starting material and maintained in order to compare with the rest of epoxides performance.

Carboxylation of glycidol and epichlorohydrin were analysed hourly at different epoxide:TBAI ratios (1:1 ; 10:1 and 100:1). Again, ratio 1:1 presented a higher conversion rate particularly differentiated for the glycidol carboxylation.

Four membered ring epoxide 3-hydroxyoxetane carboxylation was unsuccessfully attempted under these conditions (TBAI in acetonitrile, 75 °C and 1 atm pressure of CO₂).

Carbonate (2e) conversion was achieved using NH₄I in acetonitrile (low solubility of the salt was an issue) at 75 °C, under CO₂ atmosphere although as a minor product (18% after 24 hours). The main product (78%) was the halogenated alcohol formed from the ring opening by I⁻ and the protonation from the NH₄⁺ (1-iodo-3-phenoxypropan-2-ol).

Carboxylation of (*S*)-1,2-phenoxyethyl oxirane was analysed by chiral HPLC showing that the product was enantiomerically pure and rejecting the possibility of carbocation intermediates on the chiral carbon in the mechanism.

Carboxylation of epoxides under neat conditions (epoxide:TBAI 1:1 at 75 °C) was successfully achieved. Performance varied greatly depending on the starting material and the conversion after 24 hours followed the next series: allyl glycidyl ether (94%) > 1,2-phenoxyethyl oxirane (79%) > bromostyrene oxide (68%) > chlorostyrene oxide (49%) > styrene oxide (44%) > fluorostyrene oxide (31%) > 1,2-epoxyhexane (24%) > propylene oxide (3%).

A solvent screening study revealed that the more polar the solvent the higher the yield of carbonate conversion. Also protic solvents showed excellent conversions with 100% achieved after 5 hours. Conditions were 1:1 at 75 °C. Presence of hydrogen bonds from solvents –OH to carbon dioxide could be the answer to the good performance of these solvents.

Phosphonium salts as catalysts were tested under the neat reaction conditions. An optimization of the catalyst structure was concluded based on the results of different anions performance and different phosphonium structures performance.

The anions screening study was carried out using PS1 as the phosphonium structure. There is a clear trend on anion activity, sorted by higher to lower performance as follows: $I^- > Br^- > Cl^- > BF_4^- > BPh_4^-$. In order to evaluate the efficiency of different Phosphonium cations, structures PS1, PS2, PS3 and PS4 were tested for the carboxylation reactions of 1,2-phenoxyethyl oxirane and styrene oxide. The order of catalyst performance was: $PS3 > PS4 > PS1 = PS2$. However, carboxylation of allyl glycidyl ether showed a reversed on catalytic activity: $PS4 = PS1 > PS3$.

Testing these catalysts on other epoxides or functional groups would be of interest for a future project.

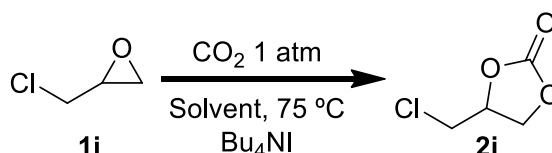
2.7 FTIR MONITORING CARBOXYLATION REACTION AND CALCULATION OF REACTION KINETICS

In order to calculate the reaction order regarding the catalyst next experiment was made possible thanks to a collaboration with Professor Matt Sigman in the Organic Chemistry department of the University of Utah. A series of cyclic carboxylation reactions of epichlorohydrin with N-tetrabutylammonium iodide were monitored with a ReactIR iC10 from Mettler Toledo. All spectra from reactions were processed by extracting values of the reference spectra of acetonitrile at 75 °C. Calculations and results can be found at the end of this section (2.7.5.4).

Calibrations of tetrabutylammonium iodide and epichlorohydrin at 1 M concentration range were carried out (see concentrations in Table 2.35). Cyclic carboxylation of epichlorohydrin in acetonitrile and in water were monitored by IR (see concentrations in Table 2.36).

Table 2.35.- IR Calibration concentrations

	TBAI (M)	Epichlorohydrin (M)
CALIBRATION 1		
CAL1_a	0.50	0.00
CAL1_b	0.75	0.00
CAL1_c	1.00	0.00
CAL1_d	1.25	0.00
CALIBRATION 2		
CAL2_a	0.00	0.50
CAL2_b	0.00	0.75
CAL2_c	0.00	1.00
CAL2_d	0.00	1.25



Scheme 2.4.- Conversion of epichlorohydrin to 4-(chloromethyl)-1,3-dioxolan-2-one through carboxylation with CO₂ and TBAI.

Table 2.36.- Cyclic carboxylation reactions of epichlorohydrin .

N	Solvent/Ratio	TBAI (M)	Epichlorohydrin (M)
1	ACN	0.56	5.60
2	ACN	1.00	10.00
3	ACN	1.00	5.00
4	ACN	0.50	5.00
5	ACN	0.25	5.00
6	ACN	0.05	5.00
7	H ₂ O	1.00	1.00

General reaction conditions: Bu₄Ni catalyst and epichlorohydrin as starting material at different ratios in Acetonitrile, 1 atm pressure of CO₂ balloon, at 75 °C.

2.7.1 Peaks

Trends of the absorbance of the following peaks (Table 2.37) are represented for every reaction and compared between them.

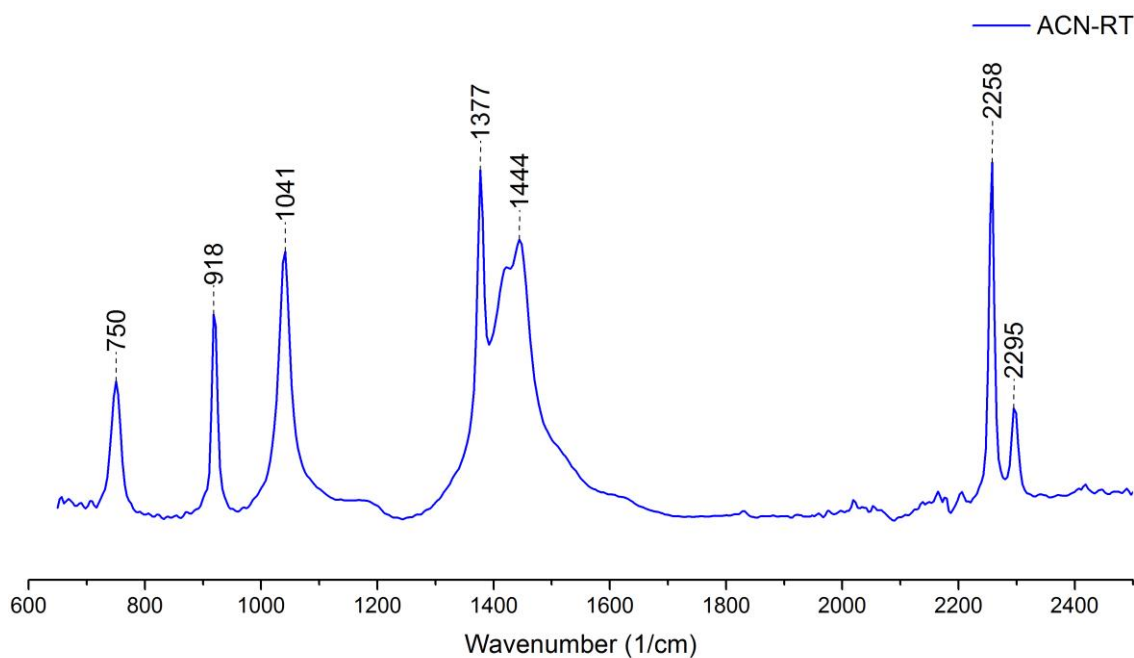
Table 2.37.- Selected peak profiles description for reaction analysis.

Peak Profile	Description (range in 1/cm wavenumber)
Cyclic carbonate	
Carbonate Peak 1	Height to Zero, Peak from 1861 to 1766
Carbonate Peak 2	Height to Zero, Peak from 1201 to 1126
Carbonate Peak 4	Height to Zero, Peak from 1090 to 1052
Carbon dioxide	
CO ₂	Height to Zero, Peak from 2363 to 2321
CO ₂ Peak 2	Height to Zero, Peak from 673 to 654
Epichlorohydrin	
Epichlorohydrin Peak 2	Height to Zero, Peak from 983 to 946
Epichlorohydrin Peak 3	Height to Zero, Peak from 869 to 823
Epichlorohydrin Peak 4	Height to Zero, Peak from 703 to 688
N-tetrabutylammonium iodide	
TBAI	Height to Zero, Peak from 1501 to 1408

All peak values were defined as heights to zero in the ReactIR iC10 software. Peaks on green were selected to analyze trends as they were not overlapping with other peaks in the reaction spectra.

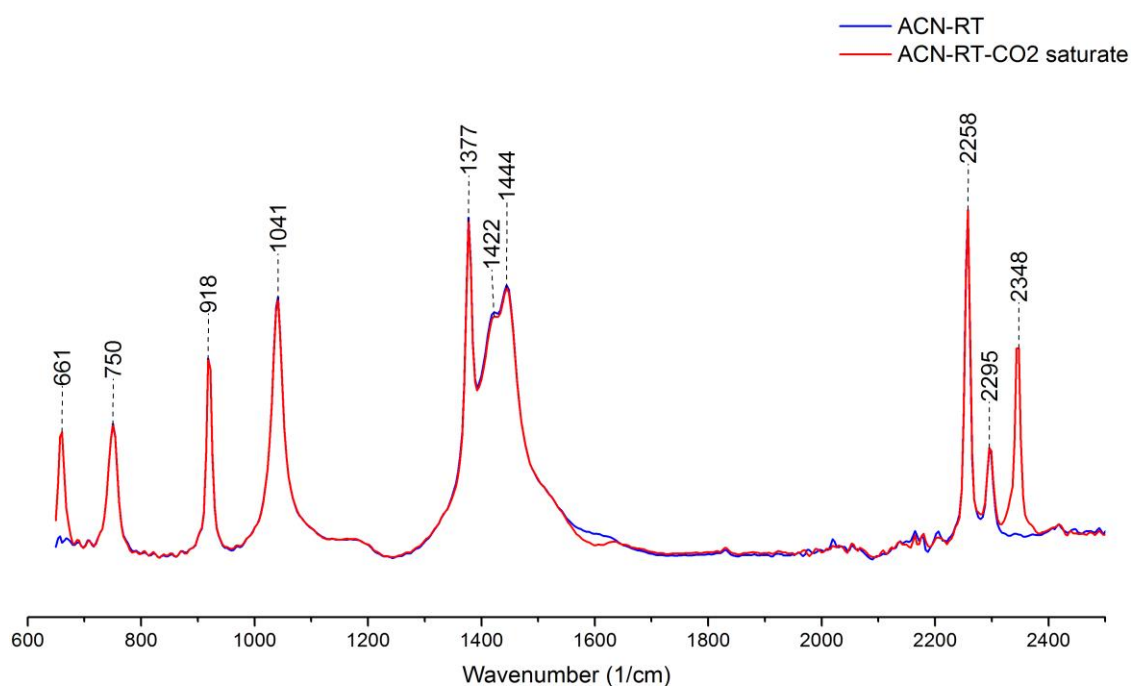
2.7.2 Infra Red reference spectra.

Acetonitrile Infra Red reference spectra: Peaks at 750, 918, 1041, 1377, 1444, 2258 and 2295 1/cm.



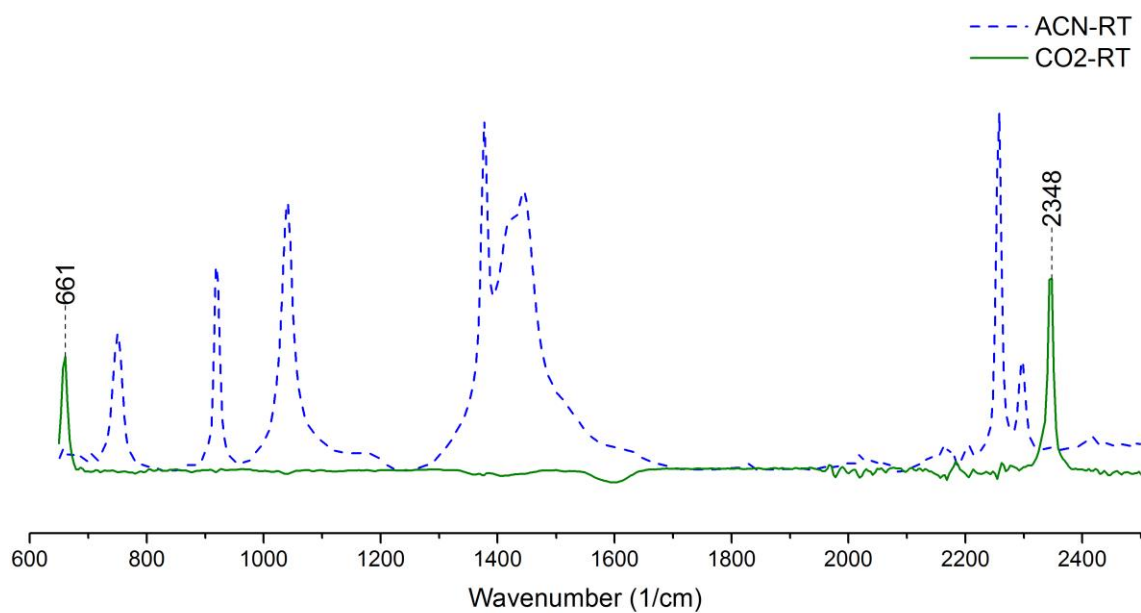
Graph 2.57.- Acetonitrile reference spectrum at room temperature.

When acetonitrile was saturated with CO₂ (dry ice pellets dissolved), new peaks appeared at 661 and 2348 1/cm (Graph 2.58 and Graph 2.59).



Graph 2.58.- Acetonitrile at room temperature saturated (red) and not saturated (blue) of CO₂.

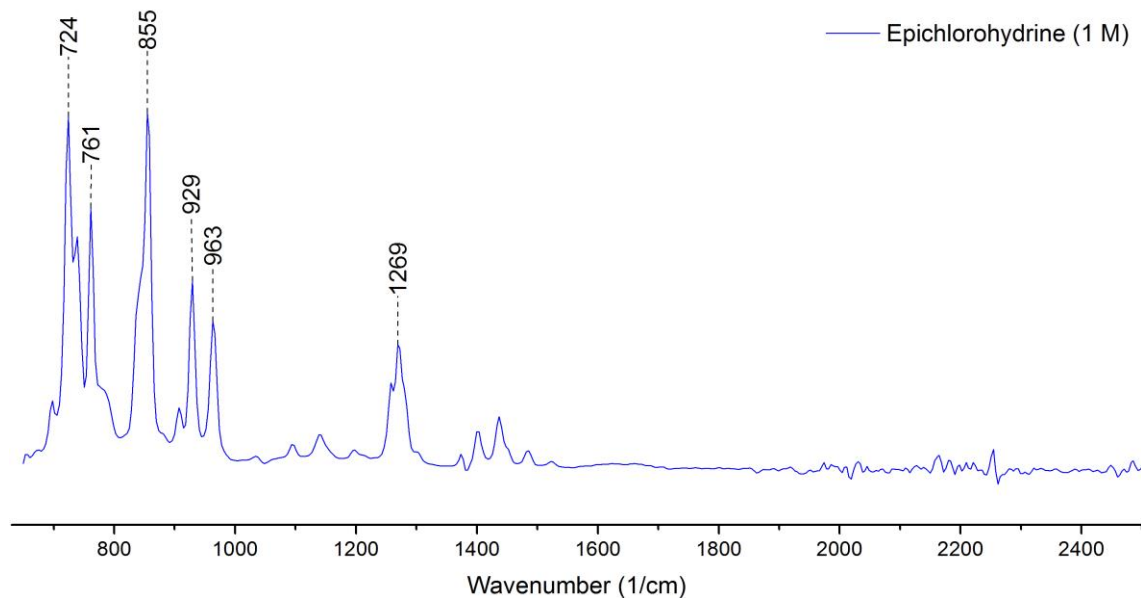
Carbon dioxide reference spectrum: CO₂ peaks at 661 and 2348 1/cm. Obtained by subtracting Acetonitrile reference spectrum to CO₂ saturated acetonitrile spectrum.



Graph 2.59.- CO₂ IR signals in a cetonitrile at room temperature.

Epichlorohydrin (1M) reference spectrum in acetonitrile:

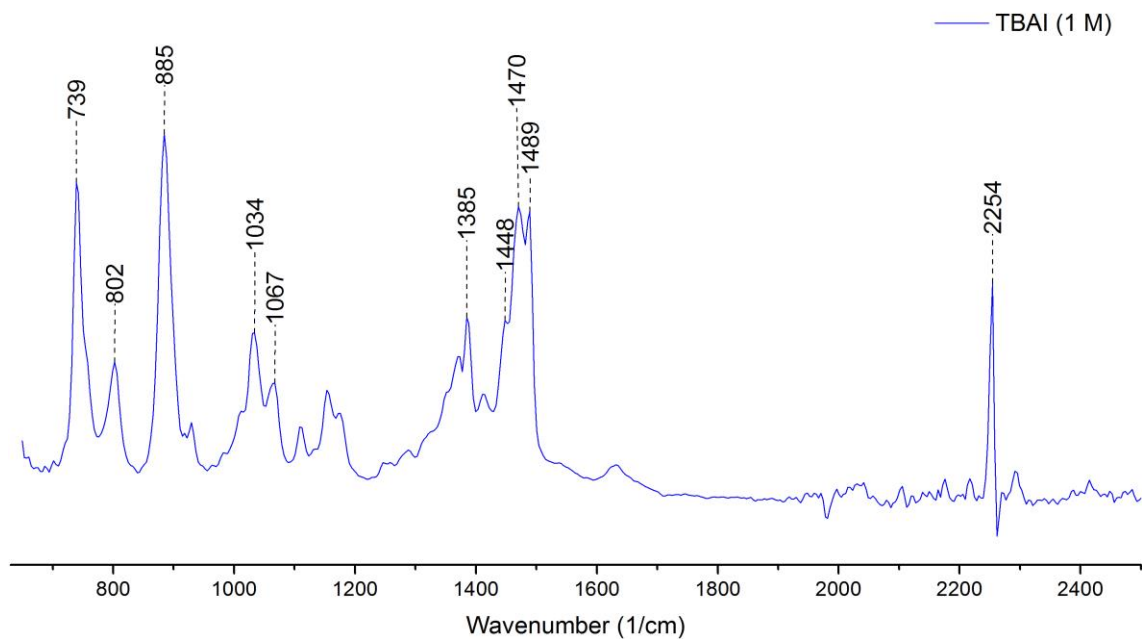
Peaks at 724, 761, 855, 929, 963 and 1269 1/cm. Obtained by subtracting Acetonitrile reference spectrum to epichlorohydrin (1M) in acetonitrile spectrum.



Graph 2.60.- Epichlorohydrin 1 M reference spectrum.

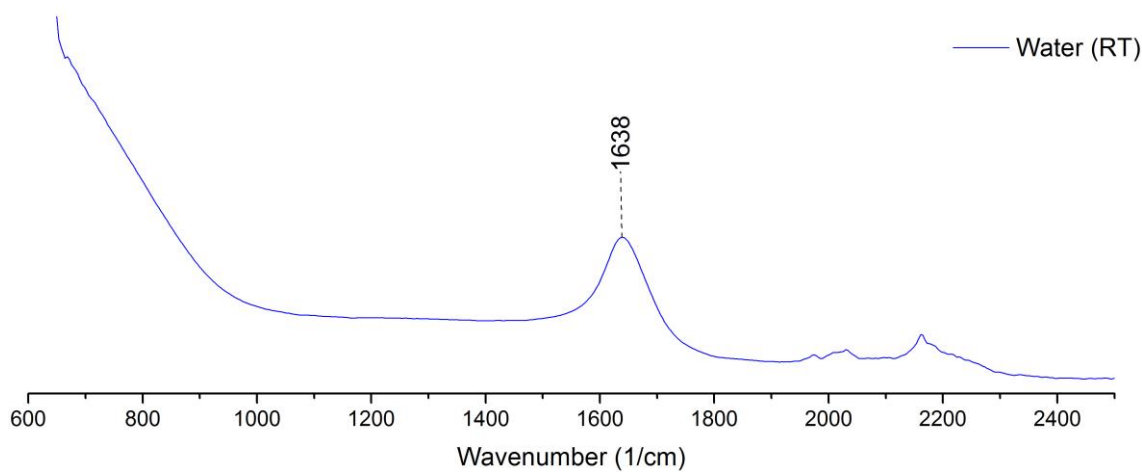
N-tetrabutylammonium iodide (1M) spectrum in acetonitrile:

Peaks at 739, 802, 885, 1034, 1067, 1385, 1448, 1470, 1489 and 2254 $1/\text{cm}$. Obtained by subtracting Acetonitrile reference spectrum to N-tetrabutylammonium iodide (1M) in acetonitrile spectrum.



Graph 2.61.- N-tetrabutylammonium iodide reference spectrum.

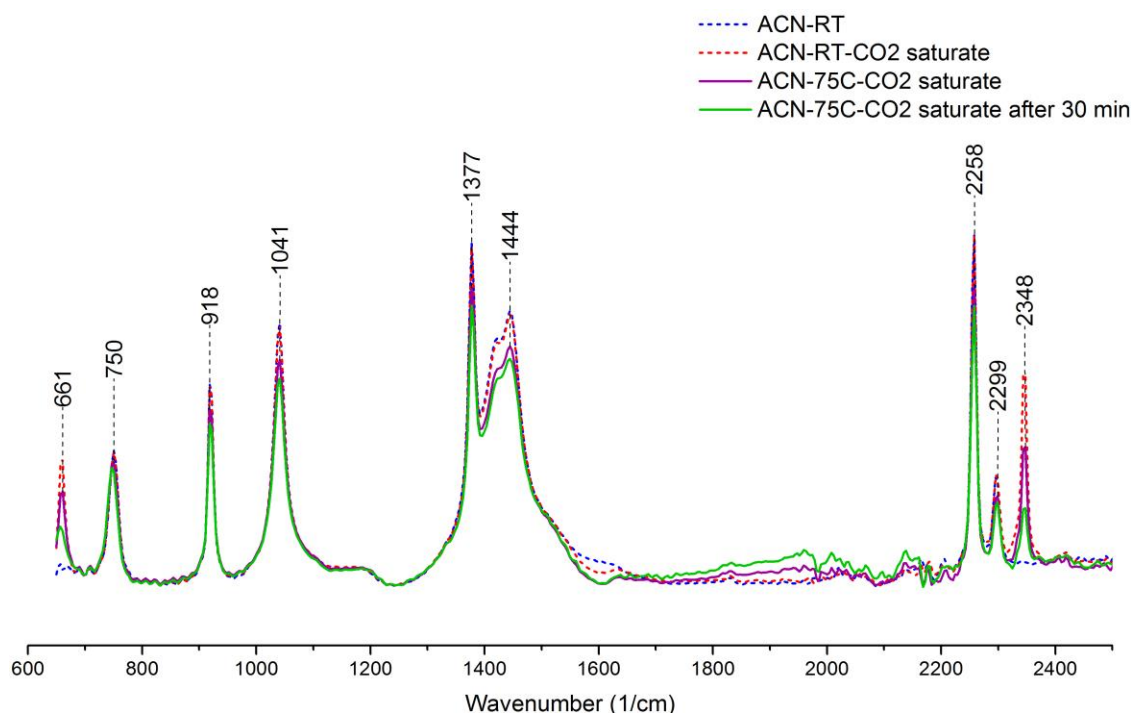
Water reference spectrum: Transmitted intensity of water is higher than acetonitrile.



Graph 2.62.- Water reference spectrum at room temperature.

2.7.3 Temperature effect on IR measurements

Higher temperature had a decreasing effect on intensity of the IR signal along the whole range of the spectrum. Graph 2.63 shows the differences between pure acetonitrile at room temperature (blue dashed line), saturated with CO₂ at room temperature (red dashed line), and acetonitrile saturated with CO₂ at 75 °C (purple and green line). When dry ice was added to pure acetonitrile and left to reach the room temperature the spectrum (red dashed line) showed two new peaks at 661 and 2348 1/cm wave number, which were both attributed to CO₂ vibrations. When the same solution was heated up to 75 °C (purple line), the intensity of most peaks decreased noticeable. When the same solution was next kept at 75 °C for 30 minutes while stirring (green line), intensity of the spectrum kept constant, but CO₂ signals considerably decreased showing that the solution had partially degassed after 30 minutes.



Graph 2.63.- Temperature effect on acetonitrile and carbon dioxide absorbance.

2.7.4 Calibrations

Calibration of the instrument is required in order to establish a mathematical relationship between absorbance and concentration of the analyte. This is accomplished by applying the Lambert-Beer

Law defined in 'A Dictionary of chemistry'¹⁶⁷ book as 'A law relating the reduction in luminous intensity of light passing through a material to the length of the light's path through the material:

$$\log\left(\frac{I}{I_0}\right) = -\varepsilon [J] l \quad \text{Eq.- (2.1)}$$

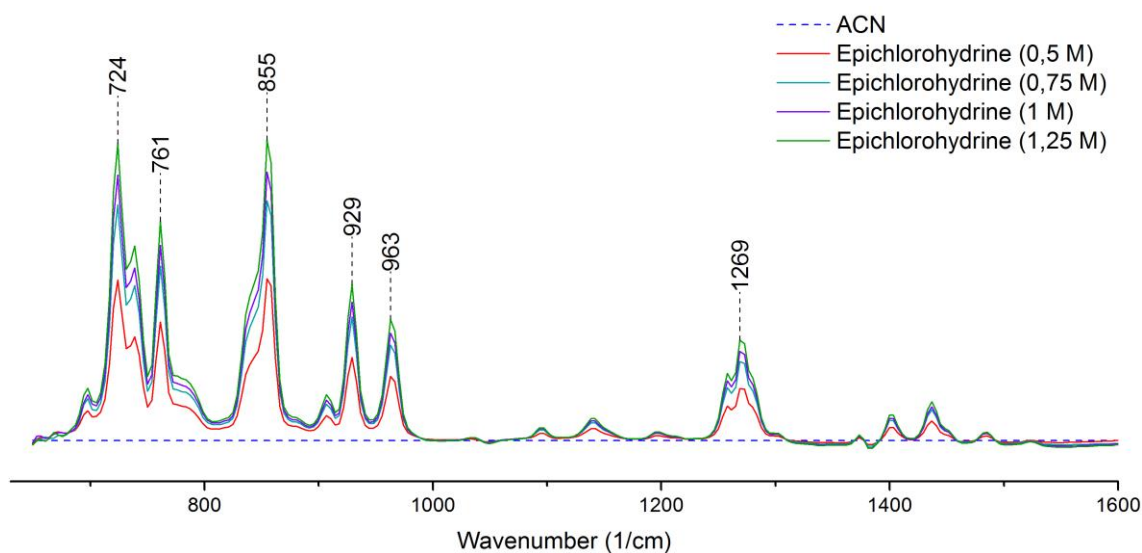
$$A = -\log\left(\frac{I}{I_0}\right) = \varepsilon [J] l \quad \text{Eq.- (2.2)}$$

Where A is absorbance, I is the intensity after passing through a sample of length l , I_0 is the incident intensity, ε is the molar absorption coefficient, and $[J]$ is the concentration of species J .

Representation of the Absorbance measured for each solution of different concentration of analyte has a lineal correlation being $(\varepsilon * l)$ the slope.

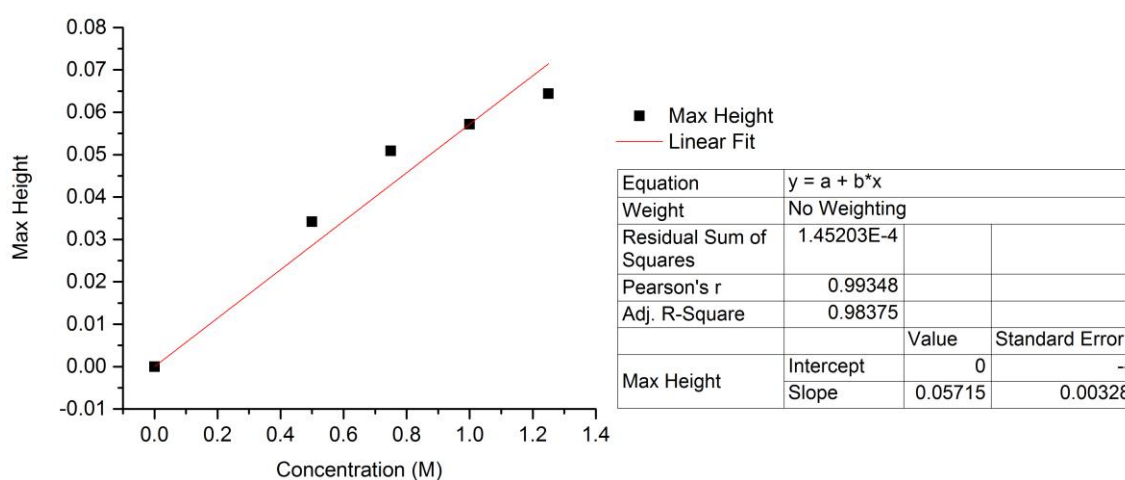
Epichlorohydrin calibration (Calibration 1):

Graph 2.64 is showing a zoom of the data from 600 to 1600 wavenumber (1/cm) in order to be able to appreciate the differences on intensity of peaks.



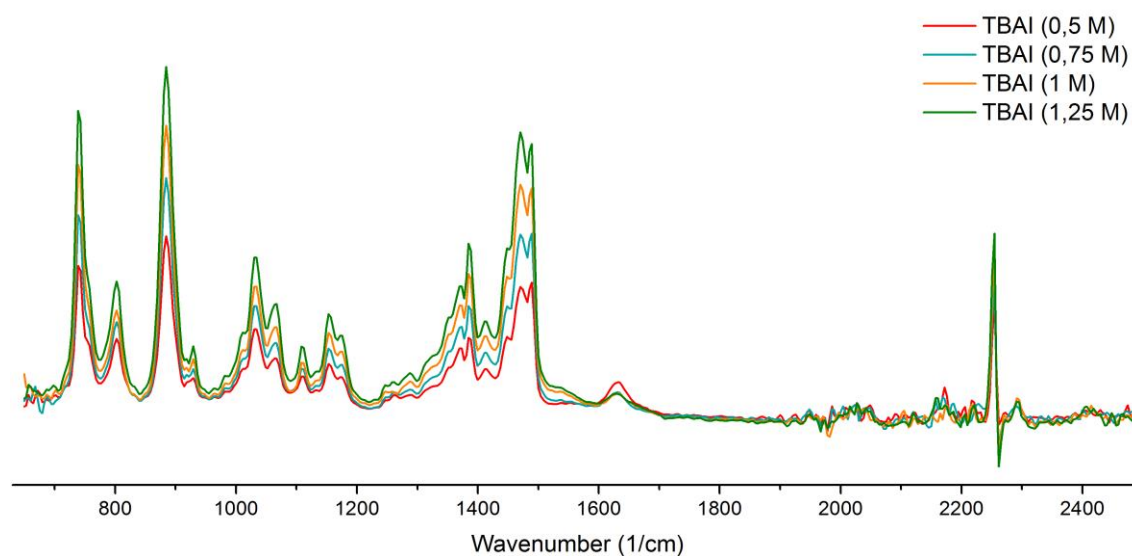
Graph 2.64.- ReactIRiC10 calibration of Epichlorohydrin in acetonitrile at 75 °C.

Representation of the height of the peak (or area of the peak) versus concentration of epichlorohydrin gave the calibration curve for this analyte (Graph 2.65). The peak selected to calculate the relation between absorbance and concentration is the same that will be used for monitoring the remaining epoxide in the reaction (peak at 963 1/cm wave number). The calibration showed that there was a linear correlation between either peak height and peak area with concentration and no significant difference between considering peak heights or peak areas was found, and both equations gave the same result for concentration of epichlorohydrin through the reactions.

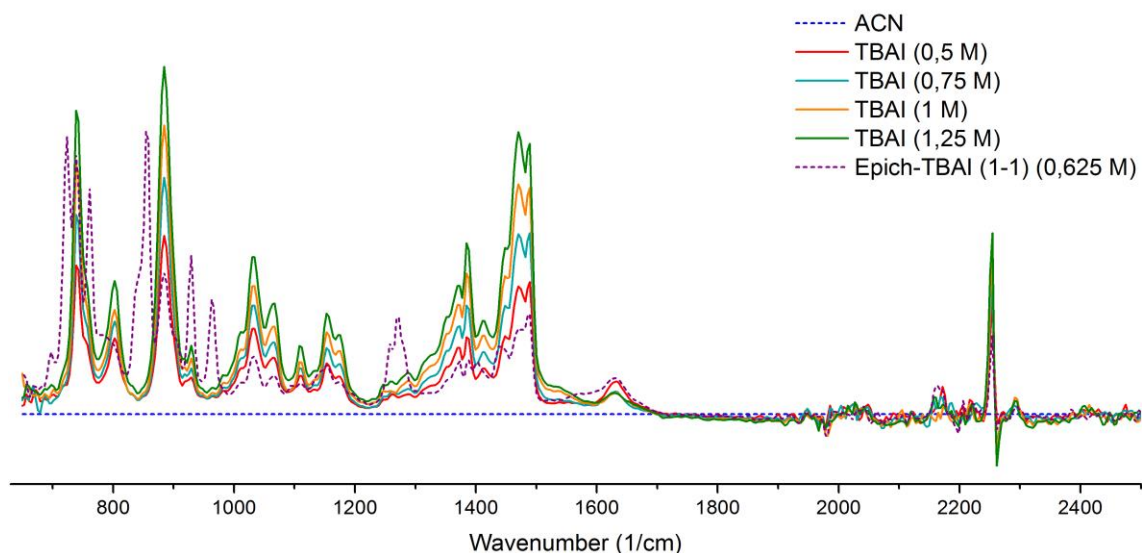


Graph 2.65.- Epichlorohydrin calibration of FTIR peak height from 947 to 986 1/cm for 4 different concentrations (0.5, 0.75, 1 and 1.25 M) ($y = 0.05715*x$; $r^2 = 0.9835$).

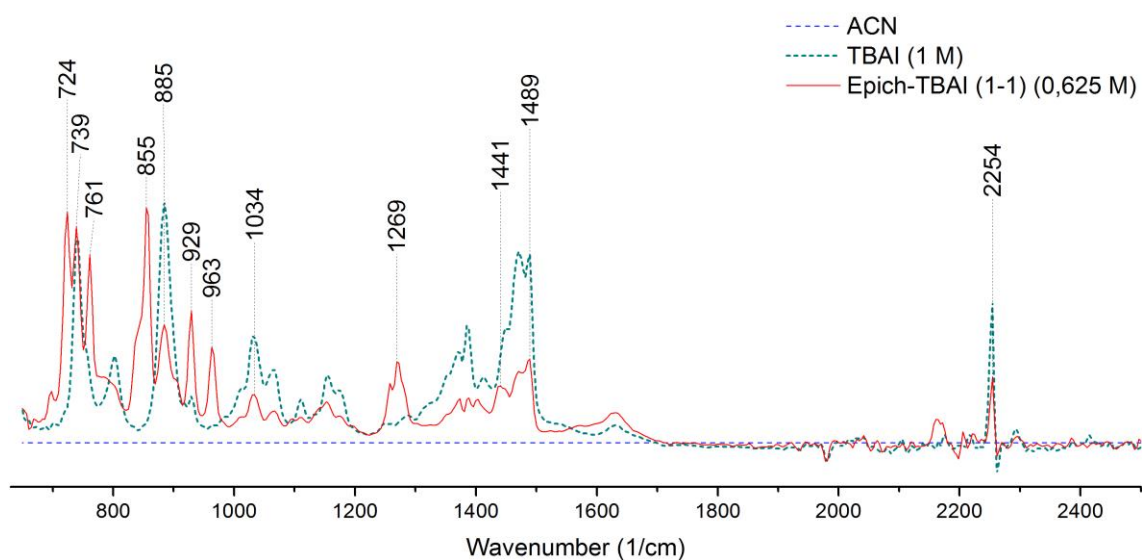
N-tetrabutylammonium iodide calibration (Calibration 2):



Graph 2.66.- ReactIR iC10 calibration of N-tetrabutylammonium iodide in acetonitrile at 75 °C.



Graph 2.67.- ReactIR iC10 calibration of N-tetrabutylammonium iodide in acetonitrile at 75 °C. ACN pattern and mixture pattern added to the overlapped spectra.



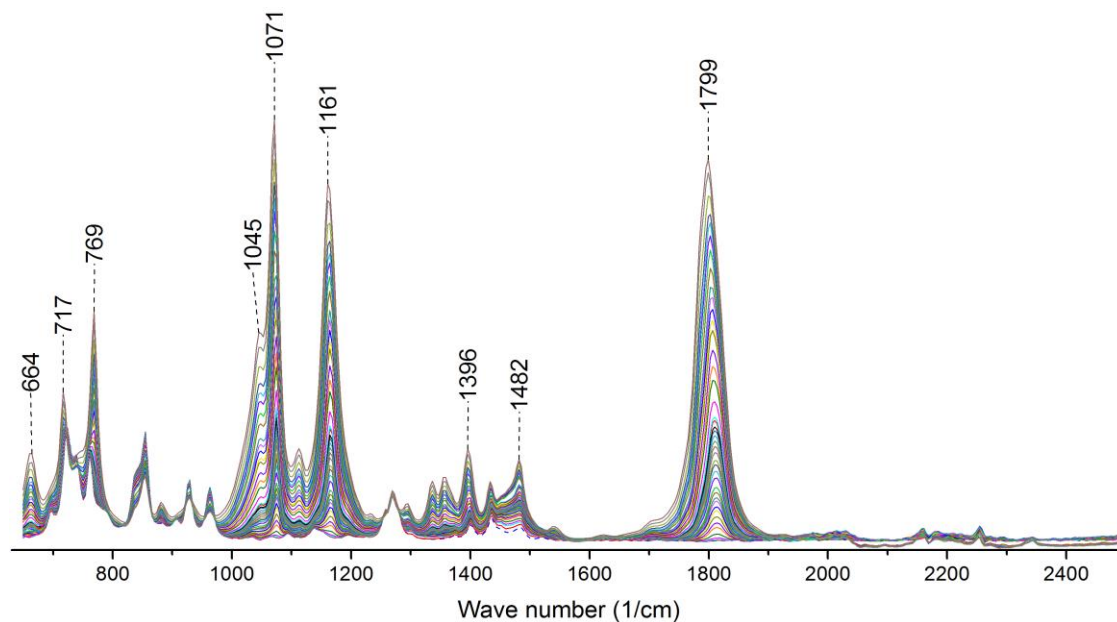
Graph 2.68.- Reference spectrum of mixture 1 to 1 of epichlorohydrin and TBAI (0.6 M) in acetonitrile.

2.7.5 Calculation of kinetics, reaction order of N-tetrabutylammonium iodide.

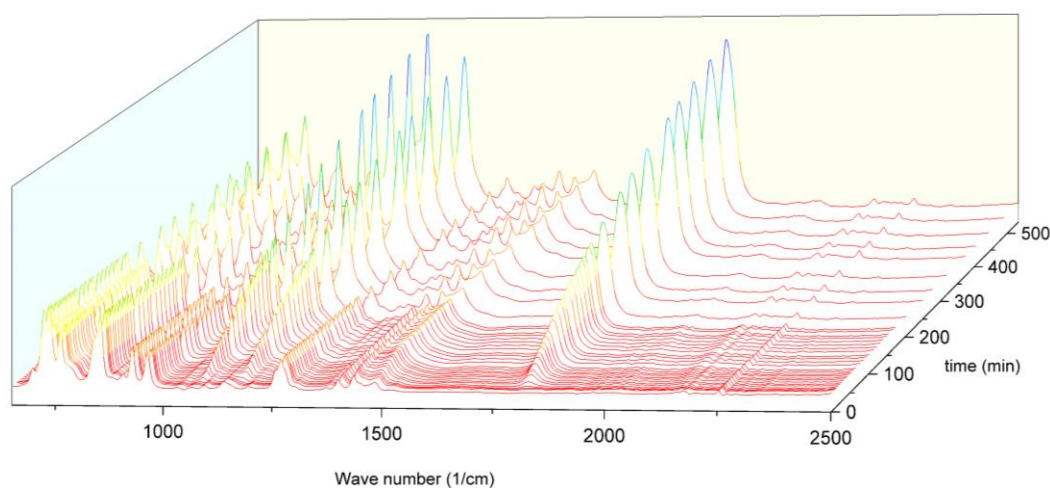
Reactions with 1M epichlorohydrin with different concentration of catalyst at 75 °C in acetonitrile were monitored in order to compare the reaction kinetics under the catalyst influence.

2.7.5.1 Reaction of epichlorohydrin 1 M – TBAI 0.5 M

An example of IR spectra collection for the carboxylation reaction of epichlorohydrin (1 M) with TBAI catalyst (0.5 M) and CO₂ is shown in the next 2 and 3 dimension graphs (Graph 2.69 and Graph 2.70). Trends of the main peaks through time are represented in Graph 2.71.

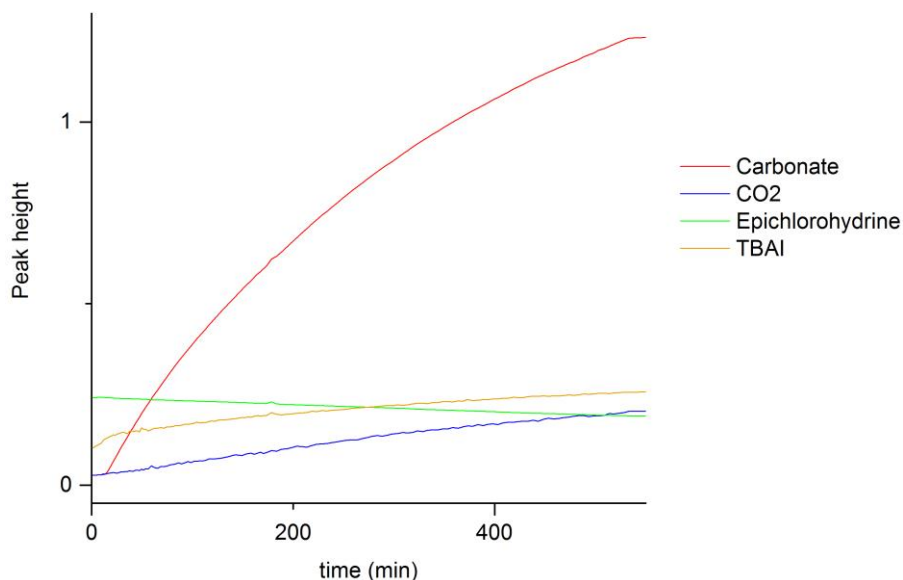


Graph 2.69.- IR monitoring reaction of cyclic carboxylation of epichlorohydrin (1M) and N-tetrabutylammonium (0.5M).



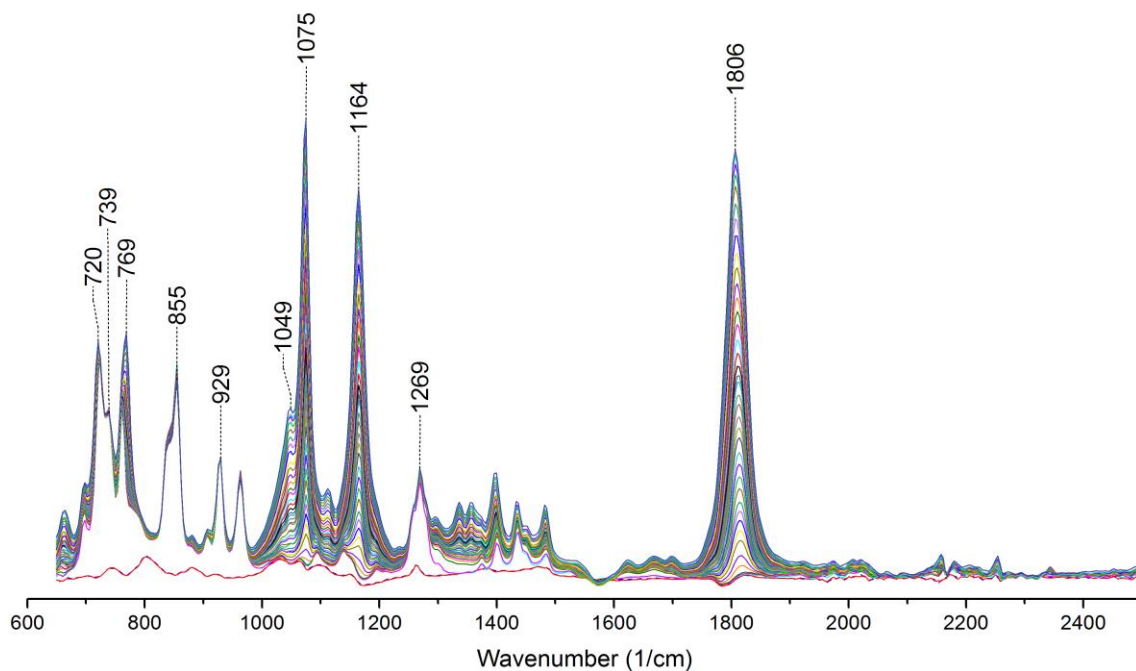
Graph 2.70.- 3D IR spectra representation versus time of the reaction of cyclic carboxylation of epichlorohydrin (1M) and N-tetrabutylammonium (0.5M).

Peak trends are represented in Graph 2.71, showing absorbance maximums of the reactants and product versus reaction times: carbonate peak at 1799 cm^{-1} in red, carbon dioxide peak at 2348 cm^{-1} in blue, epichlorohydrin peak at 963 cm^{-1} in green and tetrabutylammonium salt peak at 1470 cm^{-1} in yellow.

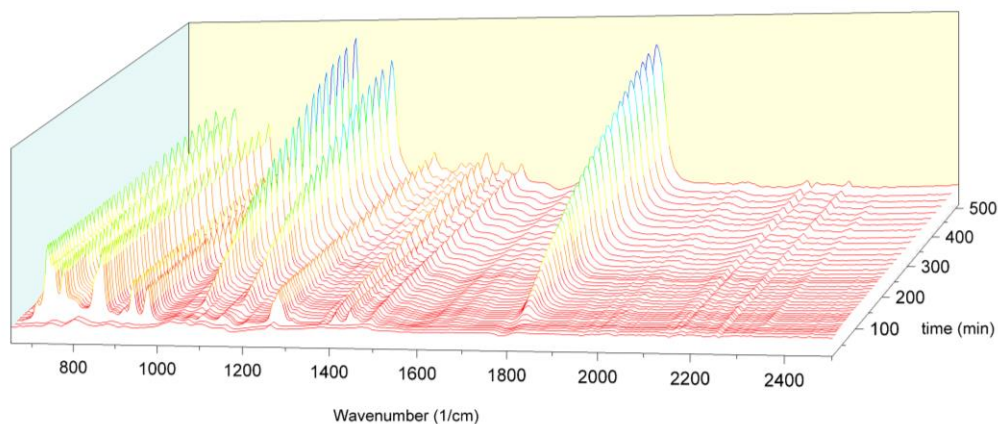


Graph 2.71.- Trends of main peak heights of the reaction of cyclic carboxylation of epichlorohydrin (1M) and N-tetra butylammonium (0.5M).

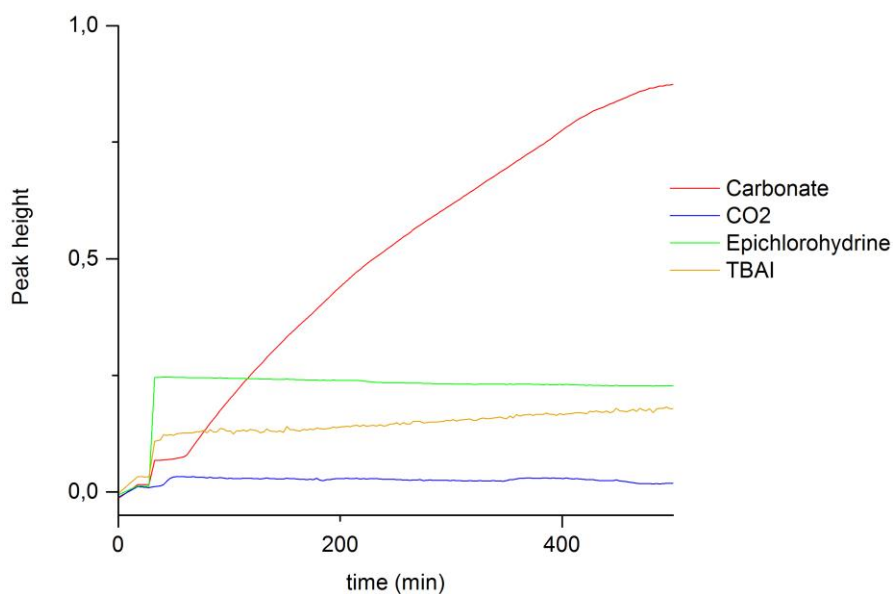
2.7.5.2 Reaction of epichlorohydrin 1 M - TBAI 0.25 M



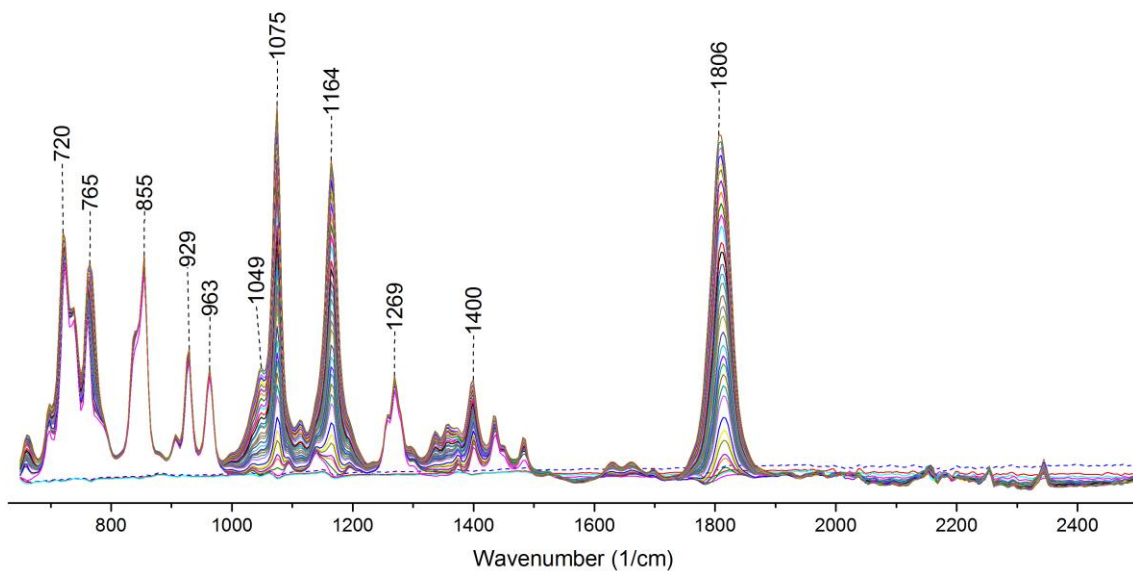
Graph 2.72.- IR monitoring reaction of cyclic carboxylation of epichlorohydrin (1M) and N-tetra butylammonium (0.25M).



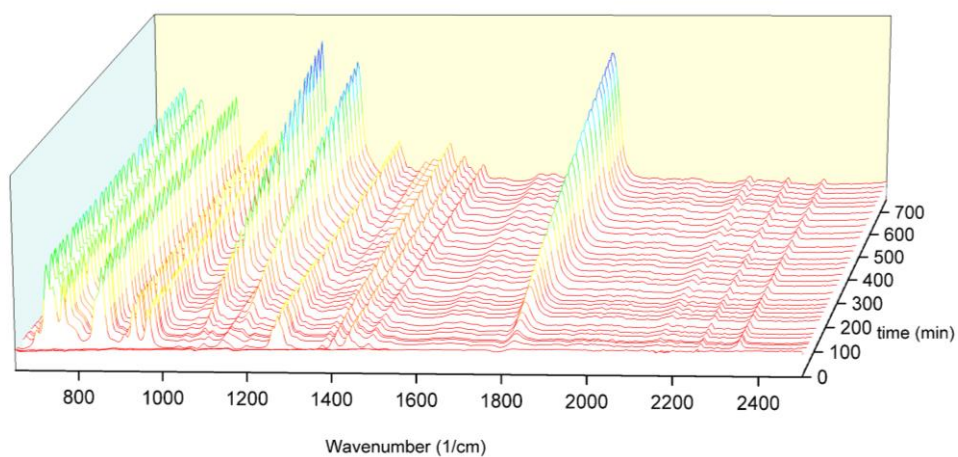
Graph 2.73.- 3D IR spectra representation versus time of the reaction of cyclic carboxylation of epichlorohydrin (1M) and N-tetrabutylammonium (0.25M).



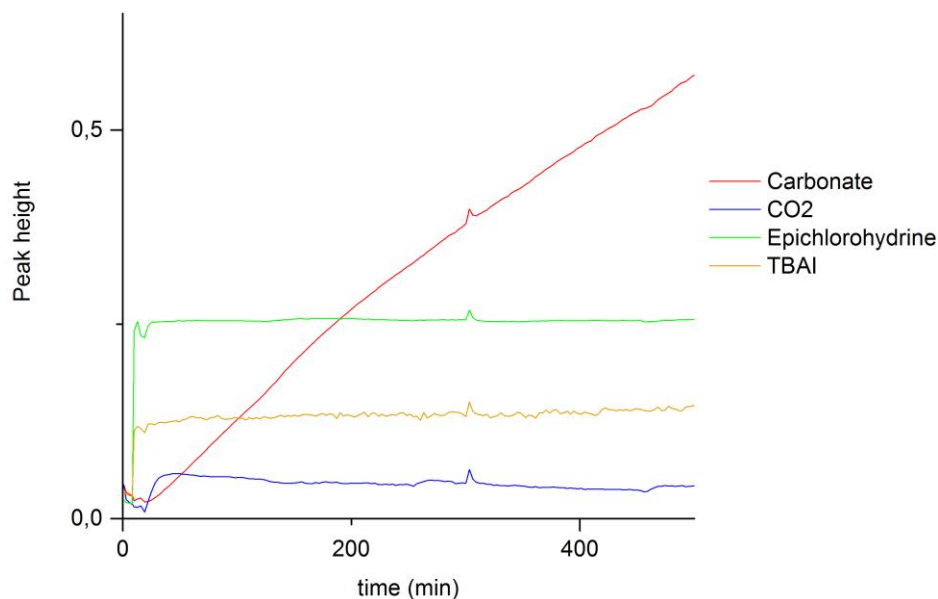
Graph 2.74.- Trends of main peak heights of the reaction of cyclic carboxylation of epichlorohydrin (1M) and N-tetrabutylammonium (0.25M).

2.7.5.3 Reaction of epichlorohydrin 1 M – TBAI 0.05 M

Graph 2.75.- IR monitoring reaction of cyclic carboxylation of epichlorohydrin (1M) and N-tetrabutylammonium (0.05M).



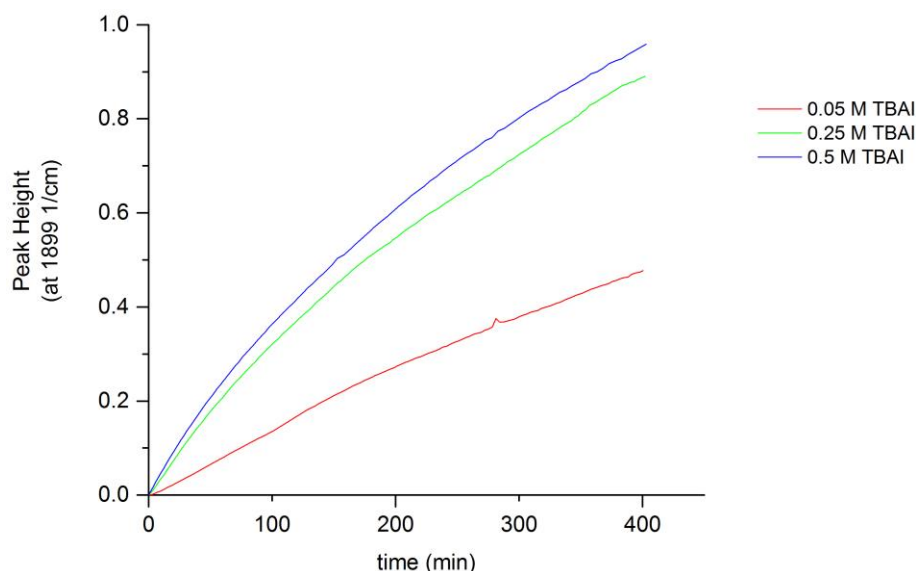
Graph 2.76.- 3D IR spectra representation versus time of the reaction of cyclic carboxylation of epichlorohydrin (1M) and N-tetrabutylammonium (0.05M).



Graph 2.77.- Trends of main peak heights of the reaction of cyclic carboxylation of epichlorohydrin (1M) and N-tetrabutylammonium (0.05M).

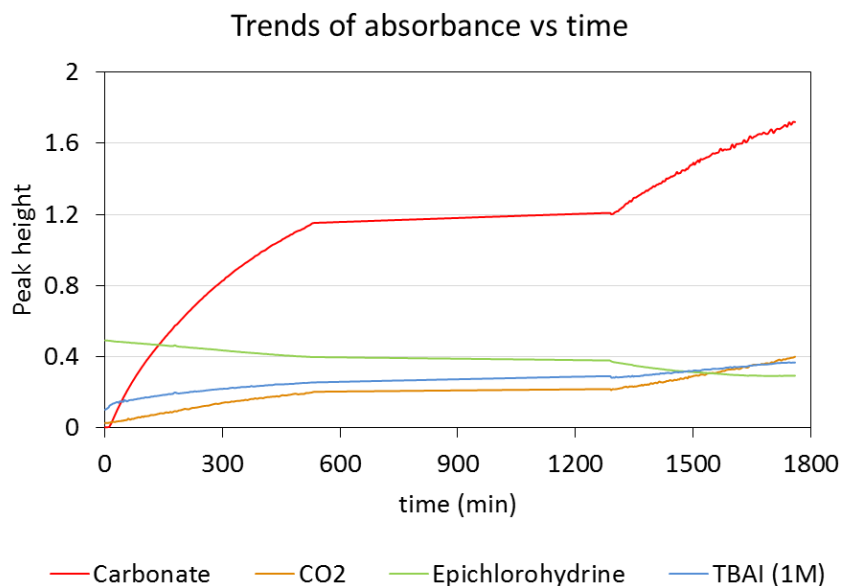
In the Graph 2.77, a pressure change can be noticed at 303 min of reaction provoked by the refill of liquid N_2 to the reactor due to its evaporation as the air conditioning of the laboratory was out of order and the temperature of the room got higher than 28 °C.

Comparison of the peak heights of the carbonate for the reactions with different concentration of TBAI is shown in Graph 2.78. Time of reaction has been normalized by setting as 0 the second at which epichlorohydrin was injected and the initial intensity of the baseline for the different spectrum.



Graph 2.78.- Comparison of height trends of carbonate peaks for the reactions of cyclic carboxylation of epichlorohydrin (1 M) and N-tetrabutylammonium (0.05 (red), 0.25 (green) and 0.5 (blue) M).

Graph 2.79 shows the peak height of each analyte for the reaction containing epichlorohydrin and TBAI (0.5 M) during 30 straight hours (1800 min). Since CO₂ is supplied with a balloon refilled with CO₂ cardice pellets the overnight reaction suffers a stand by when the CO₂ empties (see almost flat signals from 550 to 1300 min). When the balloon was refilled the next day the reaction restarted (from 1300 to 1800 min).



Graph 2.79.- Trends of absorbance of species during 30 h (1800 min) of carboxylation reaction of epichlorohydrin with TBAI (0.5 M).

2.7.5.4 Determination of reaction order with respect to N-tetrabutylammonium iodide.

The rate equation for the synthesis of 4-(chloromethyl)-1,3-dioxolan-2-one from epichlorohydrin, CO₂ and Bu₄NBr (Scheme 2.4), has the form shown in Eq.- (2.3). The kinetics calculations have been carried out studying the first 400 minutes of the reaction in order to avoid possible deviations due to the concentration of CO₂ decreasing (as seen in Graph 2.79). Within this range (0 to 400 minutes) concentration of CO₂ will be constant. Since tetrabutylammonium iodide act as a catalyst it can be assumed that its concentration does not change significantly during the reaction. Because of these two assumptions Equation 2.3 can be simplified as Eq.- (2.4).

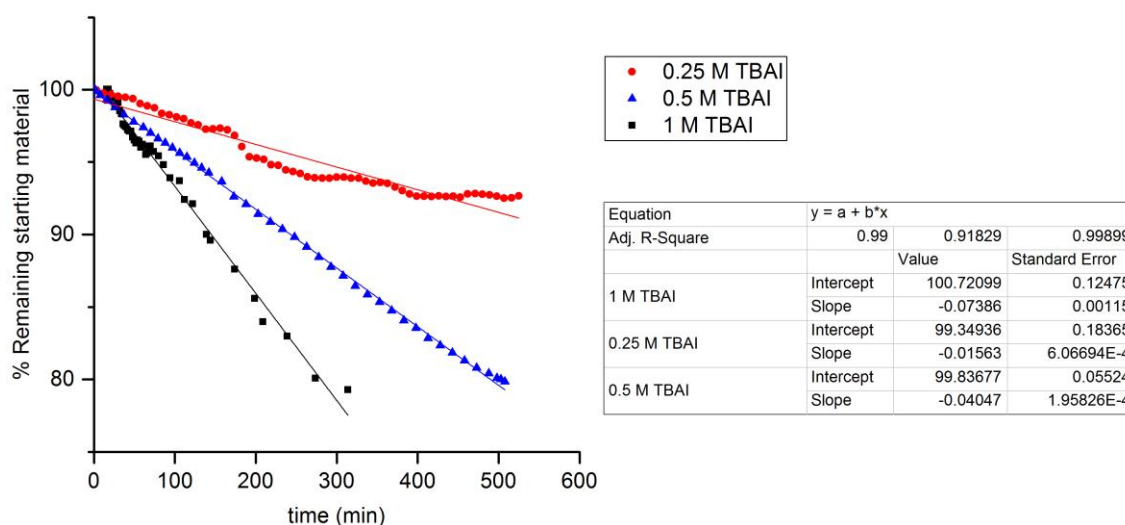
In order to calculate the reaction order with respect to tetrabutylammonium iodide, logarithm has to be taken of Eq.- (2.4) leading to Eq.- (2.5).

$$\text{Rate} = k[\text{epoxide}]^a [\text{CO}_2]^b [\text{TBAI}]^c \quad \text{Eq.-(2.3)}$$

$$\text{Rate} = k_{obs}[\text{epoxide}]^a \quad \text{where} \quad k_{obs} = k[\text{CO}_2]^b [\text{TBAI}]^c \quad \text{Eq.-(2.4)}$$

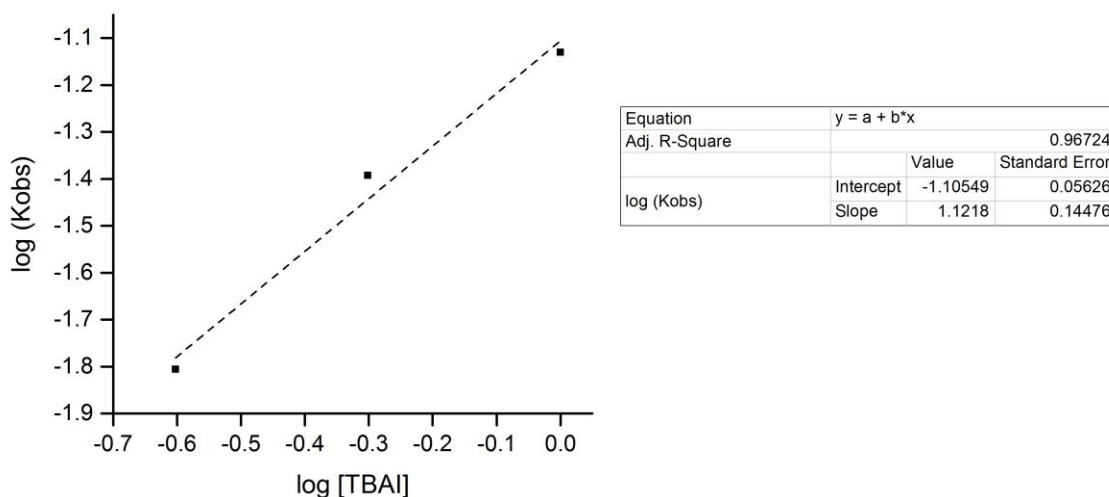
$$\log(k_{obs}) = b \log[\text{CO}_2] + c \log[\text{TBAI}] \quad \text{Eq.-(2.5)}$$

Due to the excess on starting material the reaction kinetics is of *pseudo-zero order* as it is shown in Graph 2.80.



Graph 2.80.- Zero-Order kinetics plots for the conversion of epichlorohydrin to 4-(chloromethyl)-1,3-dioxolan-2-one with different concentrations of tetrabutylammonium iodide. (Circles [TBAI] = 0.25 M $y = -0.01563x + 99.34936$. $R^2 = 0.91829$; Triangles [TBAI] = 0.5 M $y = -0.04047x + 99.83677$. $R^2 = 0.99899$; Squares [TBAI] = 1 M $y = -0.07386x + 100.72099$. $R^2 = 0.99000$).

Representation of the $\log(k_{obs})$ of each reaction against the concentration of TBAI has a slope of 1.1 suggesting a first order in the concentration of tetrabutylammonium iodide (Graph 2.81).



Graph 2.81.- Plot of k_{obs} against [TBAI], which shows that the synthesis of 4-(chloromethyl)-1,3-dioxolan-2-one is first order in [TBAI] ($y = 1.1218x - 1.10549$; $R^2 = 0.96724$).

It is worth noting that usually a number of 4 reactions are analysed in order to determine the reaction order more accurately. However, the 4th reaction (0.05 M TBAI) was discarded due to high dispersion on the data.

CHAPTER 3

CONCLUSIONS AND FUTURE WORK

3 CONCLUSIONS AND FUTURE WORK

3.1 CYCLIC VOLTAMMETRY

The electrochemical studies of the regarding cyclic carboxylation of epoxides in a two electrode system cell with tetrabutylammonium hexafluorophosphate catalyst 1% in acetonitrile were carried out. Electrode screening showed that in general (Pt, GC and Gold working electrodes) solvent decomposition started at a lower potential under N₂ atmosphere than when CO₂ was flushed through. Copper working electrode performed differently showing a broad band appearing from 0.6 to -0.6 V and decomposing acetonitrile at a lower voltage (-0.6 V). Comparison of the different working electrodes CVs showed that their ability for CO₂ reduction when Bu₄NPF₆ catalyst was used can be ranked from higher to lower as follows: Cu > Au > Pt > GC

When Cu working electrode was tested for CO₂ reduction in acetonitrile with Bu₄NBr 1% vs. RHE and platinum as counter electrode a higher dissolution of the Cu atoms occurred and the solution turned purple indicating the possible formation of a coordination complex. This colour was only visible after several scans and never spotted on the reaction mixture before (although the reaction mixture usually turns to a brown-yellowish colour depending on the starting material used). However, Anish P. Patel synthesized and tested the coordination complex [Cu(Br)₄][(Bu₄N)₃] (suspected to be forming) for carboxylation of epoxides with no success.

When magnesium was used as the counter electrode, Cu as working electrode vs RHE and Bu₄NBr 1% in acetonitrile, the changes on the CV could not be assigned to a process due to the complexity of the system when simultaneous dissolution of both Cu and Mg occurs. However, the difference on the CV under CO₂ atmosphere indicates that CO₂ is being reduced at a similar voltage range (-0.6 to -1.2 V).

From comparing the two different electrolytes used and the pairs of electrodes, a classification of performance can be listed as follows (working/counter electrodes-electrolyte 1%):

GC/Pt-Bu₄NPF₆ < Pt/Pt-Bu₄NPF₆ < Au/Pt-Bu₄NPF₆ < Cu/Pt-Bu₄NPF₆ < Cu/Pt-Bu₄NBr < Pt/Pt-Bu₄NBr

This sequence would be consistent with the experimental results obtained previously on catalyst screening for carboxylation of epoxides, being Bu_4NBr a better catalyst than Bu_4NPF_6 . The addition of styrene oxide to the system of Cu/Pt electrodes with Bu_4NBr showed a CV looking as an irreversible process. However, when the electrode pair used was Cu/Mg, a very different curve was acquired with at least three processes going on when CO_2 was flushed. Due to the complexity of the system more experiments should be carried out in order to determine the processes taking place.

A 2015 January publication by Berto, T. C., Zhang, L., Hamers, R. J. & Berry, J. F. reported a deeper analysis on this matter concluding that “the “catalytic” role of NR_4^+ salts in CO_2 electroreduction is non-existent.¹⁵³ None of the current data supports a strong electrostatic interaction between either NR_4^+ and CO_2 or NR_4^+ and the electrode surface, and the diffusion-controlled electroreduction best fits a simple direct outer-sphere reduction of dissolved CO_2 , the mechanism which was originally put forth by Savéant and co-workers.^{154”}.

Experiments using no current were designed to further understand the mechanism of the reaction.

3.2 ICP ANALYSIS OF CU AND MG CONTENT ON ELECTROCATALYTIC CYCLIC CARBOXYLATION OF EPOXIDES

Determination of Cu and Mg ions in reaction mixtures was carried out and results analysed in order to establish a relationship between the quantitative presence of those ions and the yield of the reaction. Cu and Mg content usually rose with time and so did the carbonate within the same reaction, however when comparing different starting materials, trends were not consistent. After 48 hours of reaction of styrene oxide (with TBAI in ACN at 75 °C and 1 atm of CO_2) at a concentration of 0.02 M conversion to carbonate was of 87% containing less than 10 mg/L in Cu and Mg ions. In contrast, after the same time of reaction, 1,2-epoxyhexane conversion to carbonate was of 60% while Cu and Mg ions content was more than 45 mg/L. It can be concluded that a straight relation cannot be identified between Cu and Mg in solution and concentrations and conversion when comparing different starting materials.

3.3 MEASURE OF THE ONSET POTENTIAL OF THE CELL

In order to test the presence of a current flow in a Short Circuit mode reaction the onset potential of the cell was measured with a multimeter. The positive response indicated that due to the voltage difference between the two electrodes a current was flowing from one to the other through the wire that connected them. If more information is to be obtained from this experiment instrumental improvements need to be made. A multichannel multimeter controlled by a computer has been built by A. Sertap Kavasoglu, a colleague from Hacettepe University, Engineering Faculty in Beytepe / Ankara, Turkey and sent to Loughborough University for its use on the future for this purpose. LCMS and $^1\text{H-NMR}$ analysis of reaction samples is also advisable.

3.4 CONSTRUCTION OF A GC/MS FOR ANALYSIS OF *IN-SITU* ELECTROCHEMICALLY ASSISTED CARBOXYLATION REACTIONS

The coupling of a mass spectrometer detector with the electrochemical cell was successful and spectra showed both main components of the reaction (CO_2 and acetonitrile). Different temperatures produced different ratios of intensities of CO_2/ACN and the collection of TIC spectra showed that when warm ACN run through the mass spectrometer it took at least 3 minutes to leave the system due to condensation of the solvent in the capillary. In summary, although the system was working properly, a liquid chromatography device should be added to the MS in order to be able to analyse the content of the liquid phase and to separate CO_2 signals from other possible subproducts of interest like CO. Calibration on CO_2 response of the final instrument would be required to calculate accurate contents of analytes in the reaction mixture.

3.5 BACKGROUND REACTIONS

Three different conditions of background reactions regarding the electrodes were carried out showing conversion of epoxides to carbonates in all of them at different levels: short circuit (when a wire connected both electrodes and no current was applied), open circuit (when electrodes were placed in the solution but no connection between them) and electrodes free (no electrodes were used in the reaction). The performance of these conditions at a given

concentration (0.02 M) of analytes followed the order as expected: Current > Short circuit > open circuit > no electrodes.

3.5.1 Short Circuit reactions

Yields were of 75% of conversion of styrene carbonate after 20 hours under short circuit conditions (in acetonitrile at 75 °C). Temperatures higher than 85 °C would have a degassing effect on the solvent as acetonitrile boiling point is at 83 °C and no conversion would be observed at atmospheric pressure. Different epoxides were tested under these conditions giving different conversion rates as follows: 1,2-phenoxymethyloxirane > fluorostyrene oxide > styrene oxide > chlorostyrene oxide > 1,2-epoxyhexane > bromostyrene oxide > allyl glycidyl ether.

3.5.2 Open circuit reaction

Open circuit conditions produced a 45% of styrene carbonate after 20 hours, but only 20% of chlorostyrene oxide under the same conditions. 12% of 1,2-phenoxymethyl oxirane converted to carbonate after 5 hours of reaction.

3.5.3 Carboxylation of epoxides (No Electrodes)

3.5.3.1 Dilute reactions

Carboxylation of epoxides under no electrodes conditions was as low as 5% at a concentration of 0.02 M in acetonitrile at 75 °C after 24 hours. However, and before concentration was purposely risen, two reactions suffered slow evaporation of the solvent while overnight reaction due to a difference in pressure of the CO₂ flow possibly caused by the change of temperature in the laboratory room during the night and morning. The conversion on these reactions rose from 7% after 24 hours for chlorostyrene carbonate to 70% in the next 24 hours; and from 4% after 24 hours to 92% in the next 24 hours for fluorostyrene carbonate. The ¹H NMR analysis of the crude comparing integral values of starting material and tetrabutylammonium iodide confirmed that despite the higher flow rate of CO₂ causing evaporation of the solvent starting materials did not evaporate.

A study on the ratio epoxide:catalyst was carried out with bromostyrene oxide as starting material and TBAI. 1:1 and 1:2 ratios at a concentration of 0.04 M produced a significantly slower reaction than the one held at 1:1.5 ratio and 0.26 M. Conversions were of 15, 20 and 40%

respectively after 48 hours showing that influence of concentration of the species on the reaction was higher than the influence of the catalyst ratio.

3.5.3.2 MgCO_3 and MgBr_2 as cocatalyst for cyclic carboxylation of epoxides

The possibility of MgBr_2 and MgCO_3 species causing the formation of carbonate was rejected by a series of experiments that produced no conversion after 20 to 72 hours. Although these species might form when electrodes and current are used, the inorganic form is not catalysing the carboxylation of epoxides as concluded from these experiments.

3.5.3.3 Concentration Study

A molarity study using 1,2-phenoxymethyl oxirane and TBAI (1:1) showed the clear reaction rate improvement when increasing concentration. Yield after 5 hours went from 4% at 0.1 M to 54% at 2.0 M (the actual concentration would be lower than 2 M due to partial insolubility of the catalyst as the acetonitrile got saturated).

Conduction of a study of the solubility of tetrabutylammonium iodide in acetonitrile at different temperatures could fill a gap in literature about these experimental data. In the same way, analyses of concentration of CO_2 in acetonitrile at different temperatures, with and without tetrabutylammonium iodide in solution could tell us if the ammonium salt is capturing CO_2 when dissolved in acetonitrile.

3.5.3.4 High concentrate cyclic carboxylation reactions

Reactions at higher concentrations (1 M or higher) were carried out with different CO_2 source. When a direct flow from the CO_2 cylinder was flushed through the cell reaction rates always performed better, especially after 5 hours of reaction, than when CO_2 was supplied by a balloon that was refilled as needed (expect overnight, when the balloon was left until the next day). This could be due to the fact that when heating at 75 °C the pressure in the cell is positive towards outside due to partial evaporation of the solvent. That means that the CO_2 contained in the balloon is coming to the cell at a lower rate. If instead the CO_2 is flushed with a constant flow rate, the concentration of CO_2 will be maintained. The fact that some solvent can evaporate out of the cell with the CO_2 flow, means that the actual concentration of species in solution when CO_2 flow is used could be higher than the initial one (usually 1 M). This could be improving the yields as compared to the balloon source. Also, the balloon needle got sometimes solvent condensed

inside and had to be emptied in order for the CO₂ to keep flowing (that was accomplished only by applying pressure on the balloon so the solvent would drop back to the reaction mixture).

However, due to the high volatility of styrene oxide the balloon source was chosen to avoid the loss of the starting material and maintained in order to compare with the rest of epoxides performance.

3.5.3.5 Glycidol and epichlorohydrin cyclic carboxylation

In general, reactions were analysed at 5 hours and 20 or 24 hours by sampling and running ¹H NMR of the crude. For all starting materials that got 100% of conversion at 24 hours the time at which the reaction finished was uncertain as it probably finished overnight but was not tested until the next morning. This was the case of epichlorohydrin and glycidol at 1 M in acetonitrile with TBAI (1:1) that got 100% of conversion to the corresponding carbonate after only 5 hours. Further experiments sampling hourly were carried out at different epoxide:TBAI ratios (1:1 ; 10:1 and 100:1). Again, ratio 1:1 presented a higher conversion rate particularly differentiated for the glycidol carboxylation.

3.5.3.6 Cyclic carboxylation of 3-hydroxyoxetane

Four membered ring epoxide 3-hydroxyoxetane carboxylation was unsuccessfully attempted under these conditions (TBAI in acetonitrile, 75 °C and 1 atm pressure of CO₂).

3.5.3.7 NH₄I catalyst for cyclic carboxylation of 1,2-phenoxyethyloxirane

The attempt to replicate the new reaction conditions without electrodes of the electrochemical system reported in the literature using NH₃/I₂ as electrocatalysts¹⁵² was also carried out. Carbonate conversion was achieved using NH₄I in acetonitrile (low solubility of the salt was an issue) at 75 °C, under CO₂ atmosphere although as a minor product (18% after 24 hours). The main product (78%) was the halogenated alcohol formed from the ring opening by I⁻ and the protonation from the NH₄⁺ (1-iodo-3-phenoxypropan-2-ol).

3.5.3.8 Study of enantioselectivity of cyclic carboxylation of (S)-1,2-phenoxyethyloxirane

Carboxylation of (S)-1,2-phenoxyethyl oxirane was analysed by chiral HPLC showing that the product was enantiomerically pure and rejecting the possibility of carbocation intermediates on the chiral carbon in the mechanism.

3.5.3.9 Solvent free reactions or neat reactions

Carboxylation of epoxides under neat conditions (epoxide:TBAI 1:1 at 75 °C) was successfully achieved. Performance varied greatly depending on the starting material and the conversion after 24 hours followed the next series: allyl glycidyl ether (94%) > 1,2-phenoxyethyl oxirane (79%) > bromostyrene oxide (68%) > chlorostyrene oxide (49%) > styrene oxide (44%) > fluorostyrene oxide (31%) > 1,2-epoxyhexane (24%) > propylene oxide (3%).

3.5.3.10 Solvent screening study of the cyclic carboxylation reaction of 1,2-phenoxyethyl oxirane

A solvent screening study revealed that the more polar the solvent the higher the yield of carbonate conversion. Also protic solvents showed excellent conversions with 100% achieved after 5 hours. Conditions were 1:1 at 75 °C. Reaction in H₂O went by two phases. Presence of hydrogen bonds from solvents –OH to carbon dioxide could be the answer to the good performance of these solvents. Also, that could be the explanation as well for the exceptional conversion rates for the glycidol compared to other starting materials.

3.5.3.11 Phosphonium salts as catalysts.

Resulting of a collaboration with Prof. Martin Smith and grad student Matías Giménez, phosphonium salts as catalysts were tested under the neat reaction conditions. An optimization of the catalyst structure was concluded based on the results of different anions performance and different phosphonium structures performance.

The anions screening study was carried out using PS1 (see Table 4.8) as the phosphonium structure. Conversions to carbonate after 24 hours of reaction went from 0% with PS1BPh₄ to 90% with PS1I. There is a clear trend on anion activity, sorted by higher to lower performance as follows: I⁻ > Br⁻ > Cl⁻ > BF₄⁻ > BPh₄

Synthesis of PS1I is carried out beginning with PS1Cl and LiI, so the reaction was run with PS1Cl and LiI to produce PS1I *in situ*. In this way, a whole step on the synthesis of the catalyst was saved by producing it within the reaction mixture.

The reaction mixture solidified when carbonate concentration reached the saturation point and time of completion of conversion is not accurate.

In order to evaluate the efficiency of different phosphonium cations, structures in Table 2.29 were tested (PS1, PS2, PS3 and PS4). For the carboxylation reactions of 1,2-phenoxymethyl oxirane and styrene oxide the order of catalyst performance was: PS3 > PS4 > PS1 = PS2. However, carboxylation of allyl glycidyl ether showed a reversed on catalytic activity: PS4 = PS1 > PS3.

Testing these catalysts on other epoxides or functional groups would be of interest for a future project.

3.6 FTIR MONITORING CARBOXYLATION REACTION AND CALCULATION OF REACTION KINETICS

Kinetic studies were carried out using a ReactIR to on-line monitor the conversion of epichlorohydrin to carbonate, thanks to a collaboration in Matt Sigman's laboratory in the Organic department of The University of Utah, USA. Representation of concentration of remaining epoxide versus time showed a linear correlation suggesting a zeroth order of reaction. Representation of the logarithmic k_{obs} vs $\log([TBAI])$ showed a linear correlation with a slope of 1.1 suggesting a first order with respect to TBAI concentration. Other studies to determine the reaction order with respect to CO_2 could be carried out. Other epoxides carboxylation reaction kinetics would be interesting to calculate and compare with the results obtained.

CHAPTER 4

EXPERIMENTAL

4 EXPERIMENTAL

4.1 ELECTROCHEMICAL EXPERIMENTS

4.1.1 Reagents and apparatus

Potentiometric analysis were performed using a model 760 C Potentiostat from CHInstruments, Inc. (Austin, Texas, USA).

Electrodes dimensions were 2 mm diameter for Pt and Au disk electrodes, 3 mm diameter for Glassy-Carbon disk electrode, 2 mm diameter of Cu rod and approximately 3 mm wide-0.15mm thick Mg ribbon. Before every measure, disk electrodes were polished with 1.0, 0.3 and 0.05 micron alumina in a sequence on a polishing pad. In order to eliminate the protective passivated layer, Cu rod and Mg ribbon electrodes were sanded with sand paper followed by a wipe to remove remaining powder. Hydroflex Reversible Hydrogen Electrode was used as the reference electrode.

4.1.2 Electrochemical Cell design

The three electrode system was set up in a 25 mL three necked round bottom flask as a single compartment cell and 0.1% w/v Tetrabutylammonium hexafluorophosphate (Bu_4NPF_6 or TBAHF) or Tetrabutylammonium bromide (Bu_4NBr or TBABr) acetonitrile solution as the electrolyte (Figure 4.1). The cyclic voltammograms were acquired firstly under nitrogen atmosphere by purging the solution with N_2 gas for one hour followed by a constant draft through the cell of N_2 , and secondly, in CO_2 saturated solution from bubbling CO_2 gas for one hour followed by a constant draft of CO_2 .

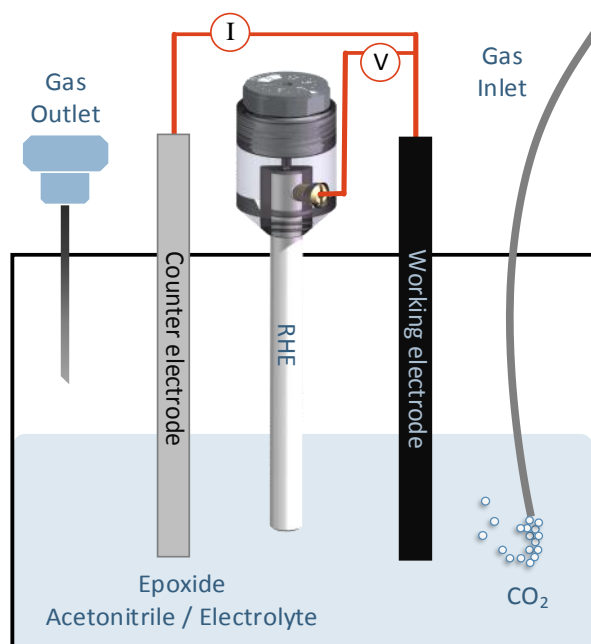


Figure 4.1.- Single compartment Electrochemical cell set up. See also section 4.1.2 for experimental conditions.

Electrochemical reduction of carbon dioxide in acetonitrile solution has been studied by cyclic voltammetry technique. Different electrodes have been tested and compared to identify the best performance system conditions. As previously discussed, electrode material is crucial in the mechanism of carbon dioxide reduction and the product of the reaction depends on the electrocatalytic activity of the cathodic metal and on other factors like the composition of the supporting electrolyte (aqueous or nonaqueous solutions), and the experimental reaction parameters (cathode potential, current density, temperature and pressure).

Table 4.1 summarizes the cyclic voltammetry experimental conditions of every experiment carried out which will be later explained in more detail. Platinum, Glassy-carbon, gold and copper electrodes were tested for carbon dioxide electrochemical reduction in acetonitrile with Bu_4NPF_6 or Bu_4NBr as electrolyte. Platinum wire was used as counter electrode except in entries 6 and 8 where Magnesium ribbon was used instead. The reference electrode employed was Standard Hydrogen Electrode from Hydroflex and a Scan Rate of 0.1 V/s.

Table 4.1.- Experimental conditions for cyclic voltammetry experiments of carbon dioxide electrochemical reduction.

Entry	Electrodes				ELECTROLYTE	Epoxide
	Working	type	Counter	type		
1	Pt	disk	Pt	wire	Bu ₄ NPF ₆	-
2	GC	disk	Pt	wire	Bu ₄ NPF ₆	-
3	Au	disk	Pt	wire	Bu ₄ NPF ₆	-
4	Cu	rod	Pt	wire	Bu ₄ NPF ₆	-
5	Cu	rod	Pt	wire	Bu ₄ NBr	-
6	Cu	rod	Mg	ribbon	Bu ₄ NBr	-
7	Cu	rod	Pt	wire	Bu ₄ NBr	Styrene oxide
8	Cu	rod	Mg	ribbon	Bu ₄ NBr	Styrene oxide

Where "GC" is Glassy-Carbon; General conditions: 0.1% electrolyte solution in acetonitrile, Reversible hydrogen electrode as reference.

4.2 ICP ANALYSIS OF CU AND MG CONTENT ON ELECTROCATALYTIC CYCLIC CARBOXYLATION OF EPOXIDES

Copper and Magnesium content in solution after Short Circuit reactions was measured by Atomic Absorption Spectrometry (AAS) using a iCE3000 AAS series from Thermo Fisher Scientific. Different range of dilutions of Cu and Mg (1000 ppm) stock solutions from Fischer Scientific were used to calibrate the instrument. The sensitivity range of the instrument to Cu is 2 to 8 ppm and to Mg is 0.1 to 0.4 ppm as listed in the manual. One stock solution of Cu (100 ppm) and one of Mg (10 ppm) were prepared as follows:



- Cu solution (100 ppm): Dilut 10 mL of Cu stock solution (1000 ppm) to 100 mL in a volumetric flask.
- Mg solution (10 ppm): Dilut 1 mL of Mg stock solution (1000 ppm) to 100 mL in a volumetric flask.

Standard solutions were prepared from Cu (100 ppm) and Mg (10 ppm) solutions as indicated in Table 4.2.

Table 4.2.- preparation of standard solutions for calibration.

Std solution	V(Cu) (mL)	V(Mg) (mL)	Final V (mL)	[Cu] (ppm)	[Mg] (ppm)
1	2	1	100	2	0.1
2	4	2	100	4	0.2
3	6	3	100	6	0.3
4	16	8	200	8	0.4

Sample preparation:

After a first dilution 1 to 10 with water, and checking the range of concentration of Cu and Mg in our sample, redilution was usually necessary for Mg analysis. The data were later normalized.

4.3 MEASURE OF THE ONSET POTENTIAL OF THE CELL

Some Short Circuit reactions were monitored looking at the onset potential of the cell. This was simply measured by connecting a multimeter to the Cu and Mg electrodes on the voltmeter mode. The usual response was in a range from 0.8 to 1 volt which is the potential at which CO₂ has been found to start to be reduced at different electrodes^{91,157,158}. If this occurs, the products of the reduction could be determined by analysing the system by LCMS coupled to the electrochemical cell.

The current has been also measured for a period of 80 minutes with the same multimeter set up on the amperimeter mode. The experimental procedure of the reaction set up is the same as explained for short circuit reactions in section 4.6.2.5.

4.4 DMS ANALYTICAL TECHNIQUE TO MONITOR IN-SITU ELECTROCATALYTIC

CYCLIC CARBOXYLATION OF EPOXIDES.

This experiment was carried out in the Analytical chemistry department in Loughborough University. Mchem student Ellie Henshall-Bell performed the DMS analysis measurements under the supervision of Dr. Jim Reynolds and Prof. Paul Thomas. I carried out the electrochemical cell set up and assisted on the connection of the cell to the DMS device and the supervision of the reaction and measurements.

Sionex Corporation differential mobility spectrometer was used for the DMS studies. Instrumental details are listed in Table 4.3.

Table 4.3.- Instrumental details for the DMS-electrochemical cell coupled experiment.

Parameter	Setting
Instrument and serial no.	Sionex Differential Mobility Spectrometer SVAC-V SVAC-0126
Transport gas	N ₂
Transport gas purity	High purity grade 5.0 (99.999%)
Transport gas flow rate, F ₂	340-350 cm ³ min ⁻¹
T _{sensor}	100 °C
RF Voltage (V _{RF})	500-1400 V
Compensation Voltage (V _C)	-45 to +12 V
Software and versión	Sionex Expert
Computer	Sionex 1004

A second device (serial no. SVAC-V0136) with same specifications was used for previous analysis in order to collect spectra of CO₂, Methanol and mixtures of both gases.

All glassware used in the experiment was fully washed with water, methanol, and dichloromethane and later dried under high vacuum oven over weekend. No grease was used in the junctions to avoid contamination and problems in measurements.

A 25 mL three necked round bottom flask was used as a single compartment electrochemical cell topped with a reflux tube and electrode couplings. Copper rod as cathode and Magnesium ribbon as anode were previously sanded to remove the passivated layer on the metal surface. The cell was filled with 10 mL of Bu₄NBr-acetonitrile electrolyte solution and styrene oxide added in a 2:1 ratio. Solution was purged for 30 min with a CO₂ gas flow of 5 mL/min which was kept along all the process. A capillary tube was introduced as the outlet to the DMS instrument (flow rate 1.6 mL/min) and an extra gas outlet (metal needle) was placed to avoid overpressure in the system (picture in Annexe, Figure 5.3). Special care was taken to avoid contact between electrodes (Annexe, Figure 5.4).

Blanks were measured in-between every addition of a new component in the cell and the reaction was monitored every hour (Table 4.4).

Table 4.4.- Blanks and measurements carried out during experiment.

Experiment		T (°C)	air	CO ₂ (5 mL/min)	Current (60 mA)	TBABr (0.1 M)	TBABr + SO
1	blank (air background)	rt	x				
2	CO ₂ blank	rt		x		x	
3	CO ₂ blank with SO	rt		x			x
4	current blank	rt		x	x	x	
5	current blank SO	rt		x	x		x
6	Current blank 50 °C	50		x	x	x	
7	current blank SO 50 °C	50		x	x		x

Acetonitrile (10 mL) was used as solvent. Bu₄NBr and styrene oxide added in a 2:1 ratio. SO stands for “styrene oxide”.

As the Table 4.4 shows, blanks were recorded in-between every addition of a new component in the cell. So that there was a background of every step: opened cell (air blank); closed cell (CO₂/air blank); CO₂ saturated electrolyte solution; CO₂ saturated electrolyte solution with constant current of 60 mA at room temperature; CO₂ saturated electrolyte solution constant current of 60 mA at 50 °C; and same blanks as before but adding the reactant, styrene oxide. Once all the conditions on (CO₂ saturated solution, 60 mA constant current, 50 °C), the reaction was monitored every hour for 4 hours.

4.5 CONSTRUCTION OF A GC/MS FOR ANALYSIS OF *IN-SITU*

ELECTROCHEMICALLY ASSISTED CARBOXYLATION REACTIONS

An attempt of mass spectrometry analysis of compounds produced in the electrocarboxylation of epoxides was made by building a mass spectrometer in the laboratory next to a fumehood in where the electrochemical cell was placed to run the reaction. A silicon tube fitted with a metal syringe connects the cell to a manual valve injector that dispenses the sample to a glass capillary that continues into the mass spectrometer. The carrier gas when the instrument was not sampling was Helium flowing at 1.5 mL/min. When a sample was taken, the positive pressure of CO₂ in the electrochemical cell carried the vapours to the loop in the manual valve.

4.6 ORGANIC SYNTHESIS PROCEDURES

4.6.1 Reagents and apparatus

The NMR spectra were recorded in a Jeol JNM-ECS400 or a Bruker Avance 400 MHz spectrometer. The solvent used for NMR spectroscopy was CDCl_3 (unless stated otherwise) using TMS (tetramethylsilane) as the internal reference.

Reactions were monitored using thin layer chromatography (TLC) visualised by UV radiation at a wavelength of 254 nm, or stained by exposure to an ethanoic solution of phosphomolybdic acid (acidified with concentrated sulfuric acid), followed by charring when appropriate. Purification by column chromatography used Merck Kiesel 60 H silica adsorbent.

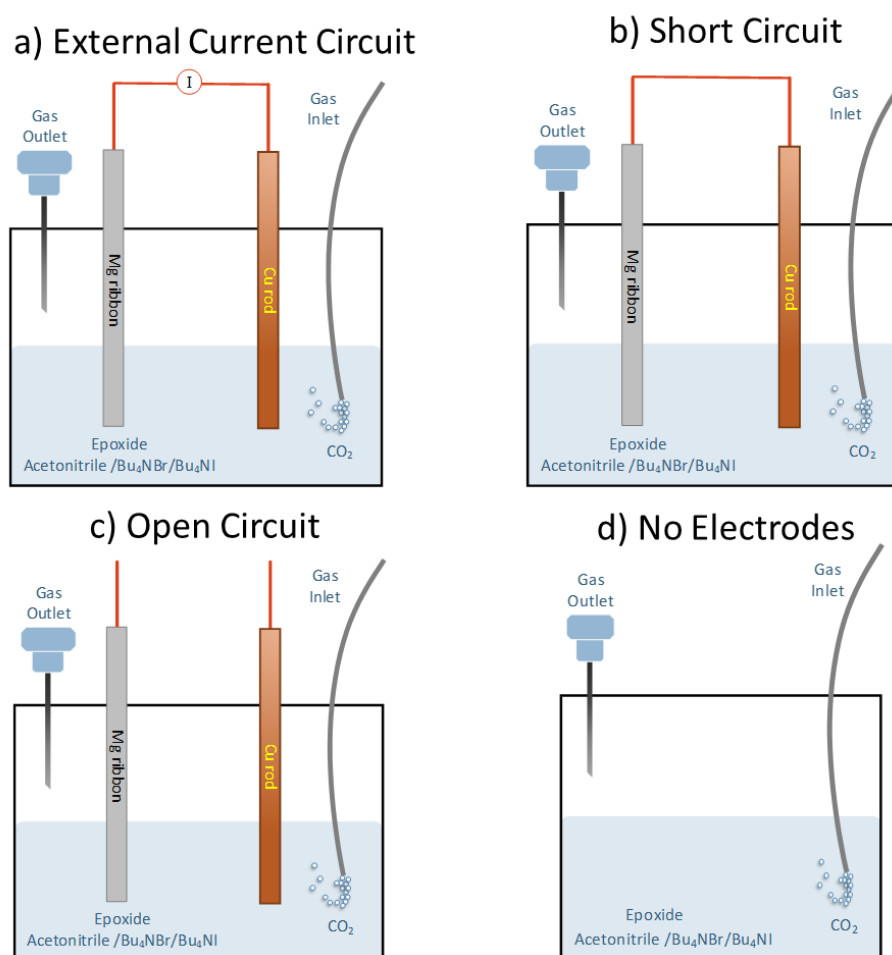
All infrared spectra were recorded in a FT-IR 8400S with GS10800-X Quest ATR diamond accessory. At the University of Utah, ReactIR iC10 from Mettler Toledo was used for monitoring cyclic carboxylation reactions of epoxides and carbon dioxide. All chemicals were used as received.

Table 4.5.- Chemicals CAS no. and supplier.

Entry	Name / IUPAC name	Grade (%)	CAS no.	Supplier
1	Styrene Oxide / 2-Phenyloxirane	97	96-09-3	Aldrich
2	Chlorostyrene Oxide / 2-(4-Chlorophenyl)oxirane	96	2788-86-5	Aldrich
3	Fluorostyrene Oxide / 2-(4-Fluorophenyl)oxirane	95	18511-62-1	Alfa Aesar
4	Bromostyrene Oxide / 2-(4-Bromophenyl)oxirane	96	32017-76-8	Aldrich
5	1,2-Phenoxyethyl oxirane / 1,2-Epoxy-3-phenoxypropane	99	122-60-1	Aldrich
6	1,2-Epoxyhexane	96	1436-34-6	Alfa Aesar
7	Allylglycidyl Ether / Allyl 2,3-epoxypropyl ether	99	106-92-3	Acros Organics
8	(+)-Propylene oxide	99	75-56-9	Sigma Aldrich
9	Epichlorohydrin / 2-(chloromethyl)oxirane	99	106-89-8	Sigma Aldrich
10	Trimethylene oxide / Oxetane / 1,3-propylene oxide	97	503-30-0	Sigma Aldrich
11	2-methyl styrene oxide / 2-Methyl-2-phenyloxirane	98	2085-88-3	Sigma Aldrich
12	alpha-methylstyrene / 2-Phenylpropene	99	98-83-9	Sigma Aldrich
13	glycidol / 2,3-Epoxy-1-propanol	96	556-52-5	Sigma Aldrich
14	4-Methylstyrene oxide / 2-(4-methylphenyl)oxirane	99	13107-39-6	Sigma Aldrich
15	2-(4-methoxyphenyl)oxirane	99	6388-72-3	Sigma Aldrich
16	4-Methoxystyrene / 4-Vinylanisole	97	637-69-4	Sigma Aldrich
17	4-Methylstyrene / 4-Vinyltoluene	96	622-97-9	Sigma Aldrich
18	3-hydroxyoxetane / oxetan-3-ol	95	7748-36-9	Sigma Aldrich
19	N-tetrabutylammonium Iodide / Bu ₄ NI / TBAI	98	311-28-4	Alfa Aesar
20	N-tetrabutylammonium Bromide / Bu ₄ NBr / TBABr	98	1643-19-2	Alfa Aesar
21	Magnesium carbonate hydroxide hydrate / MgCO ₃ •Mg(OH) ₂ •3H ₂ O	95	235-192-7	Acros Organics
22	Magnesium bromide / MgBr ₂	98	7789-48-2	Aldrich
23	Acetonitrile anhydrous / ACN / MeCN	99.8	75-05-8	Sigma Aldrich
24	Ethyl Acetate / EtOAc	99	141-78-6	Fischer Scientific
25	Diethyl ether	99.7	60-29-7	Sigma Aldrich
26	Deionized water	99.9	7732-18-5	Sigma Aldrich
27	Ethanol / EtOH	99	64-17-5	Fischer Scientific
28	Acetonitrile / ACN / MeCN	99	75-05-8	Sigma Aldrich
29	Carbon dioxide	100	124-38-9	BOC

4.6.2 Reaction conditions and procedures

Three different experimental conditions have been designed in order to carry out the control reaction blanks of the electrocarboxylation of epoxides. Scheme 4.1 shows the electrodes conditions of these experiments.



Scheme 4.1.- Electrodes experimental conditions summary for the Control reactions of electrocarboxylation of epoxides. a) An external current of 60 mA is applied to the electrodes. b) A Short Circuit using a wire to connect both electrodes. c) Open circuit where electrodes are in solution but no contact exists between them and d) Reaction with NO electrodes.

External Current conditions (Scheme 4.1, a)) refers to the electrochemical carboxylation of epoxides run by applying 60 mA of current to the electrodes. Short Circuit conditions (Scheme 4.1, b)) consists on connecting the electrodes with a wire and applying no current. Open Circuit conditions (Scheme 4.1, c)) consists on inserting the electrodes in solution with no connection between them. And No Electrodes conditions (Scheme 4.1, d)) consists on running the blank of the reaction with the only presence of the reagents and no Cu nor Mg and at different

concentrations (dilute, high concentrated and solvent free conditions). Ten different starting materials listed below have been studied under the named reaction conditions.

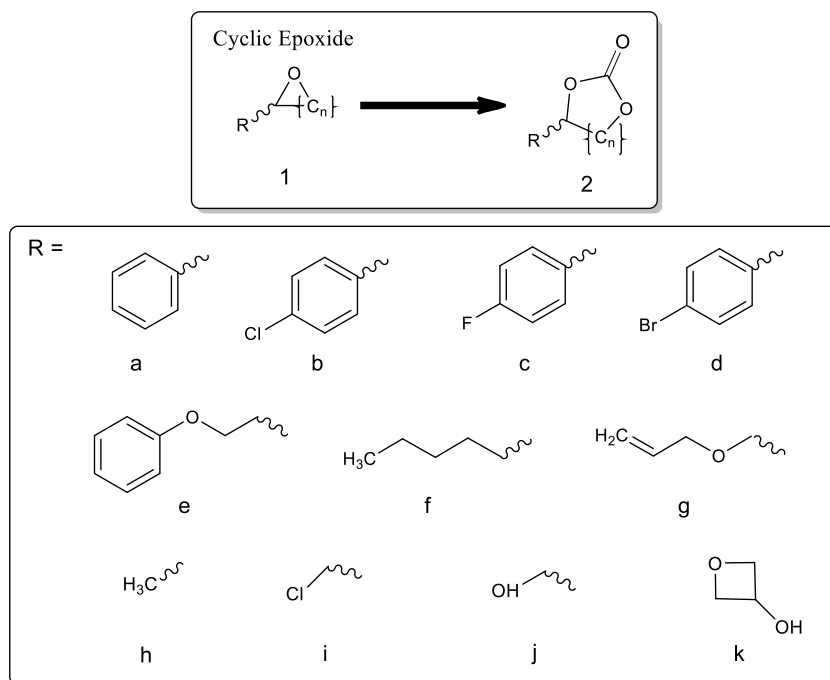
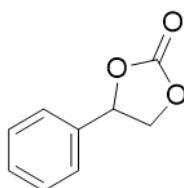


Figure 4.2.- Starting materials with different functional groups. From 1a to 1k. Products from b1 to b10.

4.6.2.1 Product characterization

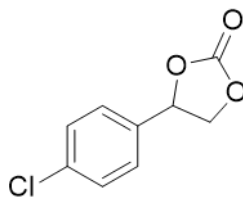
All product ^1H NMR, ^{13}C NMR and IR data are listed below:

- **4-phenyl-1,3-dioxolan-2-one (2a)**



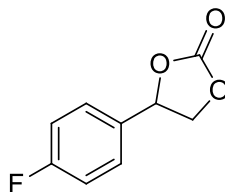
as an amber oil; $\nu_{\text{max}}(\text{CH}_2\text{Cl}_2)/\text{cm}^{-1}$ 1768 (C=O), 1165 (C-O); ^1H NMR (400 MHz, CDCl_3) δ ppm 4.36 (t, $J=8.2$ Hz, 1 H), 4.81 (t, $J=8.5$ Hz, 1 H), 5.69 (t, $J=8.0$ Hz, 1 H), 7.34 - 7.50 (m, 5 H). ^{13}C NMR (100 MHz, CDCl_3 , Me_4Si) δ_{c} ppm 71.2, 78.1, 125.94, 129.3, 129.8, 135.9, 154.9. Data in agreement with literature.¹⁶⁸

- **4-(4-chlorophenyl)-1,3-dioxolan-2-one (2b)**



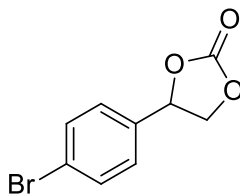
as a white solid mp 67-70 °C; $\nu_{\max}(\text{CH}_2\text{Cl}_2)/\text{cm}^{-1}$ 1645 (C=O), 1203 (C-O), 790 (C-Cl); ^1H NMR (400 MHz, CDCl_3) δ ppm 4.31 (t, $J=8.2$ Hz, 1 H), 4.84 (t, $J=8.4$ Hz, 1 H), 5.69 (t, $J=7.9$ Hz, 1 H), 7.30 - 7.35 (m, 2 H), 7.43 (m, 2 H), ^{13}C NMR (100 MHz, CDCl_3 , Me_4Si) δ_{c} ppm 71.0, 127.3, 129.5, 134.3, 135.8, 154.5. Data in agreement with literature.¹⁶⁹

- **4-(4-fluorophenyl)-1,3-dioxolan-2-one (2c)**



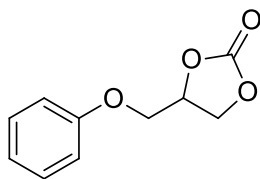
as a colorless solid. Mp 63-65 °C; $\nu_{\max}(\text{CH}_2\text{Cl}_2)/\text{cm}^{-1}$ 1643 (C=O), 1160 (C-O), 1056 (C-F); ^1H NMR (400 MHz, CDCl_3) δ ppm 4.32 (t, $J=8.2$ Hz, 1 H), 4.82 (t, $J=8.5$ Hz, 1 H), 5.73 (t, $J=8.0$ Hz, 1 H), 7.16 (m, 2 H), 7.39 - 7.49 (m, 2 H), ^{13}C NMR δ_{c} (100 MHz, CDCl_3 , Me_4Si) 71.1, 77.4, 116.0, 127.4, 131.5, 154.6, 164.6. Data in agreement with literature.¹¹⁷

- **4-(4-bromophenyl)-1,3-dioxolan-2-one (2d)**



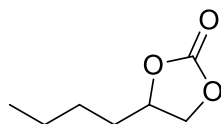
as a white solid, mp 72-74 °C; $\nu_{\max}(\text{CH}_2\text{Cl}_2)/\text{cm}^{-1}$ 2946, 2518, 2159, 2028, 1976, 1818, 1785; ^1H NMR (400 MHz, CDCl_3) δ ppm 4.30 (dd, $J=8.7, 7.8$ Hz, 1 H), 4.81 (t, $J=8.4$ Hz, 1 H), 5.65 (t, $J=8.0$ Hz, 1 H), 7.19 - 7.31 (m, 2 H), 7.54 - 7.64 (m, 2 H). ^{13}C NMR (100 MHz, CDCl_3 , Me_4Si) δ_{c} ppm 70.9, 77.2, 123.8, 127.5, 132.4, 134.7, 154.5. Data in agreement with literature.¹⁶⁹

- **4-(phenoxymethyl)-1,3-dioxolan-2-one (2e)**



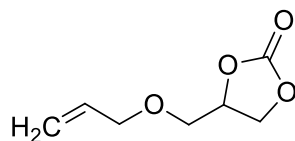
as a white solid, mp 95-97 °C; $\nu_{\max}/\text{cm}^{-1}$ 1787 (C=O); $^1\text{H NMR}$ (400 MHz, CDCl_3) δ ppm 4.13 (dd, $J=7.0, 3.5$ Hz, 1 H), 4.23 (dd, $J=10.6, 4.1$ Hz, 1 H), 4.52 (dd, $J=8.56, 5.91$ Hz, 1 H), 4.60 (t, $J=8.4$ Hz, 1 H), 4.97 - 5.06 (m, 1 H), 6.91 (d, $J=8.3$ Hz, 2 H), 6.98 (t, $J=7.9$ Hz, 1 H), 7.31 (t, $J=7.9$ Hz, 2 H). $^{13}\text{C NMR}$ (100 MHz, CDCl_3 , Me_4Si) δ_{C} ppm 66.2, 66.9, 74.1, 114.6, 121.9, 129.6, 154.7, 157.8. Data in agreement with literature.¹²²

- **4-butyl-1,3-dioxolan-2-one (2f)**



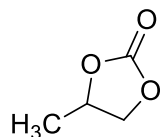
as a yellow clear oil; $\nu_{\max}(\text{CH}_2\text{Cl}_2)/\text{cm}^{-1}$ 1791 (C=O), 1165 (C-O); $^1\text{H NMR}$ (400 MHz, CDCl_3) δ ppm 0.93 (t, $J=6.9$ Hz, 3 H), 1.29 - 1.53 (m, 4 H), 1.64 - 1.75 (m, 1 H), 1.76 - 1.87 (m, 1 H), 4.08 (dd, $J=8.4, 7.2$ Hz, 1 H), 4.54 (t, $J=8.2$ Hz, 1 H), 4.67 - 4.78 (m, 1 H). $^{13}\text{C NMR}$ (100 MHz, CDCl_3 , Me_4Si) δ_{C} ppm 13.7, 22.1, 26.3, 33.4, 69.3, 77.0, 155.1. Data in agreement with literature.¹²²

- **4-((allyloxy)methyl)-1,3-dioxolan-2-one (2g)**



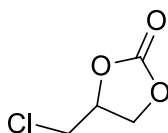
as a clear oil; $\nu_{\max}(\text{CH}_2\text{Cl}_2)/\text{cm}^{-1}$ 1781 (C=O), 1645 (C=C), 1193 (C-O); $^1\text{H NMR}$ (400 MHz, CDCl_3) δ ppm 3.61 (dd, $J=11.1, 3.8$ Hz, 1 H), 3.72 (dd, $J=11.1, 3.0$ Hz, 1 H), 4.05 (d, $J=5.6$ Hz, 2 H), 4.39 (dd, $J=8.1, 6.0$ Hz, 1 H), 4.53 (t, $J=8.3$ Hz, 1 H), 4.84 - 4.92 (m, 1 H), 5.21 (dt, $J=10.3, 1.3$ Hz, 1 H), 5.29 (dt, $J=17.4, 1.3$ Hz, 1 H), (ddt, $J=17.4, 10.5, 5.7$ Hz, 1 H). $^{13}\text{C NMR}$ (100 MHz, CDCl_3 , Me_4Si) δ_{C} ppm 66.2, 68.7, 72.4, 75.0, 117.8, 133.6, 154.9. Data in agreement with literature.¹⁷⁰

- **4-methyl-1,3-dioxolan-2-one (2h)**



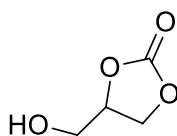
as a clear oil; $\nu_{\max}(\text{CH}_2\text{Cl}_2)/\text{cm}^{-1}$ 1782 (C=O)¹⁵¹; ^1H NMR (400 MHz, CDCl_3) δ ppm 1.26 (m, $J=6.3$ Hz, 1 H), 3.87 (dd, $J=8.2, 7.1$ Hz, 1 H), 4.43 (dd, $J=8.2, 7.1$ Hz, 1 H), 4.68 - 4.78 (m, 1 H); ^{13}C NMR (100 MHz, CDCl_3 , Me_4Si) δ_{C} ppm 19.3, 70.6, 73.5, 155.1. Data in agreement with literature.¹⁷⁰

- **4-(chloromethyl)-1,3-dioxolan-2-one (2i)**



as a yellow clear oil °C; $\nu_{\max}(\text{CH}_2\text{Cl}_2)/\text{cm}^{-1}$ 1800 (C=O), 1150 (C-O), 1050 (C-Cl); ^1H NMR (400 MHz, CDCl_3) δ ppm 3.75 (m, $J=11.4, 3.7$ Hz, 1 H), 3.81 (dd, $J=12.4, 6.0$ Hz, 1 H), 4.43 (dd, $J=8.9, 5.7$ Hz, 1 H), 4.61 (t, $J=8.5$ Hz, 1 H), 4.95 - 5.04 (m, 1 H); ^{13}C NMR (100 MHz, CDCl_3 , Me_4Si) δ_{C} ppm 44.2, 66.6, 74.3, 154.5. Data in agreement with literature.¹⁷⁰

- **4-(hydroxymethyl)-1,3-dioxolan-2-one (2j)**



as a clear oil; $\nu_{\max}(\text{CH}_2\text{Cl}_2)/\text{cm}^{-1}$ 3433 (-OH), 1767 (C=O), 1397, 1165 (C-O); ^1H NMR (400 MHz, CDCl_3) δ ppm 3.04 (s, 1 H), 3.71 (dd, $J=13.1, 3.4$ Hz, 1 H), 3.99 (dd, $J=12.8, 2.7$ Hz, 1 H), 4.47 (dd, $J=8.2, 6.9$ Hz, 1 H), 4.54 (t, $J=8.2$ Hz, 1 H), 4.77 - 4.87 (m, 1 H); ^{13}C NMR (100 MHz, CDCl_3 , Me_4Si) δ_{C} ppm 60.4, 65.6, 76.9, 155.0. Data in agreement with literature.¹

4.6.2.2 % of conversion Calculations

Due to volatility of many of the epoxides used as starting material in the reactions, ratios of conversion after work up are not reliable. A way of accurately knowing the % of conversion in every moment is by sampling the reaction solution and analysing the mixture by $^1\text{H-NMR}$ spectroscopy. If the solution is dilute the strong response of the solvent will translate on a loss of accuracy on the target signals (reactants). There exists an NMR solvent suppression technique called “presaturation at solvent signal” that allows to “hide” the solvent peak and improve the baseline and integration areas accuracy of the analyte signals resulting in a better resolution spectra.

$^1\text{H-NMR}$ analysis of solutions were made after 5/19/24/48 and/or 72 hours under this technique. See an example of $^1\text{H-NMR}$ spectrum (Figure 4.3) and $^1\text{H-NMR}$ “presaturated at ACN signal” spectrum (Figure 4.4) of 2-(4-fluorophenyl)oxirane (or fluorostyrene oxide) carboxylation after 24 hours of reaction. This technique allows us to visualize the signals corresponding to the product with higher accuracy. However, signals which δ shift is near the solvent signal (like ammonium salt H signals from 1.5 – 2.5 ppm) suffer distortion and integral values decrease considerably (almost half of its true value). The same sample was analysed by $^1\text{H NMR}$ with and without solvent suppression technique in order to confirm that only the ammonium salt signals are affected by the distortion and the epoxide signals remain constant.

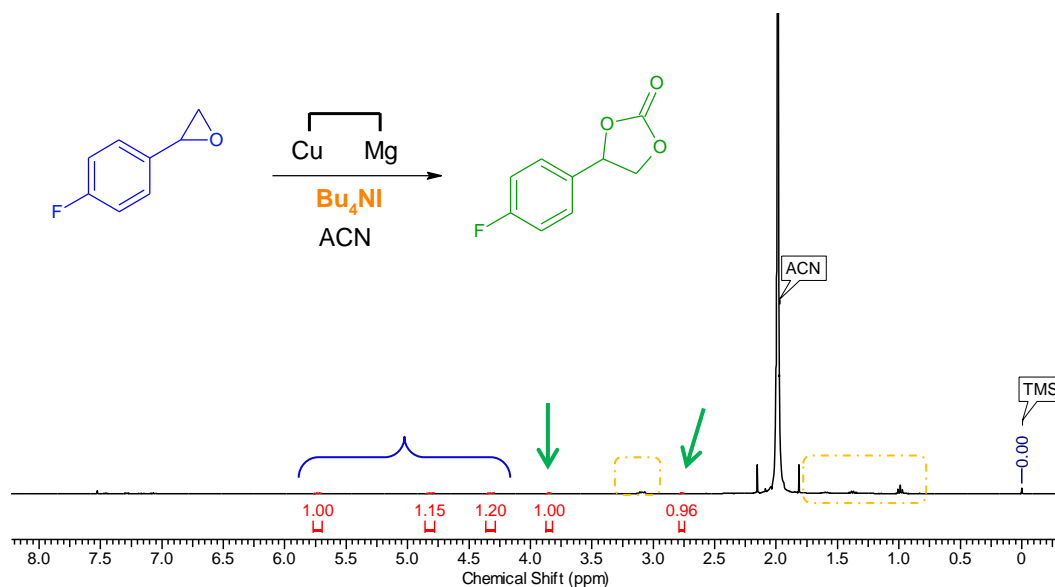


Figure 4.3.- $^1\text{H-NMR}$ of crude from 2-(4-Fluorophenyl)oxirane carboxylation reaction in ACN. Short Circuit, TBAI, 75 °C, 24 h.

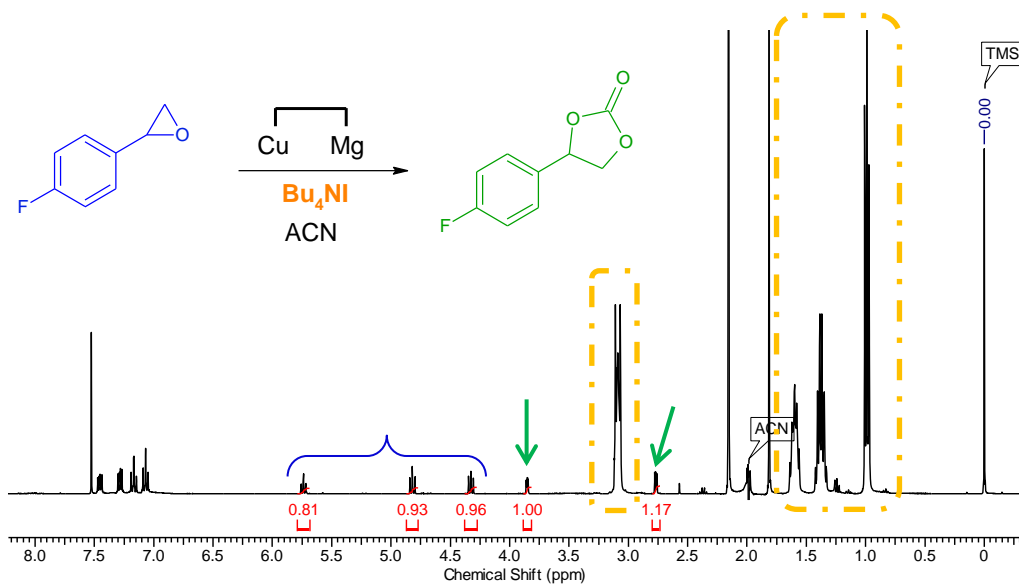


Figure 4.4.- $^1\text{H-NMR}$ presaturated at Acetonitrile signal of crude from 2-(4-Fluorophenyl)oxirane carboxylation reaction. Short Circuit, TBAI, 75 °C, 24 h

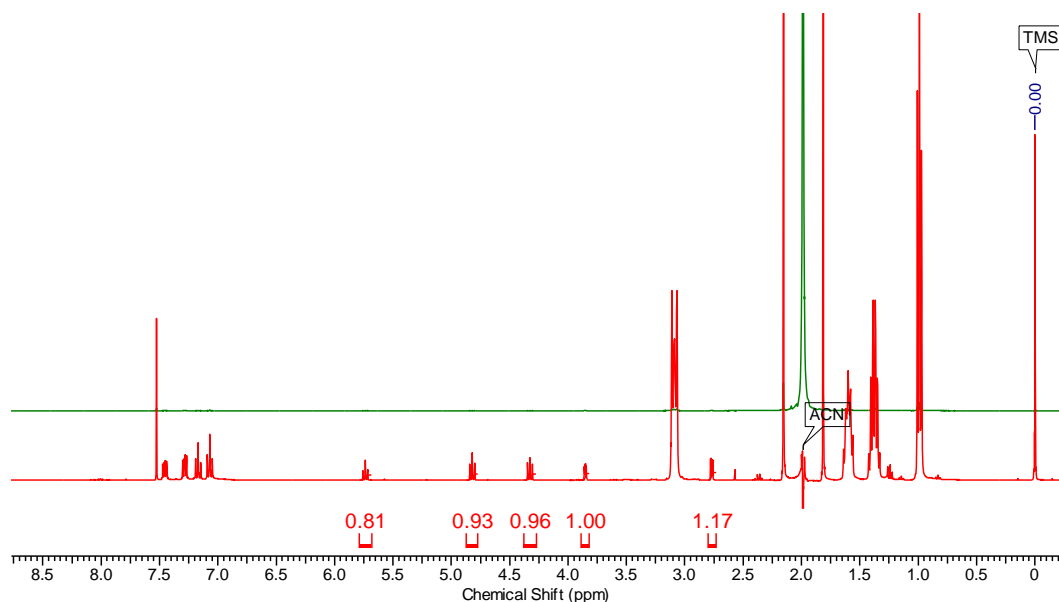


Figure 4.5.- Overlapped $^1\text{H-NMR}$ spectra before presaturation (from Figure 4.3, in green) and after presaturation at acetonitrile signal (from Figure 4.4, in red).

**When the reaction was run at a concentration of 1 M or more, suppression of solvent signal was not necessary as the signal of the solvent was of a similar height to the analytes signals and calculations were made using the normal $^1\text{H-NMR}$ spectra.

4.6.2.3 Initial improvements in procedure and work up.

The best performance conditions of the electrocarboxylation reactions carried out by Anish P. Patel¹ were chosen as starting point for the following background reaction experiments as detailed next.

Initial procedure for electrocarboxylation of epoxides (current, short circuit and open circuit modes):

The epoxide was added to a solution of supporting electrolyte (Bu_4NBr) in acetonitrile in a ratio of (1:1) (unless otherwise stated), the resulting solution was flushed with CO_2 for 1h, followed by heated electrolysis for 5h at 75 °C and constant current (60mA) with constant stirring and constant CO_2 flow, in a single compartment cell containing a magnesium anode (30 cm of Mg ribbon) and copper cathode (60 cm of Cu rod) previously sanded (to remove the oxide layer).

On completion the reaction mixture was filtered to remove the precipitate formed and hydrolysed with HCl (50 mL / 0.1 M) followed by extraction using Et_2O (3 x 35 mL). The combined organic extracts were evaporated to dryness affording a crude oil. EtOAc (5 mL) was added to precipitate Bu_4NI . After precipitation the solid was removed by filtration and the solvent evaporated to afford the corresponding carbonate (b1 or 2b). Flash Chromatography (solvent petroleum ether : ethyl acetate, 1:1) was usually needed to completely remove Bu_4NI traces from the product.

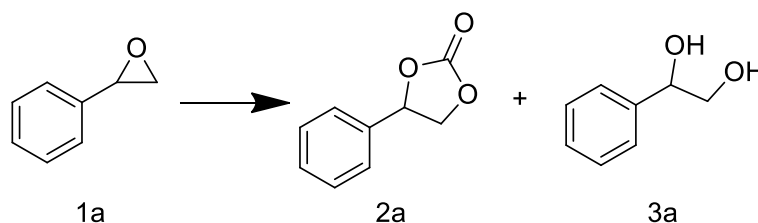


Table 4.6.- Example of diol formation in reactions carried out under initial experimental procedure.

Entry	Starting material	T (°C)	Epoxide (mol/L)	Time (h)	Carbonate (%) ^a	diol (%) ^a
Styrene Oxide						
1	SC1_10a	75	0.02	19	0.0	0.0
2	SC1_10b	75	0.02	48	56.4	15.8
3	SC1_10c	75	0.02	72	83.2	13.4
4	ER1_2	50	0.10	19	73.0	22.0

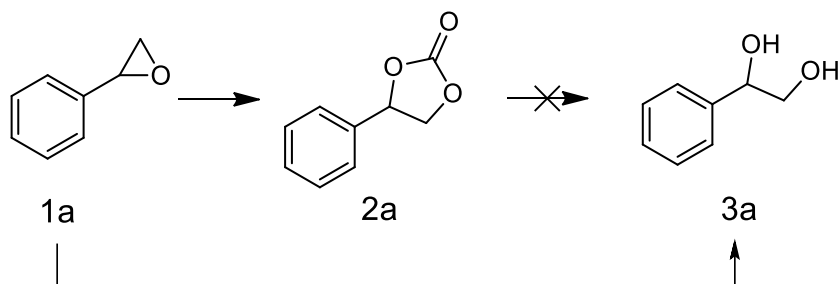


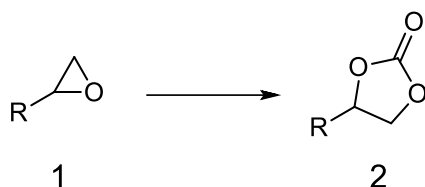
Figure 4.6.- Evolution of styrene oxide carboxylation reaction.

4.6.2.4 Electrocarboxylation of epoxides.

Improved General Procedure:

The epoxide (1a or 1b) was added to a solution of supporting electrolyte (Bu_4NBr) in acetonitrile in a ratio of (1:1) (unless otherwise stated), the resulting solution was flushed with CO_2 for 1h, followed by heated electrolysis for 5h at 75°C and constant current (60mA) with constant stirring and constant CO_2 flow, in a single compartment cell containing a magnesium anode (30 cm of Mg ribbon) and copper cathode (60 cm of Cu rod) previously sanded (to remove the oxide layer).

On completion the reaction mixture was filtered if any precipitate was formed and later concentrated under reduced pressure (in ice bath if required). EtOAc (5 mL) was added to precipitate Bu_4NI . After precipitation the solid was removed by filtration and the solvent evaporated to afford the corresponding carbonate (2a or 2b). Flash Chromatography (solvent petroleum ether : ethyl acetate, 1:1) was usually needed to completely remove Bu_4NI traces from the product.

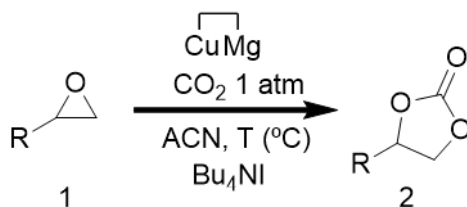


4.6.2.5 ShortCircuitreactions

General Procedure:

The epoxide (1a to 1g) was added to a solution of supporting electrolyte (Bu_4NI) in acetonitrile, the resulting solution was flushed with CO_2 for 1h, followed by heating at 75°C with constant stirring for 19h (or overnight), 24, 48 and 72 hours under constant CO_2 flow, in a single compartment cell containing a magnesium anode (15 cm of Mg ribbon) and copper cathode (30 cm of Cu rod) previously sanded. A wire connection between Cu and Mg electrodes was used to close the system, but no current was applied.

On completion the reaction mixture was concentrated under reduced pressure (in ice bath if required) and EtOAc (5 mL) was added to precipitate Bu_4NI . After precipitation the solid was removed by filtration and the solvent evaporated to afford the corresponding carbonate (2a to 2g). Flash Chromatography (solvent petroleum ether : ethyl acetate, 1:1) was usually needed to completely remove Bu_4NI traces from the product.

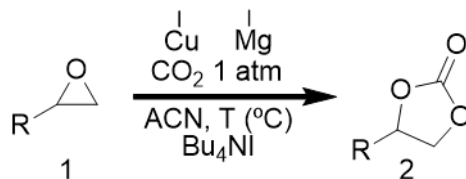


4.6.2.6 Open circuit reaction

General procedure:

Epoxide (1a, 1b or 1e) was added to a solution of supporting electrolyte (Bu_4NBr) in acetonitrile (1:1), the resulting solution was flushed with CO_2 for 1h, followed by heating at 50°C , constant stirring and constant CO_2 flow, in a single compartment cell containing a magnesium ribbon (15 cm of Mg ribbon) and copper rod (30 cm of Cu rod) previously sanded. No connection was made between the electrodes or current applied.

On completion the reaction mixture was concentrated under reduced pressure (in ice bath if required) and EtOAc (5 mL) was added to precipitate Bu_4NI . After precipitation the solid was removed by filtration and the solvent evaporated to afford the corresponding carbonate (2a, 2b or 2e). Flash Chromatography (solvent petroleum ether : ethyl acetate, 1:1) was usually needed to completely remove Bu_4NI traces from the product.



4.6.2.7 Carboxylation of epoxides (No Electrodes)

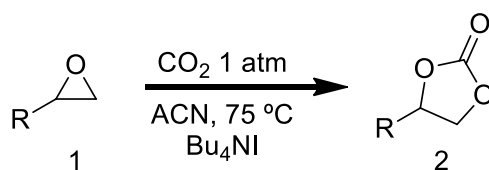
Three different ranges of concentrations of reactants were studied under No Electrodes conditions (dilute reactions from 0.02 to 0.26 M, concentrated reactions from 1 to 20 M, and neat conditions). The general procedures are described in this section.

4.6.2.8 Dilute reactions

General Procedure:

Epoxide (1a to 1g) was added to a solution of supporting electrolyte (Bu_4NI) in acetonitrile (1:1) and heated to 75 °C. Constant CO_2 flow (1 atm pressure). No electrodes were placed in the solution.

On completion the reaction mixture was concentrated under reduced pressure (in ice bath if required) and EtOAc (5 mL) was added to precipitate Bu_4NI . After precipitation the solid was removed by filtration and the solvent evaporated to afford the corresponding carbonate (2a to 2g). Flash Chromatography (solvent petroleum ether : ethyl acetate, 1:1) was usually needed to completely remove Bu_4NI traces from the product.



4.6.2.8.1 MgCO_3 and MgBr_2 as cocatalyst for cyclic carboxylation of epoxides

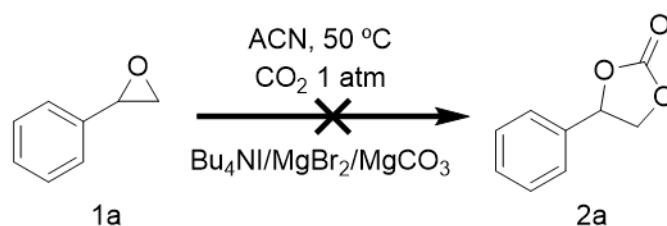
From the observation of the Magnesium electrode being a sacrificial anode and the formation of an inorganic solid (not soluble in any of the usual solvents) in solution, one of the reaction catalysts hypothesis of the electrocarboxylation of epoxides with Mg and Cu as electrodes was

that Mg metal reduced to Mg^{2+} and formed MgCO_3 (with CO_2 in solution) and/or MgBr_2 (with free bromide in solution coming from the N-tetrabutylammonium bromide).

MgCO_3 and MgBr_2 were added to a solution of styrene oxide in order to check their catalytic capacity.

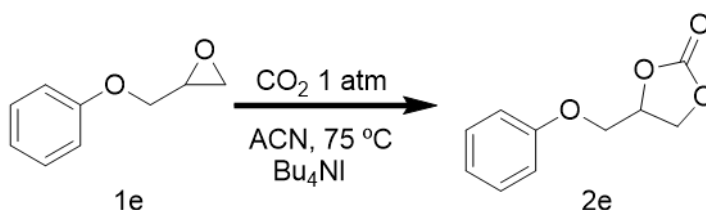
The General procedure for these reactions is as follow:

Styrene oxide (0.1 mmol) was dissolved in acetonitrile (60 mL) and heated to 50 °C. One equivalent of different catalyst/cocatalyst were tested. One reaction contained 0.1 mmol of MgBr_2 and CO_2 was supplied with a balloon at atmospheric pressure. Different species were tested as possible CO_2 source in the carboxylation of epoxides: MgCO_3 (0.1 mmol), N-tetrabutylammonium bromide (0.1 mmol), and MgBr_2 (0.1 mmol). ^1H NMR analysis were carried out after 19 hours of reaction.



4.6.2.8.2 Concentration study

A study on the influence of the concentration of the reactants on the cyclic carboxylation of epoxides was carried out. 1,2-Phenoxypropylene oxide (1e) was added to a solution of the catalyst (Bu_4NI) in acetonitrile at a 1 to 1 ratio previously heated to 75 °C. Reactions were run at concentrations of 0.1, 0.5, 1.0 and 2.0 M. CO_2 atmosphere (1 atm pressure) was maintained with balloons. No electrodes were placed in the solution. ^1H NMR analysis of the aliquots were made at 5 hours and 24 hours of reaction.

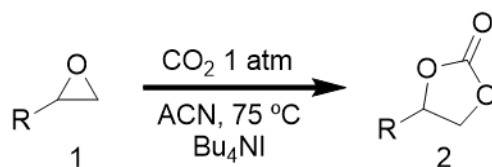


4.6.2.8.3 High concentrate reactions

The general procedure is as follows:

Epoxide (1a to 1j) was added to a concentrate solution (1 M) of supporting electrolyte (Bu_4NI) in acetonitrile and heated to 75 °C. No electrodes were placed in the solution.

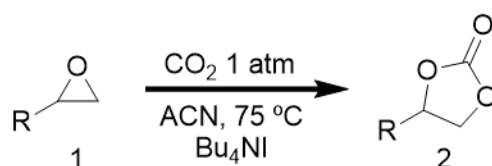
On completion the reaction mixture was concentrated under reduced pressure (in ice bath if required) and EtOAc (5 mL) was added to precipitate Bu_4NI . After precipitation the solid was removed by filtration and the solvent evaporated to afford the corresponding carbonate (2a to 2j). Flash Chromatography (solvent petroleum ether : ethyl acetate, 1:1) was usually needed to completely remove Bu_4NI traces from the product.



4.6.2.8.4 Glycidol and epichlorohydrin cyclic carboxylation

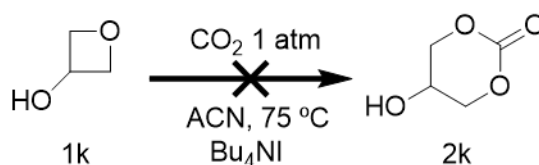
Epoxide (1i and 1j) was added in different ratios (1:1; 10:1 and 100:1) to a 1 M solution of supporting electrolyte (Bu_4NI) in acetonitrile and heated to 75 °C. CO_2 was supplied with balloons. No electrodes were placed in the solution. As seen in the results and discussion chapter glycidol and epichlorohydrin epoxides had a conversion to carbonate of 100% in 5 hours. In order to identify the reaction time and kinetics some extra measurements were taken.

On completion the reaction mixture was concentrated under reduced pressure and EtOAc (5 mL) was added to precipitate Bu_4NI . After precipitation the solid was removed by filtration and the solvent evaporated to afford the corresponding carbonate (2i and 2j). Flash Chromatography (solvent petroleum ether : ethyl acetate, 1:1) was usually needed to completely remove Bu_4NI traces from the product.



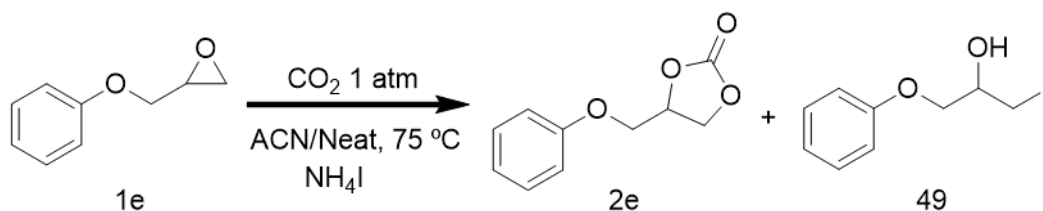
4.6.2.8.5 Cyclic carboxylation of 3-hydroxyoxetane

3-Hydroxyoxetane (Epoxide 1k) was added to a 1 M solution of supporting electrolyte (Bu_4NI) in acetonitrile (1:1) and heated to 75 °C. CO_2 was supplied with balloons. No electrodes were placed in the solution. ^1H NMR analysis were carried out after 5 and 24 hours of reaction with no success.



4.6.2.8.6 NH_4I catalyst for cyclic carboxylation of 1,2-phenoxymethyloxirane

Epoxide (1e) was added to a concentrate suspension of catalyst (NH_4I) in acetonitrile in a flask that has been previously flushed with CO_2 and heated to 75 °C. CO_2 1 atm pressure was maintained with balloons. No electrodes were placed in the solution. ^1H NMR analysis was carried out after 5 and 24 hours of reaction.

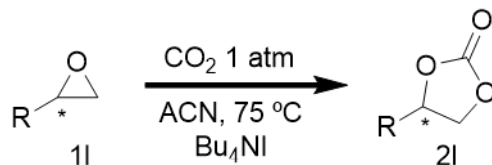


4.6.2.8.7 Study of enantioselectivity of cyclic carboxylation of (S)-1,2-phenoxymethyloxirane

Epoxide (1l, 3.6 M) was added to a 1 M solution catalyst (Bu_4NI) in acetonitrile in a flask that has been previously flushed with CO_2 and heated to 75 °C. CO_2 1 atm pressure was maintained with balloons. No electrodes were placed in the solution.

On completion the reaction mixture was concentrated under reduced pressure and EtOAc (5 mL) was added to precipitate Bu_4NI . After precipitation the solid was removed by filtration and the

solvent evaporated to afford the corresponding carbonate (2l). Flash Chromatography (solvent petroleum ether:ethyl acetate, 1:1) was usually needed to completely remove Bu₄Nl traces from the product. HPLC chirality column (Eurocel 01) was used to analyse the product stereochemistry.

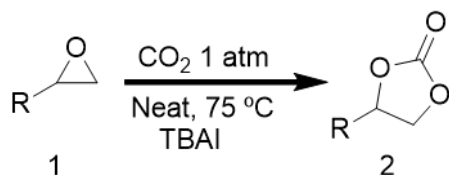


4.6.2.8.8 Solventfree reactions or neat reactions

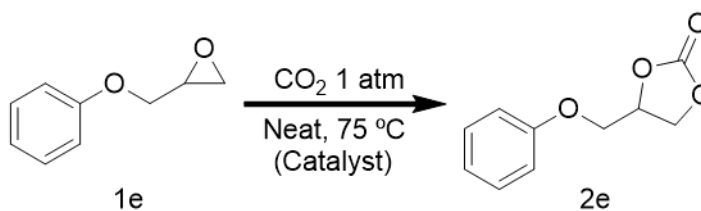
General Procedure:

The catalyst (Bu₄Nl) was added to the epoxide (1a to 1j) in absence of solvent and heated to 75 °C. The catalyst (Bu₄Nl) dissolved in the epoxide when temperature increased up to 70 °C (only if ratio epoxide:salt was equal to or lower than 100:1 regarding the catalyst). No electrodes were placed in the solution.

On completion the reaction mixture usually became an amalgam due to slow precipitation of the carbonate mixed with the non-reacted epoxide and the ammonium salt. Due to rigidity of the mixture the reaction stopped at a lower percentage of conversion compared to when the reaction took place using a solvent, as shown by NMR analysis. The mixture was homogenised by grinding it with a mortar and analysed by ¹H NMR to calculate the conversion % and further dissolved in 1 mL of EtOAc to be purified by flash chromatography (solvent petroleum ether : ethyl acetate, 1:1) to completely remove salt traces from the product and to afford the pure carbonate (2a to 2j).



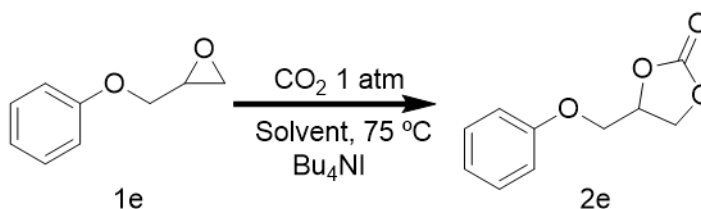
Two control reaction under neat conditions were carried out with 1,2-phenoxy-methyloxirane as epoxide one using NH₄I as catalyst and another using no catalyst.



4.6.2.8.9 Solvent screening study of the cyclic carboxylation reaction of 1,2-phenoxymethyloxirane

A study on the influence of the solvent on the cyclic carboxylation of epoxides was carried out. 1,2-Phenoxymethyloxirane (1e) was added to a 1 M solution of catalyst (Bu₄Ni) in acetonitrile 1 to 1 ratio while heating up to 75 °C. CO₂ atmosphere (1 atm pressure) was maintained with balloons. ¹H NMR analysis of the aliquots were made at 5 hours and 24 hours of reaction.

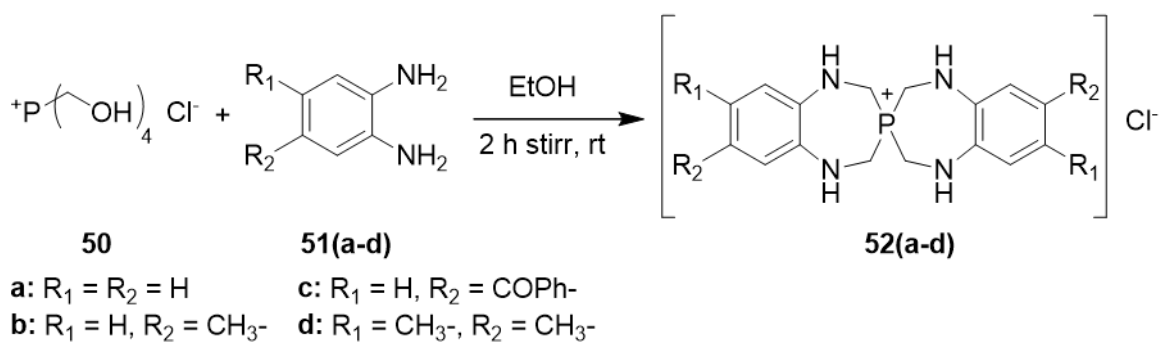
On completion the reaction mixture was concentrated under reduced pressure and EtOAc (5 mL) was added to precipitate Bu₄Ni. After precipitation the solid was removed by filtration and the solvent evaporated to afford the corresponding carbonate (2e). Flash Chromatography (solvent petroleum ether : ethyl acetate, 1:1) was usually needed to completely remove Bu₄Ni traces from the product.



4.6.2.8.10 Phosphonium salts as catalysts.

In collaboration with Professor Martin Smith from Inorganic Chemistry department in Loughborough University, Matias Giménez Toledo (Erasmus student from The University of Valencia, Spain) synthesized a series of Phosphonium salts that were tested as catalysts for the reaction of cyclic carboxylation of epoxides. Procedure of the synthesis can be found in the literature.^{164,165} In this project, phosphonium salts were synthesized from THPC

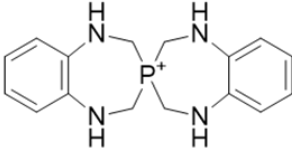
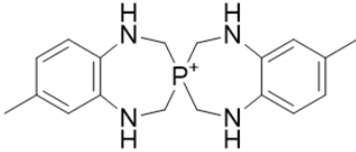
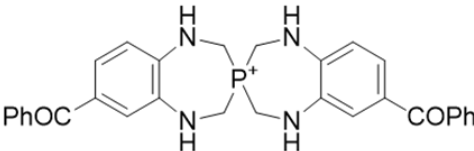
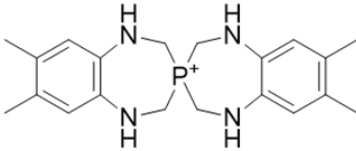
{tetrakis(hydroxymethyl)phosphonium chloride} and phenylenediamine derivatives in ethanol at room temperature while stirring during two hours (Scheme 4.2).¹⁶⁶



Scheme 4.2.- Synthesis of phosphonium salts from THPC.¹⁶⁶

The structures and molecular data of the synthesized, and tested as catalysts for carboxylation of epoxides, phosphonium salts are presented in Table 4.8.

Table 4.8.- Phosphonium salts structure and molecular data.

Cation Shortname	Anion	Cation Structure	Molecular formula	Molecular weight (g/mol)
PS1	Cl ⁻	 52a	C ₁₆ H ₂₀ ClN ₄ P	334,78
	Br ⁻		C ₁₆ H ₂₀ BrN ₄ P	379,23
	I ⁻		C ₁₆ H ₂₀ I ₄ N ₄ P	426,24
	BF ₄ ⁻		C ₁₆ H ₂₀ N ₄ PBF ₄	386,14
	BPh ₄ ⁻		C ₄₀ H ₄₀ BN ₄ P	618,56
PS2	Cl ⁻	 52b	C ₁₈ H ₂₄ ClN ₄ P	362,84
	I ⁻		C ₁₈ H ₂₄ I ₄ N ₄ P	454,29
PS3	Cl ⁻	 52c	C ₃₀ H ₂₈ ClN ₄ O ₂ P	543,00
PS4	Cl ⁻	 52d	C ₂₀ H ₂₈ ClN ₄ P	390,89

Molecular data of Phosphonium salt catalysts. Synthesis of Phosphonium salts can be found in literature.^{164,165} ¹H-NMR, ¹³C-NMR, ³¹P-NMR, IRs, X-Ray and MS analysis of samples were carried out as part of the compound characterization.¹⁶⁶

All reactions with phosphonium salts catalysts were conducted under neat conditions following the procedure described below.

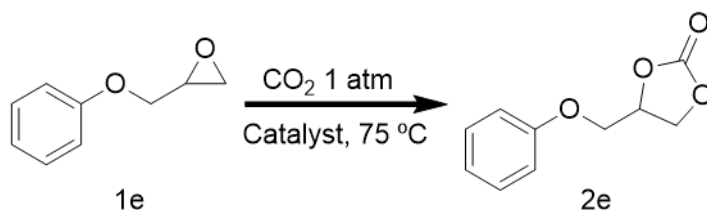
General Procedure:

The phosphonium catalyst was added to the epoxide (1a, 1f or 1g) in the absence of solvent and heated to 75 °C. The catalyst did not dissolve in the epoxide at low temperatures, but it did when reaction temperature was reached. No electrodes were placed in the solution.

On completion, if carbonate production was achieved the reaction mixture became an amalgam due to slow precipitation of the carbonate mixed with the non-reacted epoxide and the phosphonium salt. The mixture was homogenised by grinding it with a mortar and analysed by ¹H NMR to calculate the conversion %.

An initial screening study regarding catalyst performance of different anions of the phosphonium salts (PS1) over 1,2-phenoxyethyl oxirane (1e) was conducted producing the results shown in

Table 2.32. Experimental procedure was performed as detailed above using an amount of 0.1 mmol of Phosphonium (1% of catalyst loading) salt that was added to 10 mmol of epoxide.



In order to evaluate the efficiency of different Phosphonium cations the structures in Table 4.8 were synthesized and tested as catalyst for the cyclic carboxylation of epoxides under neat conditions. All salts were synthesized with Cl^- anion and later mixed with LiI (1:10) within the reaction mixture to produce *in situ* the corresponding phosphonium iodide as discussed above.

4.7 FTIR MONITORING CARBOXYLATION REACTION AND CALCULATION OF REACTION KINETICS

Next experiment was made possible thanks to a collaboration with Professor Matt Sigman in the Organic Chemistry department of the University of Utah. A series of cyclic carboxylation reactions of epichlorohydrin with N-tetrabutylammonium iodide were monitored with a ReactIR iC10 from Mettler Toledo.

The reactor chamber (shown Figure 5.5 on Annexe) consisted on a two neck Pyrex tube specifically designed to fit the mobile probe of the ReactIR iC10, assuring a complete sealing by using grease in joints. A three way tap controlled the inlet of CO_2 gas that was supplied to the reactor through a septum lid with a balloon filled with dry ice vapour which was refilled when needed.

The reactor tube was held with a clamp assuring a straight and vertical position and immersed in a heating bath provided with a magnetic stirrer. Solutions were injected through the septum lid

with a long metal needle and a plastic syringe. A minimum of 2.5 mL of solution was needed in order to reach the detector screen on the tip of the IR probe.

The probe was rinsed with acetonitrile and acetone (methanol when necessary), before and after every experiment. An air background IR was recorded before every batch of analysis started. Reference IR spectra of solvent (at different temperatures and concentrations of CO₂) and reactants were recorded. All spectra from reactions were processed by extracting values of the reference spectrum corresponding to acetonitrile at 75 °C.

Calibrations of tetrabutylammonium iodide and epichlorohydrin at 1 M concentration range were carried out. Cyclic carboxylation of epichlorohydrin in acetonitrile and in water were monitored by IR.

5 ANNEXE

5.1 GIBBS FREE ENERGY OF CO₂ AND OTHER MOLECULES.

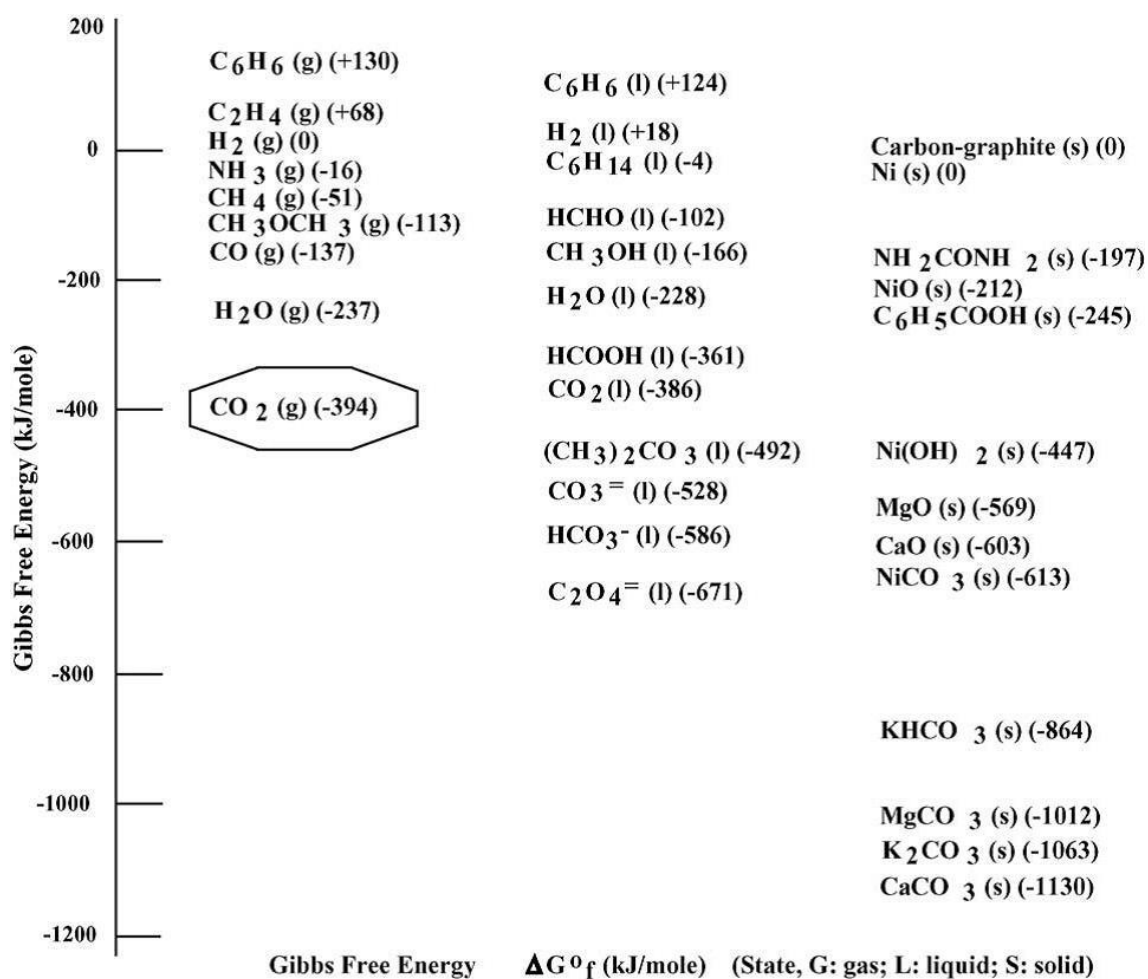


Figure 5.1.- Thermodynamic considerations for CO₂ conversion and utilization involving co-reactants (reproduced from [5]).

5.2 ELECTROCHEMICAL CELL SET UP

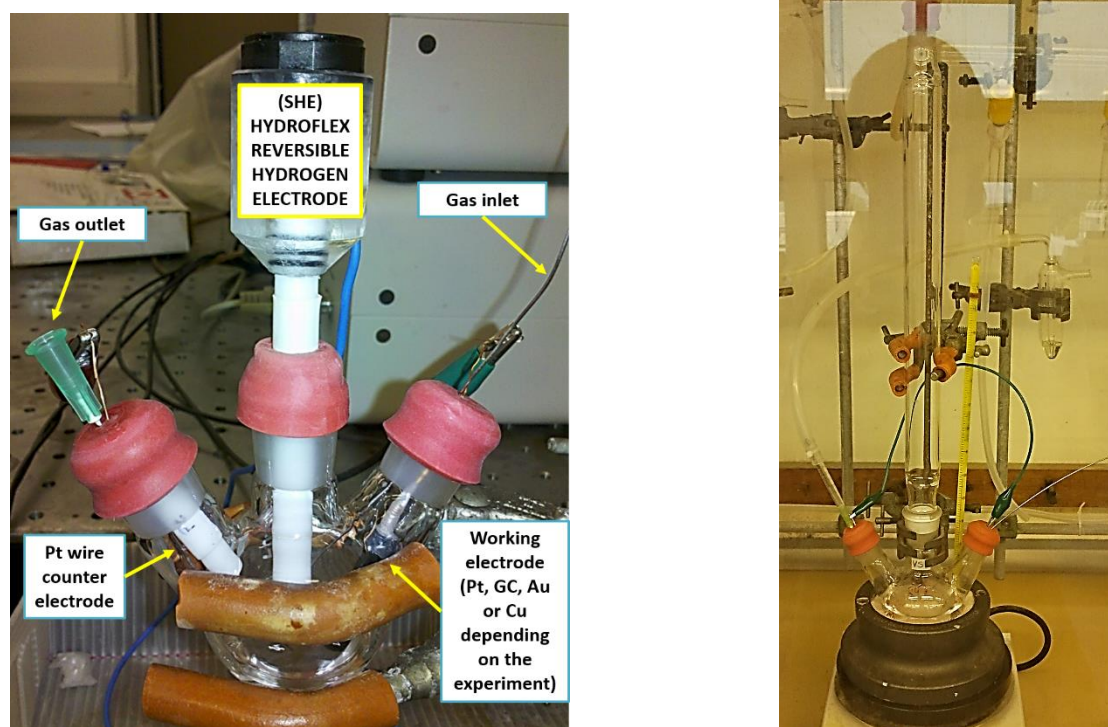


Figure 5.2.- LEFT: Electrochemical cell used to carry out cyclic voltammetry. RIGHT: Short circuit reaction conditions for the carboxylation of styrene oxide experimental set up. For open circuit conditions the set up was the same but without wire connecting the electrodes.

5.3 DMS EXPERIMENT SET UP.

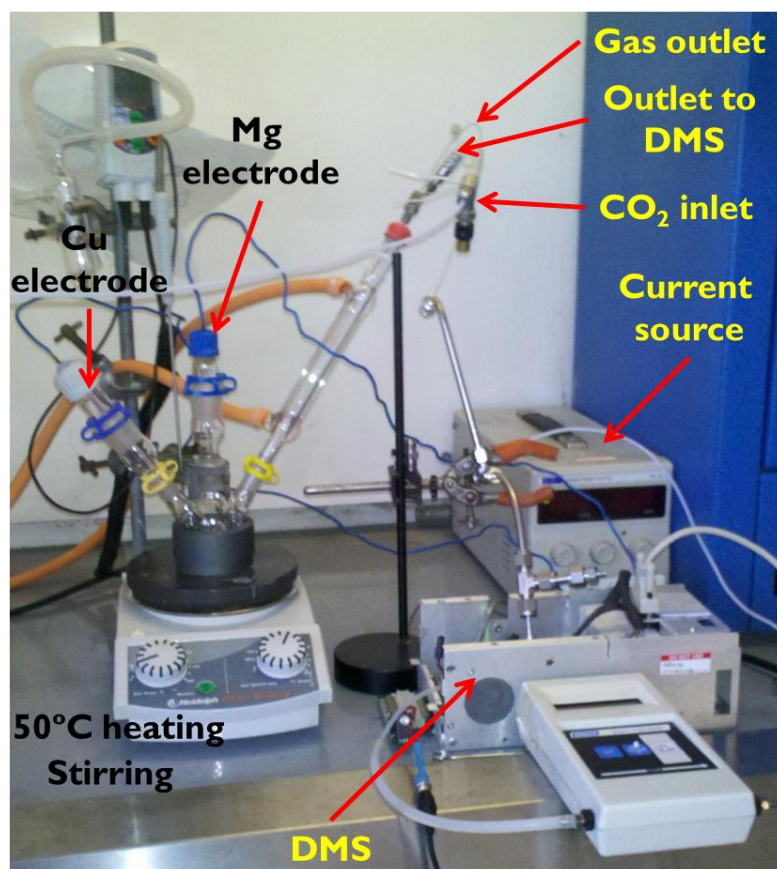


Figure 5.3.-Electrochemical cell connected to the DMS instrument.

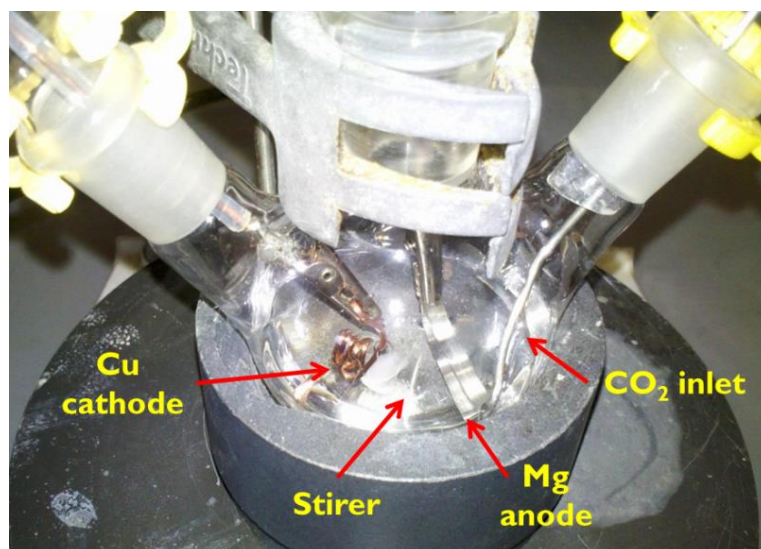
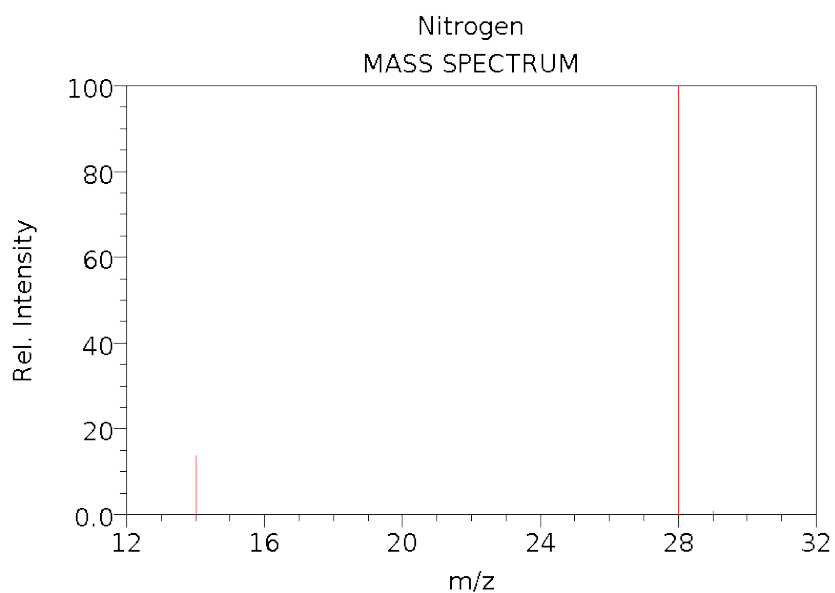


Figure 5.4.- Electrochemical cell containing Copper rod, Magnesium ribbon electrodes, the CO₂ gas inlet and the magnetic stirrer.

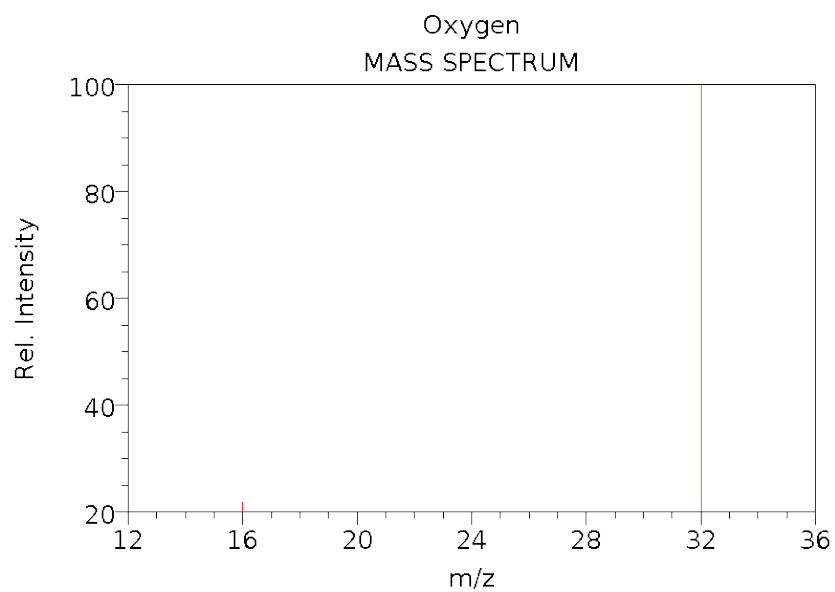
5.4 THEORETICAL MASS SPECTRA DATA.

5.4.1 N₂

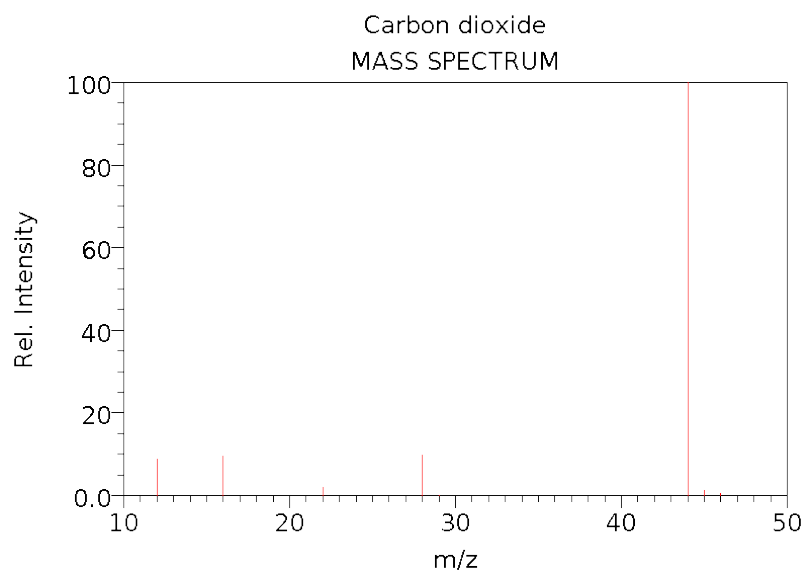


14, **28**

5.4.2 O₂

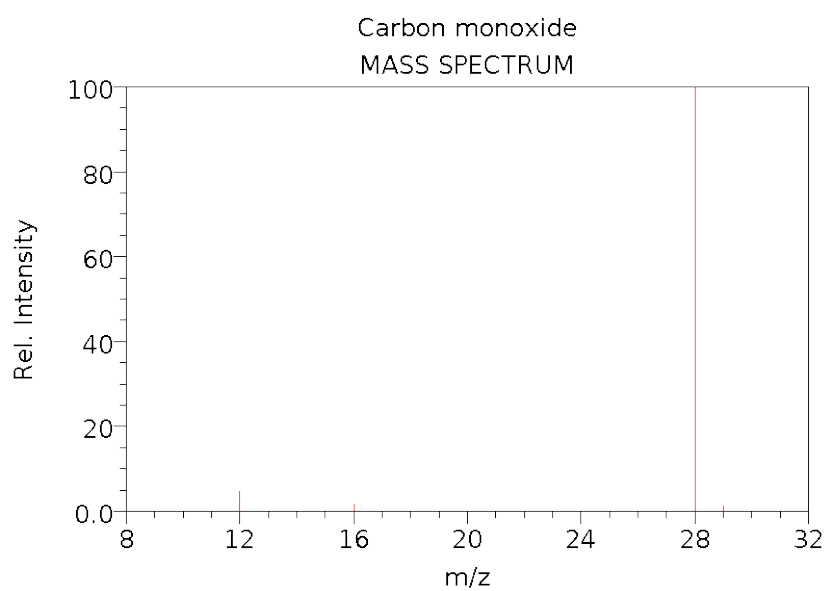


16, **32**

5.4.3 CO₂

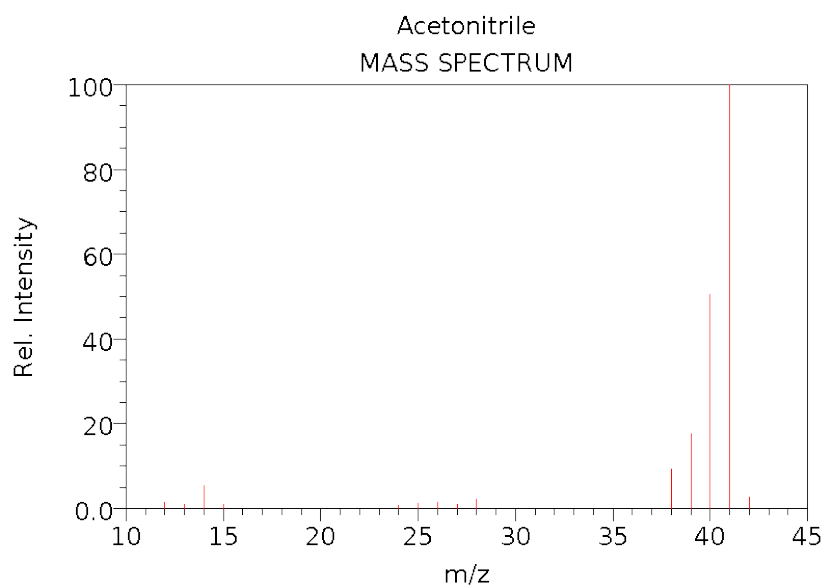
12, 16, 22, 28, 44, 45

5.4.4 CO



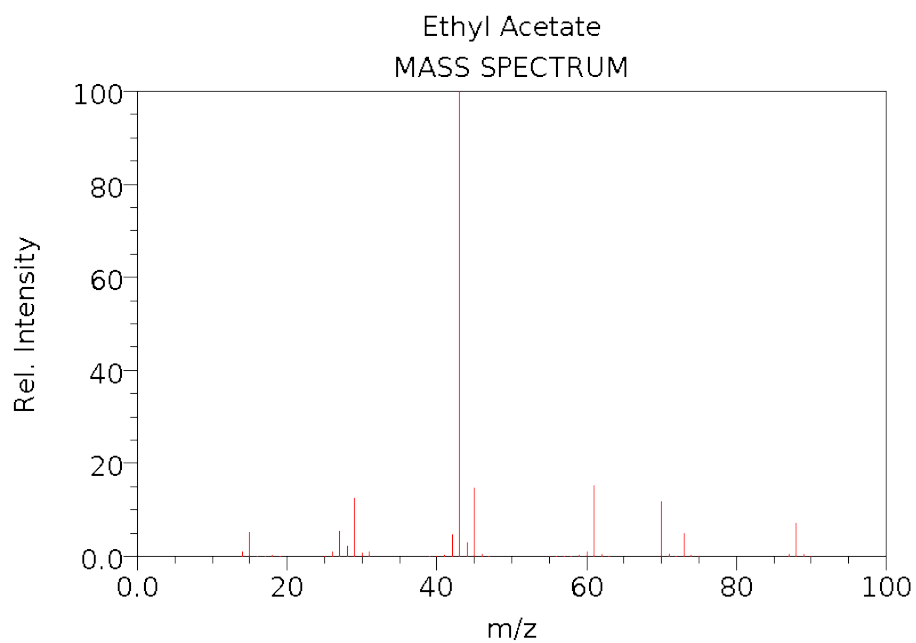
12, 16, 28, 29

5.4.5 Acetonitrile



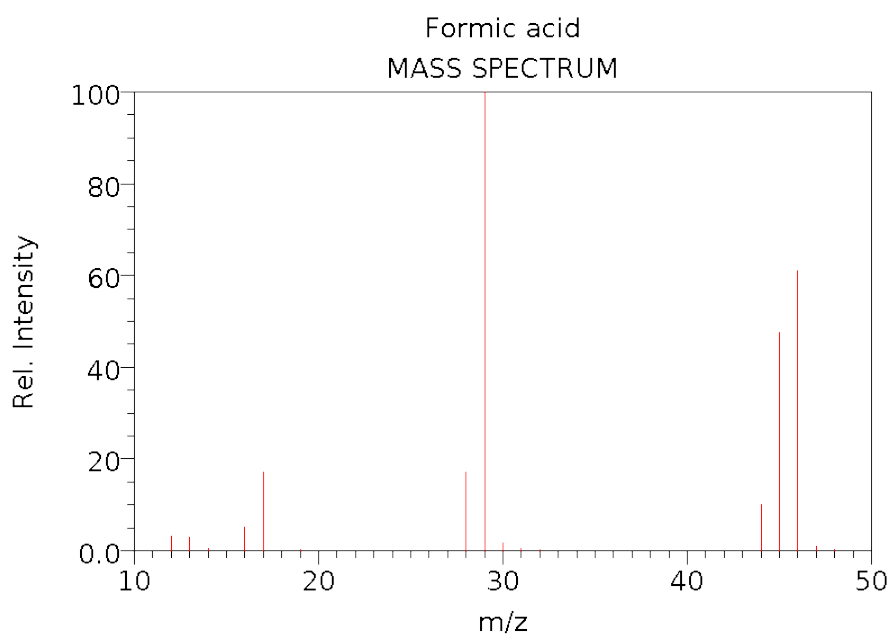
14, 39, 40, **41**

5.4.6 Ethyl Acetate



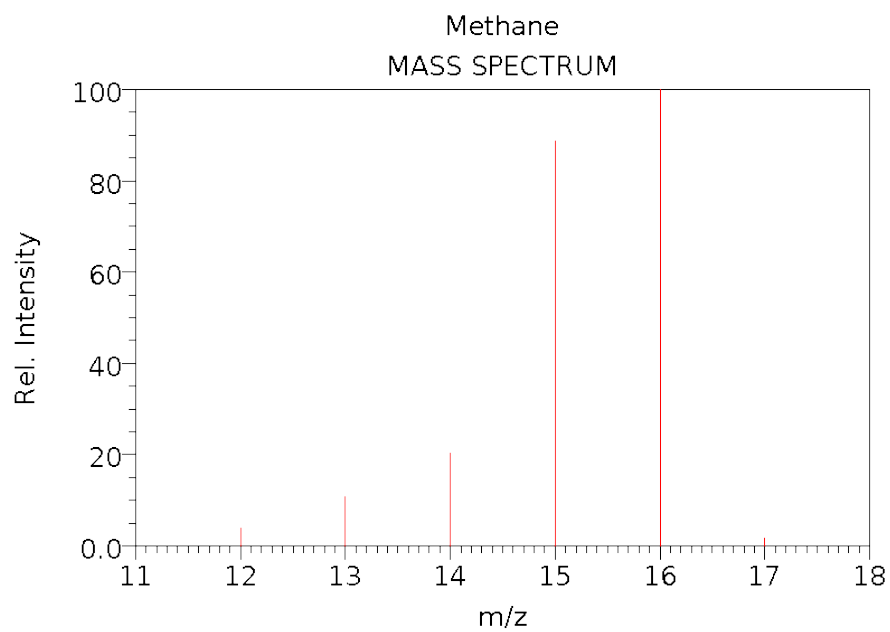
29, **43**, 45, 61, 70, 88

5.4.7 Formic Acid



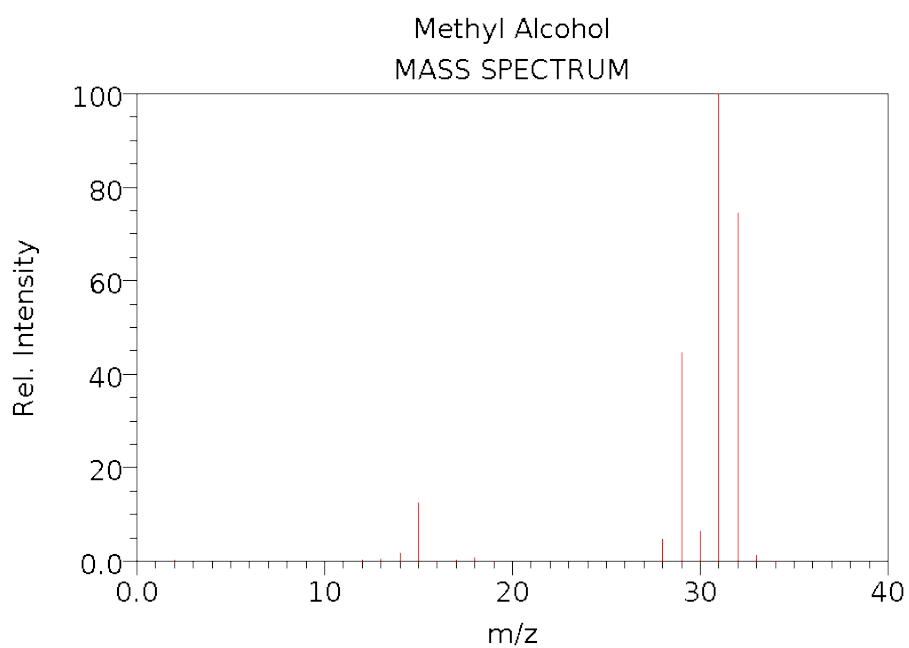
17, 28, **29**, 45, 46

5.4.8 Methane



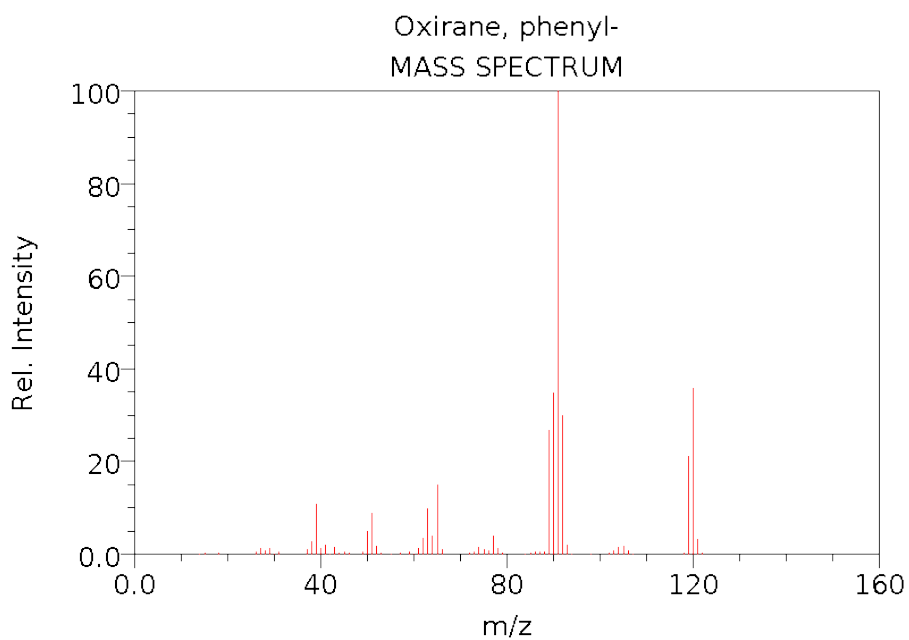
12, 13, 14, **15**, **16**

5.4.9 Methanol



15, 29, **31**, 32

5.4.9.1 Styrene oxide



39, 51, 66, 90, **91**, 119, 120

5.4.9.2 Table of main peaks

Table 5.1.- Summary of main peaks.

	1 st peak (m/z)	2 nd peak (m/z)	3 rd peak (m/z)
<i>N₂</i>	28	14	-
<i>O₂</i>	32	16	-
<i>CO₂</i>	44	28	16-12
<i>CO</i>	28	12	16-29
<i>Acetonitrile</i>	41	40	29
<i>Ethyl Acetate</i>	43	61	45
<i>Formic Acid</i>	29	46	45
<i>Methane</i>	16	15	14
<i>Methanol</i>	31	32	29
<i>Styrene oxide</i>	91	120	90

5.5 REACTIR REACTION SET UP.



Figure 5.5.-Experimental set up for the cyclic carboxylation reaction of epichlorohydrin with CO_2 and TBAI.

REFERENCES

1. Buckley, B. R., Patel, A. P. & Wijayantha, K. G. U. Electrosynthesis of cyclic carbonates from epoxides and atmospheric pressure carbon dioxide. *Chemical communications (Cambridge, England)* **47**, 11888–90 (2011).
2. DeVierno Kreuder, A., House-Knight, T., Whitford, J., Ponnusamy, E., Miller, P., Jesse, N., Rodenborn, R., Sayag, S., Gebel, M., Aped, I., Sharfstein, I., Manaster, E., Ergaz, I., Harris, A. & Nelowet Grice, L. A method for assessing greener alternatives between chemical products following the 12 principles of green chemistry. *ACS Sustainable Chemistry & Engineering* **5**, 2927–2935 (2017).
3. McNaught, A. D. & Wilkinson, A. IUPAC. Compendium of Chemical Terminology, 2nd ed. (the “Gold Book”). *Blackwell Scientific Publications, Oxford* (1997). ISBN: 0-9678550-9-8
4. Keith, D. & Mahmoudkhani, M. Carbon dioxide capture and storage. *WO Patent 2,009,155,539* (2009). ISBN: 9780521863360
5. Song, C. Global challenges and strategies for control, conversion and utilization of CO₂ for sustainable development involving energy, catalysis, adsorption and chemical processing. *Catalysis Today* **115**, 2–32 (2006).
6. Styring, P., Jansen, D., de Coninck, H., Reith, H. & Armstrong, K. *Carbon capture and utilisation in the green economy, using CO₂ to manufacture fuel, chemicals and materials*. 60 (The Centre for Low Carbon Futures 2011 and CO₂Chem Publishing 2012 For, 2011). ISBN: 978-0-9572588-1-5
7. Kennedy, C. Climate.gov. *Climate Change: Atmospheric Carbon Dioxide* available at: <http://www.dimate.gov/news-features/understanding-climate/dimate-change-atmospheric-carbon-dioxide>. (Accessed: 30th June 2013)
8. Lindsey, J. S. Encyclopedia of chemistry. *Encyclopedia of Chemistry* 157–159. (1993).
9. Jarrell, P.M., C.E. Fox, M.H. Stein, S. L. W. in *CO₂ flood environmental, health and safety planning* (Society of Petroleum Engineers, 2002). ISBN: 978-1-55563-096-6
10. Song, C. CO₂ conversion and utilization: an overview. *ACS Symposium Series; American Chemical Society* 2–30 (2002).
11. Eickemeier, P., Schlömer, S., Farahani, E., Kadner, S., Brunner, S., Baum, I. & Kriemann, B. *IPCC, 2014: Climate change 2014: mitigation of climate change. Contribution of working group III contribution to the fifth assessment report of the Intergovernmental Panel on Climate Change*. 1454 (Cambridge University Press, 2014). ISBN: 9781107654815
12. U.S. Environmental Protection Agency. *Global Greenhouse Gas Emissions Data* available at: <https://www.epa.gov/ghgemissions/global-greenhouse-gas-emissions-data#Trends>. (Accessed: 2nd September 2016)

13. Eickemeier, P., Schlömer, S., Farahani, E., Kadner, S., Brunner, S., Baum, I. & Kriemann, B. Intergovernmental Panel on Climate Change (IPCC). *Fifth Assessment Report - Mitigation of Climate Change* (2014). available at: <https://www.ipcc.ch/report/ar5/wg3/>.
14. Yang, H., Xu, Z., Fan, M., Gupta, R., Slimane, R. B., Bland, A. E. & Wright, I. Progress in carbon dioxide separation and capture: a review. *Journal of environmental sciences (China)* **20**, 14–27 (2008).
15. Yamasaki, A. An overview of CO₂ mitigation options for global warming – Emphasizing CO₂ sequestration options. *Journal of Chemical Engineering of Japan* **36**, 361–375. (2003).
16. Maroto-Valer, M. M., Fauth, D. J., Kuchta, M. E., Zhang, Y. & Andrésen, J. M. Activation of magnesium rich minerals as carbonation feedstock materials for CO₂ sequestration. *Fuel Processing Technology* **86**, 1627–1645 (2005).
17. Hughes, R. W., Lu, D. Y., Anthony, E. J. & Macchi, A. Design, process simulation and construction of an atmospheric dual fluidized bed combustion system for in situ CO₂ capture using high-temperature sorbents. *Fuel Processing Technology* **86**, 1523–1531 (2005).
18. Stewart, C. & Hessami, M.-A. A study of methods of carbon dioxide capture and sequestration: the sustainability of a photosynthetic bioreactor approach. *Energy Conversion and Management* **46**, 403–420 (2005).
19. Schrag, D. P. Preparing to capture carbon. *Science (New York, N.Y.)* **315**, 812–3 (2007).
20. Elwell, L. C. & Grant, W. S. Technology options for capturing CO₂. *Power* **150**, 60–65 (2006).
21. Working Group III of the Intergovernmental Panel on Climate Change. *Carbon dioxide capture and storage*. 443 (Cambridge University Press, 2005). ISBN: 978-0-521-86643-9
22. Sipilä, J., Teir, S. & Zevenhoven, R. *Carbon dioxide sequestration by mineral carbonation Literature review update 2005–2007. Åbo Akademi Univ., Heat Engineering Lab. ...* (2008).
23. Mikkelsen, M., Jørgensen, M. & Krebs, F. C. The teraton challenge. A review of fixation and transformation of carbon dioxide. *Energy & Environmental Science* **3**, 43 (2010).
24. Sakakura, T., Choi, J.-C. & Yasuda, H. Transformation of carbon dioxide. *Chemical reviews* **107**, 2365–87 (2007).
25. Zevenhoven, R. Inorganic CO₂ utilisation, mineralization. in “CO₂ Utilisation Potential: Summary of the joint seminar of BMBF and Siemens 22.” (2009).
26. VCI and DECHEMA. *Position Paper Utilisation and Storage of CO₂, Version 12.* (2009).
27. UK Food Standards Agency. Current EU approved additives and their E Numbers | Food Standards Agency. *Current EU approved additives and their E Numbers* (2016). available at: <https://www.food.gov.uk/science/additives/enumberlist>. (Accessed: 2nd September 2016)

28. U.S. Food and drug administration. Food additive status list | U.S. Food additives and drug. *Food additive status list* (2014). available at: <http://www.fda.gov/food/ingredientspackaginglabeling/foodadditivesingredients/ucm091048.htm>. (Accessed: 2nd September 2016)
29. Australia New Zealand Food Standards Code. Standard 1.2.4 - Labelling of Ingredients | Australia New Zealand Food Standards Code. *Schedule 10 – Generic names of ingredients and conditions for their use* (2016). available at: <https://www.legislation.gov.au/Details/F2016C00483>. (Accessed: 2nd September 2016)
30. Taylor, B. in *Carbonated soft drinks: formulation and manufacture* 48–86 (Blackwell Publishing Ltd, 2007).
31. Chen, J. H., Ren, Y., Seow, J., Liu, T., Bang, W. S. & Yuk, H. G. Intervention technologies for ensuring microbiological safety of meat: current and future trends. *Comprehensive Reviews in Food Science and Food Safety* **11**, 119–132 (2012).
32. Zhang, M., Li, T., Ji, Y., Li, M., Sha, S. & Jiang, Y. Optimization of CO₂ enrichment strategy based on BPNN for tomato plants in greenhouse. *Nongye Jixie Xuebao/Transactions of the Chinese Society of Agricultural Machinery* **46**, 239–245 (2015).
33. Hetherington Harry, C. & Krase Herbert, J. Synthesis of urea. (1933). Patent number: us1923489 a
34. Maffei. & Raymond, L. Extraction and cleaning processes. (1973). Patent number: us 4012194
35. Linning, D. A., Leyers, W. E. & Novak, R. A. Decaffeination with supercritical carbon dioxide. (1992).
36. Moret, S., Dyson, P. J. & Laurency, G. Direct synthesis of formic acid from carbon dioxide by hydrogenation in acidic media. *Nature communications* **5**, 4017 (2014).
37. Miller, J. E., Diver, R. B., Siegel, N. P., Coker, E. N., Ambrosini, A., Detric, D. E., Allendorf, M. D., McDaniel, A. H., Kellogg, G. L., Hogan, R. E., Chen, K. S. & Stechel, E. B. Sunshine to petrol: a metal oxide-based thermochemical route to solar fuels. in *Energy technology 2010: conservation, greenhouse gas reduction and management, alternative energy sources* (ed. Neelameggham, NR and Reddy, RG and Belt, CK and Hagni, AM and Das, S.) 27–38 (Minerals, metals & materials SOC, 2010). ISBN: 978-0-87339-749-0
38. Kreutz, T. Prospects for producing low carbon transportation fuels from captured CO₂ in a climate constrained world. *Energy Procedia* **4**, 2121–2128 (2011).
39. Kim, J., Johnson, T. a., Miller, J. E., Stechel, E. B. & Maravelias, C. T. Fuel production from CO₂ using solar-thermal energy: system level analysis. *Energy & Environmental Science* **5**, 8417 (2012).
40. Kim, J., Miller, J. E., Maravelias, C. T. & Stechel, E. B. Comparative analysis of environmental impact of S2P (Sunshine to Petrol) system for transportation fuel production. *Applied Energy* **111**, 1089–1098 (2013).

41. Harrison, P. & Air Fuels Synthesis. Energy conversion & storage: policy, practice, and innovation. in *Clean Transport Fuels from CO₂* (ed. Scottish Hydrogen & Fuel Cell Association Limited) (2013).
42. Smil, V. *Enriching the earth : Fritz Haber, Carl Bosch, and the transformation of world food production*. 338 (MIT Press, 2001). ISBN: 9780262693134
43. Appl, M. in *Ullmann's Encyclopedia of Industrial Chemistry* (Wiley-VCH Verlag GmbH & Co. KGaA, 2000). ISBN: 9783527306732
44. Aresta, M. & Quaranta, E. Proceedings of international conference on carbon dioxide utilization. in 63–77 (1993).
45. Dell'Amico, D. B., Calderazzo, F., Labella, L., Marchetti, F. & Pampaloni, G. Converting carbon dioxide into carbamate derivatives. *ChemInform* **103**, 3857–3898 (2003).
46. Aresta, M., Dibenedetto, A. & Quaranta, E. Reaction of alkali-metal tetraphenylborates with amines in the presence of CO₂: a new easy way to aliphatic and aromatic alkali-metal carbamates. *J. Chem. Soc. Dalton Trans.* 3359–3363 (1995).
47. Aresta, M. & Quaranta, E. Novel, CO₂-promoted synthesis of anhydrous alkylammonium tetraphenylborates: a study on their reactivity as intra- and inter-molecular proton-transfer agents. *Journal of Organometallic Chemistry* **488**, 211–222 (1995).
48. Tang, Y., Zakharov, L. N., Rheingold, A. L. & Kemp, R. A. Insertion of carbon dioxide into Mg–N bonds. Structural characterization of a previously unknown η^2 chelation mode to magnesium in magnesium carbamates. *Organometallics* **23**, 4788–4791 (2004).
49. Lill, S. O. N., Köhn, U. & Anders, E. Carbon dioxide fixation by lithium amides: DFT studies on the reaction mechanism of the formation of lithium carbamates. *European Journal of Organic Chemistry* **2004**, 2868–2880 (2004).
50. Aresta, M. & Quaranta, E. Reactivity of phosphocarbamates: transfer of the carbamate group promoted by metal-assisted electrophilic attack at the carbon dioxide moiety. *The Journal of Organic Chemistry* **53**, 4153–4154 (1988).
51. Shi, M., Jiang, J.-K., Shen, Y.-M., Feng, Y.-S. & Lei, G.-X. An unexpected carbon dioxide insertion in the reaction of Trans-2,4-disubstituted azetidine, trans-2,5-disubstituted pyrrolidine, or Trans-2,6-disubstituted piperidine with diphenylthiophosphinic chloride and diphenylselenophosphinic chloride. *The Journal of Organic Chemistry* **65**, 3443–3448 (2000).
52. Aresta, M. & Quaranta, E. in *Carbon Dioxide as Chemical Feedstock* 121–167 (Wiley-VCH Verlag GmbH & Co. KGaA, 2010). ISBN: 3527324755
53. Fukuto, T. Mechanism of action of organophosphorus and carbamate insecticides. *Environmental health perspectives* **87**, 245–254 (1990).
54. Niimi, L., Serita, K.-I., Hiraoka, S. & Yokozawa, T. Simultaneous construction of the polymer backbone and side chains by three-component polycondensation: The synthesis of

- polyurethanes with allyl side chains from dialdehydes, alkyleneN,N-bis(trimethylsilyl) carbamates, and allyltrimethylsilane. *Journal of Polymer Science Part A: Polymer Chemistry* **40**, 1236–1242 (2002).
55. North, M., Pasquale, R. & Young, C. Synthesis of cyclic carbonates from epoxides and CO₂. *Green Chemistry* **12**, 1514 (2010).
 56. Haworth, W. N. & Machemer, H. 323. Polysaccharides. Part X. Molecular structure of cellulose. *Journal of the Chemical Society (Resumed)* 2270 (1932).
 57. Brignou, P., Priebe Gil, M., Casagrande, O., Carpentier, J.-F. & Guillaume, S. M. Polycarbonates derived from green acids: ring-opening polymerization of seven-membered cyclic carbonates. *Macromolecules* **43**, 8007–8017 (2010).
 58. Matsuo, J., Nakano, S., Sanda, F. & Endo, T. Ring-opening polymerization of cyclic carbonates by alcohol–acid catalyst. *Journal of Polymer Science Part A: Polymer Chemistry* **36**, 2463–2471 (1998).
 59. Darensbourg, D. J., Andreatta, J. R. & Moncada, A. I. in *Carbon Dioxide as Chemical Feedstock* 213–248 (Wiley-VCH Verlag GmbH & Co. KGaA, 2010). ISBN: 3527324755
 60. Sugimoto, H. & Inoue, S. Copolymerization of carbon dioxide and epoxide. *Journal of Polymer Science Part A: Polymer Chemistry* **42**, 5561–5573 (2004).
 61. Seo, S. Y. & Chung, Y. G. in *Sustainable Cities Development and Environment Protection* **361**, 925–929 (Trans Tech Publications, 2013).
 62. Petrova, G. N. & Beider, E. Y. Construction materials based on reinforced thermoplastics. *Russian Journal of General Chemistry* **81**, 1001–1007 (2011).
 63. Sarva, S., Mulliken, A. D. & Boyce, M. C. Mechanics of Taylor impact testing of polycarbonate. *International Journal of Solids and Structures* **44**, 2381–2400 (2007).
 64. Omae, I. Aspects of carbon dioxide utilization. *Catalysis Today* **115**, 33–52 (2006).
 65. Shaikh, A.-A. G. & Sivaram, S. Organic Carbonates. *Chemical reviews* **96**, 951–976 (1996).
 66. Sakakura, T. & Kohno, K. The synthesis of organic carbonates from carbon dioxide. *Chemical communications (Cambridge, England)* 1312–30 (2009).
 67. Onorato, J., Pakhnyuk, V. & Luscombe, C. K. Structure and design of polymers for durable, stretchable organic electronics. *Polymer Journal* **49**, 41–60 (2017).
 68. Zevenhoven, R. & Fagerlund, J. in *Carbon Dioxide as Chemical Feedstock* 353–379 (Wiley-VCH Verlag GmbH & Co. KGaA, 2010). ISBN: 3527324755
 69. National Minerals Information Center. USGS, US Geological Survey (2009) Minerals Information. available at: <https://minerals.usgs.gov/minerals/>. (Accessed: 10th January 2012)

70. Zevenhoven, R., Eloneva, S. & Teir, S. Chemical fixation of CO₂ in carbonates: Routes to valuable products and long-term storage. *Catalysis Today* **115**, 73–79 (2006).
71. Jimoh, O. A., Shah, K., Hashim, A., Hussin, B. & Temitope, A. E. Synthesis of precipitated calcium carbonate: a review. *Carbonates Evaporites* (2017).
72. Speight, J. G. *Chemical and process design handbook*. 633 (McGraw-Hill, 2002). ISBN: 0071374337
73. Platonov, A. Y., Evdokimov, A. N., Kurzin, A. V & Maiyorova, H. D. Solubility of potassium carbonate and potassium hydrocarbonate in methanol. *J. Chem. Eng. Data* **47**, 1175–1176 (2002).
74. Berrie, J. S. & Woolley, G. E. Manufacture of magnesium carbonate and calcium sulphate from brine mud. (1980). Patent number: 4210626
75. Harnisch, H. & Tiedemann, J. Production of barium carbonate from barium sulfate. (1973). Patent number: 3726963
76. Chiang, J. S. & Goldstein, D. Preparation of strontium carbonate. (1983). Patent number: 4421729
77. Wilkomirsky, I. Production of lithium carbonate from brines. (1999). Patent number: 5993759
78. Kolbe, H. Ueber Synthese der Salicylsäure. *Justus Liebigs Annalen der Chemie* **113**, 125–127 (1860).
79. Lindsey, A. & Jeskey, H. The Kolbe-schmitt reaction. *Chemical Reviews* **1928**, 583–620 (1957).
80. Ballivet - Tkatchenko, D. & Dibenedetto, A. in *Carbon Dioxide as Chemical Feedstock* 169–212 (Wiley-VCH Verlag GmbH & Co. KGaA, 2010). ISBN: 3527324755
81. Kowalewicz, A. & Wojtyniak, M. Alternative fuels and their application to combustion engines. *Proceedings of the Institution of Mechanical Engineers, Part D: Journal of Automobile Engineering* **219**, 103–125 (2005).
82. Vitvitskaya, A. S., Naidis, F. B., Katsnel'son, E. Z. & Karpinskaya, I. A. Synthesis of ethyl cyanoethylphenylacetate. *Pharmaceutical Chemistry Journal* **15**, 512–515 (1981).
83. Halmann, M. M. & Steinberg, M. *Greenhouse Gas Carbon Dioxide Mitigation: Science and Technology*. (Lewis Publishers, 1999). ISBN: 1-56670-284-4.
84. Niemi, T., Perea-buceta, J. E., Fernandez, I., Alakurtti, S., Rantala, E. & Repo, T. Direct assembly of 2-oxazolidinones by chemical fixation of carbon dioxide. *Chemistry European Journal* **20**, 8867–8871 (2014).
85. Silvestri, G. & Scialdone, O. in *Carbon Dioxide as Chemical Feedstock* 317–334 (Wiley-VCH Verlag GmbH & Co. KGaA, 2010). ISBN: 9783527629916

86. Barton Cole, E. & Bocarsly, A. B. in *Carbon Dioxide as Chemical Feedstock* 291–316 (Wiley-VCH Verlag GmbH & Co. KGaA, 2010). ISBN: 9783527629916
87. Gibson, D. H. The organometallic chemistry of carbon dioxide. *Chemical reviews* **96**, 2063–2096 (1996).
88. Gibson, D. H. Carbon dioxide coordination chemistry: metal complexes and surface-bound species. What relationships? *Coordination Chemistry Reviews* **185-186**, 335–355 (1999).
89. Darensbourg, D. J. Chemistry of carbon dioxide relevant to its utilization: a personal perspective. *Inorganic chemistry* **49**, 10765–80 (2010).
90. Snuffin, L. L., Whaley, L. W. & Yu, L. Catalytic electrochemical reduction of CO₂ in Ionic Liquid EMIMBF₃Cl. *Journal of The Electrochemical Society* **158**, F155 (2011).
91. Hori, Y. in *Modern Aspects of Electrochemistry* (ed. Vayenas, C.) 89–189 (Springer, 2008). ISBN: 978-0-387-49489-0
92. Costentin, C., Robert, M. & Savéant, J.-M. Catalysis of the electrochemical reduction of carbon dioxide. *Chemical Society reviews* **42**, 2423–36 (2013).
93. Jitaru, M. Electrochemical carbon dioxide reduction - Fundamental and applied topics (Review). *Journal of the university of chemical technology and metallurgy* 333–344 (2007).
94. Jitaru, M., Lowy, D. & Toma, M. Electrochemical reduction of carbon dioxide on flat metallic cathodes. *Journal of Applied Electrochemistry* **27**, 875–889 (1997).
95. Finn, C., Schnittger, S., Yellowlees, L. J. & Love, J. B. Molecular approaches to the electrochemical reduction of carbon dioxide. *Chemical communications (Cambridge, England)* **48**, 1392–9 (2012).
96. Aurian-Blajeni, B., Halmann, M. & Manassen, J. Photoreduction of carbon dioxide and water. *Solar Energy* **25**, 165–170 (1980).
97. Silverman, G. S. & Rakita, P. E. *Handbook of Grignard Reagents*. (Marcel Dekker, Inc., 1996). ISBN: 0824795458
98. Carey, F. A. & Sundberg, R. J. *Advanced Organic Chemistry - Part B*. (Kluwer Academic Publishers, 2002). ISBN: 0306473801
99. Fukue, Y., Oi, S. & Inoue, Y. Direct synthesis of alkyl 2-alkynoates from alk-1-yne, CO₂, and bromoalkanes catalysed by copper(I) or silver(I) salt. *J. Chem. Soc., Chem. Commun.* 2091 (1994).
100. Mita, T., Chen, J. & Sato, Y. Synthesis of arylglycines from CO₂ through α -amino organomanganese species. *American Chemical Society, Org. Lett.* **16**, 2200–2203 (2014).
101. Shi, M. & Nicholas, K. M. Palladium-catalyzed carboxylation of allyl stannanes. *Journal of the American Chemical Society* **119**, 5057–5058 (1997).

102. Hung, T., Jolly, P. W. & Wilke, G. The insertion of the dioxides of carbon and sulphur into the palladium-carbon bond. *Journal of Organometallic Chemistry* **190**, C5 – C7 (1980).
103. Franks, R. J. & Nicholas, K. M. Palladium-catalyzed carboxylative coupling of allylstannanes and allyl halides. *Organometallics* **19**, 1458–1460 (2000).
104. Johansson, R., Jarenmark, M. & Wendt, O. F. Insertion of carbon dioxide into (PCP)Pd(II)–Me bonds. *Organometallics* **24**, 4500–4502 (2005).
105. Yeung, C. S. & Dong, V. M. Beyond Aresta's complex: Ni- and Pd-catalyzed organozinc coupling with CO₂. *Journal of the American Chemical Society* **130**, 7826–7827 (2008).
106. Johansson, R. & Wendt, O. F. Insertion of CO₂ into a palladium allyl bond and a Pd (II) catalysed carboxylation of allyl stannanes. *Dalton Transactions* 488–492 (2007).
107. Ukai, K., Aoki, M., Takaya, J. & Iwasawa, N. Rhodium(I)-catalyzed carboxylation of aryl- and alkenylboronic esters with CO₂. *Journal of the American Chemical Society* **128**, 8706–8707 (2006).
108. Takaya, J., Tadami, S., Ukai, K. & Iwasawa, N. Copper(I)-catalyzed carboxylation of aryl- and alkenylboronic esters. *Organic Letters* **10**, 2697–2700 (2008).
109. Ochiai, H., Jang, M., Hirano, K., Yorimitsu, H. & Oshima, K. Nickel-catalyzed carboxylation of organozinc reagents with CO₂. *Organic Letters* **10**, 2681–2683 (2008).
110. Hoberg, H., Schaefer, D. & Oster, B. W. Dien-carbonsäuren aus 1,3-dienen und CO₂ durch C-C-verknüpfung an nickel(0). *Journal of Organometallic Chemistry* **266**, 313–320 (1984).
111. Hoberg, H. & Oster, B. W. Nickel(0)-induzierte C-C-verknüpfung zwischen 1,2-dienen und kohlendioxid. *Journal of Organometallic Chemistry* **266**, 321–326 (1984).
112. Tsuda, T., Yasukawa, H. & Komori, K. Nickel(0)-catalyzed cycloaddition copolymerization of ether diynes with carbon dioxide to poly(2-pyrone)s. *Macromolecules* **28**, 1356–1359 (1995).
113. Tsuda, T., Kitaike, Y. & Ooi, O. Nickel(0)-catalyzed 1:1 cycloaddition copolymerization of 1,3- and 1,4-di(2-hexynyl)benzenes with carbon dioxide to poly(2-pyrone)s. *Macromolecules* **26**, 4956–4960 (1993).
114. Tsuda, T. & Maruta, K. Nickel(0)-catalyzed alternating copolymerization of 2,6-octadiyne with carbon dioxide to poly(2-pyrone). *Macromolecules* **25**, 6102–6105 (1992).
115. Meléndez, J., North, M., Villuendas, P. & Young, C. One-component bimetallic aluminium (salen)-based catalysts for cyclic carbonate synthesis and their immobilization. *Dalton Transactions* **40**, 3885–3902 (2011).
116. Meléndez, J., North, M. & Pasquale, R. Synthesis of cyclic carbonates from atmospheric pressure carbon dioxide using exceptionally active aluminium(salen) complexes as catalysts. *European Journal of Inorganic Chemistry* **2007**, 3323–3326 (2007).

117. Clegg, W., Harrington, R. W., North, M. & Pasquale, R. Cyclic carbonate synthesis catalysed by bimetallic aluminium-salen complexes. *Chemistry (Weinheim an der Bergstrasse, Germany)* **16**, 6828–43 (2010).
118. Beattie, C., North, M., Villuendas, P. & Young, C. Influence of temperature and pressure on cyclic carbonate synthesis catalyzed by bimetallic aluminum complexes and application to overall syn-bis-hydroxylation of alkenes. *The Journal of organic chemistry* **78**, 419–26 (2013).
119. North, M., Wang, B. & Young, C. Influence of flue gas on the catalytic activity of an immobilized aluminium(salen) complex for cyclic carbonate synthesis. *Energy & Environmental Science* **4**, 4163 (2011).
120. North, M., Villuendas, P. & Young, C. A gas-phase flow reactor for ethylene carbonate synthesis from waste carbon dioxide. *Chemistry (Weinheim an der Bergstrasse, Germany)* **15**, 11454–7 (2009).
121. Shin, D., Kim, J., Yu, B., Lee, M. & Park, D. Synthesis of phenoxymethyl ethylene carbonate using quaternary ammonium salt catalysts grafted onto styrene-vinylbenzylchloride-montmorillonite support. *Korean J. Chem. Eng.* **20**, 71–76 (2003).
122. Vignesh Babu, H. & Muralidharan, K. Zn(II), Cd(II) and Cu(II) complexes of 2,5-bis{N-(2,6-diisopropylphenyl)iminomethyl}pyrrole: synthesis, structures and their high catalytic activity for efficient cyclic carbonate synthesis. *Dalton transactions (Cambridge, England: 2003)* **42**, 1238–48 (2013).
123. North, M. & Pasquale, R. Mechanism of cyclic carbonate synthesis from epoxides and CO₂. *Angewandte Chemie (International ed. in English)* **48**, 2946–8 (2009).
124. Mizuno, T., Nakai, T. & Mihara, M. Facile synthesis of glycerol carbonate from glycerol using selenium-catalyzed carbonylation with carbon monoxide. *Heteroatom Chemistry* **21**, 541–545 (2010).
125. Kaneco, S., Hiei, N., Xing, Y., Katsumata, H., Ohnishi, H., Suzuki, T. & Ohta, K. Electrochemical conversion of carbon dioxide to methane in aqueous NaHCO₃ solution at less than 273 K. *Electrochimica Acta* **48**, 51–55 (2002).
126. Hori, Y. & Suzuki, S. Electrolytic reduction of carbon dioxide at mercury electrode in aqueous solution.pdf. *The chemical society of Japan* **55**, 660–665 (1981).
127. Kaneco, S., Iiba, K., Ohta, K., Mizuno, T. & Saji, A. Electrochemical reduction of CO₂ at an Ag electrode in KOH-methanol at low temperature. *Electrochimica Acta* **44**, 573–578 (1998).
128. TOMITA, Y., TERUYA, S., Koga, O. & HORI, Y. Electrochemical reduction of carbon dioxide at a platinum electrode in acetonitrile-water mixtures. *Journal of The Electrochemical Society* **147**, 4164–4167 (2000).
129. Halmann, M. M. & Steinberg, M. *Greenhouse Gas Carbon Dioxide Mitigation: Science and Technology*. (Taylor & Francis, 1998). ISBN: 9781566702843

130. Christensen, P. A., Hamnett, A. & Muir, A. V. G. CO₂ reduction at platinum, gold and glassy carbon electrodes in acetonitrile: an in-situ FTIR study. **288**, 197–215 (1990).
131. Azuma, M. Electrochemical reduction of carbon dioxide on various metal electrodes in low-temperature aqueous KHCO₃ media. *Journal of The Electrochemical Society* **137**, 1772 (1990).
132. Nagao, H., Mizukawa, T. & Tanaka, K. Carbon-carbon bond formation in the electrochemical reduction of carbon dioxide catalyzed by a ruthenium complex. *Inorganic Chemistry* **33**, 3415–3420 (1994).
133. Brisard, G. M., Amargo, A. P. M., Nart, F. C. & Iwasita, T. On-line mass spectrometry investigation of the reduction of carbon dioxide in acidic media on polycrystalline Pt. *Electrochemistry Communications* **3**, 603–607 (2001).
134. Kuhl, K. P., Hatsukade, T., Cave, E. R., Abram, D. N., Kibsgaard, J. & Jaramillo, T. F. Electrocatalytic conversion of carbon dioxide to methane and methanol on transition metal surfaces. *Journal of the American Chemical Society* **136**, 14107–14113 (2014).
135. Smolinka, T., Heinen, M., Chen, Y. X., Jusys, Z., Lehnert, W. & Behm, R. J. CO₂ reduction on Pt electrocatalysts and its impact on H₂ oxidation in CO₂ containing fuel cell feed gas – A combined in situ infrared spectroscopy, mass spectrometry and fuel cell performance study. *Electrochimica Acta* **50**, 5189–5199 (2005).
136. Willsau, J. & Heitbaum, J. The influence of Pt-activation on the corrosion of carbon in gas diffusion electrodes—A DEMS study. *Journal of Electroanalytical Chemistry and Interfacial Electrochemistry* **161**, 93–101 (1984).
137. Angelucci, C. a., Deiner, L. J. & Nart, F. C. On-line mass spectrometry of the electro-oxidation of methanol in acidic media on tungsten carbide. *Journal of Solid State Electrochemistry* **12**, 1599–1603 (2008).
138. Baltruschat, H. Differential electrochemical mass spectrometry. *Journal of the American Society for Mass Spectrometry* **15**, 1693–706 (2004).
139. Brisard, G. M., Camargo, A. P. M., Nart, F. & Iwasita, T. *A Differential Electrochemical Mass Spectrometry Study for the Investigation of the Electroreduction of Carbon Dioxide on Metal Electrodeposits*. **421**, 1997 (1997).
140. García, G., Silva-Chong, J., Rodríguez, J. L. & Pastor, E. Spectroscopic elucidation of reaction pathways of acetaldehyde on platinum and palladium in acidic media. *Journal of Solid State Electrochemistry* **18**, 1205–1213 (2013).
141. Kas, R., Kortlever, R., Milbrat, A., Koper, M. T. M., Mul, G. & Baltrusaitis, J. Electrochemical CO₂ reduction on Cu₂O-derived copper nanoparticles: controlling the catalytic selectivity of hydrocarbons. *Physical chemistry chemical physics : PCCP* **16**, 12194–201 (2014).
142. Kisadk, I., Stefanova, A., Ernst, S. & Baltruschat, H. Oxidation of carbon monoxide, hydrogen peroxide and water at a boron doped diamond electrode: the competition for hydroxyl radicals. *Physical chemistry chemical physics : PCCP* **15**, 4616–24 (2013).

143. Kuhl, K. P., Cave, E. R., Abram, D. N. & Jaramillo, T. F. New insights into the electrochemical reduction of carbon dioxide on metallic copper surfaces. *Energy & Environmental Science* **5**, 7050 (2012).
144. La Mantia, F. & Novák, P. Online detection of reductive CO₂ development at graphite electrodes in the 1 M LiPF₆, EC:DMC battery electrolyte. *Electrochemical and Solid-State Letters* **11**, A84 (2008).
145. Pastor, E. & Schmidt, V. M. Electrochemical reactions of ethene on polycrystalline Au electrodes in acid solution studied by differential electrochemical mass spectrometry and isotope labelling. *Journal of Electroanalytical Chemistry* **383**, 175–180 (1995).
146. Schnaidt, J., Heinen, M., Jusys, Z. & Behm, R. J. Oxidation of 1-propanol on a Pt film electrode studied by combined electrochemical, in situ IR spectroscopy and online mass spectrometry measurements. *Electrochimica Acta* **104**, 505–517 (2013).
147. Schnaidt, J., Heinen, M., Jusys, Z. & Behm, R. J. Mechanistic aspects of the electro-oxidation of ethylene glycol on a Pt-film electrode: A combined in situ IR spectroscopy and online mass spectrometry study of kinetic isotope effects. *Catalysis Today* **202**, 154–162 (2013).
148. Sun, S., Heinen, M., Jusys, Z. & Behm, R. J. Electrooxidation of acetaldehyde on a carbon supported Pt catalyst at elevated temperature/pressure: An on-line differential electrochemical mass spectrometry study. *Journal of Power Sources* **204**, 1–13 (2012).
149. Wang, H., Alden, L. R., DiSalvo, F. J. & Abruña, H. D. Methanol electrooxidation on PtRu bulk alloys and carbon-supported PtRu nanoparticle catalysts: a quantitative DEMS study. *Langmuir : the ACS journal of surfaces and colloids* **25**, 7725–35 (2009).
150. Wang, H., Rus, E., Sakuraba, T., Kikuchi, J., Kiya, Y. & Abruña, H. D. CO₂ and O₂ evolution at high voltage cathode materials of Li-ion batteries: a differential electrochemical mass spectrometry study. *Analytical chemistry* **86**, 6197–201 (2014).
151. Khoshro, H., Zare, H. R., Namazian, M., Jafari, A. A. & Gorji, A. Synthesis of cyclic carbonates through cycloaddition of electrocatalytic activated CO₂ to epoxides under mild conditions. *Electrochimica Acta* **113**, 263–268 (2013).
152. Gao, X., Yuan, G., Chen, H., Jiang, H., Li, Y. & Qi, C. Efficient conversion of CO₂ with olefins into cyclic carbonates via a synergistic action of I₂ and base electrochemically generated in situ. *Electrochemistry Communications* **34**, 242–245 (2013).
153. Berto, T. C., Zhang, L., Hamers, R. J. & Berry, J. F. Electrolyte dependence of CO₂ electroreduction: Tetraalkylammonium ions are not electrocatalysts. *ACS Catalysis* **703–707** (2014).
154. Lamy, E., Nadjo, L. & Saveant, J. M. Standard potential and kinetic parameters of the electrochemical reduction of carbon dioxide in dimethylformamide. *Journal of Electroanalytical Chemistry and Interfacial Electrochemistry* **78**, 403–407 (1977).

155. Tassaing, T., Foltran, S., Alsarraf, J., Robert, F., Landais, Y., Cloutet, E. & Cramail, H. On the chemical fixation of supercritical carbon dioxide with epoxides catalyzed by ionic salts: an in situ FTIR and Raman study. *Catalysis Science & Technology* **3**, 1046–1055 (2013).
156. Gazda, M., Wyrzykowski, D. & Warnke, Z. Thermal analysis of copper (II) complexes of general formula $[\text{Et}_4\text{N}]_2[\text{CuBr}_n\text{Cl}_{4-n}]$. *Journal of Thermal Analysis and Calorimetry* **91**, 979–984 (2008).
157. Batanero, B., Barba, F., Sánchez-Sánchez, C. M. & Aldaz, A. Paired electrosynthesis of cyanoacetic acid. *The Journal of organic chemistry* **69**, 2423–6 (2004).
158. Hernández, R. M., Márquez, J., Márquez, O. P., Choy, M. & Ovalles, C. Reduction of carbon dioxide on modified glassy carbon electrodes. *Journal of The Electrochemical Society* **146**, 4131–4136 (1999).
159. Chiappe, C., Leandri, E., Hammock, B. D. & Morisseau, C. Effect of ionic liquids on epoxide hydrolase-catalyzed synthesis of chiral 1,2-diols. *Green chemistry : an international journal and green chemistry resource : GC* **2007**, 162–168 (2007).
160. Zhang, W. X. & Ye, K. Hydrolysis of epoxides and aziridines catalyzed by polymer-supported quarternary ammonium bisulfate. *Chinese Chemical Letters* **19**, 146–148 (2008).
161. Kotsuki, H., Kataoka, M. & Nishizawa, H. High pressure-promoted uncatalyzed hydrolysis of epoxides. *Tetrahedron Letters* **34**, 4031–4034 (1993).
162. Wang, Z., Cui, Y.-T., Xu, Z.-B. & Qu, J. Hot water-promoted ring-opening of epoxides and aziridines by water and other nucleophiles. *The Journal of Organic Chemistry* **73**, 2270–4 (2008).
163. Yamada, W., Kitaichi, Y., Tanaka, H., Kojima, T., Sato, M., Ikeno, T. & Yamada, T. Enantioselective incorporation of carbon dioxide into epoxides catalyzed by optically active cobalt(II) complexes. *Bulletin of the Chemical Society of Japan* **80**, 1391–1401 (2007).
164. Ekudo, A. T. The chemistry of new cyclic phosphorus (III) ligands. (Loughborough University, 2009).
165. Russell, M. G. & Warren, S. Synthesis of new water-soluble phosphonium salts and their Wittig reactions in water. *J. Chem. Soc., Perkin Trans. 1* 505–513 (2000).
166. Giménez-Toledo, M. & Smith, M. *Chemical conversion of CO₂ to useful feedstocks using phosphonium salts*. (2015).
167. Miller, F. P., Vandome, A. F. & McBrewster, J. *Beer-Lambert Law*. 154 (VDM Publishing, 2009). ISBN: 9786130200602
168. Iida, T. & Itaya, T. Cydocondensation of oxalyl chloride. *Tetrahedron* **49**, 10511–10530 (1993).

169. Meléndez, J., North, M. & Villuendas, P. One-component catalysts for cyclic carbonate synthesis. *Chemical communications (Cambridge, England)* 2577–9 (2009).
170. Ren, Y. & Shim, J.-J. Efficient synthesis of cyclic carbonates by MgII/phosphine-catalyzed coupling reactions of carbon dioxide and epoxides. *ChemCatChem* **5**, 1344–1349 (2013).